

# **BIOENGINEERING CHITOSAN-BASED TUBULAR NEURO-MUSCULAR GASTROINTESTINAL TISSUE**

By

Elie Zakhem

A Thesis Submitted to the Graduate Faculty of  
WAKE FOREST UNIVERSITY GRADUATE SCHOOL OF ARTS AND SCIENCES

In Partial Fulfillment of the Requirements  
for the Degree of  
DOCTOR OF PHILOSOPHY  
Molecular Medicine and Translational Sciences

August 2016  
Winston-Salem, North Carolina

Approved by:

Khalil N. Bitar, Ph.D., AGAF, Advisor

Kenneth L. Koch, M.D., Chair

Jaime L. Bohl, M.D.

Giuseppe Orlando, M.D., Ph.D.

Sang Jin Lee, Ph.D.

ProQuest Number: 10150619

All rights reserved

INFORMATION TO ALL USERS

The quality of this reproduction is dependent upon the quality of the copy submitted.

In the unlikely event that the author did not send a complete manuscript and there are missing pages, these will be noted. Also, if material had to be removed, a note will indicate the deletion.



ProQuest 10150619

Published by ProQuest LLC (2016). Copyright of the Dissertation is held by the Author.

All rights reserved.

This work is protected against unauthorized copying under Title 17, United States Code  
Microform Edition © ProQuest LLC.

ProQuest LLC.  
789 East Eisenhower Parkway  
P.O. Box 1346  
Ann Arbor, MI 48106 - 1346

# DEDICATION

To my Dad and Mom (Redwan and Nohad) – For the continuous prayers, unconditional love and support.

To my brothers Samer and Jad – For your love and daily support.

# ACKNOWLEDGEMENTS

I would like to thank my advisor, Dr. Khalil N Bitar for the opportunity to work in his lab and for his continuous support from day one. Thank you for believing in me and for challenging me to grow as an independent researcher. Thank you for assigning me a project to start it from zero and making me see it develop and evolve over the years. Your guidance throughout my graduate studies and your encouragement were always appreciated. I would also like to thank my committee members for their continuous advice and support of this project.

I would like to extend my thanks to all members of the Bitar lab, previous and current. Each one of you had an impact on my life, at the personal and professional levels. I wouldn't have been able to initiate all this work without the mentorship I received from Dr. Shreya Raghavan. Thank you for your support, help, patience and friendship throughout the years. Thank you Dr. Sita Somara for your support and for keeping your door open all the time for questions. Thank you Saranyaraajan Varadarajan for your help and for teaching me the wet lab bench work. All the in vivo studies wouldn't have been made possible without the help and commitment of talented surgeons; Dr. Mostafa Elbahrawy and Dr. Riccardo Tamburrini. Thank you for making this project even more exciting and for your patience during surgeries.

I would like to thank all admin, core techs and animal vet staff at WFIRM for their help and assistance. Your experience broadened my knowledge in different fields. To all my friends, thank you for making grad school a fun time during the most stressful and most frustrating moments. Thank you Shreya for the laughter and great times together

and thank you for introducing me to the Indian cuisine! Thank you Abritee, my “noon thirty” lunch buddy for your support and for sponsoring my lunches when mines are usually PB&J, thank you Oula for our Lebanese chatting and for increasing the Lebanese students community by one!, thank you Riccardo for your daily funny stories that have added fun to our days, thank you Juliana for your continuous encouragement and support, you’re a great listener. It is my pleasure to call you all my friends.

Matt and Logan (and Mila) Davis, the amount of time I spend with you guys, all the activities and all the venting sessions require a whole new dissertation. You guys have been like family to me and I am delighted to call you friends for life. Thank you so much for your support.

A special thank you to my family for being always by my side. Thank you dad and mom for your unconditional love and support. I appreciated the moments you were cheering me up on my bad days and thank you for your continuous prayers, they definitely helped me survive. Thank you for celebrating my moments of success and I hope I made you proud. To my brothers Samer and Jad, I am very grateful for the daily motivation and support. I wouldn’t have been where I am today without you guys. Jennifer, thank you for being a sweet and supportive sister in law, you were a great addition to our family. And lastly, to my furry best friend Bailey, your cuteness kept all this going, I am very thankful for having you as my fist puppy during graduate school, your non-stop wagging tail added so much excitement and craziness!

# TABLE OF CONTENTS

DEDICATION.....	II
ACKNOWLEDGEMENTS.....	III
TABLE OF CONTENTS .....	V
LIST OF FIGURES .....	VI
LIST OF TABLES .....	XV
LIST OF ABBREVIATIONS .....	XVI
ABSTRACT .....	XVIII
CHAPTER I: INTRODUCTION AND BACKGROUND .....	1
CHAPTER II: DESIGN STRATEGIES OF BIODEGRADABLE SCAFFOLDS FOR TISSUE REGENERATION .....	7
CHAPTER III: TISSUE ENGINEERING AND REGENERATIVE MEDICINE: GASTROINTESTINAL APPLICATION.....	30
CHAPTER IV: EXPERIMENTAL DESIGN OF THE THESIS.....	65
CHAPTER V: CHITOSAN-BASED SCAFFOLDS FOR THE SUPPORT OF SMOOTH MUSCLE CONSTRUCTS IN INTESTINAL TISSUE ENGINEERING .....	71
CHAPTER VI: NEO-INNervation OF A BIOENGINEERED INTESTINAL SMOOTH MUSCLE CONSTRUCT AROUND CHITOSAN SCAFFOLD .....	105
CHAPTER VII: DEVELOPMENT OF CHITOSAN SCAFFOLDS WITH ENHANCED MECHANICAL PROPERTIES FOR INTESTINAL TISSUE ENGINEERING APPLICATIONS.....	133
CHAPTER VIII: IMPLANTATION OF AN ENGINEERED TUBULAR NEUROMUSCULAR TISSUE COMPOSED OF HUMAN CELLS AND CHITOSAN SCAFFOLD .....	158
CHAPTER IX: BIOMECHANICAL PROPERTIES OF AN IMPLANTED ENGINEERED TUBULAR GUT-SPHINCTER COMPLEX .....	189
CHAPTER X: TRANSLATIONAL APPLICATION OF THE TISSUE-ENGINEERED GUT (TEG) .....	224
CHAPTER XI: SUMMARY AND CONCLUSIONS .....	236
SCHOLASTIC VITA .....	239

# LIST OF FIGURES

<b>Figure 1:</b> A bioengineered smooth muscle tissue in an organ bath for testing physiological functionality.....	14
<b>Figure 2:</b> Scaffold Characterization: (A) An image of tubular chitosan scaffold prepared using the freeze-drying method. (B) Scanning Electron Microscopy (SEM) characterization of the scaffold reveals a highly porous scaffold. ....	17
<b>Figure 3:</b> Schematic for neo-innervation concept in tissue engineering: Intrinsically innervated, concentrically aligned, smooth muscle constructs were bioengineered using smooth muscle cells and enteric neural progenitor cells (innervated constructs). Three dimensional smooth muscle constructs were bioengineered using smooth muscle cells only (noninnervated constructs). The bioengineered constructs were placed next to each other around tubular chitosan scaffolds as shown in the figure. After 14 days in culture in vitro, the noninnervated constructs became neo-innervated as demonstrated by immunohistochemistry and physiological functionality assays. The intrinsically innervated construct maintained neuronal differentiation. ....	50
<b>Figure 4:</b> Paradigm of tissue engineering and regenerative medicine.....	66
<b>Figure 5:</b> Microscope evaluation of cells: Microscopic pictures of RSCMCs on tissue culture plates (A, C) and composite chitosan membranes (B, D) at day 2 (A, B) and day 7 (C, D) after cell seeding. Pictures were taken at 10X magnification. Cells attached on composite chitosan membranes and they maintained spindle-like morphology, a characteristic of smooth muscle cells. ....	83
<b>Figure 6:</b> Immunofluorescence assay: IHC on RSCMCs grown on composite chitosan membranes for $\alpha$ -smooth muscle actin (A, green color) and smooth muscle specific heavy	

Caldesmon (B, green color). Nuclei stain 4'-6-diamidino-2-phenylindole (DAPI) appears in blue. Cells stained positive for  $\alpha$ -SMA and smooth muscle specific heavy Caldesmon, indicating the maintenance of smooth muscle contractile phenotype on composite chitosan membranes.....84

**Figure 7:** Composite chitosan tubular scaffolds: Different lengths ranging from 3 cm up to 12 cm (A) and different lumen diameters and wall thicknesses (B). .....85

**Figure 8:** Scanning Electron Microscopy of the scaffolds: A section of the scaffold was mounted on a stub and coated with gold using sputter coater. Porosity was characterized by SEM under low power. The image depicted a highly porous scaffold with uniform pore structure at 300X (A) and 500X (B). The mean pore size was found to be 170  $\mu$ m. ....86

**Figure 9:** Bioengineered RCSM construct: Day 7 - Three dimensional RCSM bioengineered construct with concentrically aligned smooth muscle cells. The internal lumen diameter is 5 mm and wall thickness is 2 mm.....87

**Figure 10:** Constructs around tubular chitosan scaffold: Four bioengineered constructs were mounted around the composite chitosan tubular scaffold and maintained in culture for 2 weeks. Tissue constructs were placed 1 mm apart. ....88

**Figure 11:** Physiological functionality: KCl response. Real time force generation was measured on the constructs taken off the scaffold at day 14 and on the control constructs using a force transducer. The graphs show the average force generated up on treatment with 60 mM potassium chloride (KCl) of an average of  $0.48 \pm 0.10$  mN/mg of protein ( $n = 3$ ) in the constructs that were around the scaffold (A) and  $0.48 \pm 0.05$  mN/mg of protein ( $n = 4$ ) in the control constructs (B). Addition of KCl is marked by the arrow at 180 seconds. Representative tracings for 3D bioengineered scaffold and control constructs have been chosen. ....89

**Figure 12:** Physiological functionality: Ach response. Response in  $\mu$ N/ $\mu$ g of protein of the constructs that were around the scaffold (A) and control constructs (B) to Acetylcholine (Ach). Addition of 1 $\mu$ M of Ach is marked by the arrow. The constructs taken off the scaffold generated an average contraction of  $0.55 \pm 0.08$  mN/mg of protein ( $n = 4$ ) and the control constructs



showed an average contraction of  $0.5 \pm 0.17$  mN/mg of protein ( $n = 4$ ). This graph is a representative figure. ....91

**Figure 13:** Physiological functionality: VIP response. RSCM constructs taken off the scaffold at day 14 (A) and control constructs (B) were tested for relaxation with Vasoactive Intestinal Peptide (VIP). VIP caused an average relaxation of  $-0.79 \pm 0.06$  mN/mg ( $n = 3$ ) in the constructs that were around the scaffold and an average of  $-0.89 \pm 0.18$  mN/mg ( $n = 4$ ) in the control constructs. This graph is a representative figure. ....92

**Figure 14:** Bioengineering innervated constructs: Evaluation of the bioengineering process of the innervated smooth muscle construct. Microscopic images at day 0 (A), day 1 (B) and day 4 (C) show the cells aligning concentrically around the lumen. Macroscopic images at day 0 (D), day 1 (E) and day 4 (F) show the construct fully formed around the central post by day 4. ....114

**Figure 15:** Constructs around scaffold: (A) Both bioengineered colonic smooth muscle tissue constructs were placed next to each other around the same chitosan based scaffold. (B) Microscopic image of the junction between the 2 constructs showing cellular processes bridging the constructs. Construct 1 is the construct that initially contained enteric neural progenitor cells. Construct 2 is the construct that lacked enteric neural progenitor cells.....115

**Figure 16:** Microscopic evaluation of the constructs: (A) Initially intrinsically innervated smooth muscle construct was taken off the scaffold. Microscopic analysis reveals differentiated neuronal projections (red arrows). (B) The neo-innervated smooth muscle construct was taken off the scaffold. Microscopic view of the periphery of the construct shows cells with neural-like phenotype (red arrows). The luminal side of each construct is indicated.....116

**Figure 17:** Physiological functionality: KCl response. Smooth muscle constructs were taken off the scaffold and physiological studies were performed. (A) Intrinsically innervated construct: As the baseline was established, treatment with 60 mM KCl caused an increase in force generation. (B) Neo-innervated construct: The construct exhibited a robust response to KCl.

Constructs recovered back to baseline. Addition of calcium channel blocker, Nifedipine, inhibited contraction of both constructs in response to KCl (green trace). .....117

**Figure 18:** Physiological functionality: Ach response. Cholinergic contraction was studied using acetylcholine (Ach). (A) Intrinsically innervated construct: Treatment with Ach caused a rapid and sustained contraction. Construct recovered back to baseline. Pre-treatment of the constructs with TTX (red trace) attenuated the contraction in response to Ach by 50%. The arrow indicates the time of treatment with Ach. (B) Neo-innervated construct: When baseline was established, treatment with Ach caused a rapid and sustained contraction. In the presence of TTX, the same dose of Ach caused a contraction reduced by 30-40% (red trace).....118

**Figure 19:** Physiological functionality: VIP response. Relaxation of the constructs was studied using vasoactive intestinal peptide (VIP). (A) Intrinsically innervated construct: The construct exhibited a reduction in the basal force. The construct recovered back to baseline. In the presence of TTX, VIP caused a relaxation with 50-60% inhibition (red trace). (B) Neo-innervated construct: When the construct established baseline, treatment with VIP caused a relaxation followed by recovery back to baseline. Pre-treatment of the construct with TTX attenuated the magnitude of relaxation by 50% (red trace)......119

**Figure 20:** Physiological functionality: EFS response. Relaxation studied by electric field stimulation (EFS). (A) Intrinsically innervated construct: When the construct established baseline, electric field stimulation caused a decrease in basal force. Construct recovered back to baseline. TTX completely abolished relaxation by EFS (red trace). (B) Neo-innervated construct: Treatment of the construct with EFS caused a relaxation. Pre-treatment of the construct with TTX inhibited the relaxation seen with EFS (red trace). .....120

**Figure 21:** Smooth muscle phenotype: Bioengineered (A) intrinsically innervated construct and (B) neo-innervated construct showed positive stain for smooth muscle specific heavy Caldesmon indicating smooth muscle phenotypic characteristics in the constructs. ....121

<b>Figure 22:</b> IHC neo-innervation: (A) The intrinsically innervated construct stained positive for neural specific marker $\beta$ -III Tubulin indicating the presence of differentiated neurons in the constructs. (B) The neo-innervated construct also stained positive for $\beta$ -III Tubulin, indicating the emergence of new differentiated neurons. ....	122
<b>Figure 23:</b> Representative images of the tubular scaffolds (A) without fibers; (B) with inner fibers; (C) with outer fibers; and (D) with inner and outer fibers (fiber sandwiched scaffold). (E) Circumferentially aligned chitosan fibers were engineered using the extrusion/gelation method. (F) The mold for scaffolds consisted of an outer tube and an inner tube to create the lumen of the scaffold. ....	142
<b>Figure 24:</b> Representative SEM images of the tubular scaffold (A) without fibers; (B) the fibers; (C) scaffold with inner fibers; (D) scaffold with outer fibers; and (E) with inner and outer fibers. ....	143
<b>Figure 25:</b> Morphology of the pores: SEM of the different scaffolds shows the morphology of the pores. (A) scaffold without fibers; (B) scaffold with inner fibers; (C) scaffold with outer fibers and (D) fiber sandwiched scaffold. ....	144
<b>Figure 26:</b> Tensile properties of the different kinds of scaffolds compared to native intestine: (A) Stress-strain curve; (B) Tensile stress; (C) Tensile strain at break, and (D) Young's modulus. ....	147
<b>Figure 27:</b> Burst pressure strength of different kinds of scaffolds. ....	148
<b>Figure 28:</b> Cell alignment and phenotype around the scaffolds. Different kinds of scaffolds were seeded with aligned smooth muscle sheets. Tissues stained positive for $\alpha$ -smooth muscle actin, indicating the maintenance of smooth muscle phenotype around all scaffolds. DAPI staining demonstrated maintenance of alignment of the cells around the scaffolds. (A) Scaffolds without fibers; (B) scaffolds with inner fibers; (C) scaffolds with outer fibers; and (D) fiber-sandwiched scaffolds. Scale bars 100 $\mu$ m. ....	149
<b>Figure 29:</b> Implantation of the engineered tissue: (A) Engineered tubular neuro-muscular tissue pre-implantation. Engineered aligned smooth muscle sheet was wrapped around tubular	

chitosan scaffold to form the tubular neuro-muscular tissue. (B) A 1 cm incision was made in the back of nude athymic rats. (C) A pocket was created and the tubular neuro-muscular tissue was inserted into the subcutaneous tissue. ....169

**Figure 30:** Harvest of the implant: (A) The tubular neuro-muscular tissue was harvested after 14 days of implantation. The implant was healthy and vascularized. (B) The tubular neuro-muscular tissue was 3 cm in length and (C) 0.3 cm internal diameter. The tubular neuro-muscular tissue maintained luminal patency during the implantation period. ....170

**Figure 31:** H&E analysis of the implant: (A) The tubular neuro-muscular tissue showed maintenance of alignment of smooth muscle around the lumen with blood vessels (white arrows) and (B) absence of smooth muscle in the scaffold only (control). Masson's trichrome analysis revealed high and more compact collagen around the tubular neuro-muscular tissue (C) when compared to control scaffold (D). ....171

**Figure 32:** Immunofluorescence analysis of the implant: The tubular neuro-muscular tissue showed (A) positive stain for  $\alpha$ -smooth muscle actin and (B) smooth muscle specific heavy Caldesmon indicating the maintenance of smooth muscle contractile phenotype. (C) DAPI staining (blue) showed maintenance of alignment of smooth muscle around the lumen. (D) Differentiated neurons were demonstrated by positive stain for  $\beta$ -III tubulin. DAPI stain shows the location of the smooth muscle with respect to neurons. (E) Tubular chitosan scaffold alone (control) showed negative stain for  $\alpha$ -smooth muscle actin and (F) lack of any cellular alignment around the lumen of the scaffold. Scale bars are 100  $\mu$ m.....172

**Figure 33:** Electromechanical coupling integrity: Electromechanical coupling integrity was evaluated using potassium chloride (KCl). KCl caused a rapid and robust sustained contraction in both the implant and the native intestine. KCl response in the implants was around 50% of the force generated in the native rat intestine.....174

**Figure 34:** Cholinergic contraction: Cholinergic contraction was evaluated by addition of exogenous contractile neurotransmitter Ach. Ach caused a rapid contraction in both the implant

and the native intestine. In the presence of TTX, contraction was significantly attenuated (red trace), indicating both myogenic and neurogenic contribution to the response. TTX significantly attenuated the Ach-induced contraction ( $p < 0.05$ ). Ach-induced contraction seen in the implants was around 50% that of the native rat intestine. ....175

**Figure 35:** VIPergic relaxation: Relaxation was evaluated using the neurotransmitter VIP. Both the implanted tissue and the native intestine relaxed upon addition of 1 $\mu$ M of VIP. In the presence of TTX, the response was significantly reduced (red trace,  $p < 0.05$ ). This indicates that relaxation was mediated by both the smooth muscle and the neurons. The force generated by the implants was 30% of the force generated by the native rat intestine.....177

**Figure 36:** EFS relaxation evaluation: Relaxation was further induced using electrical field stimulation (EFS). The 2 bars indicate the time of applying EFS. The implants and the native intestine exhibited a rapid relaxation. When the tissues were pre-treated with TTX (red trace), relaxation was completely inhibited. This indicates that the response was purely neuronally mediated and that the neurons are functional. In the presence of nNOS blocker (L-NAME), EFS-induced relaxation was significantly attenuated indicating the functionality of nitrergic neurons (green trace,  $p < 0.05$ ). EFS-induced relaxation in the implants was 50% of that seen in the native rat intestine. ....178

**Figure 37:** Harvest of the gut-sphincter complex after 4 weeks of implantation. (A) The complex pre-implantation, 3 cm in length, shows a gut part and a sphincter part (white arrow). (B) After 4 weeks of subcutaneous implantation in the abdominal wall shows vascularization of the complex. (C) The complex maintained its luminal patency (0.3 cm internal diameter). ....203

**Figure 38:** In vivo intraluminal pressure measurement. The rats were anesthetized and the complex was accessed. A catheter with 4 circumferential sensors was inserted into the complex to measure luminal pressure. The catheter was connected to Sandhill equipment that records the pressures (as shown in the diagram). Mean gut luminal pressure was  $21 \pm 2$  mmHg while the sphincteric pressure was  $52 \pm 3$  mmHg.....205

**Figure 39:** Mechanical properties of the implanted complex. The tensile properties of the complex were lower than those of the native rat intestine; however they were not significantly different. (A) The tensile strength of the complex was  $0.043 \pm 0.007$  MPa compared to  $0.054 \pm 0.005$  MPa for the native rat intestine. (B) Elongation at break of the implant was  $171 \pm 30$  % compared to  $230 \pm 13$  % for the native rat intestine. (C) Young's modulus of the implanted complex was  $0.1 \pm 0.01$  MPa compared to  $0.12 \pm 0.01$  MPa for the native rat intestine. (D) Burst pressure strength of the implant was  $1396 \pm 60$  mmHg while that of rat duodena was  $1655 \pm 56$  mmHg ( $p = 0.06$ ). .....207

**Figure 40:** Histological evaluation of the implants. Representative images of H&E for the (A) sphincter and (B) gut parts of the complex show maintenance of the circular alignment of the smooth muscle around the lumen of the tubular graft. ....208

**Figure 41:** Immunofluorescence of the implants. Smooth muscle of (A) the sphincter and (B) the gut parts of the complex maintained their contractile phenotype as shown by positive stain for smoothelin after 4 weeks of implantation. (C) Innervation of the complex was demonstrated by positive stain with  $\beta$ III tubulin, indicating that the neural progenitor cells differentiated into neurons. (D) The presence of excitatory motor neurons was demonstrated by positive stain with ChAT. (E) Inhibitory motor neurons stained positive with nNOS. (F) Vascularization was demonstrated by positive stain with von Willebrand factor. ....209

**Figure 42:** In vitro physiological functionality of the implants – myogenic component. (A) The implanted sphincter maintained its capacity to generate a spontaneous basal tone of  $382 \pm 79$   $\mu$ N. (B) The addition of potassium chloride (KCl) resulted in a contraction of  $427 \pm 42$   $\mu$ N above the basal tone in the sphincter. (C) KCl resulted in a robust and sustained contraction ( $434 \pm 17$   $\mu$ N) in the gut part of the complex. ....211

**Figure 43:** In vitro physiological functionality of the implants (neural component). Electrical field stimulation (EFS) of both the (A & B) sphincter and the (C) gut parts of the complex caused relaxation of the smooth muscle (black trace). Pre-incubation of the implants with nNOS inhibitor

LNAME significantly reduced the magnitude of relaxation, indicating the presence of functional nitroergic neurons (gold trace). .....	212
<b>Figure 44:</b> Schematic diagram of the surgical process for TEG anastomosis. ....	226
<b>Figure 45:</b> Implantation of TEG in the peritoneal fold.....	227
<b>Figure 46:</b> Creation of the intestinal loop. ....	228
<b>Figure 47:</b> Anastomosis of the engineered tissue with the native intestine in the created loop area. ....	229
<b>Figure 48:</b> Organ bath studies using potassium chloride and electrical field stimulation indicated the preservation of both the smooth muscle and neural components of the implanted tissue..	230
<b>Figure 49:</b> H&E analysis of the implant indicated the re-epithelialization of the engineered tissue following anastomosis with the rat native intestine. ....	231

# LIST OF TABLES

Table 1. Summary of the mechanical properties of the different kinds of scaffolds.....	145
--	-----



# LIST OF ABBREVIATIONS

Ach	Acetylcholine
AFM	Atomic force microscopy
BMSC	Bone marrow mesenchymal stem cell
CAD	Computer aided design
ChAT	Choline acetyltransferase
DMEM	Dulbecco's modified Eagle medium
ECM	Extracellular matrix
EFS	Electrical Field Stimulation
ENS	Enteric nervous system
GERD	gastroesophageal reflux disease
GI	Gastrointestinal
HBSS	Hank's balanced salt solution
IAS	Internal Anal Sphincter
iPSC	induced pluripotent stem cell
KCl	Potassium chloride
LES	Lower esophageal sphincter

L-NAME	N $\omega$ -Nitro-L-arginine methyl ester hydrochloride
nNOS	neuronal nitric oxide synthase
PAA	poly-( $\alpha,\beta$ )-DL-aspartic acid
PBS	Phosphate buffer saline
PCL	Ploycaprolactone
PLLA	Poly-L-lactic acid
RAIR	Rectoanal inhibitory reflex
RCSMC	Rabbit circular smooth muscle cell
SEM	Scanning electron microscopic
SIS	Small intestine submucosa
TPN	Total parenteral nutrition
TTX	Tetrodotoxin
VIP	Vasoactive Intestinal Peptide
XPS	X-ray photoelectron spectroscopy

# ABSTRACT

The gastrointestinal (GI) tract is a hollow muscular tubular organ that extends from the mouth down to the rectum. Different high pressure zones exist along the tract and are referred to as sphincters. Sphincters maintain a closure tone and relax upon receiving the appropriate signal to allow movement of food. The GI tract performs 2 main functions: (1) peristalsis; a coordinated rhythmic contraction and relaxation that ensures propulsion of the ingested food along the tract and (2) absorption of nutrients through the epithelium of the tract. The GI tract is a highly complex organ system with multiple cells layers organized in a structured architecture. Peristalsis is dictated by 2 smooth muscle layers; the outer longitudinal and inner circular muscle layer along with their innervation provided by the enteric nervous system. Absorption of nutrients is performed by highly specialized epithelial cells around the lumen of the tract. Several diseases affect the tract including cancer, gastroparesis, short bowel syndrome and Hirschsprung's disease. Other diseases of the gut involve segments along with their adjacent sphincters. The most common treatment in all these conditions requires surgical resections of the diseased segment which results in motility disorders and malnutrition in patients. We hypothesized that a tissue engineered tubular neuromuscular gut can be used to lengthen the gut and restore its function. Tissue engineering and regenerative medicine aims to restore, repair or regenerate tissues and organs using a cell/scaffold/bioactive mechanism.

The material of choice in our study was chitosan. Chitosan is a natural polymer that is found in the exoskeleton of arthropods and is widely used in tissue engineering

applications. We developed different tubular chitosan scaffolds and reinforced their mechanical properties using aligned chitosan fibers. The fibers increased the tensile properties (tensile stress and elongation at break) and enhanced the burst pressure strength of the scaffolds. We also evaluated the biocompatibility of chitosan using smooth muscle cells and neural progenitor cells; the 2 main components of the neuromuscular apparatus. Smooth muscle cells maintained their morphology, phenotype and function around chitosan scaffolds. Chitosan scaffolds also enabled neural progenitor cells differentiation into functional neurons.

We then moved to engineering human innervated smooth muscle tissues. We isolated smooth muscle cells and neural progenitor cells from human gut tissues. We developed a technique to engineer intrinsically innervated aligned smooth muscle sheets. Smooth muscle cells were grown on grooves and allowed to align. A collagen gel suspension containing neural progenitor cells was overlaid on top of the aligned smooth muscle. Sheets were formed and were wrapped circumferentially around tubular chitosan scaffolds to form an innervated circular smooth muscle layer. The tissues were implanted subcutaneously in the back of athymic rats for 2 weeks. The tissues were vascularized, they maintained their luminal patency, and the cells maintained their phenotype and functionality as demonstrated by organ bath studies. In another approach to regenerate a gut segment along with its adjacent sphincter, an engineered sphincter was placed around the scaffold below the circumferential innervated smooth muscle sheets to form a gut-sphincter complex around a tubular chitosan scaffold. The complex was implanted subcutaneously in the abdomen of athymic rats for 4 weeks. The tissues were vascularized. In vivo manometric recordings indicated that the tissues

exhibited luminal pressure with a higher pressure at the sphincter zone compared to the gut zone. Tensile properties of the engineered complex matched those of a rat intestine. Histological studies indicated maintenance of smooth muscle circumferential alignment around the scaffold. Immunohistochemical studies demonstrated that the smooth muscle maintained its contractile phenotype after 4 weeks of implantation as indicated by positive stain for smoothelin. Neural differentiation was demonstrated by positive stain for  $\beta$ III tubulin. The phenotypes of the neurons were further characterized using positive staining for excitatory and inhibitory motor neurons. Functionality of the neurons was further confirmed by organ bath studies. The implanted tissues contracted in response to membrane depolarization using potassium chloride. Neural function was demonstrated by electrical field stimulation. Finally, we worked on regenerating the epithelial component of the engineered tissues. The engineered tissues were implanted in the omentum of the rats followed by intestinal bypass surgery. The intestinal bypass surgery consisted of creating an intestinal loop and anastomosing the intestine to create a secondary pathway for propulsion of luminal content. Following recovery, the implanted engineered tissue was anastomosed to the native intestine within the intestinal loop. Histological analysis showed evident regeneration of epithelial cells with villi forming in the engineered tissue.

In summary, studies presented in this thesis demonstrated the biocompatibility of chitosan for GI applications. Mechanical properties of chitosan scaffolds can be tuned using engineered chitosan fibers. Chitosan also supported the reconstruction of the neuromusculature of the gastrointestinal tract. Engineered neuromuscular tissues maintained their viability and functionality following implantation and exhibited luminal

pressure. In conclusion, the engineered tubular neuro-muscular tissues provide the essential components for regenerating the neuro-musculature. Future studies will characterize the regeneration process of the epithelium and its function. Transplantation of the engineered tissues will help patients restore the continuity of the tract, gut motility and the nutritional balance.

# CHAPTER I: INTRODUCTION AND BACKGROUND

Propulsion and digestion of ingested food is one of the main functions of the gut, achieved by the muscular apparatus. The basic unit of the gut musculature consists of smooth muscle, which performs contraction and relaxation under the regulation of the enteric nervous system (ENS) and the interstitial cells of Cajal (ICCs) <sup>1</sup>. This regulation results in a synchronized contractile pattern that is essential for peristalsis and motility. Absorption of nutrients and secretions are also major functions of the gut, regulated by the highly specialized epithelial component <sup>2</sup>. Additionally, the lymphatic and vascular system of the gut support fluid homeostasis, provide immunological defense functions and facilitate the uptake of dietary lipids from the intestinal villi <sup>3</sup>. The gut is unique in being a continuous hollow organ which should make it simple to replace. However, the complexity of the cellular composition and the different functions of the gut make its replacement a challenging process <sup>4</sup>. Thus, any disorder affecting one or more cell types can result in dysmotility and/or malnutrition.

Esophageal cancer, more specifically squamous cell carcinoma and adenocarcinoma, ranks among the most cancer-related causes of death <sup>5</sup>. The treatment strategy involves esophagectomy or endoscopic mucosal resection <sup>6</sup>. Even though short term outcomes are promising, patients still suffer from bleeding, pain and stricture at the site of surgery <sup>7</sup>. Those complications require

the patient to undergo injections of steroids, balloon dilatation or implantation of esophageal stents which impairs the patient's quality of life.

Achalasia of the lower esophageal sphincter (LES) is another disorder characterized by the inability of the LES to relax therefore preventing the food from going into the stomach. This is attributed to loss of nitric oxide neurons in the LES. Treatments include pneumatic dilation or laparoscopic Heller myotomy based on the manometric readings. Even though results were satisfactory and dependent on the type of achalasia, patients still suffered from dysphagia <sup>8</sup>.

Gastric cancer is currently being treated by gastrectomy with short-term and long-term benefits <sup>9</sup>. However, malnutrition following gastrectomy remains an issue <sup>10</sup>. Gastroparesis is a challenging motility disorder characterized by delayed gastric emptying partially due to pyloric sphincter dysfunction. There are many therapeutic approaches for gastroparesis patients, however none of them completely alleviate the symptoms. Prokinetic agents have shown some relief over short term but it has been shown that extended treatment can induce Parkinsonian symptoms, which limits the lifetime use of some of the prokinetic agents. Another way of treating gastroparesis includes botulinum toxin injection which has shown mild improvements. Gastric electric stimulation was also employed for treating gastroparesis with mixed outcomes. The main drawback from implanting the stimulator was infection which required the removal of the device <sup>11</sup>.



Short bowel syndrome is another challenging condition with multiple complications associated with the treatment approaches as listed next <sup>12, 13</sup>. One of the most common treatments is total parenteral nutrition (TPN). Patients are at high risk of developing end-stage liver disease with low survival rate. Other complications include infection of the catheter or catheter occlusion. Intestinal transplant is another option for patients with short bowel syndrome. This is also associated with the issue of available donors. If a match-donor was found, complications of intestinal transplant include rejection of the graft, non-functional graft, ischemia/bleeding, organ failure and others. In addition to health complications, patients undergoing treatments for short bowel syndrome face financial issues. Charges for home parenteral nutrition can be over \$150,000/year.

For patients presenting with Hirschsprung's disease, inflammatory bowel disease, colorectal cancer or fecal incontinence, the creation of a permanent stoma is one of the most common treatment options. Complications resulting from stoma include prolapse or stenosis <sup>14</sup>. The quality of life of the patients with a permanent stoma becomes poor and stressful. Patients suffer from skin irritation, limited physical activity, leakage, offensive odor and economic burden <sup>15</sup>.

Tissue engineering and regenerative medicine provide an alternative beneficial approach to restore gut structure and function. Cell-seeded scaffolds have been used to regenerate gut tissues. This requires an adequate cell source and a scaffolding material to support the cells <sup>16, 17</sup>. Cells such as smooth muscle

cells, epithelial cells, stem cells and organoid units are potential cell source candidates for regenerating, reconstructing or modeling gut tissues. Different scaffolds (natural and synthetic) exist as supporting matrices for the regeneration process. Results from these studies indicated the possibility of regenerating the epithelium using acellular scaffolds or using organoid units seeded onto scaffolds<sup>18</sup>. The regeneration of the epithelium is essential to restore the surface area needed for absorption and restoring nutrition balance. Other studies have focused on regenerating the neuro-musculature to restore motility in the gut<sup>19, 20</sup>. Current approaches have failed in some aspects to regenerate the musculature of the tract in terms of phenotype, architecture and its intrinsic innervation. The work described in this dissertation evaluated the use of a natural tubular chitosan scaffold to support an engineered intrinsically innervated circular smooth muscle layer for gut replacement. The phenotype and function of the engineered musculature was evaluated *in vitro* and *in vivo* in an athymic rat model. Future goals this approach can be scaled up to be evaluated in large animals for evaluation of peristalsis and regeneration of a fully differentiated epithelium. This model also provides a model to study the microbiota in the newly generated gut.

## References:

1. Sanders, K.M., Koh, S.D., Ro, S. & Ward, S.M. Regulation of gastrointestinal motility—insights from smooth muscle biology. *Nature Reviews Gastroenterology and Hepatology* **9**, 633-645 (2012).
2. Kiela, P.R. & Ghishan, F.K. Physiology of Intestinal Absorption and Secretion. *Best Practice & Research Clinical Gastroenterology* **30**, 145-159 (2016).
3. Alexander, J., Ganta, V.C., Jordan, P. & Witte, M.H. Gastrointestinal lymphatics in health and disease. *Pathophysiology* **17**, 315-335 (2010).
4. Said, H.M. Physiology of the Gastrointestinal Tract, Two Volume Set (Academic Press, 2012).
5. Zhang, Y. Epidemiology of esophageal cancer. *World Journal of Gastroenterology* **19** (2013).
6. Fujita, H. et al. Optimum treatment strategy for superficial esophageal cancer: endoscopic mucosal resection versus radical esophagectomy. *World journal of surgery* **25**, 424-431 (2001).
7. Isomoto, H., Yamaguchi, N., Minami, H. & Nakao, K. Management of complications associated with endoscopic submucosal dissection/endoscopic mucosal resection for esophageal cancer. *Digestive Endoscopy* **25**, 29-38 (2013).
8. Rohof, W.O. et al. Outcomes of treatment for achalasia depend on manometric subtype. *Gastroenterology* **144**, 718-725 (2013).
9. Gordon, A.C., Kojima, K., Inokuchi, M., Kato, K. & Sugihara, K. Long-term comparison of laparoscopy-assisted distal gastrectomy and open distal gastrectomy in advanced gastric cancer. *Surgical endoscopy* **27**, 462-470 (2013).

10. Fukuda, Y. et al. Prevalence of Malnutrition Among Gastric Cancer Patients Undergoing Gastrectomy and Optimal Preoperative Nutritional Support for Preventing Surgical Site Infections. *Annals of surgical oncology* **22**, 778-785 (2015).
11. Parkman, H.P., Hasler, W.L. & Fisher, R.S. American Gastroenterological Association technical review on the diagnosis and treatment of gastroparesis. *Gastroenterology* **127**, 1592-1622 (2004).
12. Buchman, A.L., Scolapio, J. & Fryer, J. AGA technical review on short bowel syndrome and intestinal transplantation. *Gastroenterology* **124**, 1111-1134 (2003).
13. Schalamon, J., Mayr, J. & Höllwarth, M. Mortality and economics in short bowel syndrome. *Best Practice & Research Clinical Gastroenterology* **17**, 931-942 (2003).
14. Nour, S., Beck, J. & Stringer, M. Colostomy complications in infants and children. *Annals of the Royal College of Surgeons of England* **78**, 526 (1996).
15. Dabirian, A., Yaghmaei, F., Rassouli, M. & Tafreshi, M.Z. Quality of life in ostomy patients: a qualitative study. *Patient Prefer Adherence* **5**, 1-5 (2010).
16. Bitar, K.N. & Zakhem, E. Is bioengineering a possibility in gastrointestinal disorders? *Expert review of gastroenterology & hepatology* **9**, 1463-1465 (2015).
17. Mohamed, M.S., Chen, Y. & Yao, C.-L. Intestinal stem cells and stem cell-based therapy for intestinal diseases. *Cytotechnology* **67**, 177-189 (2015).
18. Ladd, M.R., Niño, D.F., March, J.C., Sodhi, C.P. & Hackam, D.J. Generation of an artificial intestine for the management of short bowel syndrome. *Current opinion in organ transplantation* **21**, 178-185 (2016).
19. Bitar, K.N., Raghavan, S. & Zakhem, E. Tissue engineering in the gut: developments in neuromusculature. *Gastroenterology* **146**, 1614-1624 (2014).
20. Bitar, K.N. & Zakhem, E. Tissue engineering and regenerative medicine as applied to the gastrointestinal tract. *Current opinion in biotechnology* **24**, 909-915 (2013).

# **CHAPTER II: DESIGN STRATEGIES OF BIODEGRADABLE SCAFFOLDS FOR TISSUE REGENERATION**

Khalil N. Bitar<sup>1,2,3</sup> and Elie Zakhem<sup>1,2</sup>

<sup>1</sup> Wake Forest Institute for Regenerative Medicine, Wake Forest School of Medicine, Winston-Salem, NC

<sup>2</sup> Department of Molecular Medicine and Translational Science, Wake Forest School of Medicine, Winston Salem, NC

<sup>3</sup> Virginia Tech-Wake Forest School of Biomedical Engineering and Sciences, Winston-Salem, NC

***This chapter describes the strategies for designing scaffolds in tissue engineering applications.***

***This manuscript was accepted for publication in Biomedical Engineering and Computational Biology 2014, 6: 13-20.***

## **Introduction:**

Loss of tissue function is associated with various rates of morbidity and mortality depending on the degree of severity of the disease. Different therapies exist for diseases affecting different tissues or organs in the body. Therapies can include surgical replacement, surgical resection and in the case of cancer, chemotherapy and radiotherapy. End stage diseases or complete organ failure require surgical transplantation to restore functionality. The high costs of surgeries, the variability in the success of surgeries, the waiting list for organ transplantation and the limited availability of donors place the patient under socioeconomic pressure. An alternative to the above listed therapies is needed. These limitations have led to the outgrowth of new fields, whereby engineering aspects are incorporated into the principles of surgery and biology.

Regenerative medicine is an emerging field that aims to improve or repair the function of a tissue or an organ. The primary phase of regenerative medicine included the use of cells, preferably the patient's own cells, in combination with a biocompatible biomaterial as a way of delivery of these cells. Soon after that, the spectrum has broadened to include cell-based therapies, genetics, bioactive molecules, tissue engineering, and clinical approaches. This phase of regenerative medicine included the use of various technologies to precondition the cells-biomaterials composite in order to obtain a mature engineered tissue. These tissues are further characterized using molecular and genetics tools to confirm structure and function. Additionally, regenerative medicine often includes a clinical component. Surgical techniques are applied to evaluate the engineered

tissues in vivo before moving towards translational applications. This review will focus on the source of cells used in regenerative medicine, the different designs of biomaterials along with their biomechanical properties and finally the challenges encountered in regenerative medicine.

## **Cell source in regenerative medicine:**

The first step towards success in regenerative medicine is the ability to find a viable cell source. It is of paramount importance to obtain adequate number of functional cells that are able to expand in vitro and that do not cause an immune response upon their implantation. The challenge in obtaining autologous cells resides in the fact that the diseased tissue might not be a good source of cells. This shifts the search to other sources in the body. The use of stem cells in regenerative medicine has gained special attention. Different stem cells are currently being investigated to determine the best candidate. The cells must be immediately available, easy to expand in vitro, and immunocompatible. Mesenchymal stem cells are considered as the leading stem cell in tissue engineering applications. These cells can be harvested from different sources in the body for in vitro expansion. Mesenchymal stem cells from different sources have also shown comparable characteristics of cell surface markers, osteogenic and adipogenic differentiation [1].

Bone marrow-derived mesenchymal stem cells can be obtained from bone marrow aspirate. The fraction of stem cells found in the aspirate is low. However, these cells can be easily expanded in culture and can differentiate into endodermal and ectodermal cells. Bone marrow mesenchymal stem cells are

commonly used in tissue engineering and protocols for their isolation and differentiation are characterized [2-4].

Adipose derived stem cells are also a practical cell source [5, 6]. A large quantity of these cells can be obtained through a minimally invasive procedure. Methods of isolation of these cells are available, however additional optimization is required [7]. In previous studies conducted in mice, it has been documented that fat obtained from different depots share the same characteristics, however the growth rate of the cultured cells decreases with age [8]. Adipose derived stem cells have also been induced to differentiate into Schwann cells in nerve regeneration applications. Differentiated Schwann cells promoted neurite outgrowth when cultured with neurons [9]. These cell sources serve as autologous sources given that the cells can be isolated from the patient, avoiding any immune rejection after their transplantation.

Another source of stem cells is the umbilical cord mesenchymal stem cells [10]. Human umbilical cord mesenchymal stem cells isolated from the Wharton's Jelly in umbilical cords were tested in muscle tissue engineering [11]. The cells were embedded in fibrin gel at different mass fractions to determine the optimal composition for cell viability. Myogenesis was demonstrated qualitatively using immunohistochemistry and quantitatively using PCR. Umbilical cord mesenchymal stem cells have been also tested in bone tissue engineering [12]. Cells that were seeded onto collagen-calcium phosphate cement scaffolds synthesized minerals, indicating osteogenic differentiation. The advantage of using umbilical cord mesenchymal stem cells is that they are easily accessible at



low cost and without invasive procedure. These cells have high proliferative rate. However, the chance of tumorigenesis after their transplantation remains a challenge that requires further investigations.

Placenta, as other gestational tissues, is usually considered as medical waste following birth. However, a population of mesenchymal stem cells resides in the placenta, which serves as a new potential cell source in regenerative medicine [13-16]. The differentiation of placenta-derived mesenchymal stem cells and their application in tissue engineering has been demonstrated [17, 18]. Placenta can be easily obtained without an invasive procedure and with no risk to the donor. Mesenchymal stem cells can be harvested and expanded in abundance; however the issue of being immunologically rejected by the body when used in a non-autologous setting is still controversial. Recently, a pilot study aimed to determine the efficacy and safety of using allogeneic stem cells [19]. Placenta-derived mesenchymal stem cells were transplanted in patients with type 2 diabetes. Although the study was promising, a larger, more controlled study is required to confirm the results.

## **Scaffold design and synthesis: Physical and chemical modifications**

The second component in tissue engineering and regenerative medicine includes the design of a scaffold that acts to either supplement the regeneration process or to replace the diseased tissue. The scaffold is a temporary matrix that supports cell attachment, proliferation and differentiation. An ideal scaffold must have an excellent biocompatibility to ensure cell survival and minimal immune

response after implantation. Biodegradability of the scaffold is another important factor in the design of scaffolds. Biodegradability falls in line with adequate mechanical properties of the scaffold. Following implantation, the scaffold must degrade in a timely manner to ensure proper remodeling of the tissue. Highly porous scaffolds are critical for cell infiltration especially when it comes to thick scaffolds where diffusion becomes a limitation. Porosity also plays a role in providing surface area for cell attachment. An ideal scaffold is the outcome of a balance between all these factors. Finally, physical and chemical modifications can be applied to the scaffolds to enhance their bioactivity.

Given all the above listed factors, a perfect design of scaffolds for tissue engineering and regenerative medicine is still a challenge. For example, even though the trachea and the gastrointestinal tract consist of tubular organs, their architecture is very complex and requires sophisticated designing [20, 21]. Different types of cells, each with a specific alignment necessitate the synthesis of various scaffolds with precise structures that match the native tissue. Different biomaterials are available to synthesize the scaffolds and different techniques are available to modulate the design of these scaffolds.

## **Physical modification:**

The microarchitecture of the tissue is an important element that determines tissue function. Long term success of the engineered tissues requires the recapitulation of the environment in which the cells must reside. Different approaches to develop scaffolds with specific architectures have been demonstrated. An important factor in the synthesis is the reproducibility in the

manufacturing process. Recent reports emphasized the use of computer aided design (CAD) in engineering scaffolds [22-24]. This technique allows fine-tuning the geometry of the scaffold with precise structures.

Our group has previously bioengineered circumferentially aligned intrinsically innervated smooth muscle rings to mimic the circular smooth muscle layer of the gastrointestinal tract [25, 26]. Tissue culture plates were coated with Sylgard and left to cure. A cylindrical post was fixed in the center of the plate in order to create the lumen of the engineered tissue. Enteric neural progenitor cells were suspended in collagen/laminin gel and seeded onto the plate. An additional gel layer of smooth muscle cells was added on top of the first one. Within a period of 7 days, the smooth muscle cells aligned concentrically around the central post. Histological evaluation of the engineered tissues revealed smooth muscle alignment and differentiation of the neural progenitor cells into different types of neurons (excitatory and inhibitory neurons). Electromechanical integrity of the smooth muscle was demonstrated using potassium chloride in the absence and presence of calcium channel blocker, Nifedipine. The presence of muscarinic receptors was also demonstrated using acetylcholine in the absence and presence of muscarinic receptor antagonist, atropine. Neuronal functionality was also demonstrated by electrical field stimulation in the absence and presence of blockers. Although the architecture and functionality of these tissues are established, their mechanical properties are yet to be determined.

In vivo assessment of the bioengineered sphincteric smooth muscle tissues was determined in mice and rat models [27, 28]. The implanted engineered

tissues integrated with the native internal anal sphincter. The tissues were evaluated for their physiological functionality using an organ bath connected to a force transducer set up (**Figure 1**). They maintained their myogenic and neurogenic functionality and they became neo-vascularized. The animals survived throughout the study period and there were no signs of obstruction.

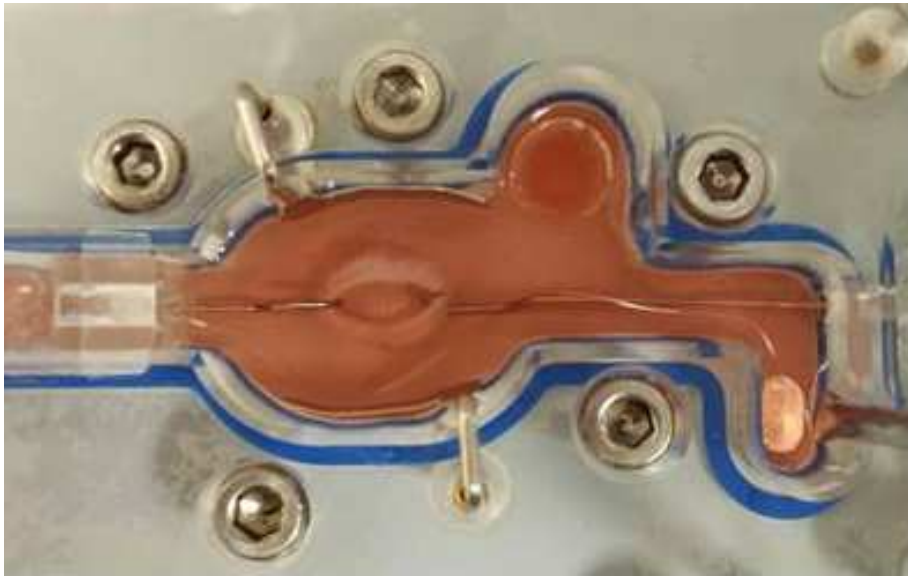


**Figure 1:** A bioengineered smooth muscle tissue in an organ bath for testing physiological functionality.

In other studies, smooth muscle tissue rings were also engineered on agarose-coated wells [29, 30]. The cells aggregated around a central post and formed a ring structure. Mechanical properties of the rings were determined at days 8 and 14 post-formation [31]. The ultimate tensile strength and ring stiffness were found to be higher in larger rings but decreased as a function of time. However, functionality of the smooth muscle was not evaluated. A correlation between the different mechanical properties of the different ring sizes and the force generated from the smooth muscle is an important factor that needs to be determined in tissue regeneration.

When designing scaffolds in tissue engineering, it is important to keep in mind the physiological condition under which the scaffold will be implanted. Tensile properties, suture retention strength, burst pressure strength and compliance are among the common properties evaluated for scaffolds. The scaffold must have enough strength not to break following suturing or when exposed to pressure. Compliance ensures that the scaffold does not compress or twist arbitrarily. To guarantee long term success, these tests must be performed in vitro before implantation. Different designs of scaffolds have been pursued to mimic the architecture of the native tissue. Lee et. al. have engineered a bilayered scaffold for blood vessel replacement using a co-electrospinning technique [32]. A polymer blend of polycaprolactone (PCL) and type 1 collagen was electrospun in a 2 step process. Small diameter fibers were electrospun as a first layer then larger diameter fibers were electrospun on top of that layer. This technique allows the seeding of endothelial cells on the small fibers from the luminal side and smooth muscle cells on the large fibers from the external side. The biomechanical and biological properties of the electrospun PCL/collagen scaffolds were also characterized [33]. Mechanical properties of the composite scaffolds are within the physiologic range.

Other approaches to control the design of the engineered tissues have attempted to prepare micropatterned thermoresponsive surfaces [34]. This technique allowed the formation of aligned cell sheet layers which were placed on top of each other to form 2 layers. Cells were grown on plates at a specific temperature and then were lifted as a layer at a different temperature. The

advantage of using thermoresponsive surfaces is that the cell sheet maintains the extracellular matrix components secreted by the cells which are beneficial for cell-cell interaction. Our group has developed a technique to align smooth muscle using a substrate microtopography technique [35]. The cells were aligned longitudinally in a similar fashion to the longitudinal smooth muscle layer of the gastrointestinal tract. The cells were lifted as a sheet using laminin/collagen gel. These smooth muscle sheets have also been tested for their physiological functionality.

Our group has used tubular chitosan scaffolds as matrices for bioengineered smooth muscle tissues. Chitosan is a natural polymer known for its wide application in tissue engineering. We demonstrated the biocompatibility of chitosan with gut smooth muscle [36]. Chitosan scaffolds also promoted the neo-innervation of bioengineered smooth muscle tissues when placed around the scaffold using enteric neural progenitor cells [37]. Our scaffolds were prepared using the freeze-drying method as described previously (**Figure 2A**). Scanning electron microscopy (SEM) revealed highly porous scaffold with average pore size of around 170  $\mu\text{m}$  (**Figure 2B**). Our scaffolds did not leak or burst when pressure was applied; however they do not possess enough strength to maintain luminal patency. Different techniques are available to improve on the mechanical properties of the chitosan scaffolds. Recently, chitosan fibers were prepared by an extrusion/gelation technique to reinforce the mechanical properties of chitosan-based heart valve scaffolds [38]. Tensile properties were improved in the reinforced scaffolds. Additionally, the fibers mechanical properties were

modulated following different methods of fabrication [39]. The benefit of this technique, where chitosan fibers were used to enhance chitosan scaffold mechanical properties, is that the same material is used but in a different structure. This reduces the issues of biocompatibility and inconsistency using other materials.

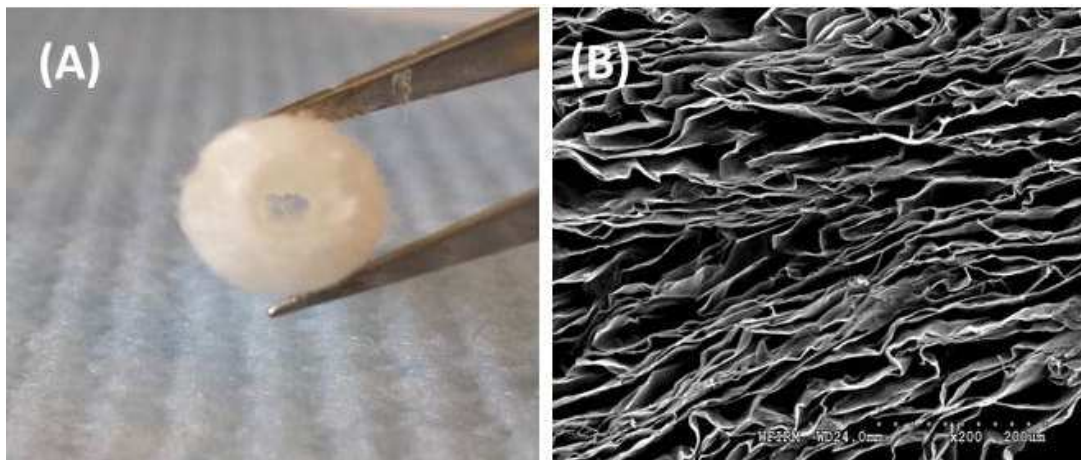


**Figure 2:** Scaffold Characterization: (A) An image of tubular chitosan scaffold prepared using the freeze-drying method. (B) Scanning Electron Microscopy (SEM) characterization of the scaffold reveals a highly porous scaffold.

## Chemical modifications:

In addition to changing the physical characteristics of the scaffolds, chemical modifications are available approaches to enhance the properties of the material. In designing a blood vessel graft, a gradient nanofibrous tubular scaffold was synthesized by electrospinning the polymer solution at different flow rates [40]. Heparin was conjugated to the nanofibers as an antithrombogenic factor. The gradient scaffolds were then loaded with VEGF in a way that heparin-

VEGF level was higher on the luminal side and lower on the external side. Gradient heparin-VEGF enhanced the release of the loaded VEGF from the scaffold and promoted cell attachment. Controlling the release of VEGF helps in tuning the attachment and function of the cells seeded on the scaffold.

In a recent study, a microporous fibrin scaffold was designed with open microchannels and adequate mechanical stiffness in an attempt to engineer cardiac tissue [41]. The design of the scaffold allows the seeding of cardiomyocytes, endothelial cells and fibroblasts in a similar alignment as the native tissue. The architecture of the scaffold also facilitated better cell seeding and survival. The tri-cell seeded scaffolds promoted the formation of a prevascular network with aligned cardiac tissue.

The disadvantage with the use of synthetic polymers is their inability to support cell attachment. Chemical surface modification can improve the biocompatibility of materials and enhance cell growth. Electrospun poly(L-lactide) scaffolds were treated with Ar/NH<sub>3</sub> plasma to introduce amine groups to the scaffold [42]. Surface characterization of the scaffolds using atomic force microscopy (AFM) and X-ray photoelectron spectroscopy (XPS) revealed an increase in hydrophilicity of the material without affecting the structure of the fibers. Surface modification promoted cell attachment, spreading and infiltration. In another study, addition of gelatin type B and fibronectin to poly( $\epsilon$ -caprolactone) improved the biological behavior of the scaffold and enhanced cell colonization and extracellular matrix (ECM) deposition[43]. Different strategies to modify the surface of scaffolds exist. These strategies can either be applied individually or in



combination. It is critical to determine the necessary modification to enhance the activity of the scaffold.

Chemical modification of the scaffold proved to be as critical as physical modification. A polymer solution composed of poly-L-lactic acid (PLLA), poly-( $\alpha,\beta$ )-DL-aspartic acid (PAA), type I and type III collagen was used to electrospin nanofibrous scaffolds[44]. Addition of functional groups to the scaffold made it more hydrophilic as demonstrated by water contact angle measurement. This characteristic allowed more cell attachment, increased the rate of proliferation and increased secretion of ECM proteins. Polyethylene glycol hydrogels were evaluated as injectable biomaterials [45]. The hydrogels were functionalized with laminin at different ratios to assess the attachment of nucleus pulposus cells. The stiffness of the hydrogels can be modulated by changing the concentration of the polyethylene glycol-laminin conjugate. This study supports the idea that manipulating different features in the design of the material provides an optimal scaffold/carrier that can be used in tissue regeneration.

In other tissue regeneration applications, chemical surface modification is used to manipulate cell differentiation. Adhesion peptides such as fibronectin and laminin and neurotrophic factors were immobilized on polymer substrates to evaluate the differentiation of neural stem cells [46]. The modified surface was characterized by AFM and SEM to look at morphology and roughness. Wettability was evaluated by water contact angle measurement. Immobilized surfaces were more hydrophilic with enhanced neuronal differentiation. On the other hand, changing the composition of the extracellular matrix components has

an influence on differentiation of neural stem cells into specific types of neurons. Our group has demonstrated the ability to differentiate enteric neural progenitor cells into specific types of neurons using different combination of extracellular matrix components [47]. The composition of the substrates modulated the extent of neuronal and glial differentiation. A higher neuronal population was observed when enteric neural progenitor cells were seeded onto composite mixtures (Collagen IV, laminin and heparan sulfate) than glial population.

Growth factor delivery is also a technique used for tissue regeneration. Delivery can be done by incorporating growth factors onto scaffolds or through carriers. However, when using carriers as means for delivery, it is critical to take into account the release kinetics of the growth factor. The activity of the growth factor must be timely controlled as well as spatially controlled. Recently, Simson et. al. have mixed chondroitin sulfate-bone marrow adhesive hydrogel with bone morphogenetic-2 protein as an attempt to regenerate cartilage tissue [48]. The carrier allowed the chondrocytes to maintain their phenotype and to produce sulfated glycosaminoglycans. The efficacy of this system is demonstrated by the retention and activity of the growth factor during the experiment and by the adhesive properties of chondroitin sulfate. A challenge that the authors have brought up to their system is the stability of the carriers, which is a pre-requisite for translational purposes.

## **Cell viability in the scaffold: Design process**

The long term success of implanted scaffolds is dependent on the delivery of an adequate number of viable and functional cells required to repair damaged

tissues. As the scaffolds or the grafts get bigger, the hypoxic regions within the scaffolds limit the performance of the cells to support regeneration. Nutrients, and most critically oxygen, need to be made available for cells post-transplantation. Recently, Wang et. al. developed oxygen-enriched scaffolds to enhance cell survival and function following implantation [49].

A major challenge in tissue engineering application is the limited diffusion ability of oxygen in the scaffold. Scaffolds design must ensure that cells have access to nutrients until neo-vascularization occurs. Uneven distribution of cells is associated with different oxygen distribution in the scaffolds. Improved expression of markers, enhanced cell functions and maintenance of cell phenotypes are the result of uniform distribution of viable cells in the scaffolds.

Mathematical models were developed to predict the oxygen gradients within engineered scaffolds taking into account scaffold dimensions and cell function[50-53]. These models can be used to organize design criteria. Studies have shown that high cellular viability correlates with higher oxygen concentration within the scaffolds. Cells at the surface of the scaffolds exhibited better viability than cells deeper in the scaffold, and this is attributed to the limited diffusivity of oxygen [54].

Diffusion-reaction models based on diffusive oxygen transport are commonly applied to correlate the distribution of oxygen within a construct cultured to the distribution of cell density and viability. These models assume that there is no convective flux within the scaffold, the oxygen diffusion coefficient is constant

and that there is homogenous distribution of cells in the scaffold. The change in oxygen concentration is described by the balance of oxygen diffusion through the scaffold and the rate of oxygen consumption by the cells. Oxygen is considered to be consumed by the cells according to the Michaelis-Menten kinetics. Defining boundary conditions, oxygen profile within the scaffold can be modeled and correlated with cell viability. Scaffolds placed in static conditions behaved differently from scaffolds exposed to flow. The profile of oxygen concentration in static conditions showed a linear decrease as a function of depth. However, flow conditions improved the oxygen concentration in the scaffold [54].

These models can become more complicated when different factors are accounted for in the design of the scaffolds. In addition to oxygen, availability of other nutrients can be also modeled. Deviations may occur during long term culture due to the remodeling of the scaffold by ECM deposition by the cells [55]. Therefore, changes in nutrient diffusivities are additional factors that must be taken in account in these models.

## **Closing remarks:**

Despite the advances in technologies and techniques used in tissue engineering and regenerative medicine, there are more questions that need to be answered. Design of scaffolds is an essential feature in regenerative medicine. It dictates cell behavior and function. Physical and chemical modifications exist to enhance the bioactivity of the scaffolds. Although different designs have proven to be

beneficial, further optimization is needed. It is critical that cells maintain their phenotypic characteristics when seeded on the scaffold. Maximum cell viability is also crucial for long term success of the implant. Additionally, design of the scaffold affects tissue remodeling and performance after implantation. Vascularization is another challenging task that must be taken into consideration in tissue regeneration. Several studies are currently being conducted to precondition tissues prior to their implantation in order to maximize vascularization. The field of regenerative medicine is still in its early stages of emergence where there is still room for optimization.

## **Acknowledgements:**

This work was supported by NIH RO1 DK 071614. Authors disclose no conflict of interests.

## References:

1. Wagner, W., et al., *Comparative characteristics of mesenchymal stem cells from human bone marrow, adipose tissue, and umbilical cord blood*. Exp Hematol, 2005. **33**(11): p. 1402-16.
2. Alves da Silva, M.L., et al., *Chondrogenic differentiation of human bone marrow mesenchymal stem cells in chitosan-based scaffolds using a flow-perfusion bioreactor*. J Tissue Eng Regen Med, 2011. **5**(9): p. 722-32.
3. Tian, H., et al., *Myogenic differentiation of human bone marrow mesenchymal stem cells on a 3D nano fibrous scaffold for bladder tissue engineering*. Biomaterials, 2010. **31**(5): p. 870-7.
4. Izal, I., et al., *Culture of human bone marrow-derived mesenchymal stem cells on of poly(L-lactic acid) scaffolds: potential application for the tissue engineering of cartilage*. Knee Surg Sports Traumatol Arthrosc, 2013. **21**(8): p. 1737-50.
5. Katz, A.J., et al., *Cell surface and transcriptional characterization of human adipose-derived adherent stromal (hADAS) cells*. Stem Cells, 2005. **23**(3): p. 412-23.
6. Anghileri, E., et al., *Neuronal differentiation potential of human adipose-derived mesenchymal stem cells*. Stem Cells Dev, 2008. **17**(5): p. 909-16.
7. Sterodimas, A., et al., *Tissue engineering with adipose-derived stem cells (ADSCs): current and future applications*. J Plast Reconstr Aesthet Surg, 2010. **63**(11): p. 1886-92.
8. Sowa, Y., et al., *Adipose-derived stem cells produce factors enhancing peripheral nerve regeneration: influence of age and anatomic site of origin*. Stem Cells Dev, 2012. **21**(11): p. 1852-62.

9. Kingham, P.J., et al., *Adipose-derived stem cells differentiate into a Schwann cell phenotype and promote neurite outgrowth in vitro*. *Experimental neurology*, 2007. **207**(2): p. 267-274.
10. Surbek, D.V., et al., *Quantitative immunophenotypic characterization, cryopreservation, and enrichment of second- and third-trimester human fetal cord blood hematopoietic stem cells (progenitor cells)*. *Am J Obstet Gynecol*, 1998. **179**(5): p. 1228-33.
11. Liu, J., et al., *Human umbilical cord stem cell encapsulation in novel macroporous and injectable fibrin for muscle tissue engineering*. *Acta Biomater*, 2013. **9**(1): p. 4688-97.
12. Thein-Han, W. and H.H. Xu, *Collagen-calcium phosphate cement scaffolds seeded with umbilical cord stem cells for bone tissue engineering*. *Tissue Eng Part A*, 2011. **17**(23-24): p. 2943-54.
13. Murphy, S.V. and A. Atala, *Amniotic fluid and placental membranes: unexpected sources of highly multipotent cells*. *Semin Reprod Med*, 2013. **31**(1): p. 62-8.
14. Semenov, O.V., et al., *Multipotent mesenchymal stem cells from human placenta: critical parameters for isolation and maintenance of stemness after isolation*. *Am J Obstet Gynecol*, 2010. **202**(2): p. 193 e1-193 e13.
15. Li, C., et al., *Human-placenta-derived mesenchymal stem cells inhibit proliferation and function of allogeneic immune cells*. *Cell Tissue Res*, 2007. **330**(3): p. 437-46.
16. Parolini, O., et al., *Toward cell therapy using placenta-derived cells: disease mechanisms, cell biology, preclinical studies, and regulatory aspects at the round table*. *Stem Cells Dev*, 2010. **19**(2): p. 143-54.

17. Hsu, S.H., et al., *Chondrogenesis from human placenta-derived mesenchymal stem cells in three-dimensional scaffolds for cartilage tissue engineering*. Tissue Eng Part A, 2011. **17**(11-12): p. 1549-60.
18. Zhang, D., et al., *Osteogenic differentiation of human placenta-derived mesenchymal stem cells (PMSCs) on electrospun nanofiber meshes*. Cytotechnology, 2012. **64**(6): p. 701-10.
19. Jiang, R., et al., *Transplantation of placenta-derived mesenchymal stem cells in type 2 diabetes: a pilot study*. Front Med, 2011. **5**(1): p. 94-100.
20. Del Gaudio, C., et al., *Are synthetic scaffolds suitable for the development of clinical tissue-engineered tubular organs?* J Biomed Mater Res A, 2013.
21. Bitar, K.N. and E. Zakhem, *Tissue engineering and regenerative medicine as applied to the gastrointestinal tract*. Curr Opin Biotechnol, 2013. **24**(5): p. 909-15.
22. Fielding, G.A., A. Bandyopadhyay, and S. Bose, *Effects of silica and zinc oxide doping on mechanical and biological properties of 3D printed tricalcium phosphate tissue engineering scaffolds*. Dental Materials, 2012. **28**(2): p. 113-122.
23. Ovsianikov, A., et al., *Laser fabrication of three-dimensional CAD scaffolds from photosensitive gelatin for applications in tissue engineering*. Biomacromolecules, 2011. **12**(4): p. 851-8.
24. Gauvin, R., et al., *Microfabrication of complex porous tissue engineering scaffolds using 3D projection stereolithography*. Biomaterials, 2012. **33**(15): p. 3824-34.
25. Somara, S., et al., *Bioengineered internal anal sphincter derived from isolated human internal anal sphincter smooth muscle cells*. Gastroenterology, 2009. **137**(1): p. 53-61.
26. Hecker, L., et al., *Development of a three-dimensional physiological model of the internal anal sphincter bioengineered in vitro from isolated smooth muscle cells*. Am J Physiol Gastrointest Liver Physiol, 2005. **289**(2): p. G188-96.



27. Raghavan, S., et al., *Successful implantation of bioengineered, intrinsically innervated, human internal anal sphincter*. Gastroenterology, 2011. **141**(1): p. 310-9.
28. Gilmont, R.R., et al., *Bioengineering of Physiologically Functional Intrinsically Innervated Human Internal Anal Sphincter Constructs*. Tissue Eng Part A, 2014.
29. Adebayo, O., et al., *Self-assembled smooth muscle cell tissue rings exhibit greater tensile strength than cell-seeded fibrin or collagen gel rings*. J Biomed Mater Res A, 2013. **101**(2): p. 428-37.
30. Gwyther, T.A., et al., *Directed cellular self-assembly to fabricate cell-derived tissue rings for biomechanical analysis and tissue engineering*. J Vis Exp, 2011(57): p. e3366.
31. Gwyther, T.A., et al., *Engineered vascular tissue fabricated from aggregated smooth muscle cells*. Cells Tissues Organs, 2011. **194**(1): p. 13-24.
32. Ju, Y.M., et al., *Bilayered scaffold for engineering cellularized blood vessels*. Biomaterials, 2010. **31**(15): p. 4313-21.
33. Lee, S.J., et al., *Development of a composite vascular scaffolding system that withstands physiological vascular conditions*. Biomaterials, 2008. **29**(19): p. 2891-8.
34. Takahashi, H., et al., *The use of anisotropic cell sheets to control orientation during the self-organization of 3D muscle tissue*. Biomaterials, 2013. **34**(30): p. 7372-80.
35. Raghavan, S., et al., *Bioengineered three-dimensional physiological model of colonic longitudinal smooth muscle in vitro*. Tissue Eng Part C Methods, 2010. **16**(5): p. 999-1009.
36. Zakhem, E., et al., *Chitosan-based scaffolds for the support of smooth muscle constructs in intestinal tissue engineering*. Biomaterials, 2012. **33**(19): p. 4810-7.
37. Zakhem, E., S. Raghavan, and K.N. Bitar, *Neo-innervation of a bioengineered intestinal smooth muscle construct around chitosan scaffold*. Biomaterials, 2014. **35**(6): p. 1882-9.

38. Albanna, M.Z., et al., *Improving the mechanical properties of chitosan-based heart valve scaffolds using chitosan fibers*. J Mech Behav Biomed Mater, 2012. **5**(1): p. 171-80.
39. Albanna, M.Z., et al., *Chitosan fibers with improved biological and mechanical properties for tissue engineering applications*. J Mech Behav Biomed Mater, 2013. **20**: p. 217-26.
40. Du, F., et al., *Gradient nanofibrous chitosan/poly varepsilon-caprolactone scaffolds as extracellular microenvironments for vascular tissue engineering*. Biomaterials, 2012. **33**(3): p. 762-70.
41. Thomson, K.S., et al., *Prevascularized microtemplated fibrin scaffolds for cardiac tissue engineering applications*. Tissue Eng Part A, 2013. **19**(7-8): p. 967-77.
42. Cheng, Q., et al., *Plasma surface chemical treatment of electrospun poly(L-lactide) microfibrous scaffolds for enhanced cell adhesion, growth, and infiltration*. Tissue Eng Part A, 2013. **19**(9-10): p. 1188-98.
43. Declercq, H.A., et al., *Synergistic effect of surface modification and scaffold design of bioplotting 3-D poly-epsilon-caprolactone scaffolds in osteogenic tissue engineering*. Acta Biomater, 2013. **9**(8): p. 7699-708.
44. Ravichandran, R., et al., *Composite poly-L-lactic acid/poly-(alpha,beta)-DL-aspartic acid/collagen nanofibrous scaffolds for dermal tissue regeneration*. Mater Sci Eng C Mater Biol Appl, 2012. **32**(6): p. 1443-51.
45. Francisco, A.T., et al., *Injectable laminin-functionalized hydrogel for nucleus pulposus regeneration*. Biomaterials, 2013. **34**(30): p. 7381-8.
46. Yang, K., et al., *Polydopamine-mediated surface modification of scaffold materials for human neural stem cell engineering*. Biomaterials, 2012. **33**(29): p. 6952-64.

47. Raghavan, S., R.R. Gilmont, and K.N. Bitar, *Neuroglial differentiation of adult enteric neuronal progenitor cells as a function of extracellular matrix composition*. Biomaterials, 2013. **34**(28): p. 6649-58.
48. Simson, J.A., et al., *An adhesive bone marrow scaffold and bone morphogenetic-2 protein carrier for cartilage tissue engineering*. Biomacromolecules, 2013. **14**(3): p. 637-43.
49. Wang, Y., et al., *A synthetic oxygen carrier in fibrin matrices promotes sciatic nerve regeneration in rats*. Acta Biomater, 2013. **9**(7): p. 7248-63.
50. Zhou, S., Z. Cui, and J.P. Urban, *Nutrient gradients in engineered cartilage: metabolic kinetics measurement and mass transfer modeling*. Biotechnol Bioeng, 2008. **101**(2): p. 408-21.
51. Rutkowski, G.E. and C.A. Heath, *Development of a bioartificial nerve graft. I. Design based on a reaction-diffusion model*. Biotechnol Prog, 2002. **18**(2): p. 362-72.
52. Malda, J., et al., *Oxygen gradients in tissue-engineered PEGT/PBT cartilaginous constructs: measurement and modeling*. Biotechnol Bioeng, 2004. **86**(1): p. 9-18.
53. Stabler, C., et al. *Modeling and in vitro and in vivo characterization of a tissue engineered pancreatic substitute*. in *Data Mining, Systems Analysis and Optimization in Biomedicine*. 2007. American Institute of Physics.
54. Radisic, M., et al., *Oxygen gradients correlate with cell density and cell viability in engineered cardiac tissue*. Biotechnol Bioeng, 2006. **93**(2): p. 332-43.
55. Obradovic, B., et al., *Glycosaminoglycan deposition in engineered cartilage: experiments and mathematical model*. AIChE Journal, 2000. **46**(9): p. 1860-1871.

# **CHAPTER III: TISSUE ENGINEERING AND REGENERATIVE MEDICINE: GASTROINTESTINAL APPLICATION**

Elie Zakhem<sup>1,2</sup> and Khalil N. Bitar<sup>1,2,3</sup>

<sup>1</sup>Wake Forest Institute for Regenerative Medicine, Wake Forest School of  
Medicine, Winston-Salem NC 27101

<sup>3</sup>Department of Molecular Medicine and Translational Sciences, Wake Forest  
School of Medicine, Winston Salem, NC 27101

<sup>3</sup>Virginia Tech-Wake Forest School of Biomedical Engineering and Sciences,  
Winston-Salem NC 27101

***This chapter describes the recent advances and current concept in  
bioengineering the gastrointestinal tract.***

***This manuscript was accepted for publication as Chapter 5, in Translating  
Regenerative Medicine to the Clinic, Elsevier 2015.***

## **Abstract:**

The gastrointestinal (GI) tract is susceptible to multiple neurodegenerative diseases that can result in motility disorders. Current surgical treatments are associated with limited outcomes and high rates of morbidity. The GI tract consists of multiple cell types arranged in a specific alignment and location. Tissue engineering and regenerative medicine provide an alternative approach by taking into account the different layers of the tract. Finding a cell source is a major challenge with the autologous source remaining the ideal one. Apart from the cell source, different biomaterials are available for scaffolds fabrication. This unique combination of cells and scaffolds dictates the biocompatibility of the scaffold, cell attachment and survival, maintenance of cell phenotype and mechanical properties of the scaffolds. All these factors are critical for successful regeneration outcomes. In this chapter, we will focus on the recent advances in the regeneration of different parts of the GI tract.

## **The gastrointestinal tract: Overview**

The gastrointestinal tract (GI) is a continuous tubular system that extends from the mouth to the anus. The GI tract exhibits diverse motility patterns that aid in performing a variety of functions including ingestion, digestion, absorption of nutritive elements and excretion of waste. The organs that make up the GI tract are not limited to, but include: mouth, esophagus, stomach, small intestine and large intestine. The food enters through the mouth where it gets ingested, chemically and mechanically. The food bolus then passes into the esophagus, where alternating contractions and relaxations, a process defined as peristalsis, initiate to help propelling the food down to the stomach. Additional peristaltic pattern in the stomach coordinate digestion and propulsion of the food into the small intestine. The food is then transferred into the large intestine and any waste products are excreted from the body. Digested materials are absorbed into the blood through the epithelium. Waste substances get excreted from the body through the anus. Discontinuity exists along the tract between the different organs. The discontinuities serve as checkpoints to ensure unidirectional flow of the food down the tract.

Coordinated chemical and electrical interactions exist between smooth muscle, intramural innervation, interstitial cells and mucosal epithelial layers. Those interactions are essential for proper GI motility. The inability of the GI tract to perform its function due to malformations or defects along the GI tract may lead to surgical resection which could cause loss of functionality. Surgical

intervention serves as a short-term cure to many of the diseases. Major drawbacks of surgical resections are classified into psychological, economic and social distress (1-6). Currently, tissue engineering provides a promising field that can offer treatment for most parts of the GI tract. The goal is to obtain a biopsy from the patient for cell isolation and expansion *in vitro*. The cells are then seeded onto biodegradable, bioactive polymer scaffolds. The result is an engineered autologous tissue that can be implanted back into the same patient to regenerate a defective segment of the GI tract. The GI is composed of multiple cell layers including smooth muscle, enteric neurons, interstitial cells of Cajal (ICCs), epithelial cells, and skeletal muscle which populate one third of the esophagus. This innate anatomical and physiological complexity dictates the requirement for a multi-disciplinary approach to regeneration of functional tissue replacements. The main challenge lies in the ability to recapitulate the architecture and function of different components of the GI tract.

Engineered scaffolds are designed to recreate the anatomic complexity of the micro-environments associated with the native tissue. Design strategies for scaffolds include physical as well as chemical modifications (7). After the design and manufacturing process, scaffolds are characterized by their porosities and stiffness. Cell-seeded scaffolds help the process of remodeling post-implantation and result in a functional final bioengineered product. The primary goal of tissue engineering is to be able to develop physiologically functional replacement tissues that have similar architecture and composition as the native tissue. Pre-conditioning the engineered tissues using bioreactors or mechanical cycling is

one way of inducing maturation to the tissue prior to implantation. The goal is to obtain a functional engineered replacement while maintaining its integrity. Although the GI tract is a hollow tubular organ, it requires sophisticated design processes in order to generate functional replacements.

This chapter will focus on the main steps in engineering the neuro-musculature of the GI tract. These steps are considered as the basic requirements for successful outcomes. An overview on the regeneration of the esophagus, stomach, small intestine and colon including the sphincters will be discussed in this chapter.

In the last couple decades, tissue engineering evolved quickly with the aim of reconstructing functional tissues and organs. Regenerative medicine approaches seek the reconstruction of tissues using cells and scaffolds.

## **Neurodegenerative diseases of the GI tract**

The integrity of the neuronal circuitry in the GI tract is essential for coordination of cell function. Loss or defects of neuronal integrity leads to diseases related to motility and secretion. The smooth muscle is the basic musculature unit in the gastrointestinal tract that is responsible for contraction and relaxation. The smooth muscle receives regulatory signals from different levels including the enteric nervous system and ICCs (8). The enteric nervous system is arranged into 2 ganglionated plexi. The myenteric plexus exists between the 2 muscle layers and contains excitatory and inhibitory motor



neurons. Neurons secrete neurotransmitters responsible for neural transmission to the smooth muscle. The submucosal plexus is located between the circular muscle layer and the submucosa. Neuro-neuronal transmission is mediated by ascending and descending interneurons. Neural dysfunction affects different parts of the GI tract and result in diseases that alter motility.

The inability of the sphincters to relax due to loss of inhibitory motor neurons, more specifically the nitrergic neurons is a condition known as achalasia. The lower esophageal sphincter (LES) mediates the transport of food from the esophagus into the stomach. Esophageal achalasia is a neurodegenerative condition where the LES fails to relax. This condition is characterized by the absence of nitrergic neurons, however the excitatory cholinergic neurons are intact (9, 10). Absence of nitrergic neurons and presence of cholinergic neurons result in tonic contraction of the sphincter. Similarly, achalasia of the internal anal sphincter (IAS) is another form of neuropathies of the GI tract. In normal conditions, the distention of the rectum by luminal content induces rectoanal inhibitory reflexes (RAIR) that allow the relaxation of the IAS. This is followed by excretion of rectal luminal content. In achalasia, RAIR is lost due to the loss of nitrergic neurons. Achalasia is characterized by the absence of nitrergic neurons (11). Both forms of achalasia can be diagnosed by manometric pressure measurement. Loss of intrinsic inhibitory innervation to the pyloric sphincter leads to pyloric stenosis, which is associated with gastric obstruction and altered gastric emptying. Current treatments for sphincteric achalasia include

injection of botulinum toxin in order to reduce the tonic contraction and thus facilitating the relaxation of the sphincter (12, 13).

Intestinal pseudo-obstruction is another form of neurodegenerative diseases resulting from loss of intrinsic innervation. This disease is characterized by altered motility in the GI tract (14). Pharmacological treatments are considered as the most effective way of relieving the symptoms and restoring intestinal motility (15). Surgical correction does not provide long term satisfactory outcomes (16).

Hirschsprung's disease is another well characterized enteric neuropathy. It is characterized by either partial or total loss of enteric neurons in the gut. Areas of aganglionosis lack intrinsic inhibitory motor neurons and are dominated by the excitatory motor neurons. Aganglionated lengths are tonically contracted which leads to obstruction of the gut (17). The most common and effective surgery involves a pull-through. Although the surgery is helpful, it often causes disruption of the anal sphincter and loss of innervation of the rectum. Patients with pull through surgeries suffer from fecal incontinence (18).

Given the limited success of surgical intervention, there is an urgent need for functional replacements of the GI tract. Tissue engineering and regenerative medicine provide a therapeutic option for diseases that affect the GI tract. The concept of tissue engineering is to recapitulate the architecture and function of the tissue using the patient's own cells in combination with a scaffolding biomaterial. In the next sections of this chapter, we will discuss the different

sources of cells and materials used in tissue engineering. The last section will also discuss the recent advances in tissue engineering of different regions of the GI tract.

## **Cell source in regenerating the neuro-musculature of the GI tract**

Cell source is an essential component in the design of bioengineering tissues/organs. The ability to find an appropriate cell source using minimally invasive surgeries has been recently the focus of research. This becomes more challenging when the organ is complex in its cellular composition, such as the GI tract. Ideally, biopsies obtained from patients are used to isolate the type of cells that is needed. It is critical to be able to culture the cells, expand them in vitro to obtain adequate number for reseeding. Depending on the tissue source and the type of cell needed, expansion might be problematic. Another challenge resides in the fact that some tissues, in their diseased state, do not provide a good source of cells. Finding other sources for biopsies might become an alternative approach. In the case of regenerating the GI tract, finding an efficient source of highly proliferative cells is a major limitation and is the focus of on-going research. Stem cells derived from different parts of the body are being investigated to overcome the concern of cell source. Mesenchymal stem cells (from different sources), induced pluripotent stem cells and organoid units are all examples of potential cell sources in tissue engineering (19-23).

Tissue-specific cells obtained from biopsies are usually considered as the ideal source given the fact that they have a determined physiological function. Tissue-specific smooth muscle cells have the contractile properties when cultured and used in the regeneration process. Smooth muscle cells can be isolated from gut segments using well established enzymatic digestion protocols. The cells have the potential to be expanded and passaged in vitro. A major concern with tissue-specific cells is their ability to maintain their phenotype after isolation and expansion, and following their implantation (24, 25). Muscle derived-stem cells have the advantage of self-renewal and multi-lineage differentiation where they have been shown to differentiate into myotubes as well as smooth muscle (26-28).

The GI tract is known to have its own nervous system which is referred to as the enteric nervous system (ENS). The ENS is considered as the intrinsic innervation of the GI tract and it is a major player in the regulatory apparatus that controls the smooth muscle function. Neural stem cells derived from both the central nervous system and the enteric nervous system are sources for neurons (29). Well established protocols have been developed to isolate enteric neural stem cells from embryonic, fetal, post-natal and adult rodent as well as human gut tissue (30-36). Enteric neural stem cells reinstated the innervation of denervated colon (37). Enteric neural stem cells have the potential to migrate, proliferate and differentiate into different subtypes of motor neurons (38-41). Additionally, neural stem cells isolated from the central nervous system have the

potential to differentiate into enteric-like neurons and treat gastrointestinal disorders (35, 42-46).

## **Scaffolds as support for neuro-musculature regeneration**

The GI tract is a hollow tubular organ that extends from the esophagus down to the rectum. Natural and/or synthetic biomaterials can be used to develop tubular scaffolds to mimic the GI tract. Biomaterials are tested for their ability to support cell attachment, survival, proliferation and differentiation. While designing scaffolds for tissue engineering applications, it is essential to characterize the scaffolds in terms of biocompatibility, porosity and pore sizes, mechanical properties and biodegradability (7, 47). Determining all these characteristics of scaffolds will help in modulating the interaction of the cells with the scaffold including cell attachment, alignment, and maintenance of phenotype. Taken all together, these elements are key for successful outcomes of the implant. A major hurdle in GI tissue engineering is the failure of the scaffold to support cell alignment (48). A wide spectrum of natural and synthetic biomaterials is under investigation for the support of GI tissue engineering.

### ***Natural materials***

The most common natural material is collagen. It is the most abundant and major component of the extracellular matrix. Collagen scaffolds were developed

as support in GI tissue engineering. Collagen was tested using smooth muscle cells (49-52). In addition to collagen scaffolds, collagen was used as a coating material to favor the regeneration process (53). Studies have already demonstrated the excellent biocompatibility of collagen by supporting cell attachment and differentiation. Some of the weaknesses of using collagen as a scaffold are the low mechanical properties and its inability to support the native architecture of the tissue. Another common natural material is chitosan (54). Chitosan is widely used natural polymer in tissue engineering and it has gained special attention due to its biocompatibility. Chitosan has been tested in several applications including skin and bone tissue engineering. Our group demonstrated the biocompatibility of chitosan in GI applications (55). Smooth muscle cells derived from the gut demonstrated attachment, proliferation and maintenance of phenotype in vitro. Fibrin is another natural biomaterial used in GI tissue engineering. Circular smooth muscle tissue constructs were engineered using fibrin gel (56). The smooth muscle cells demonstrated concentric alignment similar to the orientation of circular smooth muscle cells seen in native gut. Our group developed hollow tubular chitosan scaffolds for intestinal tissue engineering applications. Characterization of the scaffolds demonstrated high porosity. Engineered smooth muscle tissues maintained functionality around the tubular chitosan scaffolds. In order to obtain a scaffold that closely mimics the native tissue, physical and chemical modifications have been employed. Unidirectional porous structures were formed on OptiMaix collagen scaffolds (57). The scaffolds were designed to allow unidirectional smooth muscle growth.

Longitudinal smooth muscle tissues were engineered using substrate microtopography (58). The tissues contracted and relaxed in a similar manner to native longitudinal smooth muscle layer. On the other hand, decellularization protocols have been well documented to remove cellular component of the tissue while preserving the native architecture (59). The decellularized tissue is then reseeded with the appropriate cell types. The maintenance of architecture in the decellularized tissue guides the cells to orient themselves along the grooves.

### *Synthetic materials*

Apart from natural materials, synthetic materials are potential candidates for GI tissue engineering applications. Synthetic materials display strong biocompatibility and biodegradability properties. Synthetic materials lack binding domains, which makes them suitable for modifications (60). Electrospun poly(L-lactide-co-caprolactone) (PLLC) scaffolds were immobilized with fibronectin as an attempt to enhance cell attachment (61). Polyglycolic acid (PGA) scaffolds are also synthetic scaffolds that were coated with collagen to enhance the cell seeding process (53, 62).

## **Tissue engineering of different parts of the GI tract: current concepts**

The GI tract has multiple complex functions that include transporting and digesting food, absorbing nutrients and excreting waste. These functions are the

result of coordinated interactions by the different cell types that make up the GI tract. Different layers of the GI tract consist of different cell types, arranged in a specific alignment. Smooth muscle cells are considered as the main effectors of motility, performing contraction and relaxation to propel luminal content. The outer smooth muscle layer or also known as the longitudinal smooth muscle is responsible for shortening the length of the intestine when contracted. The contraction of the inner circular smooth muscle layer is responsible for narrowing the lumen of the intestine. A primary regulator of the function of smooth muscle is the ENS which contains neurons (sensory, motor, secretory, etc.) and glia (63). Regulation of function is also provided by the interstitial cells of Cajal, which have pacemaker activity within the gut (64). Unidirectional flow of luminal content is ensured by sphincters along the GI tract. Intestinal epithelial cells mediate absorption and secretion within the gut.

Post-natal diseases, damages, injuries, surgical or obstetric trauma, and age are causes of motility disorders. Additionally, motility can be altered due to congenital defects such as Hirschsprung's disease, intestinal pseudoobstruction and achalasia (65). Surgical intervention does not provide a long-lasting solution. Tissue engineering provides an approach to regenerate different parts of the GI tract using a combination of cells and scaffolds (66, 67).



### *Esophagus:*

The esophagus is a muscular tubular organ that extends from the pharynx to the stomach. A series of peristaltic waves mediate the transport of food bolus into the stomach through the lower esophageal sphincter (LES). Diseases affecting the esophagus such as esophageal atresia and tracheoesophageal fistula result in esophageal stricture and gastroesophageal reflux disease (GERD), which lead to impaired motility (68). Esophageal cancer is one the most leading causes of deaths. Patients with esophageal cancer have low quality of life. Any engineered esophagus must take into consideration the gravitational characteristic and the coordinated rhythmic activity of the tissue itself.

The basic requirements for a successful engineered esophagus include the following properties. First, the engineered esophagus must be a tubular structure with luminal patency. Second, all types of cells that make up the esophagus must be taken into account. The cells include epithelial cells along the lumen, the muscle component (striated muscle and smooth muscle). Intrinsic and extrinsic neural pathways are responsible for swallowing and for peristalsis. Third, analysis of the basement membrane of the esophagus is a pre-requisite for designing scaffolds in tissue engineering (69). The basement membrane composition of the esophagus dictates cell growth and differentiation. Defects or loss of function of any of the mentioned cell types will impair the process of motility.

The regeneration of the esophageal tissue has been studied using different natural-based scaffolds. OptiMaix collagen scaffolds with unidirectional

porous structures were seeded with smooth muscle. This resulted in successful alignment of regenerated smooth muscle (57). Removal of the cells from specific tissues using different detergents results in a matrix that lacks cells but maintains the native architecture of the tissue. This process of decellularization allows the reseeded of the tissue with healthy functional cells. A wide range of organs were decellularized and tested for their potential to regenerate esophageal tissue. These organs include the esophagus, urinary bladder, stomach and small intestinal submucosa. Studies have shown that decellularized ovine esophagi exhibited rough surfaces with preservation of the extracellular matrix component. Reseeding these matrices with specific cells can be one approach to regenerate the esophagus (70).

Porcine urinary bladders were also decellularized and resulted in matrices suitable for implantation in dog models. Results demonstrated the potential of using these tissues to reconstruct the esophagus. The mechanical properties of the regenerated tissue were similar to native esophagus. Additionally, histological analysis demonstrated the presence of organized layers that constitute the esophagus (71). Small intestine submucosa (SIS) was seeded with bone marrow-derived mesenchymal stem cells (BMSCs). The seeded SIS was used as autologous replacement in dogs. Results have shown re-epithelization, re-vascularization and muscle regeneration (72).

First attempts to reconstruct the esophagus using synthetic materials have tested nitinol and silicon rubber. These approaches were associated with complications such as anastomosis and shedding problems. Further

modifications of the model by adding polyester connecting rings reduced the risk of anastomotic leakage and improved the shedding time (73). Another synthetic material polycaprolactone (PCL) was used as a matrix to support esophageal epithelial cells. PCL was coupled to type IV collagen in order to accelerate the regeneration process, cell spreading and cell-cell interaction. The epithelial phenotype of the cells was confirmed via histological analysis (60).

Synthetic materials often require chemical modifications in order to enhance the performance of the cells. Epithelial cells adhesion and growth on electrospun poly(L-lactide-co-caprolactone) (PLLC) scaffolds was improved by fibronectin immobilization. Cells demonstrated morphological characteristics of epithelium with maintenance of function (61). Adipose-derived smooth muscle cells seeded onto PGA/PLGA scaffolds were implanted in rat models. Results have shown re-epithelialization and muscularis regeneration (74).

### *Stomach*

The stomach is the site of food mixing through cycles of coordinated rhythmic contractile activities. The luminal content then leaves the stomach and goes into the small intestine through the pylorus sphincter. Several diseases alter gastric motility. Gastroparesis is characterized by delayed gastric emptying due to autonomic neuropathy (75, 76). Current solutions include gastric electrical stimulation (77, 78). Gastric electrical stimulation requires surgical intervention which is associated with infection, pain, and device relocation.

Gastric cancer is another cause of dysmotility. The main solution is surgical removal of part of the stomach. This is also associated with high rates of morbidities including malnutrition, anemia and weight loss. Tissue engineering remains a promising field to regenerate the stomach.

Organoid units seeded onto different scaffolds have been the most common approach for regenerating the stomach. Composite scaffolds composed of polyglycolic acid (PGA), poly-L-lactic acid and collagen have been tested using organoid units. Following their implantation, the organoid units resulted into differentiated epithelium as well as muscularis layer (53). One of the drawbacks was the lack of muscularis architecture, which is critical for proper function. Gastric patch was developed by seeding organoid units onto PGA scaffolds. A defect in the stomach was created and then replaced with engineered patch. Results have shown integration of the patch with the host tissue. Regeneration of the epithelium as well as the muscularis layer was also demonstrated by immunostaining (79). Although the organoid units have resulted in successful regeneration of the epithelium, the architecture and function of the regenerated muscle remains a challenge (80).

### *Small intestine:*

As the food gets processed in the stomach, it gets emptied into the small intestine. Nutrient absorption mainly takes place in the small intestine. The microvilli structures in the epithelium enhance nutrient absorption. The smooth muscle performs peristalsis to propel food through the intestine. Inflammation or cancer of the intestine requires massive truncation of regions of the intestine

which results in short bowel syndrome. Patients often suffer from malnutrition, malabsorption and motility dysfunction. Patients experience weight loss, vitamin deficiency and potential infections (2). The most common therapies include chronic parenteral nutrition and intestinal transplantation. High costs of transplantation, availability of donors and lifetime administration of immunosuppressive drugs are some of the limitations (1-3).

A main requirement for successful regeneration of the muscularis layer of the intestine is the exact recapitulation of the alignment of the native smooth muscle. Additionally, providing the innervation using neuronal cells is essential for smooth muscle function. Pacemaker cells, ICCs, also provide additional regulation for motility. A tissue engineered intestine must take into account the complexity of the native tissue.

Regeneration of the muscularis layer is a challenge in tissue engineering. This may be due to the fact that smooth muscle has a dynamic phenotype, switching between synthetic and contractile phenotype. Mesenchymal stem cells failed to regenerate the smooth muscle components (48). Recent studies reported successful differentiation of induced pluripotent stem cells (iPSCs) into smooth muscle sheets with peristaltic features (81). This characteristic is promising to tissue engineer physiologically functional intestine.

Organoid units have also been tested in regenerating the small intestine. Following implantation of scaffolds seeded with organoid units, evidence of muscle and neuronal regeneration was observed (82, 83). The architecture of the

muscularis layer was also regenerated. PGA scaffolds coated with PLLA and type I collagen were developed. Organoid units were seeded onto the scaffolds and were implanted into the omentum of mice. Organoid units generated the epithelium with villi structures. Regeneration of the smooth muscle layer was confirmed by positive stains for smooth muscle markers (84). The regenerated muscle lacked the native orientation.

Attempts to reconstruct the small intestine employed decellularized tissues. In one study, smooth muscle cells were derived from the intestine and seeded onto SIS sheets. Following implantation, the implant became vascularized. Partial epithelialization was documented. There was a variation in the expression of smooth muscle markers (85). Recently, a new decellularization protocol was developed using rat small bowel. The study had optimized the protocol in terms of number of cycles of detergents needed to completely remove all cellular components. The advantage of using decellularized matrices is the preservation of both the native architecture and the mechanical properties of the tissue (86).

### *Large intestine:*

The last part of the GI tract is the large intestine, where water absorption and waste excretion take place. In terms of cellular composition, the large intestine is considered as a continuation of the neuro-musculature layer of the small intestine. Several diseases can affect the large intestine and therefore cause dysmotility in the large intestine. Diseases include inflammation (Crohn's disease) and loss/lack of innervation (Hirschsprung's disease). This is associated

with either constipation or diarrhea. Engineered functional replacements must be available in order to restore motility.

Well established protocols have successfully isolated organoid units directly from the large intestine. Organoid units were seeded onto polymer scaffolds. Results have shown regeneration of the musculature with a similar architecture to the native large intestine (83). Those studies haven't evaluated peristalsis in the engineered large intestine. Another approach to regenerate the innervation of the large intestine involved the use of neural crest progenitor cells. The large intestines of rats were denervated using benzalkonium chloride (87). Neural progenitor cells were delivered to the site of denervation and differentiated into neurons and glia. Results have shown restoration of motility. Our group has successfully regenerated the neuro-musculature of the GI tract using a combination of cells and biomaterials. We developed techniques to engineer the circular and longitudinal smooth muscle layers with the appropriate alignment. We were also successful in innervating the engineered smooth muscle using primary isolated neural progenitor cells derived from the gut. The engineered circular smooth muscle constructs maintained smooth muscle phenotype and contractile function around tubular chitosan scaffolds. We developed a novel approach to neo-innervate bioengineered smooth muscle constructs (**Figure 3:**). Our approach involved the use of scaffold as support for the constructs. Non-innervated smooth muscle constructs and innervated smooth muscle constructs were bioengineered. The constructs were placed next to each other around tubular chitosan scaffolds as shown in the figure. The initially

innervated constructs maintained neural differentiation and function. Neo-innervation of the abutting constructs around the scaffolds was demonstrated by immunohistochemistry and physiological functionality assays (55). Longitudinal smooth muscle layer was engineered using molds with longitudinal grooves (88, 89). The influence of the extracellular matrix composition on the differentiation of the neural progenitor cells in the engineered longitudinal smooth muscle tissue was studied. Changing the composition of the extracellular matrix modulated the extent of differentiation of neural progenitor cells into different neuronal subtypes.

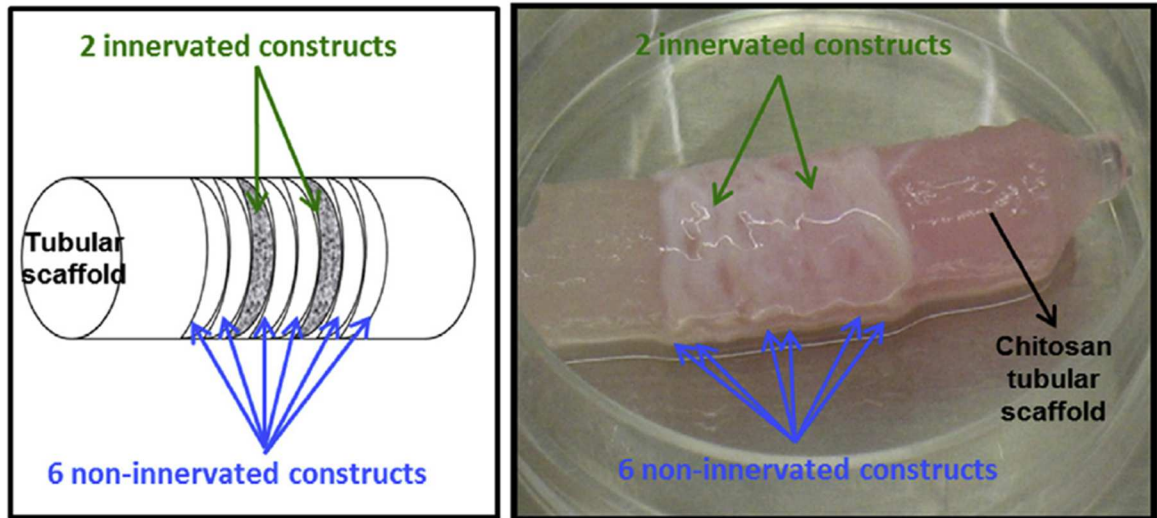


**Figure 3:** Schematic for neo-innervation concept in tissue engineering: Intrinsically innervated, concentrically aligned, smooth muscle constructs were bioengineered using smooth muscle cells and enteric neural progenitor cells (innervated constructs). Three dimensional smooth muscle constructs were bioengineered using smooth muscle cells only (noninnervated constructs). The bioengineered constructs were placed next to each other around tubular chitosan scaffolds as shown in the figure. After 14 days in culture in vitro, the noninnervated constructs became neo-innervated as demonstrated by immunohistochemistry and physiological functionality assays. The intrinsically innervated construct maintained neuronal differentiation.



Fecal incontinence is caused by the degeneration or loss of function of the internal anal sphincter (IAS) (90). This could be due to injury or aging. The sphincteric nature of the IAS smooth muscle is responsible of keeping the muscle in a constant contracture state until stimulated to relax. Current approaches involve the injection of silicone material or the use of mechanical devices (91, 92). However, these approaches fail to fully restore continence. We were successful in developing IAS constructs using primary isolated sphincteric smooth muscle and neural progenitor cells (56, 93). The engineered IAS constructs generated a spontaneous tone, which is a characteristic of native IAS. Following their implantation in situ in rodents, the engineered IAS constructs became neo-vascularized and maintained their myogenic and neurogenic phenotype and function (94, 95).

## **Conclusion**

Tissue engineering and regenerative medicine provide an alternative approach as potential therapy for disorders affecting the GI tract. Current treatments for dysmotility in the GI tract involve surgical intervention associated with high rates of complications and limited success. Ongoing research has demonstrated promising results in generating three-dimensional tissues using autologous cells. The ultimate goal of tissue engineering and regenerative medicine is to recapitulate the architecture and function of the native tissue. The GI tract is highly regulated. In a system as complex as the GI tract, it is important to keep in mind all the different cell types and the specific cell alignment in each

layer. Maintenance of cell phenotype is also critical for proper function. These characteristics are essential for peristalsis.

## **Acknowledgements**

*This work was supported by NIH/NIDDK R01DK071614.*

## **References**

1. Levitt MA, Dickie B, Pena A. Evaluation and treatment of the patient with Hirschsprung disease who is not doing well after a pull-through procedure. *Seminars in pediatric surgery*. 2010 May;19(2):146-53. PubMed PMID: 20307851.
2. Beyer-Berjot L, Joly F, Maggiori L, Corcos O, Bouhnik Y, Bretagnol F, et al. Segmental reversal of the small bowel can end permanent parenteral nutrition dependency: an experience of 38 adults with short bowel syndrome. *Annals of surgery*. 2012 Nov;256(5):739-45. PubMed PMID: 23095617.
3. Sampietro GM, Corsi F, Maconi G, Ardizzone S, Frontali A, Corona A, et al. Prospective study of long-term results and prognostic factors after conservative surgery for small bowel Crohn's disease. *Clinical gastroenterology and hepatology : the official clinical practice journal of the American Gastroenterological Association*. 2009 Feb;7(2):183-91; quiz 25. PubMed PMID: 19118641.
4. Braghetto I, Korn O, Valladares H, Debandi A, Diaz JC, Brunet L. Laparoscopic surgical treatment for patients with short- and long-segment Barrett's esophagus: which technique in which patient? *International surgery*. 2011 Apr-Jun;96(2):95-103. PubMed PMID: 22026298.
5. Songun I, Putter H, Kranenbarg EM, Sasako M, van de Velde CJ. Surgical treatment of gastric cancer: 15-year follow-up results of the randomised nationwide Dutch D1D2 trial. *The lancet oncology*. 2010 May;11(5):439-49. PubMed PMID: 20409751.

6. Prasad GA, Wu TT, Wigle DA, Buttar NS, Wongkeesong LM, Dunagan KT, et al. Endoscopic and surgical treatment of mucosal (T1a) esophageal adenocarcinoma in Barrett's esophagus. *Gastroenterology*. 2009 Sep;137(3):815-23. PubMed PMID: 19524578.
7. Bitar KN, Zakhem E. Design strategies of biodegradable scaffolds for tissue regeneration. *Biomedical engineering and computational biology*. 2014;6:13-20. PubMed PMID: 25288907. Pubmed Central PMCID: 4147780.
8. Hansen MB. The enteric nervous system I: organisation and classification. *Pharmacol Toxicol*. 2003 Mar;92(3):105-13. PubMed PMID: 12753424. Epub 2003/05/20. eng.
9. Holloway RH, Dodds WJ, Helm JF, Hogan WJ, Dent J, Arndorfer RC. Integrity of cholinergic innervation to the lower esophageal sphincter in achalasia. *Gastroenterology*. 1986 Apr;90(4):924-9. PubMed PMID: 3949120. Epub 1986/04/01. eng.
10. De Giorgio R, Di Simone MP, Stanghellini V, Barbara G, Tonini M, Salvioli B, et al. Esophageal and gastric nitric oxide synthesizing innervation in primary achalasia. *Am J Gastroenterol*. 1999 Sep;94(9):2357-62. PubMed PMID: 10483991. Epub 1999/09/14. eng.
11. Hirakawa H, Kobayashi H, O'Briain DS, Puri P. Absence of NADPH-diaphorase activity in internal anal sphincter (IAS) achalasia. *J Pediatr Gastroenterol Nutr*. 1995 Jan;20(1):54-8. PubMed PMID: 7533833. Epub 1995/01/01. eng.
12. Messineo A, Codrich D, Monai M, Martellossi S, Ventura A. The treatment of internal anal sphincter achalasia with botulinum toxin. *Pediatr Surg Int*. 2001 Sep;17(7):521-3. PubMed PMID: 11666049. Epub 2001/10/23. eng.
13. Annese V, Bassotti G, Coccia G, D'Onofrio V, Gatto G, Repici A, et al. Comparison of two different formulations of botulinum toxin A for the treatment of

- oesophageal achalasia. The Gismad Achalasia Study Group. *Aliment Pharmacol Ther.* 1999 Oct;13(10):1347-50. PubMed PMID: 10540051. Epub 1999/10/30. eng.
14. Antonucci A, Fronzoni L, Cogliandro L, Cogliandro RF, Caputo C, De Giorgio R, et al. Chronic intestinal pseudo-obstruction. *World J Gastroenterol.* 2008 May 21;14(19):2953-61. PubMed PMID: 18494042. Pubmed Central PMCID: 2712158. Epub 2008/05/22. eng.
15. Rudolph CD, Hyman PE, Altschuler SM, Christensen J, Colletti RB, Cucchiara S, et al. Diagnosis and treatment of chronic intestinal pseudo-obstruction in children: report of consensus workshop. *J Pediatr Gastroenterol Nutr.* 1997 Jan;24(1):102-12. PubMed PMID: 9093995. Epub 1997/01/01. eng.
16. Bitar KN, Raghavan S. Intestinal tissue engineering: current concepts and future vision of regenerative medicine in the gut. *Neurogastroenterol Motil.* 2012 Jan;24(1):7-19. PubMed PMID: 22188325. Pubmed Central PMCID: 3248673. Epub 2011/12/23. eng.
17. Arshad A, Powell C, Tighe MP. Hirschsprung's disease. *BMJ.* 2012;345:e5521. PubMed PMID: 23028095. Epub 2012/10/03. eng.
18. Catto-Smith AG, Coffey CM, Nolan TM, Hutson JM. Fecal incontinence after the surgical treatment of Hirschsprung disease. *J Pediatr.* 1995 Dec;127(6):954-7. PubMed PMID: 8523196. Epub 1995/12/01. eng.
19. Wang A, Tang Z, Park IH, Zhu Y, Patel S, Daley GQ, et al. Induced pluripotent stem cells for neural tissue engineering. *Biomaterials.* 2011 Aug;32(22):5023-32. PubMed PMID: 21514663. Pubmed Central PMCID: 3100451.
20. Rodrigues MT, Lee SJ, Gomes ME, Reis RL, Atala A, Yoo JJ. Amniotic Fluid-Derived Stem Cells as a Cell Source for Bone Tissue Engineering. *Tissue engineering Part A.* 2012 Aug 14. PubMed PMID: 22891759.

21. Williams C, Xie AW, Emani S, Yamato M, Okano T, Emani SM, et al. A comparison of human smooth muscle and mesenchymal stem cells as potential cell sources for tissue-engineered vascular patches. *Tissue engineering Part A*. 2012 May;18(9-10):986-98. PubMed PMID: 22145703.
22. Fuller MK, Faulk DM, Sundaram N, Shroyer NF, Henning SJ, Helmrath MA. Intestinal crypts reproducibly expand in culture. *The Journal of surgical research*. 2012 Nov;178(1):48-54. PubMed PMID: 22564827.
23. Wagner W, Wein F, Seckinger A, Frankhauser M, Wirkner U, Krause U, et al. Comparative characteristics of mesenchymal stem cells from human bone marrow, adipose tissue, and umbilical cord blood. *Experimental hematology*. 2005 Nov;33(11):1402-16. PubMed PMID: 16263424.
24. Halayko AJ, Camoretti-Mercado B, Forsythe SM, Vieira JE, Mitchell RW, Wylam ME, et al. Divergent differentiation paths in airway smooth muscle culture: induction of functionally contractile myocytes. *The American journal of physiology*. 1999 Jan;276(1 Pt 1):L197-206. PubMed PMID: 9887072.
25. Brittingham J, Phiel C, Trzyna WC, Gabbeta V, McHugh KM. Identification of distinct molecular phenotypes in cultured gastrointestinal smooth muscle cells. *Gastroenterology*. 1998 Sep;115(3):605-17. PubMed PMID: 9721158.
26. Deasy BM, Jankowski RJ, Huard J. Muscle-derived stem cells: characterization and potential for cell-mediated therapy. *Blood Cells Mol Dis*. 2001 Sep-Oct;27(5):924-33. PubMed PMID: 11783957. Epub 2002/01/11. eng.
27. Cao B, Huard J. Muscle-derived stem cells. *Cell Cycle*. 2004 Feb;3(2):104-7. PubMed PMID: 14712064. Epub 2004/01/09. eng.
28. Hwang JH, Yuk SH, Lee JH, Lyoo WS, Ghil SH, Lee SS, et al. Isolation of muscle derived stem cells from rat and its smooth muscle differentiation [corrected]. *Mol Cells*. 2004 Feb 29;17(1):57-61. PubMed PMID: 15055528. Epub 2004/04/02. eng.

29. Kulkarni S, Becker L, Pasricha PJ. Stem cell transplantation in neurodegenerative disorders of the gastrointestinal tract: future or fiction? *Gut*. 2011 Aug 4. PubMed PMID: 21816959. Epub 2011/08/06. Eng.
30. Suárez-Rodríguez R, Belkind-Gerson J. Cultured Nestin–Positive Cells from Postnatal Mouse Small Bowel Differentiate Ex Vivo into Neurons, Glia, and Smooth Muscle. *Stem cells*. 2004;22(7):1373-85.
31. Schafer KH, Hagl CI, Rauch U. Differentiation of neurospheres from the enteric nervous system. *Pediatric surgery international*. 2003 Jul;19(5):340-4. PubMed PMID: 12845455.
32. Belkind-Gerson J, Carreon-Rodriguez A, Benedict LA, Steiger C, Pieretti A, Nagy N, et al. Nestin-expressing cells in the gut give rise to enteric neurons and glial cells. *Neurogastroenterology and motility : the official journal of the European Gastrointestinal Motility Society*. 2013 Jan;25(1):61-9 e7. PubMed PMID: 22998406. Pubmed Central PMCID: 3531577.
33. Silva AT, Wardhaugh T, Dolatshad NF, Jones S, Saffrey MJ. Neural progenitors from isolated postnatal rat myenteric ganglia: Expansion as neurospheres and differentiation< i> in vitro</i>. *Brain research*. 2008;1218:47-53.
34. Lindley RM, Hawcutt DB, Connell MG, Almond SL, Vannucchi MG, Faussone-Pellegrini MS, et al. Human and mouse enteric nervous system neurosphere transplants regulate the function of aganglionic embryonic distal colon. *Gastroenterology*. 2008 Jul;135(1):205-16 e6. PubMed PMID: 18515088.
35. Metzger M, Caldwell C, Barlow AJ, Burns AJ, Thapar N. Enteric nervous system stem cells derived from human gut mucosa for the treatment of aganglionic gut disorders. *Gastroenterology*. 2009 Jun;136(7):2214-25 e1-3. PubMed PMID: 19505425.
36. Rauch U, Hänsgen A, Hagl C, Holland-Cunz S, Schäfer K-H. Isolation and cultivation of neuronal precursor cells from the developing human enteric nervous

system as a tool for cell therapy in dysganglionosis. *International journal of colorectal disease*. 2006;21(6):554-9.

37. Pan WK, Zheng BJ, Gao Y, Qin H, Liu Y. Transplantation of neonatal gut neural crest progenitors reconstructs ganglionic function in benzalkonium chloride-treated homogenic rat colon. *Journal of Surgical Research*. 2011;167(2):e221-e30.

38. Hotta R, Stamp LA, Foong JP, McConnell SN, Bergner AJ, Anderson RB, et al. Transplanted progenitors generate functional enteric neurons in the postnatal colon. *The Journal of clinical investigation*. 2013;123(3):1182.

39. Anitha M, Joseph I, Ding X, Torre ER, Sawchuk MA, Mwangi S, et al. Characterization of fetal and postnatal enteric neuronal cell lines with improvement in intestinal neural function. *Gastroenterology*. 2008 May;134(5):1424-35. PubMed PMID: 18471518. Pubmed Central PMCID: 2612783. Epub 2008/05/13. eng.

40. Tsai YH, Murakami N, Gariépy CE. Postnatal intestinal engraftment of prospectively selected enteric neural crest stem cells in a rat model of Hirschsprung disease. *Neurogastroenterology and motility : the official journal of the European Gastrointestinal Motility Society*. 2011 Apr;23(4):362-9. PubMed PMID: 21199176. Pubmed Central PMCID: 3105196.

41. Hotta R, Stamp LA, Foong JP, McConnell SN, Bergner AJ, Anderson RB, et al. Transplanted progenitors generate functional enteric neurons in the postnatal colon. *J Clin Invest*. 2013 Mar 1;123(3):1182-91. PubMed PMID: 23454768. Pubmed Central PMCID: 3582137. Epub 2013/03/05. eng.

42. Kulkarni S, Zou B, Hanson J, Micci M-A, Tiwari G, Becker L, et al. Gut-derived factors promote neurogenesis of CNS-neural stem cells and nudge their differentiation to an enteric-like neuronal phenotype. *American Journal of Physiology-Gastrointestinal and Liver Physiology*. 2011;301(4):G644-G55.

43. Micci MA, Kahrig KM, Simmons RS, Sarna SK, Espejo-Navarro MR, Pasricha PJ. Neural stem cell transplantation in the stomach rescues gastric function in neuronal nitric oxide synthase-deficient mice. *Gastroenterology*. 2005 Dec;129(6):1817-24. PubMed PMID: 16344050.
44. Dong YL, Liu W, Gao YM, Wu RD, Zhang YH, Wang HF, et al. Neural stem cell transplantation rescues rectum function in the aganglionic rat. *Transplantation proceedings*. 2008 Dec;40(10):3646-52. PubMed PMID: 19100458.
45. Kulkarni S, Zou B, Hanson J, Micci MA, Tiwari G, Becker L, et al. Gut-derived factors promote neurogenesis of CNS-neural stem cells and nudge their differentiation to an enteric-like neuronal phenotype. *American journal of physiology Gastrointestinal and liver physiology*. 2011 Oct;301(4):G644-55. PubMed PMID: 21817062. Pubmed Central PMCID: 3191554.
46. Metzger M, Bareiss PM, Danker T, Wagner S, Hennenlotter J, Guenther E, et al. Expansion and differentiation of neural progenitors derived from the human adult enteric nervous system. *Gastroenterology*. 2009 Dec;137(6):2063-73 e4. PubMed PMID: 19549531. Epub 2009/06/25. eng.
47. Yang S, Leong K-F, Du Z, Chua C-K. The design of scaffolds for use in tissue engineering. Part I. Traditional factors. *Tissue engineering*. 2001;7(6):679-89.
48. Hori Y, Nakamura T, Kimura D, Kaino K, Kurokawa Y, Satomi S, et al. Experimental study on tissue engineering of the small intestine by mesenchymal stem cell seeding. *The Journal of surgical research*. 2002 Feb;102(2):156-60. PubMed PMID: 11796013.
49. Lee M, Wu BM, Stelzner M, Reichardt HM, Dunn JC. Intestinal smooth muscle cell maintenance by basic fibroblast growth factor. *Tissue engineering Part A*. 2008 Aug;14(8):1395-402. PubMed PMID: 18680389.



50. Hori Y, Nakamura T, Kimura D, Kaino K, Kurokawa Y, Satomi S, et al. Functional analysis of the tissue-engineered stomach wall. *Artificial organs*. 2002 Oct;26(10):868-72. PubMed PMID: 12296927.
51. Araki M, Tao H, Sato T, Nakajima N, Hyon SH, Nagayasu T, et al. Development of a new tissue-engineered sheet for reconstruction of the stomach. *Artificial organs*. 2009 Oct;33(10):818-26. PubMed PMID: 19839991.
52. Nakase Y, Hagiwara A, Nakamura T, Kin S, Nakashima S, Yoshikawa T, et al. Tissue engineering of small intestinal tissue using collagen sponge scaffolds seeded with smooth muscle cells. *Tissue engineering*. 2006;12(2):403-12.
53. Speer AL, Sala FG, Matthews JA, Grikscheit TC. Murine tissue-engineered stomach demonstrates epithelial differentiation. *The Journal of surgical research*. 2011 Nov;171(1):6-14. PubMed PMID: 21571313.
54. Madhally SV, Matthew HW. Porous chitosan scaffolds for tissue engineering. *Biomaterials*. 1999 Jun;20(12):1133-42. PubMed PMID: 10382829.
55. Zakhem E, Raghavan S, Gilmont RR, Bitar KN. Chitosan-based scaffolds for the support of smooth muscle constructs in intestinal tissue engineering. *Biomaterials*. 2012 Jun;33(19):4810-7. PubMed PMID: 22483012. Pubmed Central PMCID: 3334429.
56. Somara S, Gilmont RR, Dennis RG, Bitar KN. Bioengineered internal anal sphincter derived from isolated human internal anal sphincter smooth muscle cells. *Gastroenterology*. 2009;137(1):53-61.
57. Saxena AK, Kofler K, Ainodhofer H, Hollwarth ME. Esophagus tissue engineering: hybrid approach with esophageal epithelium and unidirectional smooth muscle tissue component generation in vitro. *Journal of gastrointestinal surgery : official journal of the Society for Surgery of the Alimentary Tract*. 2009 Jun;13(6):1037-43. PubMed PMID: 19277795.

58. Raghavan S, Lam MT, Foster LL, Gilmont RR, Somara S, Takayama S, et al. Bioengineered three-dimensional physiological model of colonic longitudinal smooth muscle in vitro. *Tissue Engineering Part C: Methods*. 2010;16(5):999-1009.
59. Totonelli G, Maghsoudlou P, Garriboli M, Riegler J, Orlando G, Burns AJ, et al. A rat decellularized small bowel scaffold that preserves villus-crypt architecture for intestinal regeneration. *Biomaterials*. 2012;33(12):3401-10.
60. Zhu Y, Ong WF. Epithelium regeneration on collagen (IV) grafted polycaprolactone for esophageal tissue engineering. *Materials Science and Engineering: C*. 2009;29(3):1046-50.
61. Zhu Y, Leong MF, Ong WF, Chan-Park MB, Chian KS. Esophageal epithelium regeneration on fibronectin grafted poly(L-lactide-co-caprolactone) (PLLC) nanofiber scaffold. *Biomaterials*. 2007 Feb;28(5):861-8. PubMed PMID: 17081604.
62. Levin DE, Barthel ER, Speer AL, Sala FG, Hou X, Torashima Y, et al. Human tissue-engineered small intestine forms from postnatal progenitor cells. *Journal of pediatric surgery*. 2013;48(1):129-37.
63. Furness JB. The enteric nervous system and neurogastroenterology. *Nature Reviews Gastroenterology and Hepatology*. 2012;9(5):286-94.
64. Sanders KM, Koh SD, Ro S, Ward SM. Regulation of gastrointestinal motility—insights from smooth muscle biology. *Nature Reviews Gastroenterology and Hepatology*. 2012;9(11):633-45.
65. Chumpitazi B, Nurko S. Pediatric gastrointestinal motility disorders: challenges and a clinical update. *Gastroenterology & hepatology*. 2008;4(2):140.
66. Bitar KN, Raghavan S, Zakhem E. Tissue engineering in the gut: developments in neuromusculature. *Gastroenterology*. 2014 Jun;146(7):1614-24. PubMed PMID: 24681129. Pubmed Central PMCID: 4035447.

67. Bitar KN, Zakhem E. Tissue engineering and regenerative medicine as applied to the gastrointestinal tract. *Current opinion in biotechnology*. 2013 Oct;24(5):909-15. PubMed PMID: 23583170. Pubmed Central PMCID: 3723710.
68. Kovesi T, Rubin S. Long-term complications of congenital esophageal atresia and/or tracheoesophageal fistula. *Chest*. 2004 Sep;126(3):915-25. PubMed PMID: 15364774.
69. Li Y, Zhu Y, Yu H, Chen L, Liu Y. Topographic characterization and protein quantification of esophageal basement membrane for scaffold design reference in tissue engineering. *Journal of biomedical materials research Part B, Applied biomaterials*. 2012 Jan;100(1):265-73. PubMed PMID: 22102566.
70. Ackbar R, Ainoedhofer H, Gugatschka M, Saxena AK. Decellularized ovine esophageal mucosa for esophageal tissue engineering. *Technology and health care : official journal of the European Society for Engineering and Medicine*. 2012;20(3):215-23. PubMed PMID: 22735736.
71. Badylak SF, Vorp DA, Spievack AR, Simmons-Byrd A, Hanke J, Freytes DO, et al. Esophageal reconstruction with ECM and muscle tissue in a dog model. *The Journal of surgical research*. 2005 Sep;128(1):87-97. PubMed PMID: 15922361.
72. Tan B, Wei RQ, Tan MY, Luo JC, Deng L, Chen XH, et al. Tissue engineered esophagus by mesenchymal stem cell seeding for esophageal repair in a canine model. *The Journal of surgical research*. 2012 Aug 17. PubMed PMID: 22925499.
73. Liang JH, Zhou X, Zheng ZB, Liang XL. Long-term form and function of neoesophagus after experimental replacement of thoracic esophagus with nitinol composite artificial esophagus. *ASAIO journal*. 2010 May-Jun;56(3):232-4. PubMed PMID: 20449897.

74. Basu J, Mihalko KL, Payne R, Rivera E, Knight T, Genheimer CW, et al. Extension of bladder-based organ regeneration platform for tissue engineering of esophagus. *Medical hypotheses*. 2012 Feb;78(2):231-4. PubMed PMID: 22100629.
75. Camilleri M, Vazquez-Roque M. Gastric Dysmotility at the Organ Level in Gastroparesis. In: Parkman HP, McCallum RW, editors. *Gastroparesis. Clinical Gastroenterology*: Humana Press; 2012. p. 37-46.
76. Sachdeva P, Malhotra N, Pathikonda M, Khayyam U, Fisher RS, Maurer AH, et al. Gastric emptying of solids and liquids for evaluation for gastroparesis. *Digestive diseases and sciences*. 2011 Apr;56(4):1138-46. PubMed PMID: 21365240.
77. Guerci B, Bourgeois C, Bresler L, Scherrer ML, Böhme P. Gastric electrical stimulation for the treatment of diabetic gastroparesis. *Diabetes & Metabolism*. 2012 11//;38(5):393-402.
78. Chu H, Lin Z, Zhong L, McCallum RW, Hou X. Treatment of high-frequency gastric electrical stimulation for gastroparesis. *Journal of gastroenterology and hepatology*. 2012 Jun;27(6):1017-26. PubMed PMID: 22128901.
79. Maemura T, Kinoshita M, Shin M, Miyazaki H, Tsujimoto H, Ono S, et al. Assessment of a tissue-engineered gastric wall patch in a rat model. *Artif Organs*. 2012 Apr;36(4):409-17. PubMed PMID: 22040317.
80. Sala FG, Kunisaki SM, Ochoa ER, Vacanti J, Grikscheit TC. Tissue-engineered small intestine and stomach form from autologous tissue in a preclinical large animal model. *The Journal of surgical research*. 2009 Oct;156(2):205-12. PubMed PMID: 19665143.
81. Yoshida A, Chitcholtan K, Evans JJ, Nock V, Beasley SW. In vitro tissue engineering of smooth muscle sheets with peristalsis using a murine induced pluripotent stem cell line. *Journal of pediatric surgery*. 2012 Feb;47(2):329-35. PubMed PMID: 22325385.

82. Grikscheit TC, Siddique A, Ochoa ER, Srinivasan A, Alsberg E, Hodin RA, et al. Tissue-engineered small intestine improves recovery after massive small bowel resection. *Annals of surgery*. 2004 Nov;240(5):748-54. PubMed PMID: 15492554. Pubmed Central PMCID: 1356478.
83. Grikscheit TC, Ochoa ER, Ramsanahie A, Alsberg E, Mooney D, Whang EE, et al. Tissue-engineered large intestine resembles native colon with appropriate in vitro physiology and architecture. *Annals of surgery*. 2003 Jul;238(1):35-41. PubMed PMID: 12832963. Pubmed Central PMCID: 1422658.
84. Sala FG, Matthews JA, Speer AL, Torashima Y, Barthel ER, Grikscheit TC. A multicellular approach forms a significant amount of tissue-engineered small intestine in the mouse. *Tissue engineering Part A*. 2011 Jul;17(13-14):1841-50. PubMed PMID: 21395443. Pubmed Central PMCID: 3118603.
85. Qin HH, Dunn JC. Small intestinal submucosa seeded with intestinal smooth muscle cells in a rodent jejunal interposition model. *The Journal of surgical research*. 2011 Nov;171(1):e21-6. PubMed PMID: 21937060. Pubmed Central PMCID: 3195903.
86. Totonelli G, Maghsoudlou P, Garriboli M, Riegler J, Orlando G, Burns AJ, et al. A rat decellularized small bowel scaffold that preserves villus-crypt architecture for intestinal regeneration. *Biomaterials*. 2012 Apr;33(12):3401-10. PubMed PMID: 22305104.
87. Pan WK, Zheng BJ, Gao Y, Qin H, Liu Y. Transplantation of neonatal gut neural crest progenitors reconstructs ganglionic function in benzalkonium chloride-treated homogenic rat colon. *The Journal of surgical research*. 2011 May 15;167(2):e221-30. PubMed PMID: 21392806.
88. Raghavan S, Lam MT, Foster LL, Gilmont RR, Somara S, Takayama S, et al. Bioengineered three-dimensional physiological model of colonic longitudinal smooth

muscle in vitro. *Tissue engineering Part C, Methods*. 2010 Oct;16(5):999-1009. PubMed PMID: 20001822. Pubmed Central PMCID: 2943406.

89. Raghavan S, Bitar KN. The influence of extracellular matrix composition on the differentiation of neuronal subtypes in tissue engineered innervated intestinal smooth muscle sheets. *Biomaterials*. 2014 Aug;35(26):7429-40. PubMed PMID: 24929617. Pubmed Central PMCID: 4086147.

90. Bharucha AE. Fecal incontinence. *Gastroenterology*. 2003 May;124(6):1672-85. PubMed PMID: 12761725.

91. Nelson R, Norton N, Cautley E, Furner S. Community-based prevalence of anal incontinence. *Jama*. 1995 Aug 16;274(7):559-61. PubMed PMID: 7629985.

92. Frenckner B, Ihre T. Influence of autonomic nerves on the internal and sphincter in man. *Gut*. 1976 Apr;17(4):306-12. PubMed PMID: 773793. Pubmed Central PMCID: 1411095.

93. Gilmont RR, Raghavan S, Somara S, Bitar KN. Bioengineering of physiologically functional intrinsically innervated human internal anal sphincter constructs. *Tissue engineering Part A*. 2014 Jun;20(11-12):1603-11. PubMed PMID: 24328537. Pubmed Central PMCID: 4029137.

94. Raghavan S, Gilmont RR, Miyasaka EA, Somara S, Srinivasan S, Teitelbaum DH, et al. Successful implantation of bioengineered, intrinsically innervated, human internal anal sphincter. *Gastroenterology*. 2011 Jul;141(1):310-9. PubMed PMID: 21463628. Pubmed Central PMCID: 3129458.

95. Raghavan S, Miyasaka EA, Gilmont RR, Somara S, Teitelbaum DH, Bitar KN. Perianal implantation of bioengineered human internal anal sphincter constructs intrinsically innervated with human neural progenitor cells. *Surgery*. 2014 Apr;155(4):668-74. PubMed PMID: 24582493. Pubmed Central PMCID: 4017655.

## **CHAPTER IV: EXPERIMENTAL DESIGN OF THE THESIS**

The hypothesis of this thesis work was that tubular chitosan scaffolds will support the reconstruction of the neuro-musculature of the GI tract.

### **Tissue engineering and regenerative medicine approach:**

Surgical management of the gut remains the gold standard treatment for GI diseases. Post-operative complications such as leakage [1, 2] and stricture have shifted the focus to an alternative treatment approach. Tissue engineering and regenerative medicine aim to regenerate or reconstruct tissues and organs with restoration of their specific functions. The paradigm is described in Figure 4. The cellular and architectural complexity of the GI tract is considered as one of the greatest challenges in the regeneration process. The most common engineering tools used in the field of tissue engineering and regenerative medicine include one or multiple cellular components, scaffolding materials and bioactive components. Those tools require quality testing before translation into humans.

## The scaffold component:

A wide range of biomaterials (natural and synthetic) is available for developing scaffolds. For GI applications, tubular hollow structures facilitate the regeneration process. Synthetic materials such as poly- $\epsilon$ -caprolactone and polyglycolic acid have been previously used for regeneration of the epithelium and the musculature [3, 4]. Natural polymers such as collagen and chitosan are also widely used in different tissue engineering applications. Collagen supported the regeneration of different cell layers however; the weak mechanical properties of collagen necessitated its reinforcement using synthetic materials [5, 6].

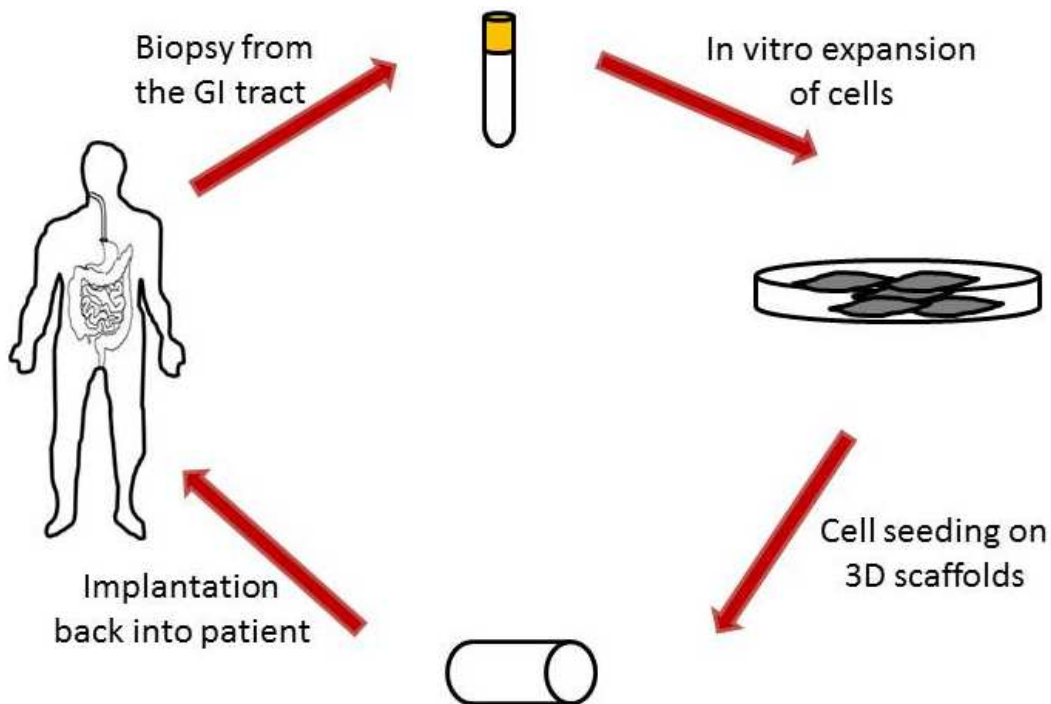


**Figure 4:** Paradigm of tissue engineering and regenerative medicine.



Chitosan has the ability to form porous structures and its mechanical properties are tunable [7]. Chitosan hasn't been previously used in GI applications. In this thesis work, we demonstrated the biocompatibility of chitosan in 2 steps; using smooth muscle cells (**Chapter 5**) and neural progenitor cells (**Chapter 6**) in terms of phenotype and functionality. After demonstrating the biocompatibility of chitosan for GI applications, we moved into developing tubular scaffolds with enhanced mechanical properties. Tubular porous chitosan scaffolds were developed with aligned chitosan fibers to reinforce their mechanical properties when compared to tubular porous scaffolds without fibers (**Chapter 7**).

## **The cellular component:**

The next step of the regeneration process is the cellular component. The neuro-musculature of the GI tract requires an adequate source of smooth muscle and neural cells. Isolation of smooth muscle cells from the GI tract has been well established, even though maintenance of its contractile phenotype in vitro is still a challenge [8]. Additionally, the GI tract is a rich source of enteric neural progenitor cells [9]. Those cells have shown the potential to differentiate into functional neurons to treat neurodegenerative diseases. Another cell source recently employed in regenerating the gut is gut-derived organoid units. Those units were seeded onto scaffolds and differentiated into a gut tissue that contains all cell layers [10-12]. Even though an innervated musculature is regenerated, assays are needed to confirm its functionality.

The gut has 2 smooth muscle layers (longitudinal and circular) that run in different directions along the tract. Circular muscle contraction induces narrowing of the luminal diameter whereas contraction of the longitudinal muscle shortens the gut. An intrinsically innervated smooth muscle layer was engineered and wrapped around hollow tubular chitosan scaffolds to form the innervated circular smooth muscle layer. The engineered tubular neuro-muscular tissues maintained their phenotype and function following their subcutaneous implantation in rats for 2 weeks (**Chapter 8**) and 4 weeks (**Chapter 9**). The tissues exhibited luminal pressure and mechanical properties comparable to native rat intestine.

In addition to the regeneration of the neuro-musculature of the GI tract, regeneration the epithelial component is also of paramount importance for absorption of nutrient [13, 14]. Therefore, incorporating the epithelium in the regeneration process is essential to achieve the translational aspect of this thesis. **Chapter 10** of this thesis work was to study the epithelial regeneration in the engineered neuro-muscular tissues. The hypothesis for this aim was that anastomosis of the engineered tubular neuro-muscular tissue with the native small intestine of the rat will allow epithelial cell migration and colonization of the engineered tissue. Cell migration and infiltration from the native intestine into the anastomosed engineered tissue was evident. These studies provided preliminary promising results about the potential of regenerating an intestinal segment with the necessary cellular components for peristalsis and for absorption/secretion.

## References:

- [1] Hyman N, Manchester TL, Osler T, Burns B, Cataldo PA. Anastomotic leaks after intestinal anastomosis: it's later than you think. *Annals of surgery*. 2007;245:254-8.
- [2] Briel JW, Tamhankar AP, Hagen JA, DeMeester SR, Johansson J, Choustoulakis E, et al. Prevalence and risk factors for ischemia, leak, and stricture of esophageal anastomosis: gastric pull-up versus colon interposition. *Journal of the American College of Surgeons*. 2004;198:536-41.
- [3] Diemer P, Markoew S, Le DQS, Qvist N. Poly- $\epsilon$ -caprolactone mesh as a scaffold for in vivo tissue engineering in rabbit esophagus. *Diseases of the Esophagus*. 2015;28:240-5.
- [4] Miyazawa M, Aikawa M, Watanabe Y, Takase K-i, Okamoto K, Shrestha S, et al. Extensive regeneration of the stomach using bioabsorbable polymer sheets. *Surgery*. 2015;158:1283-90.
- [5] Hori Y, Nakamura T, Kimura D, Kaino K, Kurokawa Y, Satomi S, et al. Functional Analysis of the Tissue-Engineered Stomach Wall. *Artificial organs*. 2002;26:868-72.
- [6] Araki M, Tao H, Sato T, Nakajima N, Hyon SH, Nagayasu T, et al. Development of a New Tissue-Engineered Sheet for Reconstruction of the Stomach. *Artificial organs*. 2009;33:818-26.
- [7] Madihally SV, Matthew HW. Porous chitosan scaffolds for tissue engineering. *Biomaterials*. 1999;20:1133-42.
- [8] Walthers CM, Lee M, Wu BM, Dunn JC. Smooth muscle strips for intestinal tissue engineering. *PloS one*. 2014;9:e114850.
- [9] Metzger M, Bareiss PM, Danker T, Wagner S, Hennenlotter J, Guenther E, et al. Expansion and differentiation of neural progenitors derived from the human adult enteric nervous system. *Gastroenterology*. 2009;137:2063-73. e4.

- [10] Grikscheit TC, Ochoa ER, Ramsanahie A, Alsberg E, Mooney D, Whang EE, et al. Tissue-engineered large intestine resembles native colon with appropriate in vitro physiology and architecture. *Annals of surgery*. 2003;238:35-41.
- [11] Grikscheit T, Srinivasan A, Vacanti JP. Tissue-engineered stomach: a preliminary report of a versatile in vivo model with therapeutic potential. *Journal of pediatric surgery*. 2003;38:1305-9.
- [12] Spurrier RG, Speer AL, Hou X, El-Nachef WN, Grikscheit TC. Murine and human tissue-engineered esophagus form from sufficient stem/progenitor cells and do not require microdesigned biomaterials. *Tissue Engineering Part A*. 2014;21:906-15.
- [13] Vrana NE, Lavalle P, Dokmeci MR, Dehghani F, Ghaemmaghami AM, Khademhosseini A. Engineering functional epithelium for regenerative medicine and in vitro organ models: a review. *Tissue Engineering Part B: Reviews*. 2013;19:529-43.
- [14] Paz AC, Soleas J, Poon JC, Trieu D, Waddell TK, McGuigan AP. Challenges and opportunities for tissue-engineering polarized epithelium. *Tissue Engineering Part B: Reviews*. 2013;20:56-72.

# **CHAPTER V: CHITOSAN-BASED SCAFFOLDS FOR THE SUPPORT OF SMOOTH MUSCLE CONSTRUCTS IN INTESTINAL TISSUE ENGINEERING**

Elie Zakhem, Shreya Raghavan, Robert R Gilmont, Khalil N Bitar\*

Wake Forest Institute for Regenerative Medicine, Wake Forest School of  
Medicine,  
Winston-Salem NC

*The study in this chapter describes the biocompatibility of chitosan using gut  
derived smooth muscle.*

*This manuscript was accepted for publication in Biomaterials 2012; 33(19): 4810-7*

## ABSTRACT

Intestinal tissue engineering is an emerging field due to a growing demand for intestinal lengthening and replacement procedures secondary to massive resections of the bowel. Here, we demonstrate the potential use of a chitosan/collagen scaffold as a 3D matrix to support the bioengineered circular muscle constructs maintain their physiological functionality. We investigated the biocompatibility of chitosan by growing rabbit colonic circular smooth muscle cells (RCSMCs) on chitosan-coated plates. The cells maintained their spindle-like morphology and preserved their smooth muscle phenotypic markers. We manufactured tubular scaffolds with central openings composed of chitosan and collagen in a 1:1 ratio. Concentrically-aligned 3D circular muscle constructs were bioengineered using fibrin-based hydrogel seeded with RCSMCs. The constructs were placed around the scaffold for 2 weeks, after which they were taken off and tested for their physiological functionality. The muscle constructs contracted in response to Acetylcholine (Ach) and potassium chloride (KCl) and they relaxed in response to vasoactive intestinal peptide (VIP). These results demonstrate that chitosan is a biomaterial possibly suitable for intestinal tissue engineering applications.

## **1. Introduction:**

Damaged or diseased segments of the intestinal tract require surgical intervention and extensive resection. This can lead to malabsorption and malnutrition eventually resulting in high mortality and morbidity rates in children and in adults [1-3]. Intestinal transplantation is a common treatment but its limitation resides in the high incidence of rejection, availability of donor organs and the size of the donor graft [4-6]. Hence, there is a clinical demand for generating physiologically functional intestinal replacement. The challenge in tissue engineering functional intestinal replacement lies in the anatomic complexity of this tubular organ. The intestine is composed of two layers of smooth muscle cells that are arranged in distinct orientations; the inner muscle layer consisting of concentrically oriented circular smooth muscle cells, and the external muscle layer consisting of parallel longitudinal smooth muscle cells. These two smooth muscle layers, along with their innervations, perform propulsive peristaltic function.

Tissue engineering provides an approach to generate new tissues using a variety of biomaterials with different cells. In intestinal tissue engineering, it is essential to develop a physiologically functional intestinal segment that could serve as a replacement. To date, both synthetic and natural polymers are used to design 3-D scaffolds to serve as temporary matrices for cell seeding until mature regeneration of the intestine occurs. Synthetic biomaterials used in intestinal tissue engineering applications include polyglycolic acid (PGA) and polycaprolactone (PCL). Vacanti et. al have successfully seeded intestinal

organoids isolated from rat guts onto PGA scaffolds and reported recovery after small bowel resection in rat models [7]. Another group has reported the biocompatibility of PCL as an alternative biomaterial for intestinal regeneration [8]. These polymers demonstrate adequate mechanical properties and are easily reproducible. Intestinal segments have been tissue engineered using collagen due to its excellent biocompatibility, cell-binding affinity and biodegradability [9, 10]. However, the mechanical properties of collagen are unsuitable for intestinal tissue engineering applications [11]. In vivo, collagen scaffolds display rapid degradation rate; therefore they do not allow enough time for tissue regeneration. This imposes limitations on the use of collagen alone as biomaterial in tissue engineering.

Chitosan is a partially or fully deacetylated form of chitin, which is the second most abundant natural polymer found in the shells of shrimps, lobsters and crabs. It is a natural polymer that is commonly used as a biomaterial in many tissue engineering applications. Chitosan is a linear polysaccharide linked by (1→4)- $\beta$ -glycosidic bonds. [12-14]. It has a degradation rate that can be controlled by enzymatic reactions and its biocompatibility has shown promising results in vivo [15-17]. The hydroxyl and amino groups of chitosan allows this polymer to be derivatized under mild conditions [15]. Chitosan has the ability to modify the mechanical properties of collagen when mixed together [18]. Little is known about the use of chitosan in intestinal tissue engineering applications; however, it is thought to be well-tolerated by the digestive system as it has been used as a component of dietary supplements for a number of studies [19-21].



Our laboratory first reported the bioengineering of 3-D physiological model of rabbit internal anal sphincter (IAS) and colonic smooth muscle constructs using fibrin-based gels. These constructs showed cellular alignment similar to native tissue [22]. Yoshikawa and colleagues have implanted collagen sponges seeded with smooth muscle cells as a potential for intestinal regeneration [10]. The smooth muscle cells demonstrated an arrangement similar to the native circular muscle layer but functionality was not assessed. Also, the degradation time of the collagen sponges in vivo was very short which caused shrinkage of the graft sites.

In our current study, we have developed a composite scaffold composed of collagen as the bioactive component combined with chitosan to provide mechanical stability to the scaffold. The composite scaffold was then cross linked with heparan sulfate using carbodiimide cross linker. We propose to use the composite chitosan scaffold as a support for the bioengineered constructs. We first investigated the biocompatibility of chitosan with intestinal smooth muscle cells on 2D composite chitosan membranes by evaluating cellular attachment and smooth muscle phenotypic markers expression. Secondly, we bioengineered 3D smooth muscle tissue constructs and placed them around the composite chitosan tubular scaffold. The bioengineered muscle constructs were taken off the scaffold after a period of 2 weeks and their physiological functionality was compared to constructs that were not around the scaffold.

## **2. Materials and Methods:**

### ***2.1. Reagents:***

All cell culture reagents including growth medium and supplements were purchased from Invitrogen (Carlsbad, CA). Growth medium consisted of Dulbecco's modified Eagle medium (DMEM) (supplemented with 10% fetal bovine serum (FBS), 1.5% antibiotic-antimycotic, and 0.6% L-glutamine. Differentiation medium consisted of 73% DMEM, 20% medium 199, 7% heat-inactivated horse serum, and 1% antibiotic-antimycotic. Collagenase type II was from Worthington (Lakewood, NJ).

Medium molecular weight chitosan (75-85% deacetylation), glycosaminoglycan heparan sulfate, 1-ethyl-3-(3-dimethylaminopropyl) carbodiimide (EDC), acetylcholine (ACh) and vasoactive intestinal peptide (VIP) were purchased from Sigma (St. Louis, MO). Sylgard [poly(dimethylsiloxane); PDMS] was from World Precision Instruments (Sarasota, FL). Type I collagen was purchased from BD Biosciences.

### ***2.2. Isolation of Rabbit Colonic Circular Smooth Muscle cells:***

Rabbit colonic circular smooth muscle cells (RCSMCs) were isolated as described previously [23]. Briefly, rabbit sigmoid colon was cleaned of fecal

content. The serosa, longitudinal smooth muscle and mucosa were removed. The circular smooth muscle was finely minced, digested twice in type II Collagenase (Worthington), and filtered through a 300  $\mu$ m mesh to eliminate cellular debris. The filtrate was centrifuged at 600 *g* for 5 min, washed three times in Hank's buffered salt solution HBSS, and then plated in growth medium. Cells were grown to confluence before use in the experiments.

### *2.3. Fabrication of composite chitosan membranes and scaffolds:*

A 2% w/v chitosan solution was prepared by dissolution in 0.2 M acetic acid. 500  $\mu$ l chitosan: type I collagen (1:1) solution was added to each well of a 12-well plate and the plate was left to air-dry overnight. The resulting dry membranes were cross linked with heparan sulfate using the carbodiimide cross linker (EDC) under moderate shaking at room temperature following the method used by Uygun et. al [24]. The membranes were neutralized with 0.2 M sodium hydroxide and washed several times with 1X PBS. Heparan sulfate (10mg/ml) solution was activated by EDC in a 1:10 ratio. The activated heparan sulfate was then applied to the dried chitosan. The plates were left under moderate shaking at room temperature overnight. This resulted in the production of composite chitosan 2D membranes, which were then sterilized with 70% ethanol and UV light. Membranes were washed several times with sterile PBS before use.

Composite chitosan scaffolds were prepared using the freezing and lyophilizing method described by Madhally et. al. [15]. Briefly, the 2 w/v % chitosan solution

was mixed with type I collagen in a volume ratio of 1:1. The mixture was poured into a custom made mold. The mold consisted of a cylindrical tube with a central port. The inner lumen was created by inserting tubing in the center of the mold. The mold, containing the mixture, was frozen at -80°C for 3 hours and then lyophilized for 24 hours. The scaffolds were neutralized in 0.2 M NaOH and covalently crosslinked with heparan sulfate using EDC. The scaffolds were then washed several times with PBS and distilled water and then placed in 70% ethanol until time of use.

#### *2.4. Microscopic Analysis:*

RCSMCs were seeded on 2D composite chitosan matrices at a density of 20,000 cells per well. Fresh growth medium was supplied every 2 days. Microscopic analysis was performed on days 2 and 7 to determine whether the smooth muscle cells had attached to the chitosan membranes and to record their morphology. Cells grown on chitosan were compared to control cell cultures, which consisted of RCSMC grown directly on tissue culture dishes (no membrane).

#### *2.5. Immunofluorescence Analysis:*

RCSMCs were grown to confluence on microscope chamber slides and were supplied with growth medium. The cells were fixed, blocked and permeabilized. Primary antibodies directed against smooth muscle markers;  $\alpha$ -smooth muscle actin (F3777; Sigma) and smooth muscle specific Caldesmon (c-4562; Sigma)

were used. Fluorophore-conjugated secondary antibodies were used to detect immunofluorescence using a Nikon Ti-E fluorescence microscope.

## *2.6. Scanning Electron Microscopy:*

Lyophilized scaffolds were sectioned using a sharp scalpel. Cross sections were placed on a stub with double sticky tape and colloidal graphite and then sputter-coated with gold prior to examination under an AMRAY 1910 Field Emission Scanning Electron Microscope (FEG-SEM). Porosity and average pore sizes were determined by scanning 3 images of the scaffold and averaging the pore size using Sigmascan Pro 5 software (Systat software Inc, San Jose, CA).

## *2.7. Fabrication of three-dimensional tissue constructs using rabbit circular smooth muscle cells and placing them around a composite chitosan scaffold:*

The process of bioengineering three dimensional circular smooth muscle constructs is similar to the one previously described using internal anal sphincter smooth muscle cells [22]. Briefly, gels were fabricated by polymerizing 20 mg/ml of fibrinogen with 10 units of thrombin. RCSMC density was adjusted to  $2 \times 10^5$  cells/ml and 2 ml of solution was added to fibrin gels. Plates were incubated in growth medium overnight. The next day, the growth medium was replaced with differentiation medium to promote smooth muscle differentiation. These fully formed, 3-dimensional bioengineered rabbit circular smooth muscle (RCSM) tissue constructs remained stable in culture for 7 days until used for the purpose of the experiment.

At day 7, RSCM tissue constructs were completely formed. Four of the constructs were placed around a tubular composite chitosan scaffold and left in culture for an additional two weeks. The four constructs were placed 1 mm apart.

### *2.8. Physiologic functionality measurement and testing protocol:*

The physiological functionality of the bioengineered rabbit colon tissue constructs was assessed in terms of real-time force generation. The force measurements of the constructs were conducted following the protocol previously described in human Internal Anal Sphincter (IAS) and implanted mouse IAS constructs [25]. All constructs were tested using an isometric force transducer with an attached vernier control (Harvard Apparatus, Holliston, MA). The force transducer set up consisted of a warm tissue bath keeping the tissue samples at conditions of  $37^{\circ}\text{C} \pm 1^{\circ}\text{C}$ . Noise and liquid measurements were evaluated by recording air tension and warm liquid force respectively. The bioengineered RSCM tissue constructs were taken off the scaffold at day 14 and real time force generation was measured on each one. RSCM constructs that were not placed around the scaffold were also tested as control.

One end of the tissue sample was hooked onto the measuring arm of the transducer and the other end was hooked onto a fixed reference pin. Tissue constructs were allowed to equilibrate in the tissue bath containing fresh medium. All reported values of force are active tension produced as a result of the tissue. The tissue constructs were immersed in the fluid throughout the testing period to

avoid any air vibration. After establishment of baseline, the tissues were stretched by 10% - 15% using the micromanipulator. The same stretch was maintained during the testing. The stretch baseline established by the tissue samples was arbitrarily set to zero and the values represent change in force generation. Potassium chloride (KCl) was used for testing electromechanical coupling, Acetylcholine (Ach) for cholinergic stimulation and Vasoactive Intestinal Peptide (VIP) for relaxation. Before addition of any reagent, the baseline was established. At the end of each experiment, the tissues were washed with buffer and supplied with fresh basal DMEM.

### *2.9. Quantification of protein:*

Rabbit colonic circular smooth muscle cells grown on tissue culture plates were scraped using PBS. Aliquots of 200,000 cells were lysed in 100  $\mu$ l of lysis buffer (Radioimmunoprecipitation assay buffer) by sonication. The lysates were centrifuged at the end of which the pellets were discarded. For protein quantification, 2  $\mu$ l of the protein extract was removed and added to water. Coomassie blue dye was added to the solution and absorbance was measured at 490 nm. The results were plotted against a standard curve made with  $\gamma$ -globulin ranging from 0 to 11.5  $\mu$ g/ $\mu$ L. Total protein was then calculated by extrapolation for the volume of the lysate. All reported forces are expressed in terms of Newtons per gram of protein content in the bioengineered constructs.

### ***2.10. Data Analysis:***

Force generation data was acquired using LabScribe2 (iWorx, Hanover, NH). GraphPad Prism 5.01 for Windows (GraphPad Software, San Diego CA; [www.graphpad.com](http://www.graphpad.com)) was used for data analysis. Data was exported at 100 samples/second. All values were normalized to millinewton per milligram of protein content in the bioengineered constructs. Second order Savitzky-Golay smoothing was applied to raw data. Expressed values represent mean and standard error of the mean. Student t-test was used to compare the means. A p-value less than 0.05 was considered significant.

## **3. Results:**

### ***3.1. Microscopic analysis:***

The ability of composite chitosan membranes to support attachment, viability and growth of circular smooth muscle cells was evaluated. Rabbit circular smooth muscle cells were seeded on composite-chitosan-coated wells and on non-coated wells of a 12 well plate for comparison. Growth medium was supplied every other day for a period of 7 days. Microscopic analysis showed good attachment of RSCMCs on composite chitosan membranes at day 2 (**Figure 5**). Cells on composite chitosan membranes displayed the normal spindle-like morphology of smooth muscle, when compared to cells on non-coated wells. The cells showed uniform distribution on the composite chitosan membrane. The smooth muscle cells maintained their spindle-like morphology at day 7 on both



coated and non-coated wells. Thus, chitosan did not change the normal morphology of the smooth muscle cells.

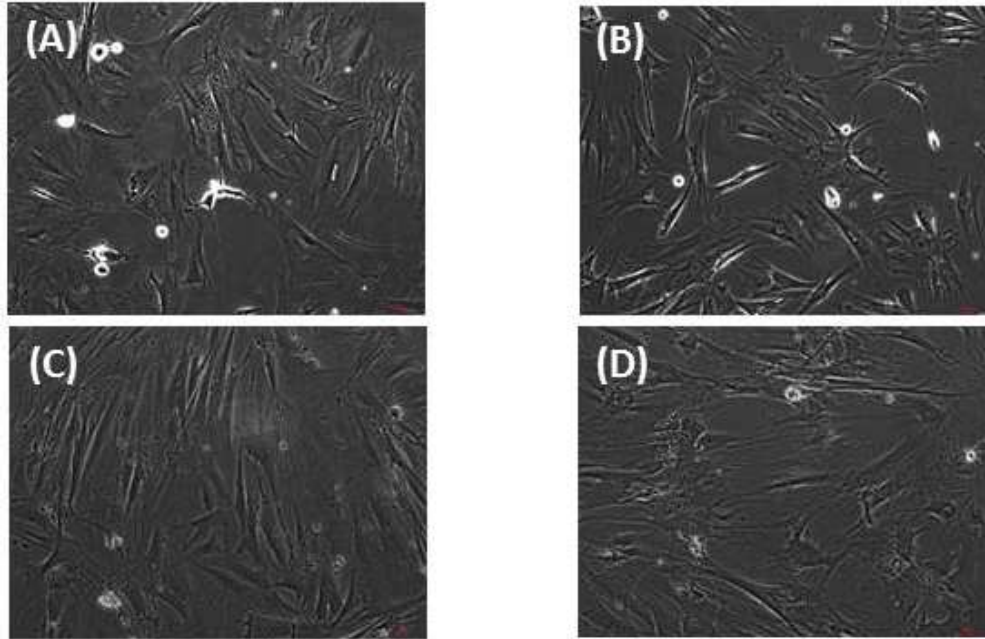


**Figure 5:** Microscope evaluation of cells: Microscopic pictures of RSCMCs on tissue culture plates (A, C) and composite chitosan membranes (B, D) at day 2 (A, B) and day 7 (C, D) after cell seeding. Pictures were taken at 10X magnification. Cells attached on composite chitosan membranes and they maintained spindle-like morphology, a characteristic of smooth muscle cells.

### 3.2. *Immunofluorescence assay:*

RSCMCs were cultured on cover slips coated with composite chitosan for one week and growth medium was applied every 48 hours. The cells were analyzed by immunofluorescence using antibodies to smooth muscle markers  $\alpha$ -smooth muscle actin and smooth-muscle-specific heavy Caldesmon (**Figure 6**). All the cells cultured on composite chitosan membranes stained positive for both

markers, indicating a highly enriched population of smooth muscle cells. The nuclei stained positive with DAPI.

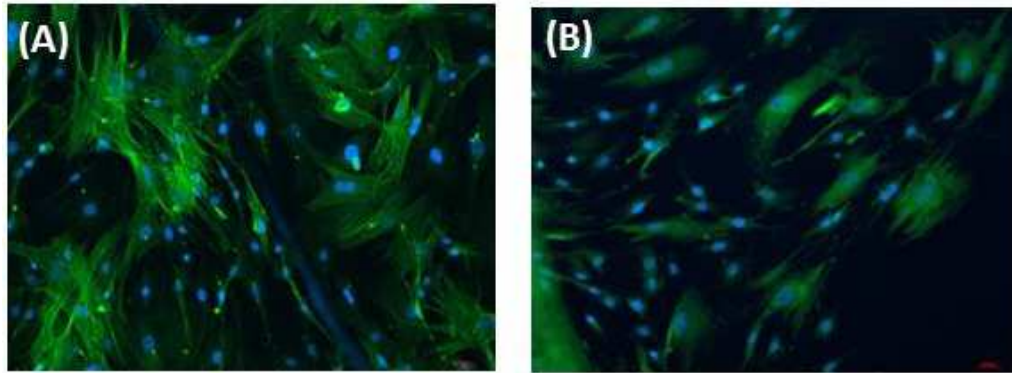


**Figure 6:** Immunofluorescence assay: IHC on RSCMCs grown on composite chitosan membranes for  $\alpha$ -smooth muscle actin (A, green color) and smooth muscle specific heavy Caldesmon (B, green color). Nuclei stain 4'-6-diamidino-2-phenylindole (DAPI) appears in blue. Cells stained positive for  $\alpha$ -SMA and smooth muscle specific heavy Caldesmon, indicating the maintenance of smooth muscle contractile phenotype on composite chitosan membranes.

### 3.3. *Characterization of composite chitosan scaffolds:*

Tubular chitosan scaffolds were fabricated using the freezing and drying method [15]. The custom-made cylindrical molds consisted of cylindrical tubes with annular spaces. The mold containing the chitosan-collagen mixture was frozen for 3 hours at  $-80^{\circ}\text{C}$  and then lyophilized for 24 hours. Figure 7 shows different tubular scaffolds fabricated with different lengths ranging from 3 cm up to 12 cm. The diameter of the inner lumen and the wall thickness of the mold were controlled during the manufacturing process by controlling the tube sizes. The

fabricated scaffolds had different wall thicknesses and different diameter of central opening. The porosity of the scaffolds was observed under low power using a scanning electron microscope. Pore sizes were measured from 3 samples and averaged using Sigmascan Pro 5 software. **Figure 8** shows highly porous scaffolds with mean pore size of 170  $\mu\text{m}$ . Additionally, the pores had a uniform and homogenous pattern.

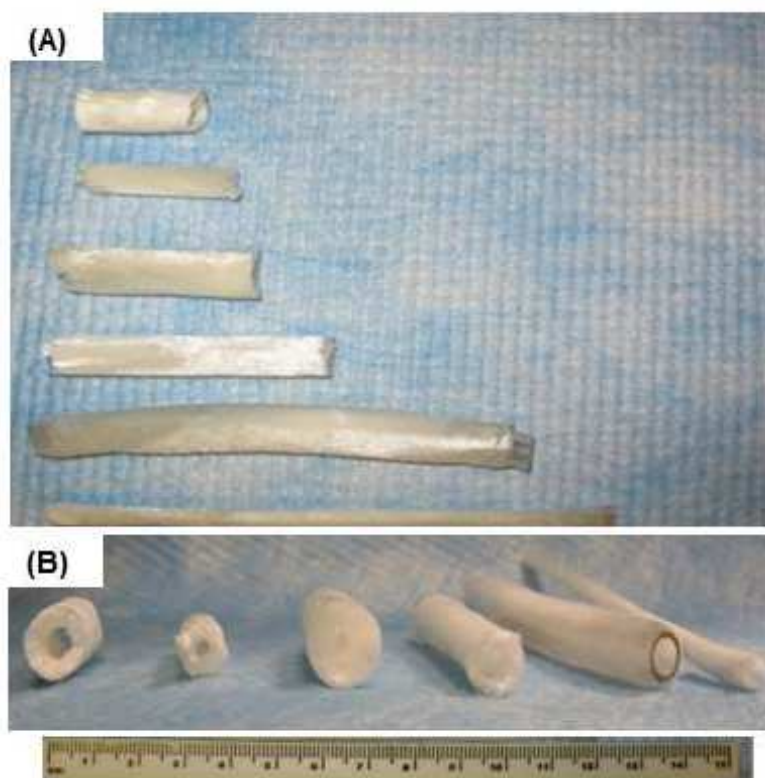


**Figure 7:** Composite chitosan tubular scaffolds: Different lengths ranging from 3 cm up to 12 cm (A) and different lumen diameters and wall thicknesses (B).

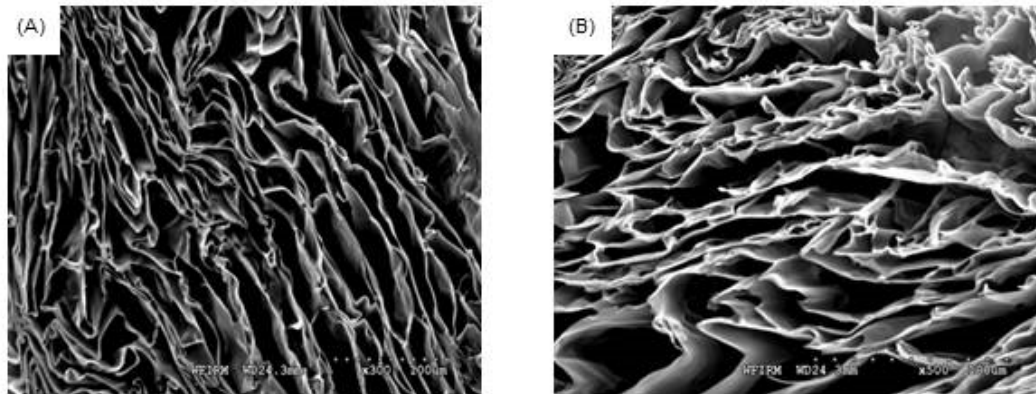


**Figure 8:** Scanning Electron Microscopy of the scaffolds: A section of the scaffold was mounted on a stub and coated with gold using sputter coater. Porosity was characterized by SEM under low power. The image depicted a highly porous scaffold with uniform pore structure at 300X (A) and 500X (B). The mean pore size was found to be 170  $\mu\text{m}$ .

#### 3.4. *Bioengineered RSCM constructs placed around the tubular scaffold:*

The RSCM constructs were formed using the fibrin-based method [22]. The circular smooth muscle cells were seeded on a fibrin gel. The cells were concentrically aligned around the post at the center of the plate. The constructs were fully formed by day 7 in culture and they were separated from the post using forceps.

**Figure 9** shows the RSCM construct with an inner diameter of 5 mm and a thickness of 2 mm. The tubular scaffold had the following dimensions: 2.5cm length, 5mm outer diameter and 3.25mm luminal diameter. The bioengineered RSCM tissue constructs were placed around the composite chitosan tubular scaffold and left in culture for 2 weeks (**Figure 10**). The scaffold was easy to handle and there was no sign of disruption or disintegration of the RSCM constructs while sliding them around the scaffold. They maintained their integrity throughout the culture period of 14 days. Precaution was taken to ensure complete immersion of the scaffold along with the constructs in medium. These bioengineered constructs did not adhere to the tubular scaffold as they were easily taken off the scaffold at the end of the culture period. The bioengineered constructs didn't appear to change the structure of the scaffold as it maintained its luminal patency.



**Figure 9:** Bioengineered RSCM construct: Day 7 - Three dimensional RSCM bioengineered construct with concentrically aligned smooth muscle cells. The internal lumen diameter is 5 mm and wall thickness is 2 mm.



**Figure 10:** Constructs around tubular chitosan scaffold: Four bioengineered constructs were mounted around the composite chitosan tubular scaffold and maintained in culture for 2 weeks. Tissue constructs were placed 1 mm apart.

### *3.5. Physiological testing of the bioengineered constructs:*

The muscle constructs were taken off the scaffold and immersed in a tissue bath for force measurements using the force transducer set up. The response of the bioengineered constructs taken off the scaffold was compared to that of the control constructs (that were not around the scaffold). Pharmacologic studies were carried out to evaluate the maximal contractile responses observed on the bioengineered constructs in response to depolarization with KCl as well as in response to acetylcholine. Relaxation was determined in response to VIP. All reported force values are expressed in Newtons per gram of protein content in the bioengineered constructs.

### a) Contractile Response:

A final concentration of 60 mmol/L of KCl was added to the 4 ml tissue bath containing the RCSM constructs taken off the scaffold or the control RCSM constructs (**Figure 11**). The bioengineered constructs that were around the scaffold and the control constructs both produced an increase in force generation with a mean maximal contractile response of  $0.48 \pm 0.10$  mN/mg of protein (n=3) and  $0.48 \pm 0.05$  mN/mg of protein (n=4) respectively

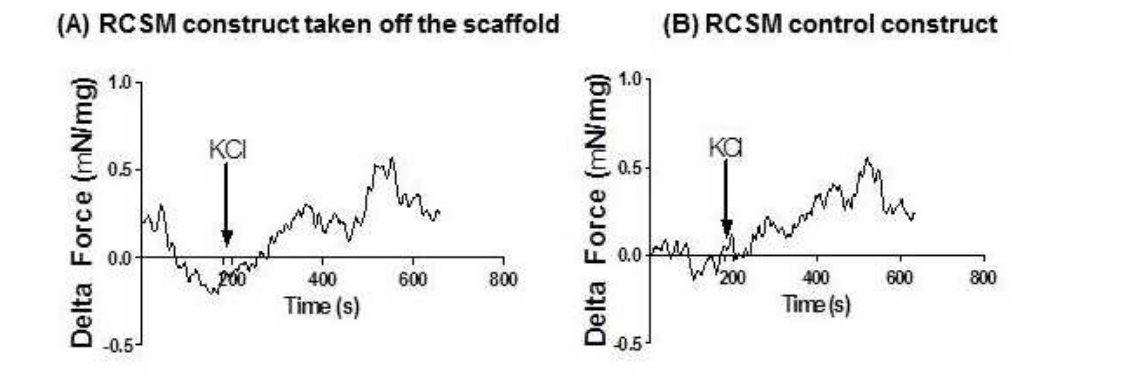


**Figure 11:** Physiological functionality: KCl response. Real time force generation was measured on the constructs taken off the scaffold at day 14 and on the control constructs using a force transducer. The graphs show the average force generated up on treatment with 60 mM potassium chloride (KCl) of an average of  $0.48 \pm 0.10$  mN/mg of protein (n = 3) in the constructs that were around the scaffold (A) and  $0.48 \pm 0.05$  mN/mg of protein (n = 4) in the control constructs (B). Addition of KCl is marked by the arrow at 180 seconds. Representative tracings for 3D bioengineered scaffold and control constructs have been chosen.

Acetylcholine was added after the bioengineered constructs established baseline. The arrow indicates the time of treatment with Ach. Addition of 1  $\mu$ M Acetylcholine to the RCSM constructs that were around the scaffold for 14 days caused a mean contractile force of  $0.55 \pm 0.08$  mN/mg of protein (n=4). Similarly, treatment of the control constructs with 1  $\mu$ M Acetylcholine caused a contraction with an average of  $0.5 \pm 0.17$  mN/mg of protein (n=4) (**Figure 12**). Both groups of bioengineered RCSM constructs showed a sustained contraction in response to Ach. The bioengineered constructs that were around the scaffold preserved the integrity of their cellular receptors. Their maximal contractile response seen with KCl and Ach was similar to that observed for the corresponding responses in the control constructs that were not around the scaffold.



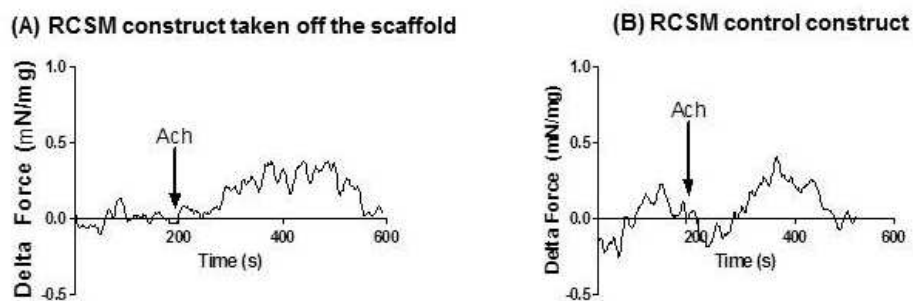


**Figure 12:** Physiological functionality: Ach response. Response in  $\mu\text{N}/\mu\text{g}$  of protein of the constructs that were around the scaffold (A) and control constructs (B) to Acetylcholine (Ach). Addition of  $1\mu\text{M}$  of Ach is marked by the arrow. The constructs taken off the scaffold generated an average contraction of  $0.55 \pm 0.08$  mN/mg of protein ( $n = 4$ ) and the control constructs showed an average contraction of  $0.5 \pm 0.17$  mN/mg of protein ( $n = 4$ ).

#### **b) Relaxation Response:**

The ability of the RCSM constructs to relax in response to  $1\mu\text{M}$  VIP was investigated. The observed relaxation in both the constructs that were around the scaffold and the control constructs was rapid. An average relaxation of  $-0.79 \pm 0.06$  mN/mg of protein ( $n=3$ ) was shown in the constructs that were around the scaffold following the addition of VIP. The control constructs showed an average relaxation of  $-0.89 \pm 0.18$  mN/mg of protein ( $n=4$ ) up on treatment with VIP (**Figure 13**). There was no difference seen in relaxation in response to VIP between the constructs taken off the scaffold and the control constructs.

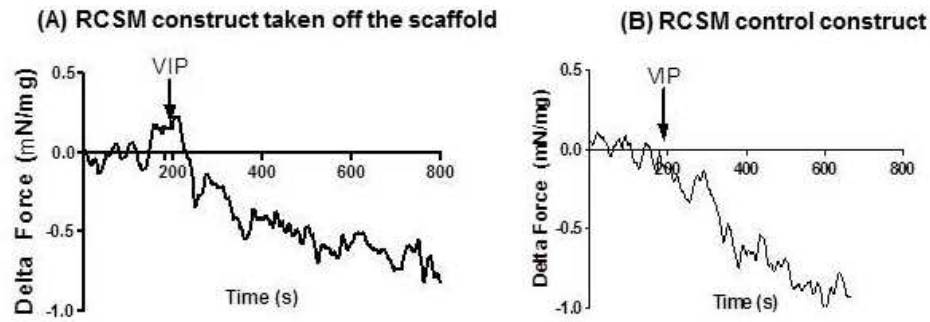


**Figure 13:** Physiological functionality: VIP response. RCSM constructs taken off the scaffold at day 14 (A) and control constructs (B) were tested for relaxation with Vasoactive Intestinal Peptide (VIP). VIP caused an average relaxation of  $-0.79 \pm 0.06$  mN/mg ( $n = 3$ ) in the constructs that were around the scaffold and an average of  $-0.89 \pm 0.18$  mN/mg ( $n = 4$ ) in the control constructs. This graph is a representative figure.

#### 4. Discussion:

Severe weight loss and malnutrition constitute a major threat to patients with extensive bowel resections. Patients with inflammatory bowel disease typically require surgical intervention. Surgical resection has shown improved conditions in patients but the chance of recurrence is still high [26]. Tissue engineered intestinal grafts are beneficial to create intestinal replacements or to lengthen the bowel. Smooth muscle is a crucial component of the gastrointestinal system, and the myoarchitecture of the intestinal wall is of paramount importance. The use of oriented smooth muscles to mimic the native tissue arrangement is more advantageous than randomly seeding smooth muscle cells onto a scaffold. In

dysmotility, smooth muscle layer loses its ability to function normally. Thus, in intestinal tissue engineering it is necessary to duplicate the structure and function of the muscle layers in vitro. Dunn et. al. used fibroblast growth factor incorporated into a scaffold seeded with smooth muscle cells in order to induce vascularization and to help regenerating the smooth muscle layer of the intestine, which is a significant challenge in intestinal tissue engineering [27].

Several challenges to tissue-engineer intestinal grafts reside in mimicking in vivo arrangement of cells and extracellular components. Research is ongoing to bioengineer scaffolds with aligned structure to serve the purpose of their application. Our group has previously bioengineered longitudinally aligned colonic smooth muscle constructs [28]. The specific alignment of these constructs is thought to be responsible for the similarity in force generation between the bioengineered constructs and the native tissue. Other examples include the use of tissue scaffolds with longitudinal grooves structures to enhance the alignment of vascular smooth muscle cells [29]. A biodegradable polymer scaffold made out of aligned nanofibers improved the adhesion, proliferation and alignment of vascular smooth muscle cells while maintaining contractile phenotype [30]. Scaffolds with longitudinally oriented structures are shown to be required for the reconstruction of injured peripheral axons [31]. Graft replacements are usually developed using scaffolds and seeding them with cells, but in our method, we successfully developed concentrically oriented smooth muscle constructs to mimic the native architecture. The alignment of the cells was done using fibrin-based 3D culture. The potential of placing the muscle

constructs around the tubular composite chitosan scaffold for 14 days with the ability to maintain physiological functionality in vitro is promising for intestinal regeneration. Our approach has the advantage of combining bioengineered muscle constructs aligned in an identical way to the native tissue with a biodegradable chitosan scaffold.

In this study, a 2 w/v % medium molecular weight chitosan solution was used to prepare the scaffolds by the freeze-drying method. Scanning electron microscopy was employed to characterize the porosity of the scaffold. Our results revealed a porous scaffold with an average pore size of 170  $\mu\text{m}$ . Porosity is essential in intestinal tissue engineering in order to facilitate vascularization. Previous attempts to induce vascularization and to enhance cell survival have seeded smooth muscle cells in bFGF-releasing collagen scaffolds [27]. To mimic the physiological environment, we cross linked the scaffolds with heparan sulfate because of the abundance of this glycosaminoglycan in the intestinal extracellular matrix [32]. This is the first report that assesses the biocompatibility of chitosan using intestinal smooth muscle. Our data indicates that chitosan was not toxic to these cells as they maintained their spindle-like morphology. The rabbit intestinal smooth muscle cells preserved their contractile phenotype and their smooth muscle specificity as shown by the positive expression of differentiation markers ( $\alpha$ -smooth muscle actin and smooth muscle specific heavy Caldesmon). Moreover, the above findings show that these smooth muscle cells were able to contract and relax in response to contractile and relaxant agonists, which are functions associated with high level of differentiation.

In recent years, acellular collagen scaffolds or collagen scaffolds seeded with mesenchymal stem cells have been developed. Results have shown lack of smooth muscle layer regeneration which is essential for the functionality of the tissue-engineered intestine [9, 33]. Other approaches have used collagen sponges seeded with smooth muscle cells as a potential for intestinal regeneration [10]. The main limitation is the lack of a functional smooth muscle layer. In our study, the three-dimensional circular smooth muscle tissue constructs were bioengineered by seeding circular smooth muscle cells isolated from rabbit colon in a thrombin polymerized fibrinogen hydrogel. The cells were self-organized concentrically around the central post of the plate and formed three-dimensional ring-like structures. We showed that 14 days post-placing the muscle constructs around the composite scaffold in culture, they displayed characteristics of colonic physiology, including contraction and relaxation mediated by physiologically relevant neurotransmitters like Acetylcholine and Vasoactive Intestinal Peptide. We were able to slide the constructs without causing rupture, and this shows the flexibility of the composite chitosan scaffold. During the culture period, the composite chitosan scaffold did not cause damage to the tissue constructs as they maintained their integrity and morphology. Also, there was no sign of damage to the scaffold throughout the culture period as it retained its luminal patency.

Some studies have seeded collagen scaffolds with autologous smooth muscle cells to regenerate the intestine. The smooth muscle cells formed a circular smooth muscle layer similar to in vivo arrangement, but there was no evidence for functionality [10]. The group of Vacanti has reported the use of intestinal organoids derived from animal guts to seed polymer scaffolds in order to regenerate the intestine [7, 34]. Histological studies have shown positive staining for the muscularis propria and electrophysiological studies have shown similar parameters to the native colon tissue [34]. In our case, the force generated by the constructs that were around the scaffold was compared to that of the control ones. Force was expressed in terms of Newton per microgram of protein content in the constructs. The RSCM constructs taken off the scaffold displayed a physiologic response to KCl in a way similar to the control constructs. This shows the maintenance of the electromechanical coupling and integrity of the cell membrane of the constructs after being placed around the composite chitosan scaffold for 14 days. Smooth muscle receptor-mediated contraction in response to Ach has been previously reported [35, 36]. Both the constructs that were around the scaffold and the control constructs demonstrated a similar sustained contraction with the addition of 1  $\mu$ M Ach. This indicates that the smooth muscle cells in the RSCM constructs maintained their receptor integrity after being around the composite chitosan scaffold for 14 days. Smooth muscle relaxation has been documented to be dependent on protein kinase PKA [37, 38]. There was no difference in relaxation response between the constructs taken off the scaffold and the control constructs, which proves again that chitosan did not

affect the receptors on the smooth muscle cells. Preincubation of our bioengineered constructs in a medium containing PKA inhibitor abolished the relaxation seen with VIP (data not shown), which means that the intracellular signaling pathway leading to relaxation was also preserved. Our constructs produced only a fraction of the contractile response (13%) compared to muscle strips from rabbit sigmoid native colon tissues (data not shown). The difference in response compared to native tissue was reported in previous studies using vascular smooth muscle cells [39, 40].

Alignment of smooth muscle cells is essential for muscle peristaltic function and therefore for the coordination of motility. To date, several scaffolds have been successfully seeded with smooth muscle cells and have shown to be capable of maintaining the smooth muscle characteristics. However, these structures lack the orientation of the native tissue, which is considered as the gold standard for treating colonic motility. Until today, no work has been done to successfully bioengineer concentrically oriented smooth muscle tissue constructs however our bioengineered constructs are expected to provide promising results in regenerating gut motility and functionality. Hori et. al. have used collagen sponges seeded with mesenchymal stem cells to reconstruct the intestine. Their results showed cells positively stained with  $\alpha$ -SMA on the scaffold but there was no regeneration of the muscle layer [33]. Our model suggests the potential use of chitosan as an appealing biomaterial in the field of intestinal regeneration. Chitosan can easily form a porous tubular scaffold that can serve as a temporary support for physiologically functional smooth muscle constructs. In this study, we

provide evidence that RCSM constructs exhibited fundamental functional characteristics of intestinal tissues. In the future, it will be necessary to include other cell types in the bioengineering of these muscle constructs in order to gain higher force.

## **5. Conclusion:**

Tissue engineering of the intestine imposes the challenge of regeneration the smooth muscle layer. This present study describes the use of chitosan as a biomaterial in intestinal tissue engineering applications. The use of aligned smooth muscle constructs is beneficial to the restoration of intestinal motility and propulsion of the intestinal content. The evidence of functionality of the smooth muscle constructs after being placed around the composite chitosan scaffold suggests the potential use of this biomaterial to produce a functional tissue. Ongoing work in our laboratory aims to create a continuous circular smooth muscle layer around the tubular scaffold and to characterize its physiological functionality and mechanical properties. Additional studies also intend to explore the ability of chitosan to support the regeneration of the intestine.

## **6. Acknowledgment:**

The authors would like to thank Sita Somara and Saranyaraajan Varadarajan for their assistance with this study and the colleagues at Wake Forest Institute for Regenerative Medicine for providing assistance with the microscopy. The authors gratefully acknowledge the funding support provided by National Institutes of Health RO1 DK-042876 and RO1 DK-071614.



***The work described in this chapter demonstrated the biocompatibility of chitosan using gut-derived smooth muscle cells as a first step for engineering the neuro-musculature of the GI tract. This was shown by maintenance of morphology, phenotype and function of smooth muscle. The next step was to demonstrate the biocompatibility of chitosan using neural progenitor cells, which will be described in the next chapter.***

## 7. References:

- [1] Cosnes J, Gendre JP, Le Quintrec Y. Role of the ileocecal valve and site of intestinal resection in malabsorption after extensive small bowel resection. *Digestion*. 1978;18:329-36.
- [2] Galea MH, Holliday H, Carachi R, Kapila L. Short-bowel syndrome: a collective review. *J Pediatr Surg*. 1992;27:592-6.
- [3] Schmidt T, Pfeiffer A, Hackelsberger N, Widmer R, Meisel C, Kaess H. Effect of intestinal resection on human small bowel motility. *Gut*. 1996;38:859-63.
- [4] Kato T, Ruiz P, Thompson JF, Eskind LB, Weppler D, Khan FA, et al. Intestinal and multivisceral transplantation. *World J Surg*. 2002;26:226-37.
- [5] Gillian B. Quality of life issues: parenteral nutrition to small bowel transplantation—a review. *Nutrition*. 1998;14:813-6.
- [6] Janson DD. Commentary on "Three years clinical experience with intestinal transplantation" and the nutritional implications. 1994. *Nutr Clin Pract*. 2002;17:361-4.
- [7] Grikscheit TC, Siddique A, Ochoa ER, Srinivasan A, Alsberg E, Hodin RA, et al. Tissue-engineered small intestine improves recovery after massive small bowel resection. *Ann Surg*. 2004;240:748-54.
- [8] Gupta A, Vara DS, Punshon G, Sales KM, Winslet MC, Seifalian AM. In vitro small intestinal epithelial cell growth on a nanocomposite polycaprolactone scaffold. *Biotechnol Appl Biochem*. 2009;54:221-9.
- [9] Hori Y, Nakamura T, Matsumoto K, Kurokawa Y, Satomi S, Shimizu Y. Tissue engineering of the small intestine by acellular collagen sponge scaffold grafting. *Int J Artif Organs*. 2001;24:50-4.

- [10] Nakase Y, Hagiwara A, Nakamura T, Kin S, Nakashima S, Yoshikawa T, et al. Tissue engineering of small intestinal tissue using collagen sponge scaffolds seeded with smooth muscle cells. *Tissue Eng.* 2006;12:403-12.
- [11] Sachlos E, Gotor D, Czernuszka JT. Collagen scaffolds reinforced with biomimetic composite nano-sized carbonate-substituted hydroxyapatite crystals and shaped by rapid prototyping to contain internal microchannels. *Tissue Eng.* 2006;12:2479-87.
- [12] Di Martino A, Sittlinger M, Risbud MV. Chitosan: A versatile biopolymer for orthopaedic tissue-engineering. *Biomaterials.* 2005;26:5983-90.
- [13] Francis Suh JK, Matthew HWT. Application of chitosan-based polysaccharide biomaterials in cartilage tissue engineering: a review. *Biomaterials.* 2000;21:2589-98.
- [14] Kim IY, Seo SJ, Moon HS, Yoo MK, Park IY, Kim BC, et al. Chitosan and its derivatives for tissue engineering applications. *Biotechnol Adv.* 2008;26:1-21.
- [15] Madihally SV, Matthew HW. Porous chitosan scaffolds for tissue engineering. *Biomaterials.* 1999;20:1133-42.
- [16] VandeVord PJ, Matthew HW, DeSilva SP, Mayton L, Wu B, Wooley PH. Evaluation of the biocompatibility of a chitosan scaffold in mice. *J Biomed Mater Res.* 2002;59:585-90.
- [17] Ma L, Gao C, Mao Z, Zhou J, Shen J, Hu X, et al. Collagen/chitosan porous scaffolds with improved biostability for skin tissue engineering. *Biomaterials.* 2003;24:4833-41.
- [18] Tare MN, Domard A. Collagen and its interactions with chitosan, III some biological and mechanical properties. *Biomaterials.* 1996;17:451-5.
- [19] Mhurchu CN, Poppitt SD, McGill AT, Leahy FE, Bennett DA, Lin RB, et al. The effect of the dietary supplement, Chitosan, on body weight: a randomised controlled trial in 250 overweight and obese adults. *Int J Obes Relat Metab Disord.* 2004;28:1149-56.

- [20] Mhurchu CN, Dunshea-Mooij C, Bennett D, Rodgers A. Effect of chitosan on weight loss in overweight and obese individuals: a systematic review of randomized controlled trials. *Obes Rev.* 2005;6:35-42.
- [21] Muzzarelli RAA. Chitosan-based dietary foods. *Carbohydr Polym.* 1996;29:309-16.
- [22] Hecker L, Baar K, Dennis RG, Bitar KN. Development of a three-dimensional physiological model of the internal anal sphincter bioengineered in vitro from isolated smooth muscle cells. *Am J Physiol Gastrointest Liver Physiol.* 2005;289:G188-96.
- [23] Somara S, Gilmont RR, Varadarajan S, Bitar KN. Phosphorylated HSP20 modulates the association of thin-filament binding proteins: caldesmon with tropomyosin in colonic smooth muscle. *Am J Physiol Gastrointest Liver Physiol.* 2010;299:G1164-76.
- [24] Uygun BE, Stojish SE, Matthew HW. Effects of immobilized glycosaminoglycans on the proliferation and differentiation of mesenchymal stem cells. *Tissue Eng Part A.* 2009;15:3499-512.
- [25] Somara S, Gilmont RR, Dennis RG, Bitar KN. Bioengineered internal anal sphincter derived from isolated human internal anal sphincter smooth muscle cells. *Gastroenterology.* 2009;137:53-61.
- [26] Krupnick AS, Morris JB. The long-term results of resection and multiple resections in Crohn's disease. *Semin Gastrointest Dis.* 2000;11:41-51.
- [27] Lee M, Wu BM, Stelzner M, Reichardt HM, Dunn JC. Intestinal smooth muscle cell maintenance by basic fibroblast growth factor. *Tissue Eng Part A.* 2008;14:1395-402.
- [28] Raghavan S, Lam MT, Foster LL, Gilmont RR, Somara S, Takayama S, et al. Bioengineered three-dimensional physiological model of colonic longitudinal smooth muscle in vitro. *Tissue Eng Part C Methods.* 2010;16:999-1009.
- [29] Sarkar S, Dadhania M, Rourke P, Desai TA, Wong JY. Vascular tissue engineering: microtextured scaffold templates to control organization of vascular smooth muscle cells and extracellular matrix. *Acta Biomater.* 2005;1:93-100.

- [30] Xu CY, Inai R, Kotaki M, Ramakrishna S. Aligned biodegradable nanofibrous structure: a potential scaffold for blood vessel engineering. *Biomaterials*. 2004;25:877-86.
- [31] Hu X, Huang J, Ye Z, Xia L, Li M, Lv B, et al. A novel scaffold with longitudinally oriented microchannels promotes peripheral nerve regeneration. *Tissue Eng Part A*. 2009;15:3297-308.
- [32] de Toledo OMS, Marquezini MV, Jia KB, Pinheiro MdC, Mora OA. Biochemical and Cytochemical Characterization of Extracellular Proteoglycans in the Inner Circular Smooth Muscle Layer of Dog Small Intestine. *IUBMB Life*. 2002;54:19-25.
- [33] Hori Y, Nakamura T, Kimura D, Kaino K, Kurokawa Y, Satomi S, et al. Experimental study on tissue engineering of the small intestine by mesenchymal stem cell seeding. *J Surg Res*. 2002;102:156-60.
- [34] Grikscheit TC, Ochoa ER, Ramsanahie A, Alsberg E, Mooney D, Whang EE, et al. Tissue-engineered large intestine resembles native colon with appropriate in vitro physiology and architecture. *Ann Surg*. 2003;238:35-41.
- [35] An JY, Yun HS, Lee YP, Yang SJ, Shim JO, Jeong JH, et al. The intracellular pathway of the acetylcholine-induced contraction in cat detrusor muscle cells. *Br J Pharmacol*. 2002;137:1001-10.
- [36] Hosey MM. Diversity of Structure, Signaling and Regulation within the Family of Muscarinic Cholinergic Receptors. *Faseb J*. 1992;6:845-52.
- [37] Van Geldre LA, Lefebvre RA. Interaction of NO and VIP in gastrointestinal smooth muscle relaxation. *Curr Pharm Des*. 2004;10:2483-97.
- [38] Murthy KS, Makhoul GM. Interaction of cA-kinase and cG-kinase in mediating relaxation of dispersed smooth muscle cells. *Am J Physiol*. 1995;268:C171-80.

[39] Neff LP, Tillman BW, Yazdani SK, Machingal MA, Yoo JJ, Soker S, et al. Vascular smooth muscle enhances functionality of tissue-engineered blood vessels in vivo. *J Vasc Surg.* 2011;53:426-34.

[40] L'Heureux N, Stoclet JC, Auger FA, Lagaud GJ, Germain L, Andriantsitohaina R. A human tissue-engineered vascular media: a new model for pharmacological studies of contractile responses. *Faseb J.* 2001;15:515-24.

# **CHAPTER VI: NEO-INNervation OF A BIOENGINEERED INTESTINAL SMOOTH MUSCLE CONSTRUCT AROUND CHITOSAN SCAFFOLD**

Elie Zakhem, Shreya Raghavan and Khalil N Bitar

Wake Forest Institute for Regenerative Medicine, Wake Forest School of  
Medicine,

Winston-Salem NC

***The work described in this chapter demonstrated the biocompatibility of  
chitosan using neural progenitor cells.***

***This manuscript was accepted for publication in Biomaterials 2014; 35(6): 1882-9***

## ABSTRACT

Neuromuscular disorders of the gut result in disturbances in gastrointestinal transit. The objective of this study was to evaluate the neo-innervation of smooth muscle in an attempt to restore lost innervation. We have previously shown the potential use of composite chitosan scaffolds as support for intestinal smooth muscle constructs. However, the constructs lacked neuronal component. Here, we bioengineered innervated colonic smooth muscle constructs using rabbit colon smooth muscle and enteric neural progenitor cells. We also bioengineered smooth muscle only tissue constructs using colonic smooth muscle cells. The constructs were placed next to each other around tubular chitosan scaffolds and left in culture. Real time force generation conducted on the intrinsically innervated smooth muscle constructs showed differentiated functional neurons. The bioengineered smooth muscle only constructs became neo-innervated. The neo-innervation results were confirmed by immunostaining assays. Chitosan supported (1) the differentiation of neural progenitor cells in the constructs and (2) the neo-innervation of non-innervated smooth muscle around the same scaffold.

### **Keywords:**

Chitosan, Neo-innervation, Enteric neural progenitor cells, Force generation, Smooth muscle constructs



## 1. Introduction:

The large intestine has an extensive intrinsic innervation through the enteric nervous system (ENS). It displays a coordinated contraction/relaxation process known as peristalsis. The ENS and the smooth muscle are two major regulators of motility patterns in the colon [1, 2]. Neuromuscular diseases of the gastrointestinal tract result in dysmotility due to impaired peristalsis. Hirschsprung's disease is a well-understood neuropathic disorder of the ENS characterized by the absence of intrinsic enteric innervation at variable lengths of the distal colon. Symptoms of hirschsprung's disease include distention of the abdomen, megacolon and inability to defecate [3-5]. Current treatments include surgical removal of the defective, aganglionic section of the bowel. However, the outcome of these surgeries is associated with post-operative complications and poor long-term quality of life [6]. Hirschsprung's disease and other diseases affecting the large intestine represent targets for tissue engineering and regenerative therapies.

Attempts to regenerate the enteric nervous system involve cell transplantation as a therapeutic strategy to treat neurodegenerative disorders of the gut. The therapeutic use of neural stem cells derived from the central nervous system for gastrointestinal disorders was initially evaluated [7]. Neural stem cells were isolated from rat central nervous system and transplanted into denervated rat recta [8]. Following transplantation, differentiation of the cells into neurons and glial cells was observed in the aganglionic rectum. A recent study aimed to

deliver colon-derived neural crest progenitor cells to denervated areas of the colon [9]. Differentiation of the neurons was observed with partial restoration of functionality. While these results are promising, cell transplantation therapy requires additional studies to optimize the survival, differentiation and source of the neural stem cells [10, 11]. In our study, we employ a tissue engineering approach where we use post-migratory adult enteric neural progenitor cells in combination with gut smooth muscle cells to neo-innervate bioengineered smooth muscle tissue construct around chitosan scaffold.

Different scaffolds have been engineered to promote neuronal regeneration. Chitosan scaffolds have gained special attention in supporting neural stem cells survival and differentiation [12-14]. Wang et. al. studied the use of chitosan matrices and demonstrated their ability to promote neural stem cell proliferation and differentiation [15]. In recent studies, neural stem cells were obtained from animal brains and seeded onto chitosan scaffolds to investigate the ability to repair spinal cord injury. Chitosan was reported to support neural stem cells survival, proliferation and differentiation [16]. However, there are no studies reporting the use of chitosan to support the differentiation of gut-derived enteric neural progenitor cells in an attempt to treat neuromuscular disorders of the gut.

We have previously demonstrated the potential use of chitosan based scaffolds to support bioengineered circular smooth muscle constructs [17]. The constructs mimicked the architecture of the circular smooth muscle layer of the intestine. However, the constructs lacked the neuronal circuitry which will be

required to coordinate motility. Here, we bioengineered concentrically aligned circular smooth muscle constructs by co-culturing gut-derived neural progenitor cells and intestinal smooth muscle cells. The aim of this study was to evaluate the ability of the enteric neural progenitor cells to differentiate into neurons around chitosan scaffolds and to evaluate the neo-innervation of smooth muscle tissues around the same scaffold.

## **2. Materials and methods**

### **2.1. *Reagents***

All cell culture reagents including growth medium and supplements were purchased from Invitrogen (Carlsbad, CA). Growth media for smooth muscle consisted of Dulbecco's modified Eagle medium (DMEM) supplemented with 10% fetal bovine serum (FBS), 1.5% antibiotic-antimycotic, and 0.6% l-glutamine. Growth media for neural progenitor cells consisted of neurobasal, N2 supplement and antibiotic-antimycotic. Neural differentiation media consisted of neurobasal medium-A supplemented with fetal calf serum, B27 supplement and antibiotic-antimycotic. Collagenase type II was purchased from Worthington Biochemicals (Lakewood, NJ). Type I rat tail collagen was purchased from BD Biosciences (Bedford, MA), and Hank's balanced salt solution (HBSS) was purchased from Hyclone (Logan, UT). Medium molecular weight chitosan (75–85% deacetylation), glycosaminoglycan heparan sulfate, 1-ethyl-3-(3-dimethylaminopropyl) carbodiimide (EDC), acetylcholine (ACh), vasoactive intestinal peptide (VIP) and tetrodotoxin (TTX) were purchased from Sigma (St.

Louis, MO). Sylgard [poly(dimethylsiloxane); PDMS] was from World Precision Instruments (Sarasota, FL).

## ***2.2. Isolation of rabbit colonic circular smooth muscle cells and enteric neural progenitor cells***

Rabbit colonic circular smooth muscle cells (RCSMCs) were isolated as described previously from rabbit sigmoid colon [18]. Briefly, colon tissue was cleaned and washed in ice-cold HBSS. The serosa, longitudinal smooth muscle and mucosa were removed. The circular smooth muscle was finely minced, digested twice in type II Collagenase (Worthington), and filtered to eliminate cellular debris. Digested cells were washed, resuspended in growth media and plated on tissue culture flasks. Cells were grown to confluence before use in the experiments.

Neuronal progenitor cells were isolated as described previously [19]. Briefly, a biopsy of rabbit jejunum was cleaned of any material using HBSS. The tissue was minced and digested in a collagenase/dispase mixture. The cell suspension was then filtered through a 40µm mesh and plated on petri dishes.

## ***2.3. Preparation of composite chitosan scaffolds***

Composite chitosan scaffolds were prepared as described previously [17, 20]. Briefly, the 2 w/v % chitosan solution was mixed with type I collagen (0.1 mg/ml) in a volume ratio of 1:1. The mixture was poured into a tubular mold with a central opening, frozen at -80 °C for 3 h and then lyophilized for 24 h. The scaffolds were neutralized in 0.2 M NaOH and covalently cross linked with

heparan sulfate using EDC. The scaffolds were then washed several times with PBS and distilled water. The scaffolds were UV sterilized and then coated with laminin (0.05 mg/ml) for 2 hours at room temperature.

#### ***2.4. Bioengineering of three-dimensional rabbit colon smooth muscle constructs:***

Intrinsically innervated, concentrically aligned, smooth muscle constructs were bioengineered following the method used previously with bioengineered internal anal sphincters [21]. Collagen/laminin gel containing  $2 \times 10^5$  rabbit neural progenitor cells was overlaid down on a Sylgard-coated plate with a central cylindrical post. A second layer of collagen gel containing  $5 \times 10^5$  rabbit colon circular smooth muscle cells was overlaid down on top of the first layer of gel. After gelation, neural differentiation media was added to the plate and incubated at  $37^{\circ}\text{C}$ . Three-dimensional circular smooth muscle constructs were bioengineered by laying down  $5 \times 10^5$  rabbit colon circular smooth muscle cells in collagen gel on a Sylgard-coated plate with a central post. After gelation, the same neural differentiation media was added to the plate. Both bioengineered smooth muscle tissue constructs were placed next to each other around the same tubular composite chitosan scaffold.

#### ***2.5. Microscopic evaluation of the constructs***

Five days post-placing the constructs around the scaffold, microscopic analysis of the junction between the two bioengineered smooth muscle constructs was evaluated. The scaffolds with the constructs were left in neural differentiation media for a period of 16 days, at the end of which, each construct

was taken off the scaffold. Microscopic evaluation was conducted on each construct.

## *2.6. Measurement of physiological functionality of the constructs*

The protocol for physiologic functionality was described previously [21]. An isometric force transducer (Harvard Apparatus, Holliston, MA) was used to record real time force generated by the constructs. The constructs were kept incubated in a warm tissue bath keeping the tissue samples at  $37^{\circ}\text{C} \pm 1^{\circ}\text{C}$ . The bioengineered tissue constructs were taken off the scaffold at days 16 for force generation measurement. One side of the tissue constructs was looped around the measuring arm of the transducer and the other side was attached to a fixed reference pin. Tissue constructs were allowed to equilibrate in the tissue bath containing fresh medium. All reported values of force represent active tension produced as a result of the tissue. After establishment of baseline, a 10%–15% stretch was applied to the tissues using the micromanipulator. The stretch baseline established by the tissue samples was arbitrarily set to zero and the values represent change in force generation.

Testing protocols were designed to determine the feasibility of neo-innervation of the smooth muscle construct that initially lacked neural progenitor cells. Electromechanical coupling was tested using potassium chloride (KCl) in the absence and presence of calcium channel blocker nifedipine. Cholinergic contraction was studied using acetylcholine (Ach) in the absence and presence of TTX. Relaxation was evaluated by studying the effect of vasoactive intestinal peptide (VIP) and electrical field stimulation, in the absence and presence of

nerve blocker tetrodotoxin (TTX). The tissues were washed with fresh buffer between each experiment.

### ***2.7. Immunofluorescence of bioengineered constructs***

Sixteen days post placing them around the scaffolds, constructs were taken off and were fixed in 3.7% formaldehyde and paraffin-embed. Cross sections of 6 $\mu$ m thickness were obtained using a microtome. Sections were then deparaffinized and rehydrated. Immunostaining analysis for smooth muscle specific Caldesmon (c-4562; Sigma) and neuron specific  $\beta$ -III tubulin (ab25770, Abcam) were performed on both constructs. Slides were visualized using a Nikon Ti-E fluorescence microscope (Tokyo, Japan).

### ***2.8. Data analysis***

GraphPad Prism 5.01 for Windows (GraphPad Software, San Diego CA; [www.graphpad.com](http://www.graphpad.com)) was used to analyze acquired force generation data. All values were expressed as means and SEM of 3-5 experiments. Second order Savitzky–Golay smoothing was applied to raw data. Student paired t-test was used to compare the means of forces in the absence and presence of neurotoxin TTX. A *p*-value less than 0.05 was considered significant.

## **3. Results:**

### ***3.1. Analysis of the bioengineered constructs:***

Rabbit colon circular smooth muscle cells were overlaid along with rabbit enteric neural progenitor cells in a collagen/laminin gel. Neural differentiation media was supplied to the constructs every other day. The process of the

bioengineering is shown in **Figure 14**. **Figure 14** A&D show the smooth muscle cells and neural progenitor cells in co-culture at day 0. At day 1, the cells are concentrically aligning around the post in the center of the plate (**Figure 14** B&E). At day 4, **Figure 14** C&F show a fully formed bioengineered colon smooth muscle construct with enteric neural progenitor cells arranged towards the periphery of the construct. At day 4 post formation, the constructs were placed around the chitosan scaffold.

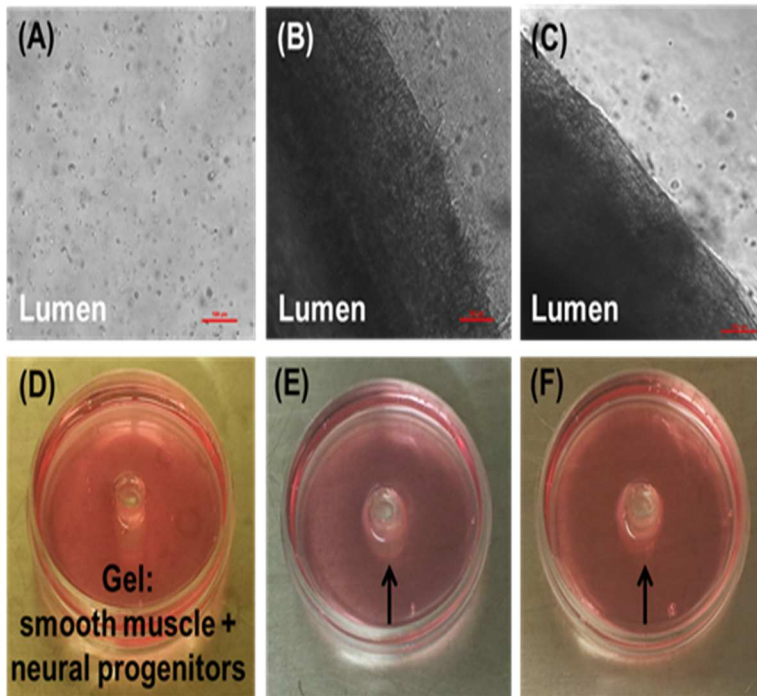


**Figure 14:** Bioengineering innervated constructs: Evaluation of the bioengineering process of the innervated smooth muscle construct. Microscopic images at day 0 (A), day 1 (B) and day 4 (C) show the cells aligning concentrically around the lumen. Macroscopic images at day 0 (D), day 1 (E) and day 4 (F) show the construct fully formed around the central post by day 4.

### 3.2. Microscopic evaluation of the bioengineered constructs

The smooth muscle construct containing neural progenitor cells was placed attached to a smooth muscle construct lacking neural progenitor cells around the same composite chitosan scaffold (**Figure 15A**). The scaffold along



with the constructs was incubated in neural differentiation media. Day 5 post-placing the constructs around the scaffold, microscopic evaluation of the junction between the 2 constructs was evaluated. **Figure 15B** shows elongated cellular processes bridging the constructs and forming a continuous network.

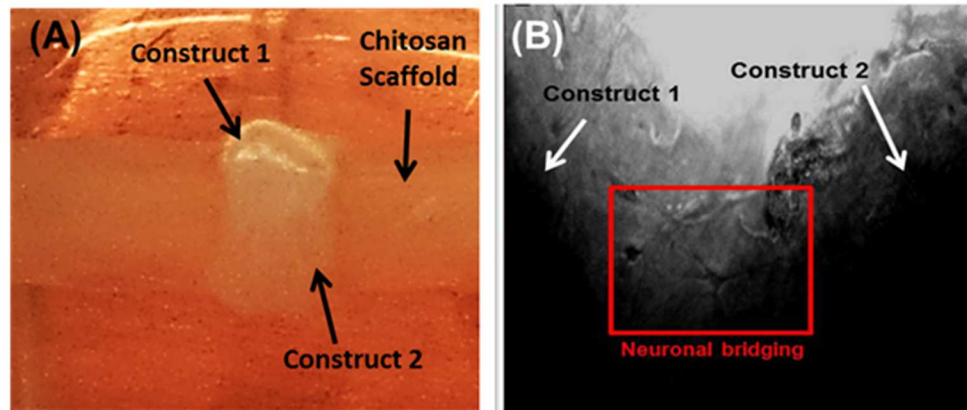


**Figure 15:** Constructs around scaffold: (A) Both bioengineered colonic smooth muscle tissue constructs were placed next to each other around the same chitosan based scaffold. (B) Microscopic image of the junction between the 2 constructs showing cellular processes bridging the constructs. Construct 1 is the construct that initially contained enteric neural progenitor cells. Construct 2 is the construct that lacked enteric neural progenitor cells.

At day 16, both tissue constructs were taken off the scaffold and were microscopically evaluated. **Figure 16A** shows axonal projections forming in the construct that initially contained neural progenitor cells. Cellular projections were also visualized in the smooth muscle construct that was initially lacking neural progenitor cells (**Figure 16B**).

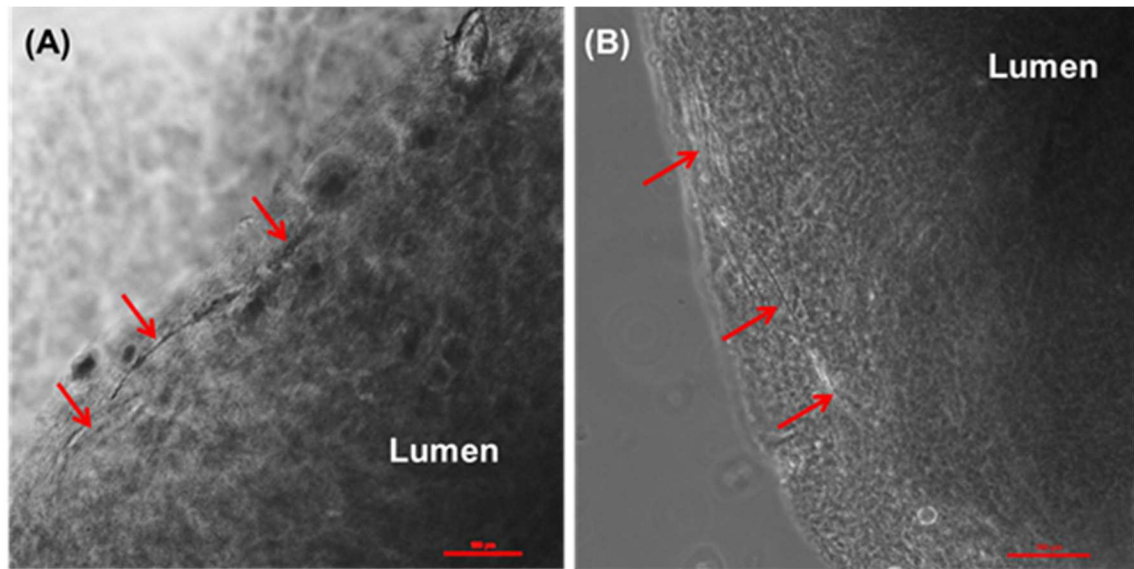


**Figure 16:** Microscopic evaluation of the constructs: (A) Initially innervated smooth muscle construct was taken off the scaffold. Microscopic analysis reveals differentiated neuronal projections (red arrows). (B) The neo-innervated smooth muscle construct was taken off the scaffold. Microscopic view of the periphery of the construct shows cells with neural-like phenotype (red arrows). The luminal side of each construct is indicated.

### 3.3. *Physiologic functionality of the constructs:*

The constructs were left around the composite chitosan scaffold for a period of 16 days, at the end of which they were taken off. Physiological functionality of the constructs was evaluated using real time force generation.

### a) Contractile response:

To test the electromechanical coupling integrity in the smooth muscle, the constructs were treated with 60 mM KCl. A rapid-rising contraction was generated in the intrinsically innervated constructs (**Figure 17A**) and in the neo-innervated constructs (**Figure 17B**). An average contraction of  $300 \pm 24 \mu\text{N}$  was seen in the innervated constructs and  $224 \pm 42 \mu\text{N}$  in the non-innervated constructs. In the presence of calcium channels blocker nifedipine, the same concentration of KCl did not induce an equivalent contraction in either constructs (green tracings) suggesting the presence and maintenance of calcium channels in these constructs. Response to KCl shows the maintenance of the integrity of the smooth muscle component.

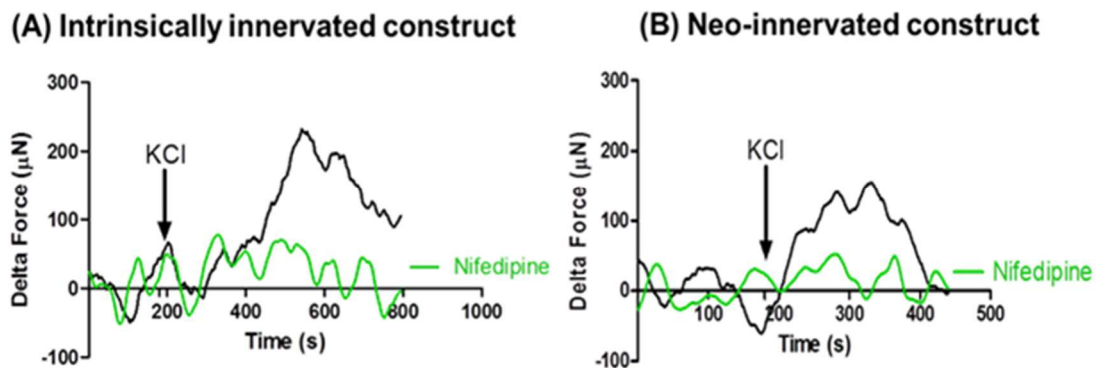


**Figure 17:** Physiological functionality: KCl response. Smooth muscle constructs were taken off the scaffold and physiological studies were performed. (A) Intrinsically innervated construct: As the baseline was established, treatment with 60 mM KCl caused an increase in force generation. (B) Neo-innervated construct: The construct exhibited a robust response to KCl. Constructs recovered back to baseline. Addition of calcium channel blocker, Nifedipine, inhibited contraction of both constructs in response to KCl (green trace).

Cholinergic contraction was studied using acetylcholine (Ach). Treatment with 1  $\mu$ M Ach induced immediate contractions in the intrinsically innervated constructs with an average contraction of  $150 \pm 26$   $\mu$ N (**Figure 18A**). An immediate rise in force generation was also seen in the neo-innervated constructs with an average contraction of  $130 \pm 24$   $\mu$ N (**Figure 18B**). Peak maximal contractions in the intrinsically innervated constructs were attenuated by 50-60% in the presence of the neuronal blocker TTX (**Figure 18A**, red tracing). Similarly, TTX reduced the maximal contraction in the neo-innervated constructs (**Figure 18B**, red tracing). Constructs were able to return back to the resting basal force. In both constructs, contractile responses induced by the excitatory neurotransmitter Ach displayed a neuronal component (contraction without TTX) as well as a myogenic component (contraction in presence of TTX).

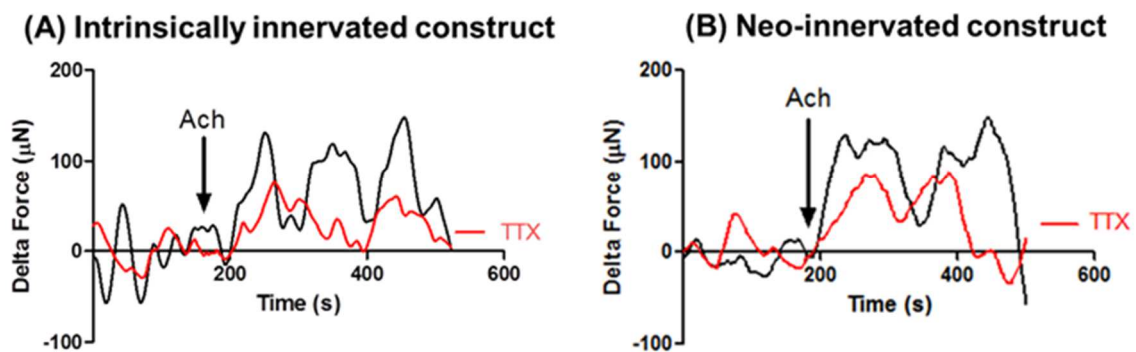


**Figure 18:** Physiological functionality: Ach response. Cholinergic contraction was studied using acetylcholine (Ach). (A) Intrinsically innervated construct: Treatment with Ach caused a rapid and sustained contraction. Construct recovered back to baseline. Pre-treatment of the constructs with TTX (red trace) attenuated the contraction in response to Ach by 50%. The arrow indicates the time of treatment with Ach. (B) Neo-innervated construct: When baseline was established, treatment with Ach caused a rapid and sustained contraction. In the presence of TTX, the same dose of Ach caused a contraction reduced by 30-40% (red trace).

### b) Relaxation response:

Relaxation of these constructs was first studied by treatment with VIP (**Figure 19**). Addition of 1  $\mu\text{M}$  VIP induced a rapid decrease of baseline with a maximal relaxation averaging  $175 \pm 10 \mu\text{N}$  in the intrinsically innervated constructs and  $147 \pm 28 \mu\text{N}$  in the neo-innervated constructs. In the presence of TTX, the same concentration of VIP induced an attenuated relaxation (60% inhibition) in the intrinsically innervated constructs (red tracing). TTX also inhibited (50%) the relaxation in response to VIP in the neo-innervated constructs (red tracing). The responses of both constructs to VIP in the absence and presence of TTX indicate the involvement of myogenic and neuronal component.

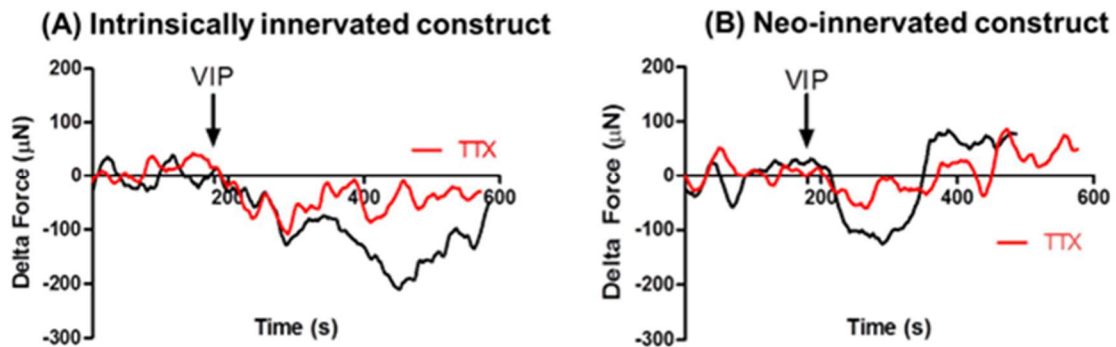


**Figure 19:** Physiological functionality: VIP response. Relaxation of the constructs was studied using vasoactive intestinal peptide (VIP). (A) Intrinsically innervated construct: The construct exhibited a reduction in the basal force. The construct recovered back to baseline. In the presence of TTX, VIP caused a relaxation with 50-60% inhibition (red trace). (B) Neo-innervated construct: When the construct established baseline, treatment with VIP caused a relaxation followed by recovery back to baseline. Pre-treatment of the construct with TTX attenuated the magnitude of relaxation by 50% (red trace).

Electric field stimulation (EFS) of the bioengineered colonic smooth muscle tissue constructs at 8 Hz, 0.9ms induced a rapid relaxation of the basal force followed by recovery back to baseline (**Figure 20**). An average relaxation of  $291 \pm 13 \mu\text{N}$  was assessed in the intrinsically innervated constructs. Preincubating these constructs with TTX completely abolished the response to EFS indicating that the relaxation originated from the stimulation of fully differentiated intrinsic neurons (red tracing). Same parameters of EFS applied to the neo-innervated constructs caused a relaxation with an average of  $125 \pm 15 \mu\text{N}$ . The relaxation was completely blocked in the presence of TTX (red tracing). This indicates that the relaxation was partially neuronally mediated in these constructs as well.

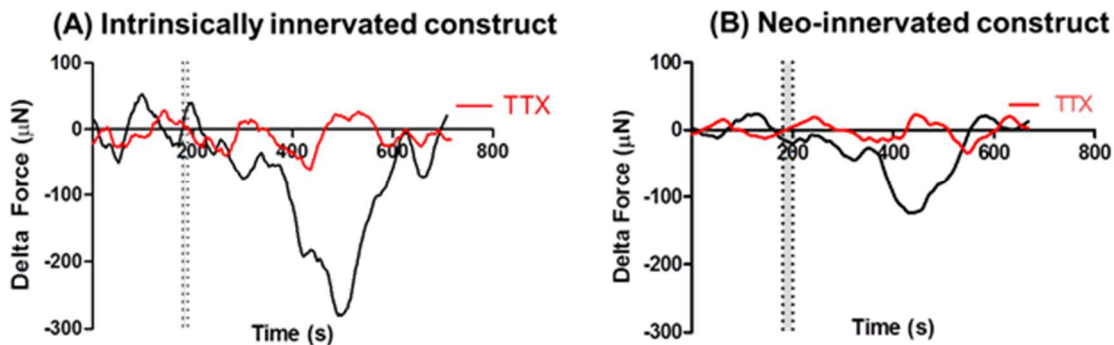


**Figure 20:** Physiological functionality: EFS response. Relaxation studied by electric field stimulation (EFS). (A) Intrinsically innervated construct: When the construct established baseline, electric field stimulation caused a decrease in basal force. Construct recovered back to baseline. TTX completely abolished relaxation by EFS (red trace). (B) Neo-innervated construct: Treatment of the construct with EFS caused a relaxation. Pre-treatment of the construct with TTX inhibited the relaxation seen with EFS (red trace).

### 3.4. Immunofluorescence of bioengineered constructs

Both bioengineered smooth muscle constructs were taken off the scaffold at day 16, fixed in 3.7% formaldehyde and embedded in paraffin.

Immunofluorescence assays demonstrated positive stain for smooth muscle specific Caldesmon, indicating a contractile smooth muscle phenotype in both constructs (**Figure 21**). Cross-sections of the intrinsically innervated constructs stained positive for the neuron-specific marker  $\beta$ -III tubulin confirming neuronal differentiation. The neo-innervation was confirmed by the positive  $\beta$ -III tubulin stain of the constructs (**Figure 22**). Immunofluorescence demonstrated the presence of functional neurons in both constructs.

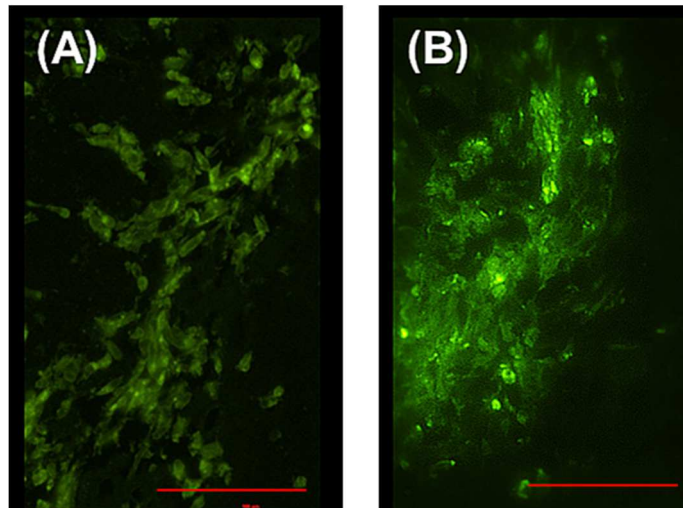


**Figure 21:** Smooth muscle phenotype: Bioengineered (A) intrinsically innervated construct and (B) neo-innervated construct showed positive stain for smooth muscle specific heavy Caldesmon indicating smooth muscle phenotypic characteristics in the constructs.



#### 4. Discussion:

The enteric neurons coordinate the activity of the smooth muscle of the gastrointestinal tract. This coordination is necessary for proper peristaltic patterns required for postprandial mixing and motility. Neuromuscular diseases of the large intestine are associated with loss or dysfunction of the smooth muscle as well as the enteric neurons resulting in gut paralysis and dysmotility. Regeneration of both the smooth muscle and the enteric neurons is critical to ensure proper motility in the colon. Here, we showed that chitosan scaffolds support enteric neural progenitor cells differentiation and promote neo-innervation of bioengineered smooth muscle constructs.

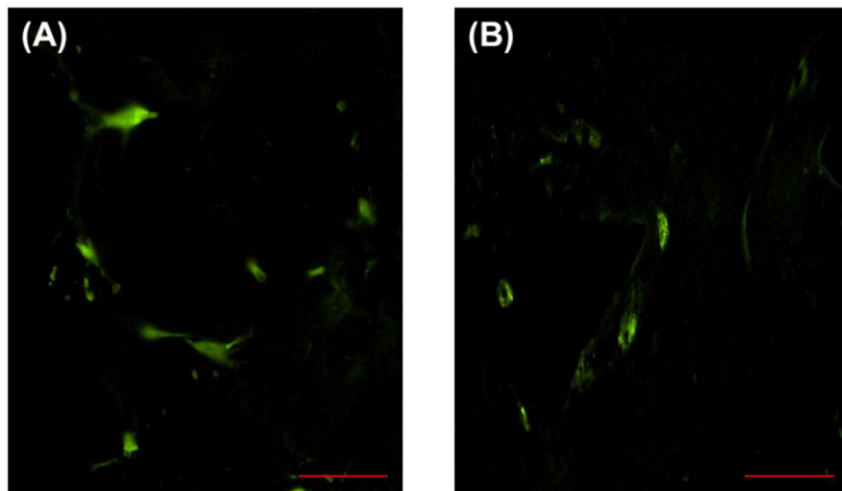


**Figure 22:** IHC neo-innervation: (A) The intrinsically innervated construct stained positive for neural specific marker  $\beta$ -III Tubulin indicating the presence of differentiated neurons in the constructs. (B) The neo-innervated construct also stained positive for  $\beta$ -III Tubulin, indicating the emergence of new differentiated neurons.



Regenerative medicine approaches to repair neural tissues considered the use of scaffolds combined with bioactive components to provide a microenvironment for cell survival and differentiation [22, 23]. In this study, laminin is used as a coating material. Laminin is one of the ECM components commonly used with chitosan to enhance axonal outgrowths and neural regeneration [24, 25]. Additionally, chitosan scaffolds were cross linked with heparan sulfate. Laminin and heparan sulfate are two molecules that are detected in the basement membrane of the enteric ganglia [26]. Incorporation of laminin and heparan sulfate into the chitosan scaffolds serves to mimic the extracellular matrix component of the enteric nervous system and the surrounding smooth muscle cells.

In intestinal tissue engineering, the proper architecture and innervation of the smooth muscle layers are crucial components for adequate functionality [27-29]. The use of organoid units in combination with synthetic polymers is being investigated for the potential to regenerate different layers of the intestine [30, 31]. We previously bioengineered concentrically aligned intestinal smooth muscle constructs to mimic the architecture of the circular smooth muscle layer of the intestine. We have also demonstrated that the constructs maintained physiological functionality around chitosan scaffolds. In this current study, we also incorporated a neuronal component in the bioengineered smooth muscle constructs to provide the necessary innervation around the chitosan scaffold.

Contractile phenotype of smooth muscle is an indicative of fully differentiated cells. In a recent study, intestinal smooth muscle cells were seeded

onto small intestinal submucosa [32]. Following implantation, contraction of the cell-seeded scaffold was assessed by immunostaining assays of contractile proteins (alpha smooth muscle actin, smooth muscle myosin heavy chain and calponin). The expression of these markers was variable at different time points. The maturation of the smooth muscle in our study was confirmed by the positive stain for smooth muscle specific heavy Caldesmon. Heavy Caldesmon is expressed specifically in differentiated smooth muscle and is a characteristic of the contractile state of smooth muscle cells [33]. This demonstrated that the smooth muscle cells did not dedifferentiate into a synthetic state.

Peristalsis and motility in the GI tract depend on smooth muscle activity which is controlled by the enteric neurons. Tissue engineering of the intestine attempts to restore motility by reinstating the contraction and relaxation patterns of the smooth muscle. Force generation studies were designed to test the differentiation of neurons and the neo-innervation of bioengineered smooth muscle. In the gut, smooth muscles are innervated by excitatory and inhibitory enteric neurons [34, 35]. Cholinergic contraction is mediated by the excitatory neurotransmitter acetylcholine, which is the principal contractile neurotransmitter in gastrointestinal motility [36]. Contractile activity is fundamental in propelling the luminal content throughout the colon. Our results indicated that TTX markedly reduced Ach contraction in the intrinsically innervated constructs, demonstrating the presence of differentiated enteric neurons that could be responsible for releasing Ach. The decrease in Ach contraction in the presence of TTX is consistent with our previous work with intrinsically innervated IAS constructs [21].

Neo-innervation of the abutting construct was demonstrated by the reduction in Ach contraction post treatment with TTX. In the presence of TTX, treatment with Ach caused a contraction that is lower in magnitude compared to Ach contraction in the absence of TTX. This showed that contraction was mediated by both a myogenic and neuronal component. The maintenance of smooth muscle electromechanical integrity was also demonstrated in both constructs by the inhibition of KCl contraction in the presence of nifedipine.

VIP is one of the neurotransmitters that contribute to inhibitory neurotransmission in the GI tract. It acts through VPAC1/2 receptors on the smooth muscle, causing the activation of adenylyl cyclase. This leads to the production of cAMP and activation of cAMP-dependent protein kinase A [37]. Both the intrinsically innervated and neo-innervated constructs relaxed rapidly in response to exogenous VIP, indicating the preservation of VIP receptors on the smooth muscle. The VIP relaxation in both constructs was shown to be TTX sensitive. This suggested that the response is partially mediated by VIP-ergic neurons that mediate inhibitory neurotransmission to the smooth muscle in both constructs. These results correlate well with our previous work involving TTX-sensitive VIP relaxation in intrinsically innervated constructs [21]. Constructs retained their ability to recover back to baseline.

Direct stimulation of the enteric neurons in the constructs was studied using EFS. EFS stimulated the release of neurotransmitters that caused relaxation in both, the intrinsically innervated and neo-innervated constructs. EFS-induced relaxation was completely abolished in the presence of TTX in both

constructs. These results indicated that relaxation was purely neuronally mediated. The parameters were previously used for direct stimulation of enteric neurons in colonic strips in vitro [38]. To further confirm the presence of differentiated neurons, constructs were stained for the neuronal marker  $\beta$ -III tubulin. Both constructs stained positive, therefore, differentiation of enteric neurons and neo-innervation occurred around chitosan scaffold.

Chitosan scaffolds have shown promising results in spinal cord injury repair, nerve regeneration and functional recovery [16, 39-41]. Here, we provide a proof of concept for the ability of chitosan scaffold to support (1) differentiation of enteric neural progenitor cells and (2) neo-innervation of smooth muscle. Loss of intrinsic innervation in large segments of the GI tract could have devastating impact on the quality of life of patients. The goal is to bioengineer larger, continuously innervated, smooth muscle tube that functions as a replacement. This study shows that gut-derived adult enteric neural progenitor cells can be used as a source to innervate smooth muscle around chitosan scaffolds. Further studies will require evaluating the distance that the neural progenitor cells can cross along smooth muscle around chitosan scaffold in order to ensure adequate innervation.

## **5. Conclusion:**

Intestinal tissue engineering aims to create functional tissue replacements. Peristalsis in the gut requires coordination between the smooth muscle and the enteric nervous system. This study showed that the use of chitosan is advantageous in tissue engineering GI neuromuscular segments. Chitosan

provides a promising material in combination with enteric neural progenitor cells. We show that enteric neural progenitor cells have the potential to innervate bioengineered smooth muscle constructs around the scaffold. We also provide an evidence of functionality of both the smooth muscle and the neuronal component of the constructs around chitosan scaffolds.

## **6. Acknowledgment:**

The authors would like to thank Robert Gilmont for his assistance with this study. The authors gratefully acknowledge the funding support provided by National Institutes of Health/DDK RO1 DK-042876 and RO1 DK-071614.

***The work described in this chapter demonstrated the biocompatibility of chitosan using the neural component of the neuro-muscular apparatus of the GI tract. Chitosan supported the survival, differentiation and function of the neurons.***

## 7. References:

- [1] Newgreen D, Young HM. Enteric nervous system: development and developmental disturbances--part 1. *Pediatric and developmental pathology : the official journal of the Society for Pediatric Pathology and the Paediatric Pathology Society*. 2002;5:224-47.
- [2] Goyal RK, Hirano I. The enteric nervous system. *N Engl J Med*. 1996;334:1106-15.
- [3] Furness JB. The enteric nervous system: normal functions and enteric neuropathies. *Neurogastroenterol Motil*. 2008;20 Suppl 1:32-8.
- [4] Knowles CH. New Horizons in the Pathogenesis of Gastrointestinal Neuromuscular Disease. *Journal of pediatric gastroenterology and nutrition*. 2007;45:S97-S102  
10.1097/MPG.0b013e31812e6569.
- [5] Brann L, Wood JD. Motility of the large intestine of piebald-lethal mice. *The American journal of digestive diseases*. 1976;21:633-40.
- [6] McKeown SJ, Stamp L, Hao MM, Young HM. Hirschsprung disease: a developmental disorder of the enteric nervous system. *Wiley Interdisciplinary Reviews: Developmental Biology*. 2013;2:113-29.
- [7] Kulkarni S, Zou B, Hanson J, Micci MA, Tiwari G, Becker L, et al. Gut-derived factors promote neurogenesis of CNS-neural stem cells and nudge their differentiation to an enteric-like neuronal phenotype. *Am J Physiol Gastrointest Liver Physiol*. 2011;301:G644-55.
- [8] Dong YL, Liu W, Gao YM, Wu RD, Zhang YH, Wang HF, et al. Neural stem cell transplantation rescues rectum function in the aganglionic rat. *Transplant Proc*. 2008;40:3646-52.
- [9] Pan WK, Zheng BJ, Gao Y, Qin H, Liu Y. Transplantation of neonatal gut neural crest progenitors reconstructs ganglionic function in benzalkonium chloride-treated homogenic rat colon. *The Journal of surgical research*. 2011;167:e221-30.

- [10] Peterson J, Pasricha PJ. Regenerative Medicine and the Gut. *Gastroenterology*. 2011;141:1162-6.e2.
- [11] Schafer KH, Micci MA, Pasricha PJ. Neural stem cell transplantation in the enteric nervous system: roadmaps and roadblocks. *Neurogastroenterology and motility : the official journal of the European Gastrointestinal Motility Society*. 2009;21:103-12.
- [12] Yang Z, Duan H, Mo L, Qiao H, Li X. The effect of the dosage of NT-3/chitosan carriers on the proliferation and differentiation of neural stem cells. *Biomaterials*. 2010;31:4846-54.
- [13] Leipzig ND, Wylie RG, Kim H, Shoichet MS. Differentiation of neural stem cells in three-dimensional growth factor-immobilized chitosan hydrogel scaffolds. *Biomaterials*. 2011;32:57-64.
- [14] Li X, Yang Z, Zhang A. The effect of neurotrophin-3/chitosan carriers on the proliferation and differentiation of neural stem cells. *Biomaterials*. 2009;30:4978-85.
- [15] Wang G, Ao Q, Gong K, Wang A, Zheng L, Gong Y, et al. The effect of topology of chitosan biomaterials on the differentiation and proliferation of neural stem cells. *Acta biomaterialia*. 2010;6:3630-9.
- [16] Zahir T, Nomura H, Guo XD, Kim H, Tator C, Morshead C, et al. Bioengineering neural stem/progenitor cell-coated tubes for spinal cord injury repair. *Cell transplantation*. 2008;17:245-54.
- [17] Zakhem E, Raghavan S, Gilmont RR, Bitar KN. Chitosan-based scaffolds for the support of smooth muscle constructs in intestinal tissue engineering. *Biomaterials*. 2012;33:4810-7.
- [18] Somara S, Gilmont RR, Varadarajan S, Bitar KN. Phosphorylated HSP20 modulates the association of thin-filament binding proteins: caldesmon with tropomyosin in colonic smooth muscle. *American journal of physiology Gastrointestinal and liver physiology*. 2010;299:G1164-76.

- [19] Raghavan S, Gilmont RR, Bitar KN. Neuroglial differentiation of adult enteric neuronal progenitor cells as a function of extracellular matrix composition. *Biomaterials*. 2013.
- [20] Uygun BE, Stojisic SE, Matthew HW. Effects of immobilized glycosaminoglycans on the proliferation and differentiation of mesenchymal stem cells. *Tissue engineering Part A*. 2009;15:3499-512.
- [21] Raghavan S, Gilmont RR, Miyasaka EA, Somara S, Srinivasan S, Teitelbaum DH, et al. Successful implantation of bioengineered, intrinsically innervated, human internal anal sphincter. *Gastroenterology*. 2011;141:310-9.
- [22] Zhong Y, Bellamkonda RV. Biomaterials for the central nervous system. *Journal of the Royal Society, Interface / the Royal Society*. 2008;5:957-75.
- [23] Orive G, Anitua E, Pedraz JL, Emerich DF. Biomaterials for promoting brain protection, repair and regeneration. *Nature reviews Neuroscience*. 2009;10:682-92.
- [24] Patel M, Mao L, Wu B, VandeVord P. GDNF blended chitosan nerve guides: an in vivo study. *Journal of biomedical materials research Part A*. 2009;90:154-65.
- [25] Itoh S, Suzuki M, Yamaguchi I, Takakuda K, Kobayashi H, Shinomiya K, et al. Development of a Nerve Scaffold Using a Tendon Chitosan Tube. *Artificial Organs*. 2003;27:1079-88.
- [26] Bannerman PC, Mirsky R, Jessen K, Timpl R, Duance V. Light microscopic immunolocalization of laminin, type IV collagen, nidogen, heparan sulphate proteoglycan and fibronectin in the enteric nervous system of rat and guinea pig. *J Neurocytol*. 1986;15:733-43.
- [27] Hori Y, Nakamura T, Matsumoto K, Kurokawa Y, Satomi S, Shimizu Y. Tissue engineering of the small intestine by acellular collagen sponge scaffold grafting. *The International journal of artificial organs*. 2001;24:50-4.



- [28] Nakase Y, Hagiwara A, Nakamura T, Kin S, Nakashima S, Yoshikawa T, et al. Tissue engineering of small intestinal tissue using collagen sponge scaffolds seeded with smooth muscle cells. *Tissue engineering*. 2006;12:403-12.
- [29] Hori Y, Nakamura T, Kimura D, Kaino K, Kurokawa Y, Satomi S, et al. Experimental study on tissue engineering of the small intestine by mesenchymal stem cell seeding. *J Surg Res*. 2002;102:156-60.
- [30] Sala FG, Kunisaki SM, Ochoa ER, Vacanti J, Grikscheit TC. Tissue-Engineered Small Intestine and Stomach Form from Autologous Tissue in a Preclinical Large Animal Model. *Journal of Surgical Research*. 2009;156:205-12.
- [31] Sala FG, Matthews JA, Speer AL, Torashima Y, Barthel ER, Grikscheit TC. A multicellular approach forms a significant amount of tissue-engineered small intestine in the mouse. *Tissue Engineering Part A*. 2011;17:1841-50.
- [32] Qin HH, Dunn JC. Small intestinal submucosa seeded with intestinal smooth muscle cells in a rodent jejunal interposition model. *The Journal of surgical research*. 2011;171:e21-6.
- [33] Ueki N, Sobue K, Kanda K, Hada T, Higashino K. Expression of high and low molecular weight caldesmons during phenotypic modulation of smooth muscle cells. *Proceedings of the National Academy of Sciences*. 1987;84:9049-53.
- [34] Bennett MR, Burnstock G, Holman ME. Transmission from intramural inhibitory nerves to the smooth muscle of the guinea-pig taenia coli. *The Journal of Physiology*. 1966;182:541-58.
- [35] Bennett M. Transmission from intramural excitatory nerves to the smooth muscle cells of the guinea-pig taenia coli. *The Journal of physiology*. 1966;185:132.
- [36] Liddle RA. Gastrointestinal hormones and neurotransmitters. *Sleisenger and Fordtran's Gastrointestinal and Liver Disease Philadelphia, Saunders-Elsevier*. 2010:3-20.

- [37] Hagen BM, Bayguinov O, Sanders KM. VIP and PACAP regulate localized Ca<sup>2+</sup> transients via cAMP-dependent mechanism. *American Journal of Physiology - Cell Physiology*. 2006;291:C375-C85.
- [38] Hasler WL, Kurosawa S, Chung OY. Regional cholinergic differences between distal and proximal colonic myenteric plexus. *American Journal of Physiology - Gastrointestinal and Liver Physiology*. 1990;258:G404-G10.
- [39] Scanga VI, Goraltchouk A, Nussaiba N, Shoichet MS, Morshead CM. Biomaterials for neural-tissue engineering — Chitosan supports the survival, migration, and differentiation of adult-derived neural stem and progenitor cells. *Canadian Journal of Chemistry*. 2010;88:277-87.
- [40] Nomura H, Zahir T, Kim H, Katayama Y, Kulbatski I, Morshead CM, et al. Extramedullary chitosan channels promote survival of transplanted neural stem and progenitor cells and create a tissue bridge after complete spinal cord transection. *Tissue engineering Part A*. 2008;14:649-65.
- [41] Li X, Yang Z, Zhang A, Wang T, Chen W. Repair of thoracic spinal cord injury by chitosan tube implantation in adult rats. *Biomaterials*. 2009;30:1121-32.

# **CHAPTER VII: DEVELOPMENT OF CHITOSAN SCAFFOLDS WITH ENHANCED MECHANICAL PROPERTIES FOR INTESTINAL TISSUE ENGINEERING APPLICATIONS**

Elie Zakhem<sup>1,2</sup> and Khalil N. Bitar<sup>1,2,3</sup>

<sup>1</sup> Wake Forest Institute for Regenerative Medicine, Wake Forest School of Medicine, Winston-Salem, NC

<sup>2</sup> Department of Molecular Medicine and Translational Science, Wake Forest School of Medicine, Winston Salem, NC

<sup>3</sup> Virginia Tech-Wake Forest School of Biomedical Engineering and Sciences, Winston-Salem, NC

***The work described in this manuscript focuses on the mechanical properties of chitosan as a potential scaffold for tissue engineering applications.***

***This manuscript was accepted for publication in Journal of Functional Biomaterials 2015, 6(4): 999-1011;***

## ABSTRACT

Massive resections of segments of the gastrointestinal (GI) tract lead to intestinal discontinuity. Functional tubular replacements are needed. Different scaffolds were designed for intestinal tissue engineering application. However, none of the studies have evaluated the mechanical properties of the scaffolds. We have previously shown the biocompatibility of chitosan as a natural material in intestinal tissue engineering. Our scaffolds demonstrated weak mechanical properties. In this study, we enhanced the mechanical strength of the scaffolds with the use of chitosan fibers. Chitosan fibers were circumferentially aligned around the tubular chitosan scaffolds either from the luminal side or from the outer side or both. Tensile strength, tensile strain and Young's modulus were significantly increased in the scaffolds with fibers when compared with scaffolds without fibers. Burst pressure was also increased. The biocompatibility of the scaffolds was maintained as demonstrated by the adhesion of smooth muscle cells around the different kinds of scaffolds. The chitosan scaffolds with fibers provided a better candidate for intestinal tissue engineering. The novelty of this study was in the design of the fibers in a specific alignment and their incorporation within the scaffolds.

## 1. Introduction

Diseases of the gastrointestinal tract including short bowel syndrome result from massive resections of the intestine [1]. Patients usually suffer from malabsorption and malnutrition which is associated with high mortality and morbidity rates [2]. One of the treatment options includes intestinal transplantation but it is limited by many factors such as immuno-rejection of the graft, shortage of donor organs, and the size of the graft to be transplanted [3,4]. Another option for patients is total parenteral nutrition [5]. This is associated with complications related to the catheter and liver diseases [6]. Therefore, engineered intestinal replacements offer an alternative promising solution.

A wide range of materials exists for tissue engineering applications; natural, synthetic or a hybrid of the two. Previously, synthetic biomaterials polyglycolic acid (PGA) and polycaprolactone (PCL) were evaluated for intestinal tissue engineering applications [7,8]. Even though the polymers supported the regeneration of intestinal segments, the mechanical properties of the scaffolds were not evaluated. Collagen, as a natural material, was also evaluated for its potential in intestinal tissue engineering [9,10]. Collagen alone has weak mechanical properties which makes it unsuitable for intestinal tissue engineering applications. One of the limitations of using collagen alone as a scaffold is its fast degradation *in vivo* due to its low mechanical properties.

Chitosan is another natural material that is widely used in different tissue engineering applications [11]. Chitosan is a natural material derived from chitin with various degrees of deacetylation. Structurally, chitosan is a linear polysaccharide of

2-amino-2-deoxy- $\beta$ -D-glucopyranose units linked by (1 $\rightarrow$ 4)- $\beta$ -glycosidic bonds. The advantage of using chitosan in tissue engineering is its biocompatibility *in vivo*, its controllable degradation rate and mechanical properties. One of the approaches to modulate the mechanical properties of chitosan scaffolds involves modifying the manufacturing process [12]. Chitosan fibers have been recently reported to enhance the mechanical properties of chitosan scaffolds.

We have previously demonstrated the biocompatibility of chitosan scaffolds in intestinal tissue engineering [13,14]. Smooth muscle and enteric neurons maintained their phenotype and functionality around chitosan scaffolds. In our previous studies, we engineered porous tubular chitosan-collagen scaffolds using the freeze/dry method. The mechanical properties of the porous tubular scaffolds did not match those of native intestines. The scaffolds failed to maintain their luminal patency. The aim of this study was to engineer circumferentially-aligned chitosan fibers and to incorporate them into the tubular scaffolds as a way to enhance the mechanical properties. We demonstrated that chitosan fibers circumferentially embedded in the tubular scaffolds have higher Young's Modulus and burst strength than tubular chitosan scaffolds without fibers.

## **2. Materials and Methods**

### ***2.1. Reagents***

Medium molecular weight chitosan (75%–85% deacetylation) was purchased from Sigma-Aldrich (St. Louis, MO, USA). Type I collagen was purchased from BD Biosciences.

### ***2.2. Chitosan Fibers Preparation***

A 2% w/v chitosan solution was prepared by dissolution in 0.2 M acetic acid. Chitosan fibers were formed using the extrusion/gelation method as described previously [15]. Chitosan solution was extruded using a syringe pump through a catheter into a flask containing 10 wt % ammonia solution. Fibers were allowed to neutralize in the ammonia solution and then dried at room temperature in different forms as described below.

### ***2.3. Scaffolds Preparation***

Four different kinds of scaffolds were engineered, all having the same basic components (chitosan and collagen). A 2% w/v chitosan solution was prepared by dissolution in 0.2 M acetic acid. A 0.1 mg/mL collagen type I solution was prepared by dissolution in acetic acid. Tubular chitosan-collagen scaffolds were prepared using the freeze/dry method as described previously [14]. Briefly, the 2% w/v chitosan solution was mixed with 0.1 mg/mL rat tail type I collagen in a volume ratio of 1:1. A custom made mold was used to prepare the scaffolds. The mold consisted of an outer cylindrical tube of 0.7 cm diameter. An additional tube of 0.3 cm diameter was inserted in the center of the outer tube to create the inner lumen of the scaffold.

#### **c) Porous scaffolds**

The chitosan-collagen mixture was poured into the space between the two tubes of the mold. The composite was then frozen at  $-80\text{ }^{\circ}\text{C}$  for 3 h and then lyophilized for 24 h.

#### **d) Scaffolds with inner fibers**

Chitosan fibers were consistently wrapped circumferentially, attached to each other, around the inner tube of the mold and allowed to dry at room temperature. Following drying, the tube was inserted into the center of the mold. The same chitosan-collagen mix was then poured into the space between the two tubes of the mold. The mold was then frozen at  $-80\text{ }^{\circ}\text{C}$  for 3 h and then lyophilized for 24 h.

#### **e) Scaffolds with outer fibers**

The chitosan-collagen solution was first poured into the space between the two tubes of the mold followed by freezing the sample at  $-80\text{ }^{\circ}\text{C}$  for 3 h and then lyophilizing for 24 h. Following lyophilization, the prepared chitosan fibers were wrapped circumferentially, attached to each other, around the dried chitosan scaffold. The fibers were allowed to dry around the scaffold at room temperature in a similar manner as described above.

#### **f) Fiber-sandwiched scaffolds**

Fiber-sandwiched scaffolds were prepared as a combination of the two previously described scaffolds. Briefly, after preparing the scaffolds with inner fibers as described in (b), additional chitosan fibers were wrapped



circumferentially around the lyophilized scaffolds and allowed to dry. After drying, the scaffolds were analyzed.

#### *2.4. Characterization of the Fibers and Scaffolds*

The chitosan fibers and scaffolds were observed under scanning electron microscopy. Chitosan fibers were allowed to dry at room temperature and used for imaging. Different types of lyophilized scaffolds were sectioned using a sharp scalpel. Fibers and cross sections of scaffolds were mounted on a stub with double sticky tape and colloidal graphite. Samples were then sputter-coated with gold prior to examination under scanning electron microscopy (SEM; Model S-2260N, Hitachi Co. Ltd., Tokyo, Japan).

#### *2.5. Tensile Properties of the Scaffolds*

Lyophilized scaffolds were neutralized in 0.2 M NaOH and then washed with phosphate buffer saline (PBS) at room temperature. Scaffolds were cut into tubular structures of 30 mm length, 30 mm inner diameter and 0.2 mm thickness. Tensile properties were measured using a uniaxial load test machine (Model # 5544, Instron Corporation, Issaquah, WA, USA) equipped with a maximum 2 kN load cell at a crosshead speed of 0.5 mm/s. Measurements of tensile strength, Young's modulus and elongation at break were obtained from stress-strain curves. Native rat intestine was used as control.

## *2.6. Burst Pressure Strength*

The burst pressure strength of the different kinds of scaffolds was measured by increasing the luminal pressure inside the scaffolds until failure. The test was performed using a pressure transducer catheter which was inserted inside the scaffolds. The luminal pressure was gradually increased using a pressure syringe until failure of the scaffolds occurred. The pressures were then recorded.

## *2.7. Cell Adhesion and Alignment on the Scaffolds*

Smooth muscle sheets were engineered following our previously published methods. Briefly, intestine-derived smooth muscle cells were isolated by collagenase digestion. Cells were then grown on wavy molds with longitudinal grooves. Following cell alignment along the grooves, a collagen gel was then overlaid on top of the aligned smooth muscle. A smooth muscle sheet formed and was lifted off the plate. The sheets were then wrapped circumferentially around the different tubular scaffolds and left in culture *in vitro* for 14 days. At the end of the culture period, the scaffolds were fixed in 3.7% formaldehyde and processed. Cross sections of 6  $\mu\text{m}$  thickness were stained with  $\alpha$ -smooth muscle actin (Sigma-Aldrich, Saint Louis, MO, USA) and DAPI to evaluate maintenance of cell phenotype and alignment on the scaffolds.

## *2.8. Statistical Analysis*

The differences in tensile strength, tensile strain, Young's modulus, and burst strength between the different types of scaffolds and the native tissue were

evaluated using ANOVA. Values reported are mean  $\pm$  SEM. Differences were considered statistically significant for  $p < 0.05$ .

### 3. Results

#### *3.1. Characterization of the Fibers and Scaffolds*

Tubular chitosan scaffolds with luminal opening were prepared following the freeze/dry method. The scaffolds were 3 cm in length and 0.3 cm internal diameter. We developed a technique to form continuous, circumferentially-aligned, chitosan fibers using the extrusion/gelation method. Representative images of the mold, the scaffolds and the fibers are shown in **Figure 23**. Representative SEM images of the fibers and the different scaffolds are illustrated in **Figure 24**: Representative SEM images **of the tubular scaffold (A)** without fibers; **(B)** the fibers; **(C)** scaffold with inner fibers; **(D)** scaffold with outer fibers; and **(E)** with inner and outer fibers.

The fibers appeared to be incorporated within the scaffold, either from the luminal side or from the outer side of the tube. The scaffolds without fibers had a wall thickness of  $1.7 \pm 0.1$  mm.

Those scaffolds did not maintain their luminal patency in wet conditions. The fibers had a diameter of 100  $\mu$ m (). For the scaffolds with inner fibers, the inner tube of the mold was used to wrap the fibers around it. The fibers were then allowed to dry. The chitosan-collagen solution was poured into the annular space of the mold, frozen, and then lyophilized. The fibers became incorporated within the lumen of the scaffold.

The fibers were uniformly aligned around the inner tube. The distance between the inner fibers was 0.4 mm. The engineering process was consistent in that the fibers were uniformly distributed within the lumen of the scaffolds. The wall thickness of the scaffolds with inner fibers was 1.3 mm. For the chitosan scaffolds with outer fibers, the fibers were wrapped circumferentially around the scaffolds and allowed to dry. The scaffolds shrunk and their wall thickness was 0.4 mm. The distance between the outer fibers was 2.9 mm. The fiber-sandwiched scaffolds had two layers of circumferentially aligned fibers; one layer on the outside and one layer on the inside. The scaffolds also shrunk with wall thickness of 0.4 mm. Figure 25 shows an SEM of the porosity of the different scaffolds. A non-uniform morphology was seen, especially in the scaffolds with outer fibers and the fiber-sandwiched scaffolds.

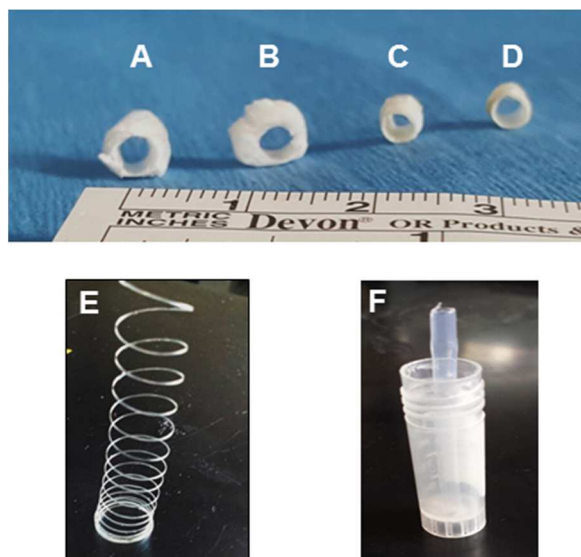


**Figure 23:** Representative images of the tubular scaffolds (A) without fibers; (B) with inner fibers; (C) with outer fibers; and (D) with inner and outer fibers (fiber sandwiched scaffold). (E) Circumferentially aligned chitosan fibers were engineered using the extrusion/gelation method. (F) The mold for scaffolds consisted of an outer tube and an inner tube to create the lumen of the scaffold.

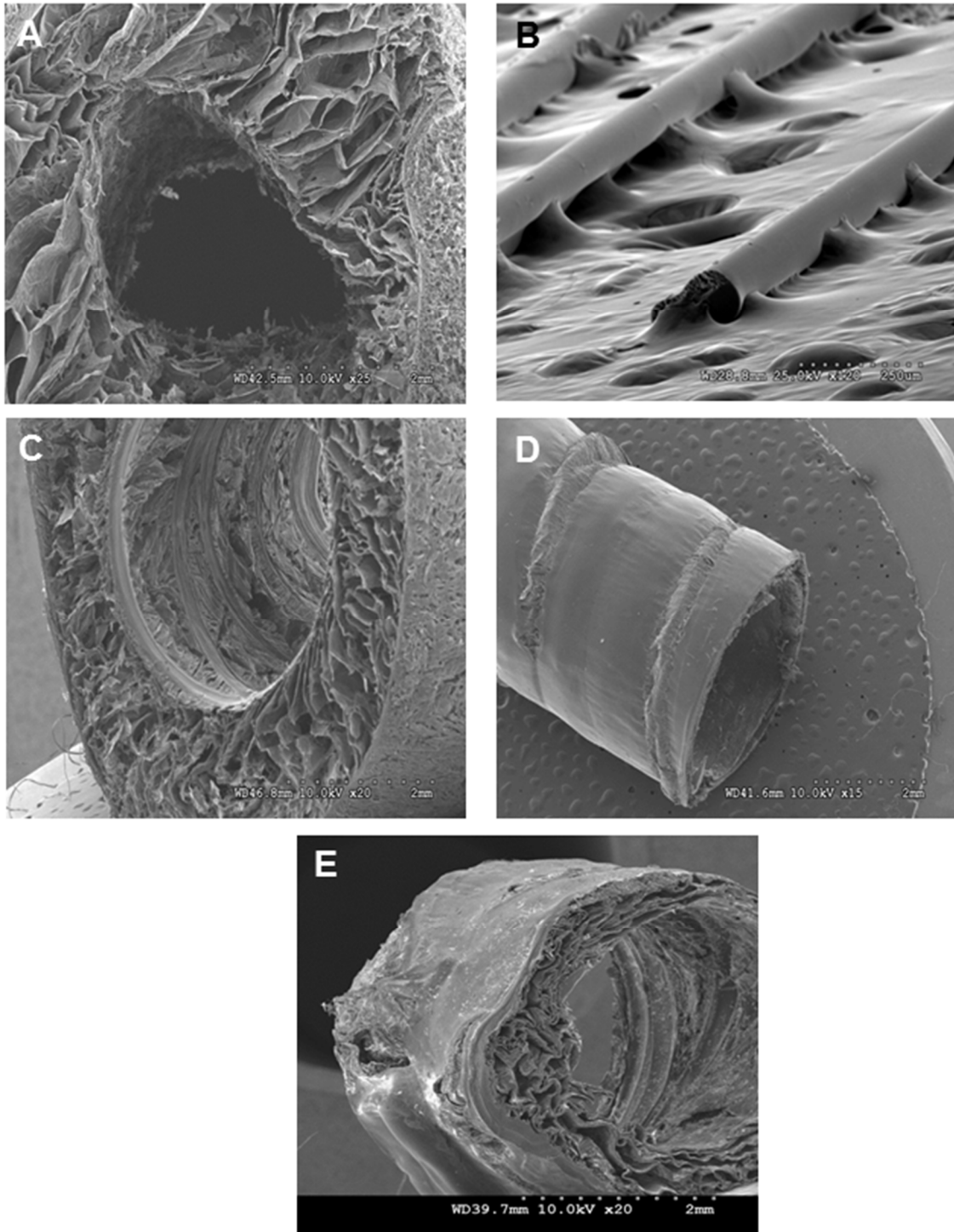


**Figure 24:** Representative SEM images of the tubular scaffold (A) without fibers; (B) the fibers; (C) scaffold with inner fibers; (D) scaffold with outer fibers; and (E) with inner and outer fibers.

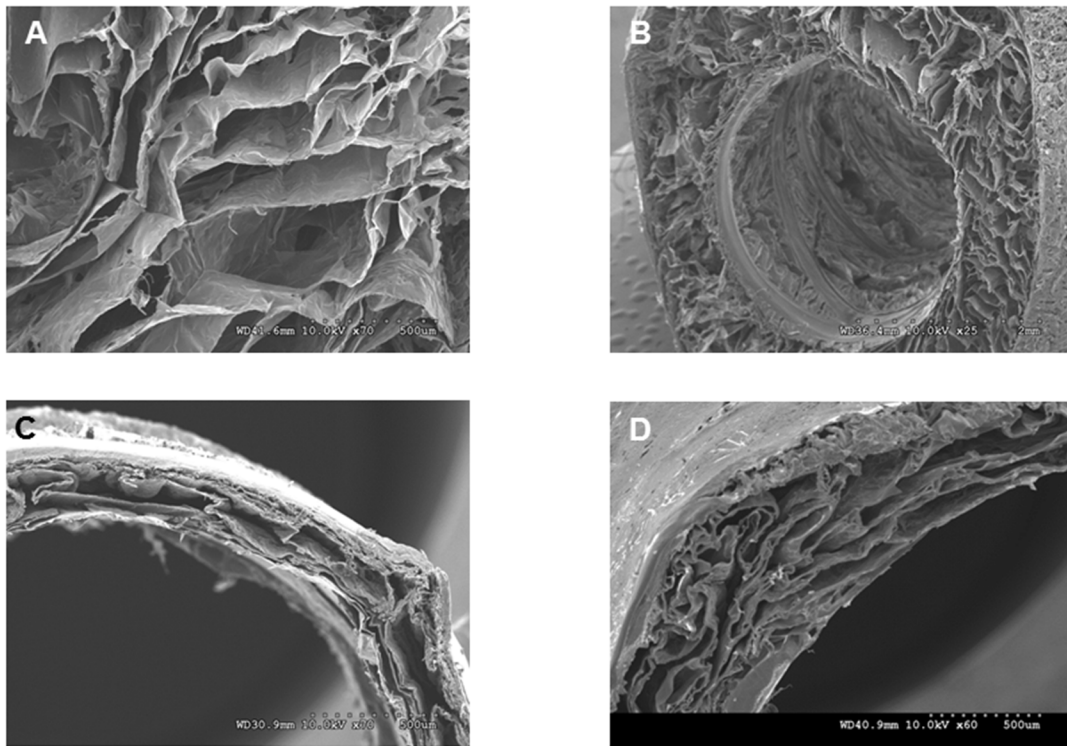


**Figure 25:** Morphology of the pores: SEM of the different scaffolds shows the morphology of the pores. **(A)** scaffold without fibers; **(B)** scaffold with inner fibers; **(C)** scaffold with outer fibers and **(D)** fiber sandwiched scaffold.

### 3.2. Mechanical Properties

The summary of the mechanical properties of the different kinds of scaffolds is presented in Table 1.

**Table 1.** Summary of the mechanical properties of the different kinds of scaffolds.

Samples	Tensile Stress (MPa)	Elongation at Break (%)	Young's Modulus (MPa)	Burst Pressure (mmHg)
Native intestine	0.076 ± 0.007	230 ± 13	0.122 ± 0.01	–
Scaffolds without fibers	0.013 ± 0.003	124 ± 6	0.022 ± 0.004	715 ± 38
Scaffolds with inner fibers	0.065 ± 0.008	262 ± 35	0.117 ± 0.007	1327 ± 75
Scaffolds with outer fibers	0.071 ± 0.01	137 ± 10	0.101 ± 0.019	1276 ± 75
Fiber sandwiched scaffolds	0.243 ± 0.033	114 ± 9	0.392 ± 0.089	–

#### a) Tensile properties

Tensile properties of the different scaffolds and the native intestines were compared (**Figure 26**). The tensile properties were measured using the Instron machine which generated the stress-strain curve of the various scaffolds and tissues. Tensile strength, elongation at break, and Young's modulus were obtained from stress strain curves. The tensile stress of the scaffolds with inner or outer fibers was significantly increased when compared to the porous scaffolds without fibers and not significantly different from the native intestine. However, the tensile stress of the fiber-sandwiched scaffolds was significantly higher from the rest of the scaffolds and the native intestine. The tensile stress of

the porous chitosan scaffolds increased from  $0.013 \pm 0.003$  MPa to  $0.065 \pm 0.008$  MPa (inner fibers),  $0.071 \pm 0.01$  MPa (outer fibers) and  $0.243 \pm 0.033$  MPa (fiber-sandwiched scaffolds). Elongation at break of chitosan scaffolds with inner fibers ( $262\% \pm 35\%$ ) was significantly increased to match that of the native intestine ( $230\% \pm 13\%$ ). Elongation at break for the chitosan scaffolds without fibers ( $124\% \pm 6\%$ ), the chitosan scaffolds with outer fibers ( $137\% \pm 10\%$ ), and fiber-sandwiched scaffolds ( $114\% \pm 9\%$ ) were significantly lower than the native intestine and the scaffolds with inner fibers. Additionally, the Young's modulus of the chitosan scaffolds reinforced with inner fibers was increased to  $0.117 \pm 0.007$  MPa and that of chitosan scaffolds with outer fibers increased to  $0.101 \pm 0.019$  MPa. The values were not significantly different from the native intestine ( $0.122 \pm 0.01$  MPa). Young's modulus of the chitosan scaffolds without fibers ( $0.022 \pm 0.004$  MPa) was significantly lower than that of the native intestine. Young's modulus of the fiber-sandwiched scaffolds ( $0.392 \pm 0.089$  MPa) was significantly higher than the native intestine and all other scaffolds.



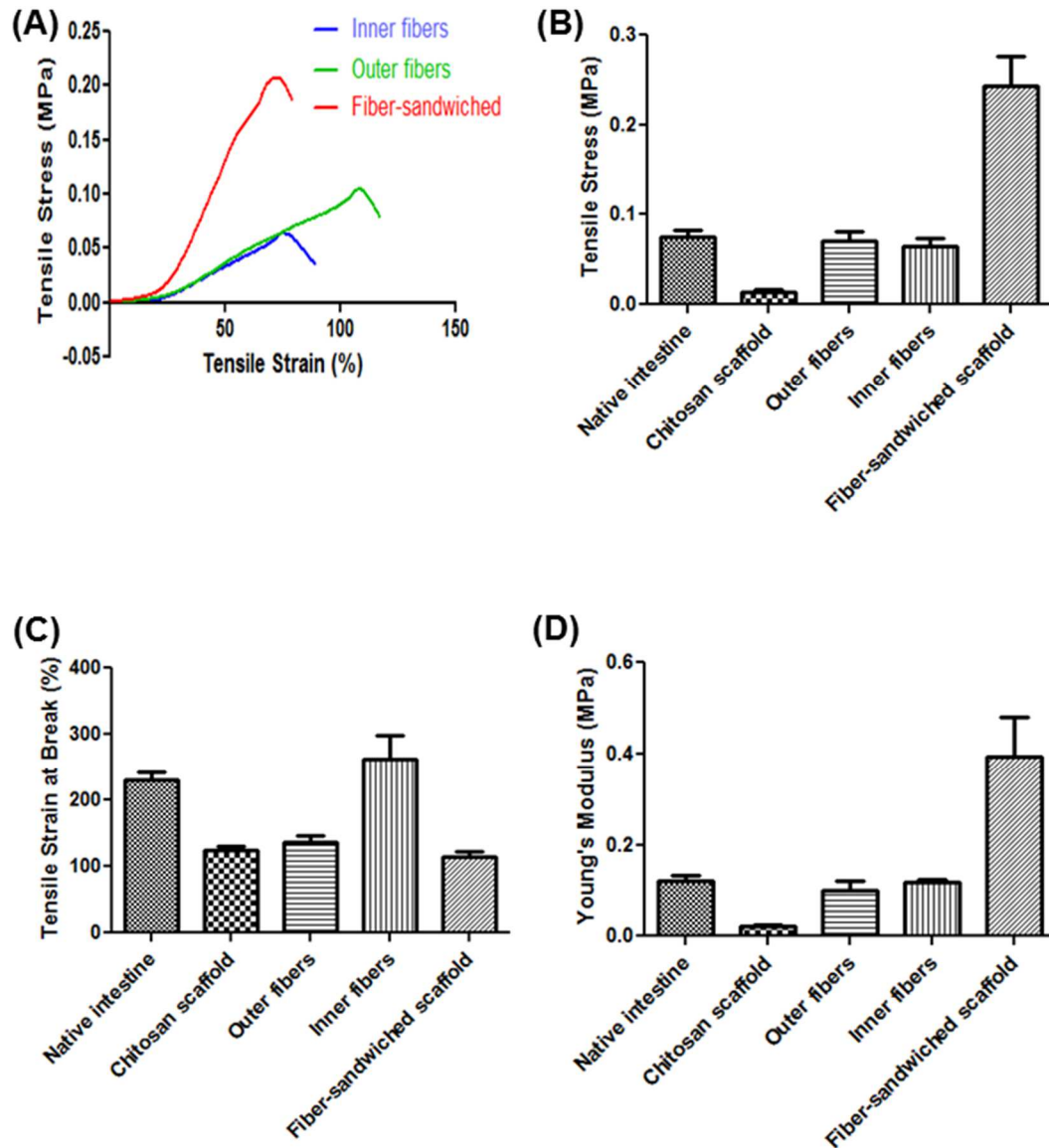


**Figure 26:** Tensile properties of the different kinds of scaffolds compared to native intestine: **(A)** Stress-strain curve; **(B)** Tensile stress; **(C)** Tensile strain at break, and **(D)** Young's modulus.

## b) Burst pressure strength

Burst pressure strength test was performed to evaluate the maximum pressure that the scaffolds can withstand following increasing the luminal pressure of the tubular scaffolds. The pressures reported are the pressures at which the scaffolds

failed (Figure 27). Both chitosan scaffolds with outer ( $1276 \pm 75$  mmHg) and inner ( $1327 \pm 75$  mmHg) fibers demonstrated significantly increased burst pressure strength when compared to porous chitosan scaffolds ( $715 \pm 38$  mmHg).

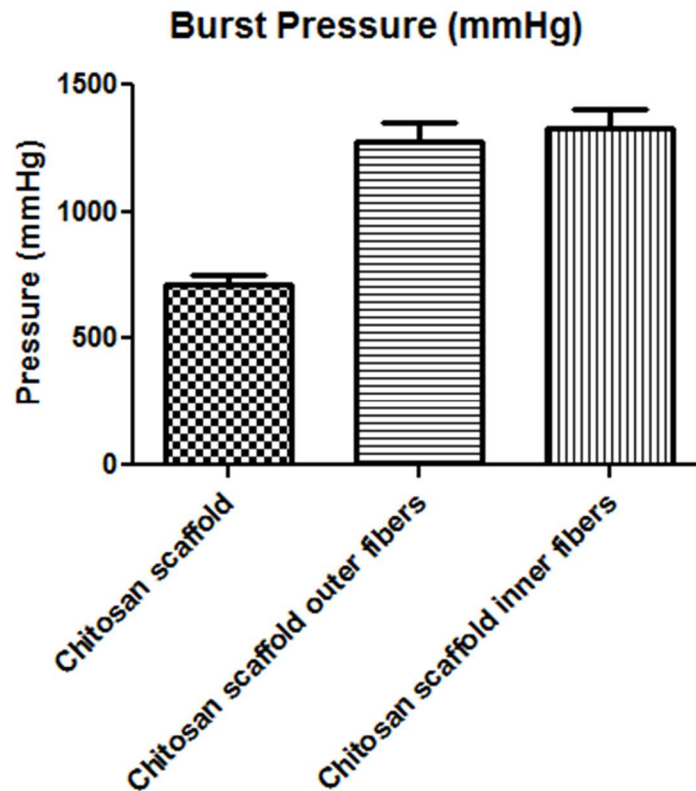


**Figure 27:** Burst pressure strength of different kinds of scaffolds.

### 3.3. Cell Adhesion and Alignment on the Scaffolds

Smooth muscle cells aligned along the grooves of the molds. Five days following alignment, collagen gel was overlaid on top of the smooth muscle. Smooth muscle sheets were formed and wrapped circumferentially around the different tubular scaffolds. The tissues were left in culture for 14 days. Cross sections were stained with  $\alpha$ -smooth muscle actin and DAPI to evaluate cell attachment and alignment (**Figure 28**). In all kinds of scaffolds, cells were shown

to align circumferentially around the scaffold. Smooth muscle cells stained positive for  $\alpha$ -smooth muscle actin indicating preservation of smooth muscle phenotype. DAPI staining showed maintenance of alignment of smooth muscle cells around the lumen of the tubular scaffolds.

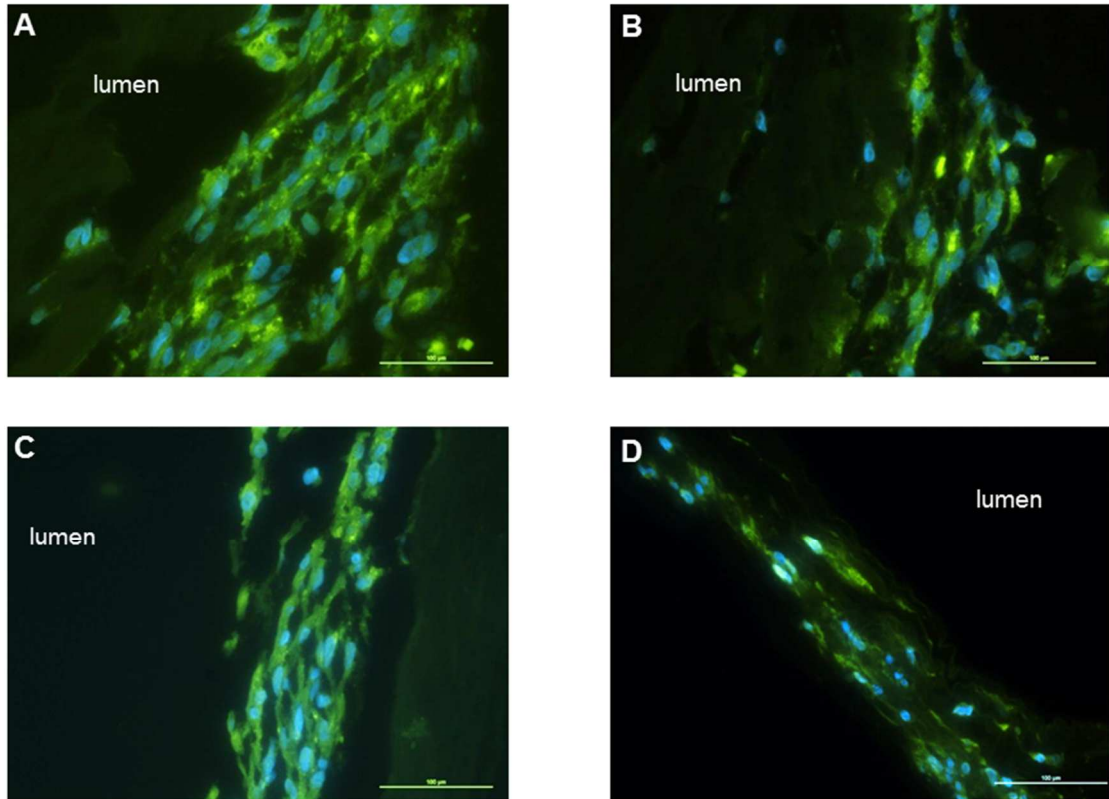


**Figure 28:** Cell alignment and phenotype around the scaffolds. Different kinds of scaffolds were seeded with aligned smooth muscle sheets. Tissues stained positive for  $\alpha$ -smooth muscle actin, indicating the maintenance of smooth muscle phenotype around all scaffolds. DAPI staining demonstrated maintenance of alignment of the cells around the scaffolds. (A) Scaffolds without fibers; (B) scaffolds with inner fibers; (C) scaffolds with outer fibers; and (D) fiber-sandwiched scaffolds. Scale bars 100  $\mu$ m.

## 4. Discussion

The selection of biomaterials is an essential factor in tissue engineering applications. When designing scaffolds, several factors must be taken into account, including biocompatibility of the scaffolds, biodegradability, and their mechanical properties. All these factors taken together result in engineered tissues with the characteristics required for successful outcomes. In intestinal tissue engineering, hollow tubular scaffolds are needed.

Even though the intestine is considered as a simple tubular structure, the complexity lies in the different types of cells that line the intestine. The mechanical properties of native gut tissues were previously tested. Given that there are different cell layers in the intestine, the contribution of each layer to the mechanical strength of the GI tract was an area of study. Previous reports have shown that the muscularis and the submucosal layers contribute the most to the mechanical strength of the intestinal wall [16,17]. Additionally, the physical properties of the luminal material of the GI tract change from liquid (small intestine) to solid (large intestine). In rats, the tensile strength increases from the proximal to the distal colon [18]. This is attributed to the increased stress as the luminal content gets harder. The difference in mechanical strength of different segments of the gut is an essential factor when designing scaffolds for intestinal tissue engineering application. Another factor to take into account is the age of the patient. In the aging population, the connective tissue composition differs and the mechanical strength of the tissue decreases [19]. A successful scaffold must be compliant with the native tissue. Therefore, the mechanical properties of the

engineered intestinal segments must match those of the native tissue and must be specific to the site of implantation and the age of the patients.

Previous attempts to regenerate the intestine have focused on the source of cells seeded onto the scaffolds. There has been little focus on the mechanical properties of the engineered scaffolds. Studying the mechanics of the gastrointestinal tract helps in developing scaffolds suitable for the application. Natural and synthetic materials have been investigated as potential candidates in intestinal tissue engineering. Synthetic scaffolds can be consistently reproducible; however, these scaffolds lack the biomimetic properties which are essential for cell-scaffold interaction. Additionally, disadvantages include degradability byproducts and variation in mechanical properties which can be limiting in certain applications [20]. The synthetic polymer polyglycolic acid (PGA) was used as support for isolated organoid units [7]. The scaffolds were coated with collagen I as a way to enhance cell attachment.

Poly- $\epsilon$ -caprolactone (PCL) was also evaluated for its biocompatibility in intestinal tissue engineering [8]. Even though the mechanical properties can be modulated, the degradation rate of PCL is slow. This raises the problem of tissue remodeling *in vivo*. Even though the synthetic scaffolds showed promising results following their implantation in animal models, the mechanical properties of the scaffolds were not studied. Confirming the mechanical strength of the scaffolds is essential especially when it comes to scaling up the scaffolds for translational purposes.

On the other hand, the most common natural material collagen has been tested for intestinal tissue engineering application. Collagen has excellent

biocompatibility, however, its low mechanical properties limits its use as the sole composition of the scaffold. We have previously-prepared scaffolds made of chitosan and collagen. We demonstrated the biocompatibility of chitosan-collagen composite scaffolds in intestinal tissue engineering [13,14]. The benefit of using chitosan as a component of our scaffold is its tunable mechanical properties, biocompatibility, controllable degradation rate and, finally, its ability to form porous scaffolds with different shapes. Our previous studies focused on engineering porous chitosan-collagen tubular scaffolds. We demonstrated that gut-derived smooth muscle cells and neurons maintained phenotype, morphology, and function when seeded onto the tubular scaffolds. However, the scaffolds failed to maintain their luminal patency. In this study, we investigated the possibility of increasing the mechanical strength of our scaffolds. We prepared chitosan fibers with a specific alignment. The advantage of our technique is the use of fibers made of the same material as the scaffold itself but in different physical property. Chitosan fibers have been previously used to enhance the mechanical properties of heart valve scaffolds [21]. In previous applications, small-cut fibers were randomly incorporated within the scaffolds and were able to improve the mechanical properties of the scaffolds. One disadvantage of this technique is the reproducibility of the manufacturing process. The randomness and the inconsistency in the amount of fibers incorporated within the scaffolds increase the variability of the mechanical properties. In our study, the fibers were consistently and uniformly prepared with a certain alignment. The fibers also improved the tensile properties of the tubular

scaffolds. The scaffolds with fibers demonstrated mechanical strength similar to native intestine. The burst pressure is a measure of the maximal pressure that the scaffold can withstand before it fails and leaks. The burst pressure in intestinal tissue engineering application is important to ensure that the scaffold does not burst or leak due to luminal pressure. Our results indicated that the fiber-reinforced scaffolds have burst pressure that is almost 50% more than porous scaffolds without fibers.

In conclusion, we showed in this study that chitosan fibers can be developed with a specific and consistent pattern. We incorporated the fibers within tubular chitosan scaffolds. The mechanically reinforced scaffolds had higher tensile properties and burst pressure than scaffolds without fibers. In our case, we found that scaffolds with inner or outer fibers enhanced the mechanical properties of the tubular scaffolds to a similar extent. However, the scaffolds with outer fibers had decreased in wall thickness, which may be a limiting factor during surgical anastomosis with the native tissue and for cell infiltration during the regeneration process. Additionally, the fiber-sandwiched scaffolds have mechanical properties beyond the range of the native intestine, which make them non-suitable for our application. Future studies will be conducted to implant the scaffolds and evaluate their mechanical properties following implantation. This is important to ensure that the implants will maintain their integrity *in vivo* for long term success.

## Acknowledgments

This study was supported by Wake Forest School of Medicine Institutional Funds.

*The work discussed in this chapter demonstrated the ability to improve the mechanical properties of chitosan scaffolds using engineered chitosan fibers. This study concludes the in vitro characterization of chitosan as a support for reconstructing the neuro-musculature of the GI tract. The next chapters focus on the in vivo evaluation of the engineered neuromuscular tissues.*



## References

1. Sundaram, A.; Koutkia, P.; Apovian, C.M. Nutritional management of short bowel syndrome in adults. *J. Clin. Gastroenterol.* **2002**, *34*, 207–220.
2. Wilmore, D.W.; Robinson, M.K. Short bowel syndrome. *World J. Surg.* **2000**, *24*, 1486–1492.
3. Kato, T.; Ruiz, P.; Thompson, J.F.; Eskind, L.B.; Weppler, D.; Khan, F.A.; Pinna, A.D.; Nery, J.R.; Tzakis, A.G. Intestinal and multivisceral transplantation. *World J. Surg.* **2002**, *26*, 226–237.
4. Brook, G. Quality of life issues: Parenteral nutrition to small bowel transplantation—A review. *Nutrition* **1998**, *14*, 813–816.
5. Amiot, A.; Messing, B.; Corcos, O.; Panis, Y.; Joly, F. Determinants of home parenteral nutrition dependence and survival of 268 patients with non-malignant short bowel syndrome. *Clin. Nutr.* **2013**, *32*, 368–374.
6. Lao, O.B.; Healey, P.J.; Perkins, J.D.; Horslen, S.; Reyes, J.D.; Goldin, A.B. Outcomes in children after intestinal transplant. *Pediatrics* **2010**, *125*, e550–e558.
7. Grikscheit, T.C.; Siddique, A.; Ochoa, E.R.; Srinivasan, A.; Alsberg, E.; Hodin, R.A.; Vacanti, J.P. Tissue-engineered small intestine improves recovery after massive small bowel resection. *Ann. Surg.* **2004**, *240*, 748–754.
8. Gupta, A.; Vara, D.S.; Punshon, G.; Sales, K.M.; Winslet, M.C.; Seifalian, A.M. *In vitro* small intestinal epithelial cell growth on a nanocomposite polycaprolactone scaffold. *Biotechnol. Appl. Biochem.* **2009**, *54*, 221–229.

9. Hori, Y.; Nakamura, T.; Matsumoto, K.; Kurokawa, Y.; Satomi, S.; Shimizu, Y. Tissue engineering of the small intestine by acellular collagen sponge scaffold grafting. *Int. J. Artif. Organs* **2001**, *24*, 50–54.
10. Nakase, Y.; Hagiwara, A.; Nakamura, T.; Kin, S.; Nakashima, S.; Yoshikawa, T.; Fukuda, K.-I.; Kuriu, Y.; Miyagawa, K.; Sakakura, C.; *et al.* Tissue engineering of small intestinal tissue using collagen sponge scaffolds seeded with smooth muscle cells. *Tissue Eng.* **2006**, *12*, 403–412.
11. Madihally, S.V.; Matthew, H.W. Porous chitosan scaffolds for tissue engineering. *Biomaterials* **1999**, *20*, 1133–1142.
12. Ma, L.; Gao, C.; Mao, Z.; Zhou, J.; Shen, J.; Hu, X.; Han, C. Collagen/chitosan porous scaffolds with improved biostability for skin tissue engineering. *Biomaterials* **2003**, *24*, 4833–4841.
13. Zakhem, E.; Raghavan, S.; Bitar, K.N. Neo-innervation of a bioengineered intestinal smooth muscle construct around chitosan scaffold. *Biomaterials* **2014**, *35*, 1882–1889.
14. Zakhem, E.; Raghavan, S.; Gilmont, R.R.; Bitar, K.N. Chitosan-based scaffolds for the support of smooth muscle constructs in intestinal tissue engineering. *Biomaterials* **2012**, *33*, 4810–4817.
15. Albanna, M.Z.; Bou-Akl, T.H.; Blowytsky, O.; Walters, H.L.; Matthew, H.W. Chitosan fibers with improved biological and mechanical properties for tissue engineering applications. *J. Mech. Behav. Biomed. Mater.* **2013**, *20*, 217–226.

16. Egorov, V.I.; Schastlivtsev, I.V.; Prut, E.V.; Baranov, A.O.; Turusov, R.A. Mechanical properties of the human gastrointestinal tract. *J. Biomech.* **2002**, *35*, 1417–1425.
17. Goyal, R.K.; Biancani, P.; Phillips, A.; Spiro, H.M. Mechanical properties of the esophageal wall. *J. Clin. Investig.* **1971**, *50*, doi:10.1172/JCI106630.
18. Watters, D.; Smith, A.; Eastwood, M.; Anderson, K.; Elton, R. Mechanical properties of the rat colon: The effect of age, sex and different conditions of storage. *Q. J. Exp. Physiol.* **1985**, *70*, 151–162.
19. Watters, D.; Smith, A.; Eastwood, M.; Anderson, K.; Elton, R.; Mugerwa, J. Mechanical properties of the colon: comparison of the features of the African and European colon *in vitro*. *Gut* **1985**, *26*, 384–392.
20. Gunatillake, P.A.; Adhikari, R. Biodegradable synthetic polymers for tissue engineering. *Eur. Cell Mater.* **2003**, *5*, 1–16.
21. Albanna, M.Z.; Bou-Akl, T.H.; Walters, H.L.; Matthew, H.W. Improving the mechanical properties of chitosan-based heart valve scaffolds using chitosan fibers. *J. Mech. Behav. Biomed. Mater.* **2012**, *5*, 171–180.

# CHAPTER VIII: IMPLANTATION OF AN ENGINEERED TUBULAR NEUROMUSCULAR TISSUE COMPOSED OF HUMAN CELLS AND CHITOSAN SCAFFOLD

Elie Zakhem<sup>1,2</sup>, Mostafa El Bahrawy<sup>1\*</sup>, Giuseppe Orlando<sup>1</sup>, Khalil N. Bitar<sup>1,2,3</sup>

<sup>1</sup>Wake Forest Institute for Regenerative Medicine, Wake Forest School of Medicine, Winston Salem, NC

<sup>2</sup>Department of Molecular Medicine and Translational Sciences, Wake Forest School of Medicine, Winston Salem, NC

<sup>3</sup>Virginia Tech-Wake Forest School of Biomedical Engineering and Sciences, Winston Salem, NC

***The work in this chapter described the remodeling of the engineered tubular neuromuscular tissues upon subcutaneous implantation in the back of athymic rats.***

***This manuscript was accepted for publication in Surgery 2015; 158(6): 1598-608***

## ABSTRACT

**Background:** There is an urgent need for gut lengthening secondary to massive resections of the gastrointestinal (GI) tract. In this study, we propose to evaluate the remodeling, vascularization and functionality of a chitosan-based tubular neuro-muscular tissue upon subcutaneous implantation in the back of athymic rats. **Methods:** Aligned innervated smooth muscle sheets were bioengineered using human smooth muscle and neural progenitor cells. The innervated sheets were wrapped around tubular chitosan scaffolds. The engineered tubular neuro-muscular tissue was implanted subcutaneously in the back of athymic rats. The implant was harvested after 14 days and assessed for morphology, vascularization and functionality. **Results:** Gross examination of the implants showed healthy color with no signs of inflammation. The implanted tissue became vascularized as demonstrated by gross and histological analysis. Chitosan supported the luminal patency of the tissue. The innervated muscle remodeled around the tubular chitosan scaffold. Smooth muscle maintained its circumferential alignment and contractile phenotype. Functionality of the implant was further characterized using real time force generation. Cholinergic response was demonstrated by robust contraction in response to Ach. VIP and EFS caused relaxation. In the presence of neurotoxin TTX, the magnitude of Ach-induced contraction and VIP-induced relaxation was attenuated while EFS-induced relaxation was completely abolished, indicating neuronal contribution to the response. **Conclusion:** Our results indicated the successful subcutaneous implantation of engineered tubular neuro-muscular tissues. The tissues became

vascularized and maintained their myogenic and neurogenic phenotype and function. This provides potential therapeutic prospects for providing implantable replacement GI segments for treating GI motility disorders.

## 1. Introduction:

Short bowel syndrome (SBS) is the result of massive resections (over 70%) of the small intestine [1]. Severity and treatment of SBS are dependent on the specific regions of the bowel that are resected [2]. Due to reduced absorptive surface area following resection of the intestine, patients usually suffer from dehydration, weight loss, disturbances in electrolytes and deficiencies in minerals and vitamins [1, 3]. Current standard treatments for SBS require extensive nutritional management [4]. Parenteral nutrition is usually associated with liver failure and catheter-related complications. Intestinal transplantation provides an alternative treatment, however complications including graft rejection and failure still exist [5]. Therefore, there is a clinical need for gut lengthening to restore intestinal function. Previous studies demonstrated the feasibility of re-implanting a mechanically-lengthened intestinal segment in pig models [6]. This resulted in mucosal and muscle function. Tissue engineering is another viable option to restore gut continuity. The goal is to duplicate the architecture and function of all cell types of the GI tract using a combination of cells and scaffolds.

The GI tract is a complex system with multiple cell types, organized in different layers. The smooth muscle is considered as the basic unit of the musculature of the tract. The alignment and the phenotype of gut smooth muscle are critical for proper function [7]. The GI tract has its own intrinsic regulatory apparatus which includes the enteric nervous system and the interstitial cells of Cajal (ICC). Smooth muscle receives and interprets signals from the regulatory

apparatus required for proper function [8]. Another major component of the GI tract includes the epithelium which is required for enzyme secretion, nutrient absorption and defense barrier. All these functions are dictated by specialized cell types. Taken together, an ideal functional gut replacement requires the regeneration of all of these cell types.

In our previous studies, sphincteric ring structures were engineered using the co-culturing system of smooth muscle and neural progenitor cells [9]. Those ring structures became vascularized and maintained their phenotype and function following their implantation around the internal anal sphincter of rats [10]. Results presented in this work demonstrate that we can successfully develop tubular tissues as a first stage for future gut replacements. We engineered innervated human smooth muscle sheets. We also introduced a tubular chitosan scaffold as support for those sheets. The tubular tissues were implanted subcutaneously in athymic rats and evaluated for vascularization, remodeling and functionality. Following 14 days of subcutaneous implantation, the engineered tubular neuro-muscular tissues became vascularized and maintained their myogenic and neurogenic characteristics as demonstrated by histological and physiological analysis.



## **2. Materials and methods:**

### **2.1. Reagents:**

Cell culture reagents were purchased from Invitrogen (Carlsbad, CA). Smooth muscle growth medium consisted of Dulbecco's modified Eagle medium (DMEM), 10% fetal bovine serum (FBS), 1.5% antibiotic-antimycotic, and 0.6% L-glutamine. Neural progenitor cell growth medium consisted of neurobasal, N2 supplement and antibiotic-antimycotic. Neural differentiation media consisted of neurobasal medium-A supplemented with 2% fetal calf serum, 1X B27 supplement and 1X antibiotic-antimycotic. Medium molecular weight chitosan (75–85% deacetylation), acetylcholine (ACh), vasoactive intestinal peptide (VIP), tetrodotoxin (TTX), and nNOS-blocker *N*<sub>ω</sub>-Nitro-L-arginine methyl ester hydrochloride (L-NAME) were purchased from Sigma (St. Louis, MO). Sylgard [poly (dimethylsiloxane); PDMS] was purchased from World Precision Instruments (Sarasota, FL). Type I collagen was purchased from BD Biosciences.

### **2.2. Cell Isolation:**

Human intestinal tissues were ethically obtained from organ donors through Carolina Donor Services and Wake Forest Baptist Medical Center (IRB No. 00007586).

#### **a) Human circular smooth muscle cells:**

A segment of 10 cm of the duodenum right below the pyloric sphincter was consistently obtained from all donors for cell isolation. Human smooth muscle

cells were isolated from human duodenum following the protocols previously described by our lab [11]. Briefly, human duodena were cleaned of any luminal content and washed extensively in ice-cold Hank's balanced salt solution. The circular smooth muscle layer was stripped off and separated from the mucosa and the longitudinal muscle layer. The circular smooth muscle was minced and digested twice in type II collagenase (Worthington, Lakewood, NJ) and DNase (Roche, Indianapolis, IN) for one hour each. Digested cells were washed, resuspended in smooth muscle growth media and cultured on tissue culture flasks until confluent.

**b) Human enteric neural progenitor cells:**

Human enteric neural progenitor cells were isolated following previously published protocols [9, 10, 12]. Briefly, human intestinal tissues were extensively washed in ice-cold Hank's balanced salt solution supplemented with gentamicin and antibiotics/antimycotics. The tissues were finely minced followed by additional washing. Tissues were then subjected to digestion using a mixture of collagenase type II, dispase, and DNase I. Cells were then passed through 70  $\mu\text{m}$  followed by 40  $\mu\text{m}$  cell strainers. Cells were recovered by centrifugation and cultured in non-tissue culture treated plates in neural growth medium that enhances cell proliferation. Cells were maintained at 37°C and 7% CO<sub>2</sub> with regular media change. These cultured cells formed floating clusters known as neurospheres. These neurospheres stained positive for neural crest-derived cell marker p75 [9].

### *2.3. Engineering tubular neuro-muscular tissue:*

Tubular chitosan scaffolds were engineered as described previously [11]. Briefly, chitosan solution was prepared in 0.2 M acetic acid and mixed with type I collagen. Chitosan/collagen mixture was poured into a custom made tubular mold with a central opening to create the lumen of the scaffold. The whole assembly was frozen at  $-80^{\circ}\text{C}$  for 3 h and then lyophilized for 24 h. The scaffolds were neutralized in NaOH and washed extensively with PBS and distilled water.

Innervated smooth muscle sheets (2x4 cm) were bioengineered following our previously published method [13]. Briefly, smooth muscle cells were trypsinized and collected. A suspension of 500,000 smooth muscle cells was seeded onto a Sylgard wavy mold coated with laminin and cultured in muscle growth medium. Smooth muscle cells were left in culture for 5 days to allow smooth muscle cell alignment along the grooves of the mold. On day 5, human enteric neuronal progenitor cells were suspended in a collagen gel mixture, which was overlaid on top of the aligned smooth muscle cells. Innervated smooth muscle sheets were formed through the process of delamination of the smooth muscle cell layer. Neural differentiation media was supplied every other day to enhance neural differentiation. The innervated smooth muscle sheets were then wrapped around the tubular chitosan scaffolds and prepared for implantation.

#### *2.4. Implantation of the engineered tubular neuro-muscular tissues:*

The engineered tubular neuro-muscular tissues were implanted subcutaneously in the back of female athymic rats (n=5). All surgical procedures were performed following the guidelines set forth by IACUC. This surgical procedure has been previously described [14]. Athymic rats were anesthetized under continuous isoflurane masking. Surgical area in the back of anesthetized rats were shaved and aseptically prepared. A 1 cm transverse incision was made in the upper back of the rat. A subcutaneous pocket was created into which the engineered tissue was inserted and fixed using 5-0 prolene sutures in order to locate it at the time of harvest. Tubular chitosan scaffolds that were not seeded with the innervated smooth muscle were implanted in a similar fashion and served as control. The rats were allowed to recover in their cages in standard fashion.

#### *2.5. Implant harvest:*

The rats were euthanized 14 days post-implantation. The site of incision was reopened and the tissues were located using the 5-0 prolene sutures. The neuro-muscular tissues and the control scaffolds were dissected from the surrounding tissue. The harvested tissues and scaffolds were evaluated as described below.

#### *2.6. Histological and immunofluorescence evaluation of the implant:*

Following harvest, the tissues were fixed in formaldehyde, processed and paraffin embedded. Cross sections of 6  $\mu\text{m}$  thickness were obtained,

deparaffinized and hydrated in water. Hematoxylin and eosin (H&E) and Masson's Trichrome stains were performed for morphological analysis. Immunofluorescence studies were designed to evaluate (i) smooth muscle phenotype using primary antibodies directed against  $\alpha$ -smooth muscle actin and smooth muscle specific heavy-Caldesmon and (ii) differentiated neurons using  $\beta$ -III tubulin.

### *2.7. Physiological analysis of the implant:*

Cross sections of the harvested neuro-muscular tissues were tested for physiological functionality using a force transducer apparatus (Harvard Apparatus, Holliston, MA) following our previously published protocols [15]. The physiological functionality of the implanted neuro-muscular tissues was compared to forces generated by native rat intestines of same size as the implants. The tissues were incubated in a warm tissue bath and connected to the measuring arm of the transducer.

The tests were designed to evaluate the (i) electromechanical coupling integrity of the smooth muscle using potassium chloride (KCl), (ii) cholinergic responsiveness of the smooth muscle using Acetylcholine (Ach) and (iii) relaxation of smooth muscle in response to vasoactive intestinal peptide (VIP) and electrical field stimulation (EFS). The tissues were washed after each experiment. KCl response was evaluated in the absence and presence of calcium channel blocker, Nifedipine. Neural contribution to cholinergic contraction, VIP and EFS relaxation was tested in the absence and presence of

neurotoxin, tetrodotoxin (TTX). EFS-induced relaxation was further characterized for nitrergic neurotransmitters involved in the response by pre-treating the tissues with nitric oxide synthase (nNOS) blocker *N<sub>ω</sub>*-Nitro-L-arginine methyl ester hydrochloride (L-NAME).

## **2.8. Statistical analysis:**

Analysis of acquired force data was acquired using Powerlab and exported to GraphPad Prism 5.0 for Windows (GraphPad Software, San Diego CA; [www.graphpad.com](http://www.graphpad.com)). Second order Savitzky–Golay smoothing was applied to data. Student paired *t*-test was used to compare the means of forces in the absence and presence of inhibitors. Student *t*-test was used to compare the forces generated by the implant and the native intestine. A *p*-value less than 0.05 was considered significant. All values were expressed as means  $\pm$  SEM (n=5).

### 3. Results:

#### 3.1. *Implantation and harvest of the tubular neuro-muscular tissues:*

Innervated smooth muscle sheets were cultured in the presence of neural differentiation media to allow neural differentiation. The Sheets were then wrapped around sterile tubular chitosan scaffolds and prepared for implantation (**Figure 29A**). A 1 cm incision was made in the back of the rat (**Figure 29B**) and a pocket was created to implant the tubular neuro-muscular tissues (**Figure 29C**). The implants were secured in place by sutures and the skin was closed. Tubular chitosan scaffolds without innervated muscle were implanted as control.



**Figure 29:** Implantation of the engineered tissue: (A) Engineered tubular neuro-muscular tissue pre-implantation. Engineered aligned smooth muscle sheet was wrapped around tubular chitosan scaffold to form the tubular neuro-muscular tissue. (B) A 1 cm incision was made in the back of nude athymic rats. (C) A pocket was created and the tubular neuro-muscular tissue was inserted into the subcutaneous tissue.

All rats maintained normal activity and survival was 100%. Incision sites were completely healed at the time of harvest with no signs of infection. Gross inspection of the neuro-muscular tissues showed no signs of inflammation, abscess formation or necrosis (**Figure 30A**). The tissues appeared healthy in color and surrounded by blood vessels. The tubular neuro-muscular tissues were

3 cm in length (**Figure 30B**). The tissues maintained their luminal patency following implantation, with an internal diameter of 0.3 cm and external diameter of 0.5 cm (n=5) (**Figure 30C**).



**Figure 30:** Harvest of the implant: (A) The tubular neuro-muscular tissue was harvested after 14 days of implantation. The implant was healthy and vascularized. (B) The tubular neuro-muscular tissue was 3 cm in length and (C) 0.3 cm internal diameter. The tubular neuro-muscular tissue maintained luminal patency during the implantation period.

### 3.2. *Histological and immunofluorescence evaluation of the implant:*

#### a) **H&E and Masson's Trichrome:**

Harvested implants were fixed in formaldehyde, processed and paraffin embedded. Cross sections of 6  $\mu\text{m}$  thickness were prepared. Representative H&E staining of the neuro-muscular tissues after implantation is shown in **Figure 31A**. Stains showed preservation of circumferentially aligned smooth muscle layer around the lumen. Blood vessel structures were observed in the periphery of the implant (white arrows). H&E of scaffolds only showed lack of cellular alignment around the scaffold (**Figure 31B**). Masson's trichrome staining demonstrated deposition of collagen in the tubular neuro-muscular tissues



(**Figure 31C**) when compared to scaffolds only without smooth muscle (**Figure 31D**).

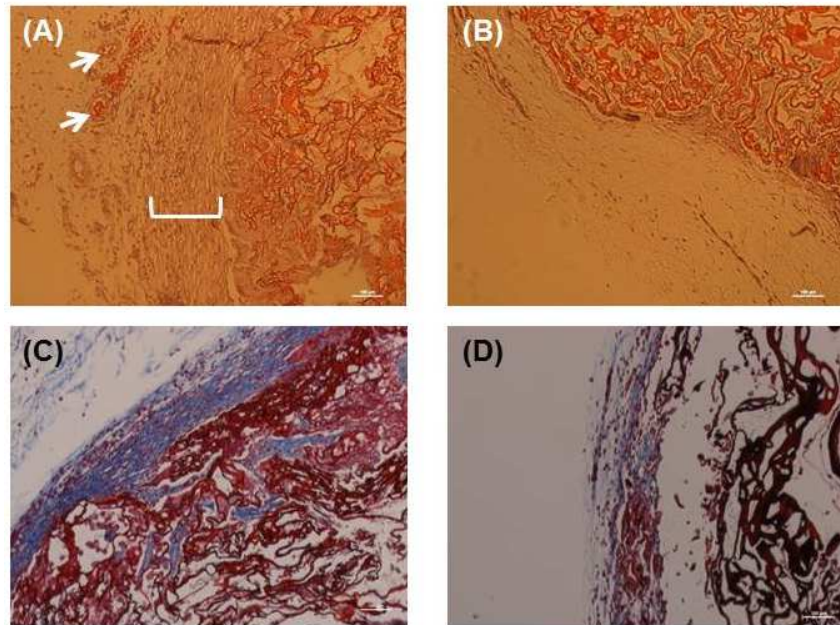


**Figure 31:** H&E analysis of the implant: (A) The tubular neuro-muscular tissue showed maintenance of alignment of smooth muscle around the lumen with blood vessels (white arrows) and (B) absence of smooth muscle in the scaffold only (control). Masson's trichrome analysis revealed high and more compact collagen around the tubular neuro-muscular tissue (C) when compared to control scaffold (D).

#### **b) Immunofluorescence:**

Implant sections were deparaffinized and rehydrated. Sections stained positive with  $\alpha$ -smooth muscle actin (**Figure 32A**) and smooth muscle specific heavy Caldesmon (**Figure 32B**). This indicated that smooth muscle contractile phenotype was maintained during the 2 week period of implantation. DAPI

staining showed maintenance of concentric alignment of the smooth muscle around the lumen of the tubular scaffold (**Figure 32C**).

Sections of the neuro-muscular tissues stained positive for  $\beta$ III tubulin, indicating the presence of differentiated mature neurons (**Figure 32D**). Scaffolds that served as control stained negative for  $\alpha$ -smooth muscle actin (**Figure 32E**) and showed no specific cellular alignment around the scaffold (**Figure 32F**).

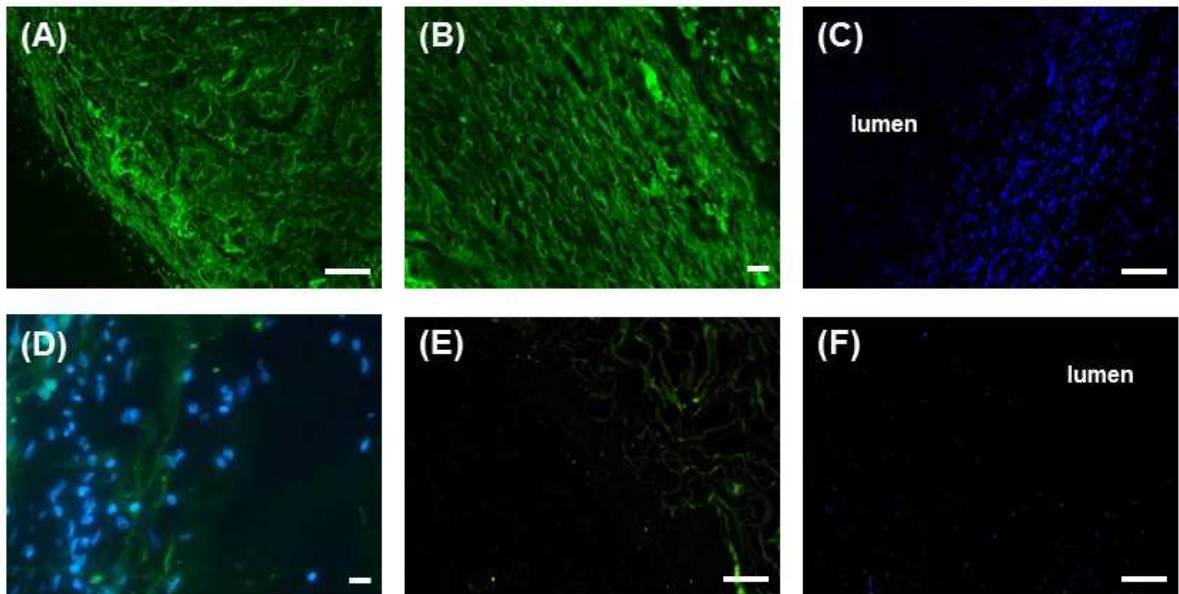


**Figure 32:** Immunofluorescence analysis of the implant: The tubular neuro-muscular tissue showed (A) positive stain for  $\alpha$ -smooth muscle actin and (B) smooth muscle specific heavy Caldesmon indicating the maintenance of smooth muscle contractile phenotype. (C) DAPI staining (blue) showed maintenance of alignment of smooth muscle around the lumen. (D) Differentiated neurons were demonstrated by positive stain for  $\beta$ -III tubulin. DAPI stain shows the location of the smooth muscle with respect to neurons. (E) Tubular chitosan scaffold alone (control) showed negative stain for  $\alpha$ -smooth muscle actin and (F) lack of any cellular alignment around the lumen of the scaffold. Scale bars are 100  $\mu$ m.

### 3.3. *Physiological studies:*

Further confirmation of functionality of the neuro-muscular tissues is critical for successful outcomes. Cross sections of the tissues were obtained after harvest for real time force generation. Cross sections of similar sizes were obtained from rat intestines for comparison. One end of the tissue was connected to the fixed pin of the organ bath while the other end was connected to the measuring arm of the force transducer. The tissues were allowed to establish baseline. Tissues were washed with fresh warm buffer after every experiment.

#### **a) Electromechanical coupling integrity:**

After establishing baseline, the tissues were treated with 60 mM KCl. A robust and rapid contraction of  $470 \pm 78 \mu\text{N}$  ( $n=5$ ) was observed in the neuro-muscular tissues compared to  $992 \pm 170 \mu\text{N}$  in the native tissue (**Figure 33**). In the presence of calcium channel blocker, Nifedipine, the response to the same concentration of KCl was significantly diminished. The response of the implanted tissue to KCl demonstrated that smooth muscle component was maintained and the calcium channels were preserved.

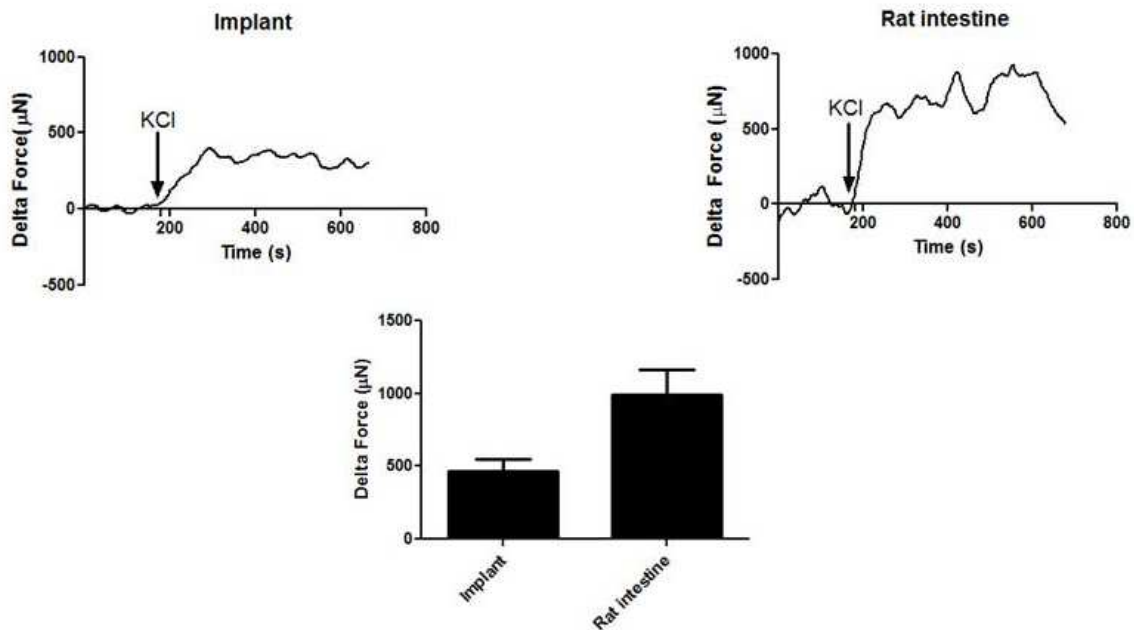


**Figure 33:** Electromechanical coupling integrity: Electromechanical coupling integrity was evaluated using potassium chloride (KCl). KCl caused a rapid and robust sustained contraction in both the implant and the native intestine. KCl response in the implants was around 50% of the force generated in the native rat intestine.

#### b) Cholinergic response:

Smooth muscle contraction was tested using the major contractile neurotransmitter in the gut, Acetylcholine (ACh). As the tissues established baseline, 1 µM ACh induced a rapid contraction of  $427 \pm 39$  µN in the implants (n=5) compared to  $827 \pm 103$  µN generated in the native intestine (**Figure 34**). In the presence of 1 µM TTX, the same dose of ACh caused a significant decrease in the magnitude of contraction ( $215 \pm 18$  µN in the implants and  $482 \pm 48$  µN in native intestine) (**Figure 34** - red trace). This indicated that the contractile

response in the implants is mediated by both a myogenic and neurogenic component.

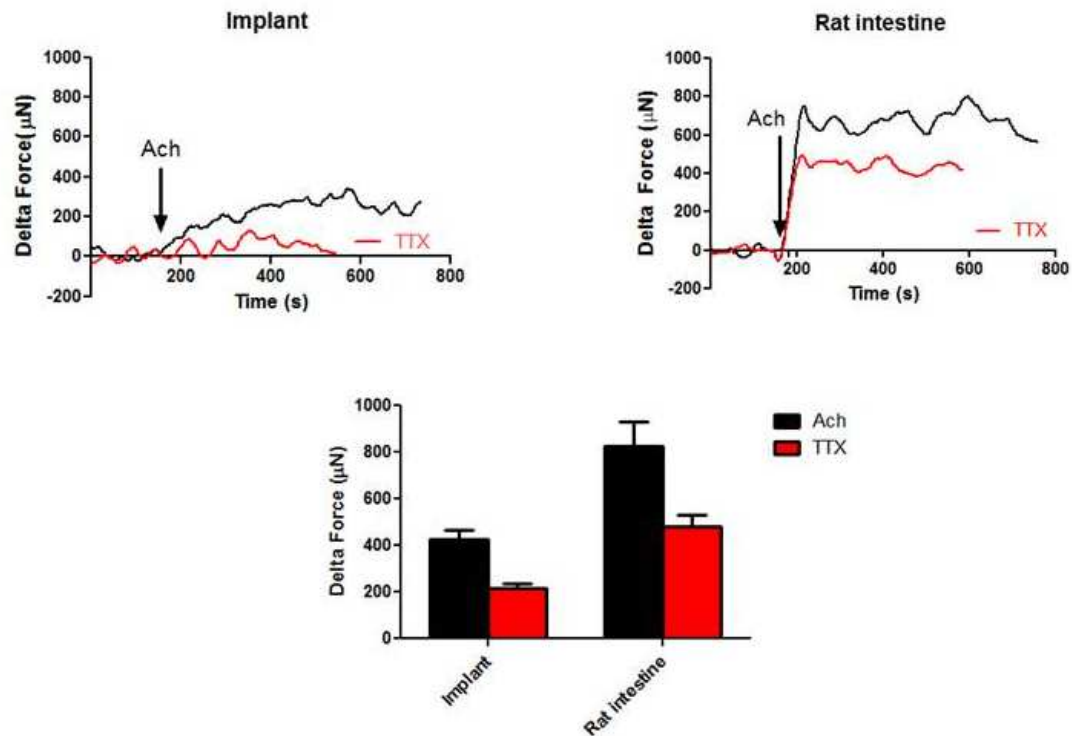


**Figure 34:** Cholinergic contraction: Cholinergic contraction was evaluated by addition of exogenous contractile neurotransmitter Ach. Ach caused a rapid contraction in both the implant and the native intestine. In the presence of TTX, contraction was significantly attenuated (red trace), indicating both myogenic and neurogenic contribution to the response. TTX significantly attenuated the Ach-induced contraction ( $p < 0.05$ ). Ach-induced contraction seen in the implants was around 50% that of the native rat intestine.

**c) VIPergic relaxation:**

Relaxation of the tissues was studied using vasoactive intestinal peptide (VIP). Upon addition of 1  $\mu$ M VIP, tissues rapidly relaxed (**Figure 35**). The average maximal relaxation magnitude in the implants was  $-240 \pm 12$   $\mu$ N (n=5) compared to  $-350 \pm 31$   $\mu$ N in the native intestines. In the presence of TTX, the magnitude of relaxation was significantly attenuated to  $-182 \pm 14$   $\mu$ N (n=5), indicating that VIP-induced relaxation in the implants has myogenic and neurogenic components (**Figure 35** – red trace). VIP-relaxation of native intestine in the presence of TTX was  $-205 \pm 59$   $\mu$ N.

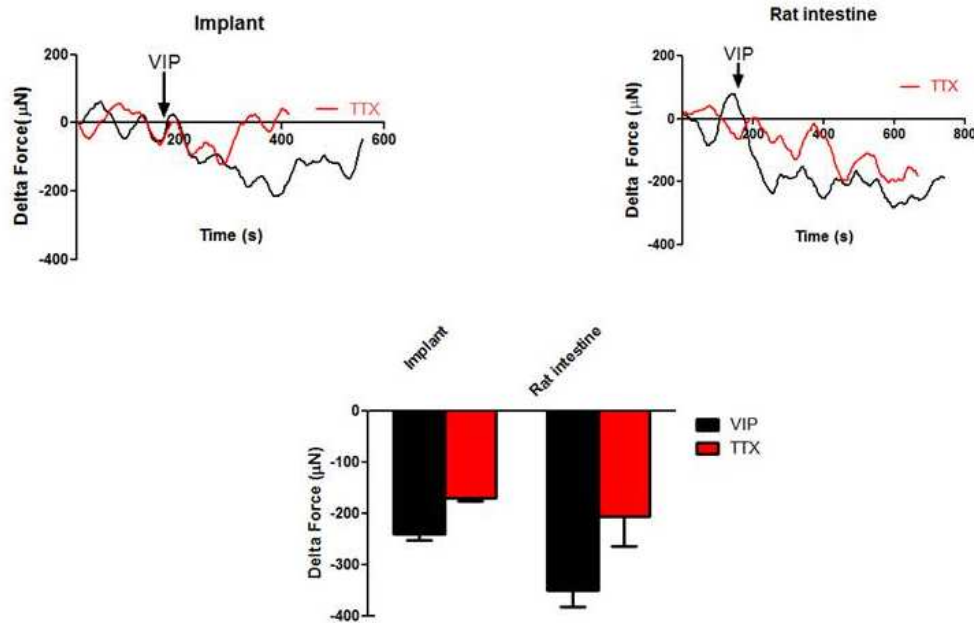


**Figure 35:** VIPergic relaxation: Relaxation was evaluated using the neurotransmitter VIP. Both the implanted tissue and the native intestine relaxed upon addition of 1μM of VIP. In the presence of TTX, the response was significantly reduced (red trace,  $p < 0.05$ ). This indicates that relaxation was mediated by both the smooth muscle and the neurons. The force generated by the implants was 30% of the force generated by the native rat intestine.

#### d) Electrical Field Stimulation (EFS):

Neuronal excitation was performed using EFS (8 Hz and 0.5 ms). Upon stimulating the nerves with electrical field, a rapid and robust relaxation was observed (**Figure 36**). The maximal relaxation averaged  $-250 \pm 16 \mu\text{N}$  ( $n=5$ ) in the implants versus  $-510 \pm 145 \mu\text{N}$  in the native intestine. In the presence of TTX, the relaxation response was completely abolished (**Figure 36** – red trace). This indicated that the relaxation was purely neuronally mediated and caused by neurotransmitters released from the neurons upon stimulation by electrical field.

In the presence of nNOS inhibitor LNAME, the EFS-induced relaxation was significantly reduced to  $-163 \pm 14 \mu\text{N}$  ( $n=5$ ) in the implants and to  $-187 \pm 36 \mu\text{N}$  in the native intestines (green trace). This inhibition indicates the presence of functional nitrergic neurons.

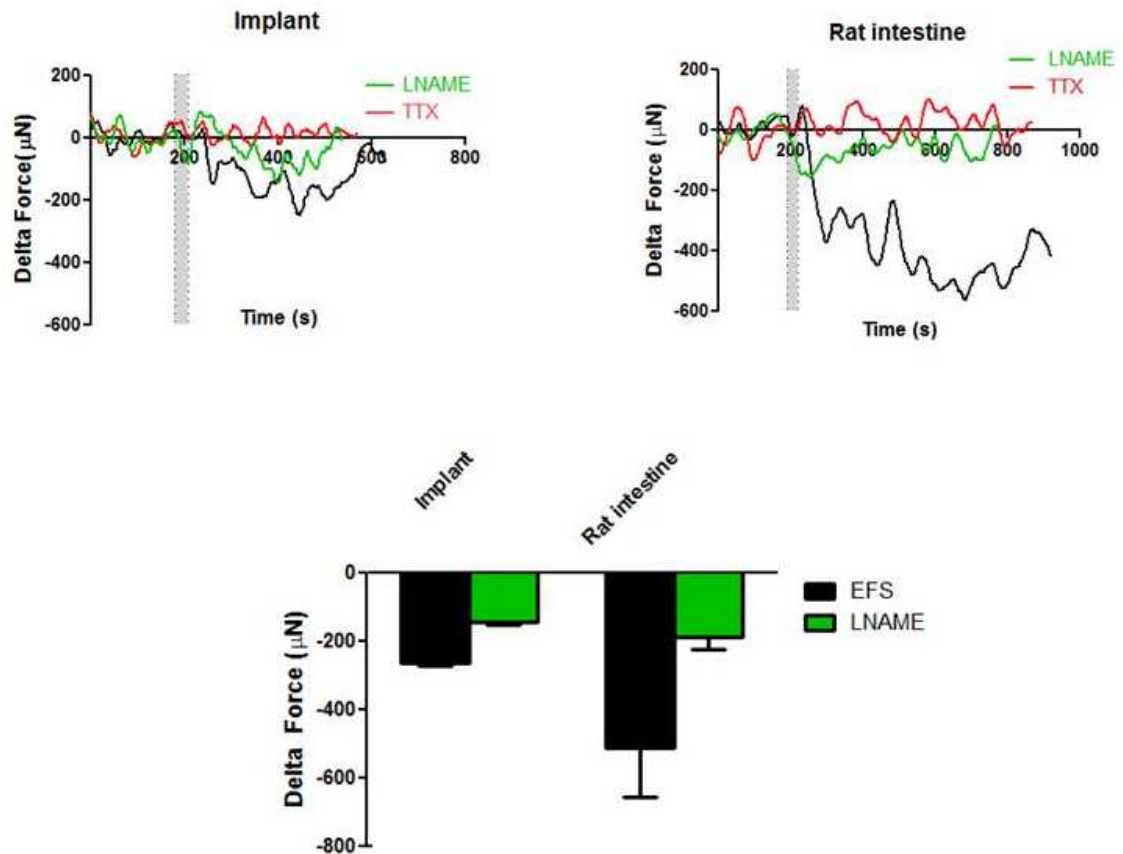


**Figure 36:** EFS relaxation evaluation: Relaxation was further induced using electrical field stimulation (EFS). The 2 bars indicate the time of applying EFS. The implants and the native intestine exhibited a rapid relaxation. When the tissues were pre-treated with TTX (red trace), relaxation was completely inhibited. This indicates that the response was purely neuronally mediated and that the neurons are functional. In the presence of nNOS blocker (L-NAME), EFS-induced relaxation was significantly attenuated indicating the functionality of nitrergic neurons (green trace,  $p<0.05$ ). EFS-induced relaxation in the implants was 50% of that seen in the native rat intestine.



#### **4. Discussion:**

The challenges and limitations of current surgical treatments have switched the focus to a tissue engineering approach for generating functional segments to lengthen the gut. The use of scaffolds in combination with cells has shown promising outcomes in tissue engineering. Chitosan is a natural biomaterial used in different tissue engineering application [16]. Recently, we introduced tubular chitosan scaffolds in the field of GI tissue engineering and evaluated its biocompatibility in vitro [11, 15]. The next step in order to move this study toward translational aspects was to evaluate the tubular tissues in vivo. In our previous studies, we implanted engineered innervated smooth muscle rings for sphincter replacements. In this study, we sought an approach to develop tubular gut tissues. We developed tubular neuro-muscular tissues by wrapping sheets of innervated smooth muscle around 3 cm long tubular chitosan scaffolds. As early as 2 weeks following subcutaneous implantation, the tubular tissues were vascularized, maintained luminal patency and preserved viability and functionality. This is essential for maintenance of survival in future long term implantation studies. Since the engineered tubular neuro-muscular tissue is human derived, nude athymic rats were used in this study in order to avoid any immune rejection of the implant.

The smooth muscle is the basic effector responsible for contraction and relaxation [17]. Plasticity of smooth muscle and the switch between synthetic and contractile phenotype is an extensive area of study [7, 18, 19]. Different smooth muscle markers exist and their expression varies [18, 20]. At 2 weeks post-

implantation, the engineered neuro-muscular tissue showed positive expression of  $\alpha$ -smooth muscle actin. This is consistent with a previous study where  $\alpha$ -smooth muscle actin expression was extensive at 2 weeks [19]. The implant also exhibited smooth muscle specific heavy Caldesmon expression. Smooth muscle specific heavy Caldesmon is a smooth muscle marker of later events of contractility and maturation [21]. The positive stain indicates that the implanted neuro-muscular tissue maintained contractile phenotype for 2 weeks in vivo.

Previous attempts to develop gut segments have used scaffolds seeded with organoid units isolated from different parts of the GI tract [22-25]. Massive bowel resection was performed in rats followed by anastomosis to tissue-engineered small intestine [26]. The engineered intestine grew into a mature tissue with differentiated epithelial, muscular and neural components. Organoid units were shown to be successful in generating a muscularis layer, ganglionated plexi and a differentiated functional epithelium in small and large animal studies. However, the functionality of the innervated muscularis layer was not evaluated, which is essential for motility purposes. Additionally, early reports investigated the ability to regenerate the musculature of the GI tract but showed lack of proper smooth muscle alignment or phenotype [27-29]. In our study, we generated tubular neuro-muscular tissues of 3 cm in length with luminal patency. Our immunostaining studies demonstrated differentiated phenotype of the muscle and the neurons. The innervated muscle maintained proper alignment and displayed key aspects of GI physiology when treated with exogenous contractile/relaxant neurotransmitters that are normally found in the GI tract. Both

the myogenic and neurogenic components of the tissue proved to be preserved. KCl-induced contraction was reversed in the presence of calcium channel blocker Nifedipine, which is consistent with previous studies [30]. The inhibition of the Ach, VIP and EFS responses in the presence of TTX indicated that the responses were partially mediated by the neural component. All of these responses were consistent with the in vitro functionality studies [15]. The ability of our engineered tissues to generate force indicates that the innervated muscle remodeled around the scaffold and was able to respond to pharmacological stimuli.

We demonstrated the successful development of a viable and functional tubular neuro-muscular tissue in athymic rat models. This tissue is a first step towards generating a gut segment that contains the epithelial component. Our technique is advantageous by providing a pre-aligned innervated smooth muscle around tubular scaffolds to regenerate the neuro-musculature of the gut. However, this study has some limitations that need to be considered in the future. The first limitation is that our engineered tissue lacks the epithelial component, which is crucial for complete gut function. The epithelial part is important for patients receiving intestinal replacement to ensure proper absorption and secretion balance. Our engineered hollow tubular neuro-muscular tissue is a first step towards developing a complete functional gut segment that can be used as tubular replacement for different parts of the GI tract. Further investigations on the regeneration of the epithelial component are currently being conducted in our lab. There are different approaches in the literature for the

regeneration of the epithelium, including the use of organoid units or isolated epithelial cells [31-35]. Additionally, findings from previous reports demonstrated the proliferation of the epithelial cells following mechanical lengthening of an intestinal segment after its isolation from the intestinal continuity [6]. The capacity of the epithelium to proliferate and grow following resection of the intestine provides promising insights for our study. It will be interesting in the future to determine the ability of the epithelium to grow and proliferate into our engineered tissues following anastomosis with the native intestine. The second limitation of our study is the site of implantation. Even though the tissues became vascularized in the back of the rats, it is important to test vascularization in a more clinically relevant area. Our previous in vivo studies using engineered IAS have shown the capacity of our constructs to become vascularized when implanted subcutaneously in the back or in situ. This current study was intended to provide a proof that the engineered neuro-muscular tissues survived around tubular chitosan scaffolds of 3 cm length. We have initiated studies in our lab where the tissues are implanted in the abdominal area and vascularization was achieved. The outcomes of this paper will allow us to extend our studies to further evaluate the tissue following anastomosis with the native intestine. The third limitation is the lower force generated by our engineered tissues compared to native rat intestines. A recent study reported force values generated by an implanted engineered intestine to be one-fourth of native intestine [36]. The forces generated by our engineered tissues were 50%-70% those of the native intestine. Even though the forces generated by our engineered tissues were

lower than native rat intestines, our engineered tissues displayed similar neuro-motility characteristics of native intestine. KCl and Ach induced sustained contraction in both types of tissues. Also, the responses were inhibited to the same level in the presence of TTX and LNAME. The lower force generated in our case might be due to the short period of implantation (2 weeks) which did not allow complete maturation of the tissue. Longer implantation periods are needed to confirm our hypothesis. In conclusion, we provided a custom-made multi-purpose system to engineer 3 cm tubular neuro-muscular human tissues using smooth muscle and neural progenitor cells obtained from the same donor. Our tubular tissues can be used for applications including small intestine and/or large intestine. The engineered tissues presented in this work are considered as a first successful stage of engineering the neuro-musculature of a gut. Next, we aim to incorporate the epithelial component in order to develop a functional gut.

## **5. Acknowledgment:**

This work was supported by NIH/NIDDK R01DK071614 and Wake Forest School of Medicine Institutional Funds. \*Dr. Mostafa Elbahrawy is a visiting medical doctor from Al-Azhar University, School of Medicine, Cairo, Egypt.

***This chapter demonstrated the survival and maintenance of function of the engineered human neuro-muscular tissues following their subcutaneous implantation in athymic rats. The engineered tissues could be used to lengthen the gut and to replace lost gut segments as in the case of short bowel syndrome or gut cancer.***

## 6. References:

- [1] Sundaram A, Koutkia P, Apovian CM. Nutritional management of short bowel syndrome in adults. *Journal of clinical gastroenterology*. 2002;34:207-20.
- [2] Yang I, Boushey RP. Short Bowel Syndrome. *Complexities in Colorectal Surgery*: Springer; 2014. p. 447-62.
- [3] Wilmore DW, Robinson MK. Short bowel syndrome. *World journal of surgery*. 2000;24:1486-92.
- [4] Amiot A, Messing B, Corcos O, Panis Y, Joly F. Determinants of home parenteral nutrition dependence and survival of 268 patients with non-malignant short bowel syndrome. *Clinical Nutrition*. 2013;32:368-74.
- [5] Lao OB, Healey PJ, Perkins JD, Horslen S, Reyes JD, Goldin AB. Outcomes in children after intestinal transplant. *Pediatrics*. 2010;125:e550-e8.
- [6] Koga H, Sun X, Yang H, Nose K, Somara S, Bitar KN, et al. Distraction-induced intestinal enterogenesis: Preservation of intestinal function and lengthening after re-implantation into normal jejunum. *Annals of surgery*. 2012;255:302.
- [7] Lee M, Wu BM, Stelzner M, Reichardt HM, Dunn JC. Intestinal smooth muscle cell maintenance by basic fibroblast growth factor. *Tissue engineering Part A*. 2008;14:1395-402.
- [8] Bitar KN, Raghavan S, Zakhem E. Tissue engineering in the gut: developments in neuromusculature. *Gastroenterology*. 2014;146:1614-24.

- [9] Gilmont RR, Raghavan S, Somara S, Bitar KN. Bioengineering of physiologically functional intrinsically innervated human internal anal sphincter constructs. *Tissue engineering Part A*. 2014;20:1603-11.
- [10] Raghavan S, Miyasaka EA, Gilmont RR, Somara S, Teitelbaum DH, Bitar KN. Perianal implantation of bioengineered human internal anal sphincter constructs intrinsically innervated with human neural progenitor cells. *Surgery*. 2014;155:668-74.
- [11] Zakhem E, Raghavan S, Gilmont RR, Bitar KN. Chitosan-based scaffolds for the support of smooth muscle constructs in intestinal tissue engineering. *Biomaterials*. 2012;33:4810-7.
- [12] Almond S, Lindley RM, Kenny SE, Connell MG, Edgar DH. Characterisation and transplantation of enteric nervous system progenitor cells. *Gut*. 2007;56:489-96.
- [13] Raghavan S, Gilmont RR, Bitar KN. Neuroglial differentiation of adult enteric neuronal progenitor cells as a function of extracellular matrix composition. *Biomaterials*. 2013;34:6649-58.
- [14] Hashish M, Raghavan S, Somara S, Gilmont RR, Miyasaka E, Bitar KN, et al. Surgical implantation of a bioengineered internal anal sphincter. *Journal of pediatric surgery*. 2010;45:52-8.
- [15] Zakhem E, Raghavan S, Bitar KN. Neo-innervation of a bioengineered intestinal smooth muscle construct around chitosan scaffold. *Biomaterials*. 2014;35:1882-9.

- [16] Lee HJ, Cho HS, Park E, Kim S, Lee SY, Kim CS, et al. Rosmarinic acid protects human dopaminergic neuronal cells against hydrogen peroxide-induced apoptosis. *Toxicology*. 2008;250:109-15.
- [17] Murthy KS. Signaling for contraction and relaxation in smooth muscle of the gut. *Annual review of physiology*. 2006;68:345-74.
- [18] Huber A, Badylak SF. Phenotypic changes in cultured smooth muscle cells: limitation or opportunity for tissue engineering of hollow organs? *Journal of tissue engineering and regenerative medicine*. 2012;6:505-11.
- [19] Qin HH, Dunn JC. Small intestinal submucosa seeded with intestinal smooth muscle cells in a rodent jejunal interposition model. *The Journal of surgical research*. 2011;171:e21-6.
- [20] Kofler K, Ainoedhofer H, Tausendschön J, Höllwarth M, Saxena A. Esophageal smooth muscle cells dedifferentiate with loss of  $\alpha$ -smooth muscle actin expression after 8 weeks of explant expansion in vitro culture: Implications on esophagus tissue engineering. *European Surgery*. 2011;43:168-73.
- [21] Frid MG, Shekhonin BV, Koteliensky VE, Glukhova MA. Phenotypic changes of human smooth muscle cells during development: late expression of heavy caldesmon and calponin. *Developmental biology*. 1992;153:185-93.
- [22] Grant CN, Salvador GM, Sala FG, Hill JR, Levin DE, Speer AL, et al. Human and Mouse Tissue-Engineered Small Intestine Both Demonstrate Digestive And Absorptive Function. *American Journal of Physiology-Gastrointestinal and Liver Physiology*. 2015:ajpgi. 00111.2014.



- [23] Sala FG, Kunisaki SM, Ochoa ER, Vacanti J, Grikscheit TC. Tissue-engineered small intestine and stomach form from autologous tissue in a preclinical large animal model. *Journal of Surgical Research*. 2009;156:205-12.
- [24] Sala FG, Matthews JA, Speer AL, Torashima Y, Barthel ER, Grikscheit TC. A multicellular approach forms a significant amount of tissue-engineered small intestine in the mouse. *Tissue Engineering Part A*. 2011;17:1841-50.
- [25] Grikscheit TC, Ochoa ER, Ramsanahie A, Alsberg E, Mooney D, Whang EE, et al. Tissue-engineered large intestine resembles native colon with appropriate in vitro physiology and architecture. *Annals of surgery*. 2003;238:35.
- [26] Grikscheit TC, Siddique A, Ochoa ER, Srinivasan A, Alsberg E, Hodin RA, et al. Tissue-engineered small intestine improves recovery after massive small bowel resection. *Annals of surgery*. 2004;240:748.
- [27] Hori Y, Nakamura T, Matsumoto K, Kurokawa Y, Satomi S, Shimizu Y. Tissue engineering of the small intestine by acellular collagen sponge scaffold grafting. *The International journal of artificial organs*. 2001;24:50-4.
- [28] Hori Y, Nakamura T, Kimura D, Kaino K, Kurokawa Y, Satomi S, et al. Experimental study on tissue engineering of the small intestine by mesenchymal stem cell seeding. *The Journal of surgical research*. 2002;102:156-60.
- [29] Nakase Y, Hagiwara A, Nakamura T, Kin S, Nakashima S, Yoshikawa T, et al. Tissue engineering of small intestinal tissue using collagen sponge scaffolds seeded with smooth muscle cells. *Tissue engineering*. 2006;12:403-12.
- [30] Janssen LJ, Tazzeo T, Zuo J, Pertens E, Keshavjee S. KCl evokes contraction of airway smooth muscle via activation of RhoA and Rho-kinase.

American journal of physiology Lung cellular and molecular physiology. 2004;287:L852-8.

[31] Grikscheit T, Ochoa ER, Srinivasan A, Gaisert H, Vacanti JP. Tissue-engineered esophagus: experimental substitution by onlay patch or interposition. The Journal of thoracic and cardiovascular surgery. 2003;126:537-44.

[32] Maemura T, Ogawa K, Shin M, Mochizuki H, Vacanti JP. Assessment of tissue-engineered stomach derived from isolated epithelium organoid units. Transplantation proceedings. 2004;36:1595-9.

[33] Grikscheit TC, Siddique A, Ochoa ER, Srinivasan A, Alsberg E, Hodin RA, et al. Tissue-engineered small intestine improves recovery after massive small bowel resection. Annals of surgery. 2004;240:748-54.

[34] Grikscheit TC, Ochoa ER, Ramsanahie A, Alsberg E, Mooney D, Whang EE, et al. Tissue-engineered large intestine resembles native colon with appropriate in vitro physiology and architecture. Annals of surgery. 2003;238:35-41.

[35] Beckstead BL, Pan S, Bhrany AD, Bratt-Leal AM, Ratner BD, Giachelli CM. Esophageal epithelial cell interaction with synthetic and natural scaffolds for tissue engineering. Biomaterials. 2005;26:6217-28.

[36] Nakao M, Ueno T, Oga A, Kuramitsu Y, Nakatsu H, Oka M. Proposal of intestinal tissue engineering combined with Bianchi's procedure. Journal of pediatric surgery. 2014.

# CHAPTER IX: BIOMECHANICAL PROPERTIES OF AN IMPLANTED ENGINEERED TUBULAR GUT- SPHINCTER COMPLEX

Elie Zakhem<sup>1,2</sup>, Mostafa El Bahrawy<sup>1\*</sup>, Giuseppe Orlando<sup>3</sup>, Khalil N. Bitar<sup>1,2,4</sup>

<sup>1</sup> Wake Forest Institute for Regenerative Medicine, Wake Forest School of Medicine, Winston Salem, NC

<sup>2</sup> Department of Molecular Medicine and Translational Sciences, Wake Forest School of Medicine, Winston Salem, NC

<sup>3</sup> Department of General Surgery, Wake Forest School of Medicine, Winston-Salem, NC

<sup>4</sup> Virginia Tech-Wake Forest School of Biomedical Engineering and Sciences, Winston Salem, NC

\*Dr. Mostafa Elbahrawy is a visitor from the department of pediatric surgery, Al-Azhar University, School of Medicine, Cairo, Egypt.

***In this chapter, the work discusses the engineering of a gut-sphincter complex and its subcutaneous implantation in rats for 4 weeks.***

***This manuscript was accepted for publication in the Journal of Tissue Engineering and Regenerative Medicine***

## ABSTRACT

**Introduction:** Neuro-muscular diseases of the gut alter the normal motility patterns. Even though surgical intervention remains the standard treatment, preservation of the sphincter attached to the rest of the gut is challenging.

**Objective:** This study aimed to evaluate a bioengineered gut-sphincter complex following its subcutaneous implantation for 4 weeks in rats. **Methods:**

Engineered innervated human smooth muscle sheets and innervated human sphincters with a pre-defined alignment were placed around tubular scaffolds to create a gut-sphincter complex. The engineered complex was subcutaneously implanted in the abdomen of the rats for 4 weeks. **Results:** The implanted tissues were vascularized. In vivo manometry revealed luminal pressure at the gut and the sphincter zone. Tensile strength, elongation at break and Young's modulus of the engineered complexes were similar to those of native rat intestine. Histological and immunofluorescence assays showed maintenance of smooth muscle circular alignment in the engineered tissue, maintenance of smooth muscle contractile phenotype and innervation of the smooth muscle. Electrical field stimulation induced a relaxation of the smooth muscle of both the sphincter and the gut parts. Relaxation was partially inhibited by nitric oxide inhibitor indicating nitrergic contribution to the relaxation. **Conclusion:** In this study for the first time, we successfully developed and subcutaneously implanted a tubular human-derived gut-sphincter complex. The sphincteric part of TGSC maintained the basal tone characteristic of a native sphincter. The gut part also

maintained its specific neuro-muscular characteristics. The results of this study provide a promising therapeutic approach to restore gut continuity and motility.

## 1. Introduction:

The gut is responsible for ingestion of food, propulsion of luminal content and excretion of waste. These functions are conducted by the basic unit of the musculature of the gut, which is the smooth muscle. Function of the smooth muscle of the gut is highly regulated, mainly by the enteric nervous system (ENS) and the interstitial cells of Cajal (ICCs) [1]. The smooth muscle receives regulatory inputs which are critical to produce a coordinated response. While the gut is considered a continuous tubular muscular organ (except for the stomach), several sphincters exist as checkpoints along the length of the gut. Those sphincters possess high pressure zone that regulate the propulsion of luminal content.

Motility disorders result when neuro-muscular functions of the gut are disturbed. In certain cases of neuro-muscular diseases, sphincter integrity and function is also impaired. In esophageal achalasia, impairment of the enteric neurons at the level of the smooth muscle of the lower esophagus causes loss of relaxation of the lower esophageal sphincter (LES) [2, 3]. Treatments aim to reduce the contractility of the LES. This can be done using different drugs/blockers, balloon dilatation, injection of botulinum toxin or myotomy of the LES [4]. On the other hand, gastroparesis is characterized by delayed gastric emptying. This is partially attributed to the inability of the pyloric sphincter to relax. Common treatments include botulinum toxin injection, drugs/diet change, gastric electric stimulation or pyloroplasty [5, 6]. In patients with colorectal cancer, preservation of the sphincter following surgical resection of the tumor is

challenging. The formation of a stoma is a common treatment; however patients suffer from low quality of life (social and physical problems) [7, 8]. In other cases, congenital anomalies such as anorectal malformation involve the rectum along with the anus. Children with anorectal malformation require surgical intervention which consists of either surgical repair or a colostomy [9]. Fecal incontinence is a major complication among other physical and social morbidities resulting from anorectal malformation [10-13]. All of the listed treatments for neuro-muscular disorders are either associated with complications or provide a short-term relief for the patients. New long term therapeutic strategies are needed.

Tissue engineering provides an alternative approach that has been shown to be promising in the field of gut bioengineering [14]. Our group has previously developed a technique to engineer different gut smooth muscle layers with the appropriate alignment [15, 16]. We have also engineered intrinsically innervated sphincteric tissues [17, 18]. The engineered sphincters became vascularized and maintained viability and functionality following their implantation in mice and rats. Recently, we expanded our engineering technique to develop tubular neuro-muscular intestinal tissues [19]. The tissues maintained their cellular alignment, became vascularized and maintained neuro-muscular phenotype and functionality following their subcutaneous implantation in rats. The objective of this study was to engineer a human gut-sphincter complex by combining the engineered sphincters and engineered tubular gut tissues around tubular chitosan scaffolds. We subcutaneously implanted the engineered human segment for 4 weeks in the abdomen of rats. The tissues were vascularized,

exhibited both luminal pressure and baseline force, and possessed mechanical properties close to native intestine.

## **2. Materials and methods:**

### **2.1. Reagents:**

Cell culture reagents were purchased from Life Technologies (Grand Island, NY, US) unless otherwise specified. Smooth muscle growth medium consisted of Dulbecco's modified Eagle medium, 10% fetal bovine serum, 1X antibiotic-antimycotic, and 2 mM L-glutamine. Neural growth medium consisted of neurobasal, 1X N2 supplement, recombinant human Epidermal Growth Factor (EGF 20 ng/mL, Stemgent, San Diego, CA, US), recombinant basic Fibroblast Growth Factor (bFGF 20 ng/mL, Stemgent, CA, US), and 1X antibiotic-antimycotic. Neural differentiation media consisted of neurobasal medium-A supplemented with 2% fetal bovine serum, 1X B27 supplement and 1X antibiotic-antimycotic. Medium molecular weight chitosan (75–85% deacetylation), tetrodotoxin (TTX; 1 µmol/L), and neuronal nitric oxide synthase (nNOS)-blocker *N*<sub>ω</sub>-Nitro-L-arginine methyl ester hydrochloride (L-NAME; 300 µmol/L) were purchased from Sigma (St. Louis, MO). Sylgard [poly(dimethylsiloxane); PDMS] was purchased from World Precision Instruments (Sarasota, FL). Type I rat tail collagen was purchased from BD Biosciences.

### **2.2. Cell Isolation:**

Autologous healthy human intestinal and pyloric tissues were ethically obtained from organ donors through Carolina Donor Services and Wake Forest Baptist



Medical Center (IRB No. 00007586). Tissues were obtained from 3 donors of ages 2, 18 and 67 years old.

**a) Human intestinal circular smooth muscle cells:**

Smooth muscle cells were isolated from human duodenum following the protocols previously described by our lab [19]. The duodena (10 cm below the pyloric sphincter) were consistently obtained for cell isolation. Human duodena were cleaned of any luminal content and were washed extensively in ice-cold Hank's balanced salt solution (HBSS) containing antibiotics-antimycotics. The tissues were cut into smaller pieces and the circular smooth muscle was obtained by stripping off the mucosa and the longitudinal muscle. The circular smooth muscle tissue was then minced and washed extensively in HBSS. The muscle was then finely minced, washed extensively in HBSS and incubated in a digestion mix containing 1mg/ml type II collagenase (Worthington, Lakewood, NJ) and 30 µg/mL DNase (Roche, Indianapolis, IN) for one hour at 37°C with agitation. The digested tissue was then extensively washed in HBSS and subjected to a second digest for an hour. Digested cells were washed by centrifugation, resuspended in warm smooth muscle growth media and expanded in tissue culture flasks at 37°C with 5% CO<sub>2</sub>.

**b) Human pyloric smooth muscle cells:**

Human pylori were dissected off for smooth muscle isolation following previously published protocols [20]. Pylorus tissues were cleaned of any fat and mucosa and extensively washed with HBSS. Tissues were then cut into smaller pieces,

minced and washed again with sterile HBSS. Minced tissues were digested in 1mg/ml type II collagenase (Worthington Biochemical, Lakewood, NJ) and 30 µg/mL DNase (Roche, Indianapolis, IN) mix solution twice at 37°C with agitation at 100rpm for one hour each digest. Cells were pelleted down with centrifugation at 800 g, resuspended in smooth muscle growth media and expanded in tissue culture flasks at 37°C with 5% CO<sub>2</sub>.

**c) Human enteric neural progenitor cells:**

Human enteric neural progenitor cells were isolated from the small intestine as previously published [19]. Human duodenal tissues were finely minced followed by extensive washing in HBSS. Tissues were then digested in a mixture of 0.85 mg/ml type II collagenase, 0.85 mg/ml dispase II, and 30 µg/mL DNase for one hour. Following digestion, the tissues were recovered by centrifugation and the cells in the supernatant were passed through 70 µm cell strainer followed by extensive washing. The pelleted tissues were subjected for a second digest followed by centrifugation and recovery of the cells through 70 µm cell strainer. The recovered cells from both digests were then passed through 40 µm cell strainers. Following centrifugation, cells were resuspended in neural growth media and cultured in non-tissue culture treated plates at 37°C and 7% CO<sub>2</sub>. The cultured cells formed free-floating clusters referred to as neurospheres which have been shown to stain positive for neural crest-derived cell marker p75 [21].

### *2.3. Preparation of tubular gut-sphincter segment:*

Tubular chitosan/collagen scaffolds were engineered using the freezing and lyophilizing method as described previously [22, 23]. A 2% w/v chitosan solution was prepared in 0.2M acetic acid. The chitosan solution was then mixed with type I collagen in a 1:1 ratio. The mix was then poured into a custom-made 3 cm long tubular mold with a diameter of 0.7 cm. The lumen of the scaffold was created by inserting an inner tubing of 0.3 cm diameter in the center of the main tubular mold. This created a scaffold with length of 3 cm and internal diameter of 0.3 cm. The mixture in the molds was frozen at -80°C for 3 hours followed by lyophilization overnight. The scaffolds were then neutralized in 0.2 M NaOH and washed extensively with PBS and distilled water. The scaffolds were sterilized in 70% ethanol and then washed extensively with sterile 1X PBS before cell seeding.

Innervated aligned smooth muscle sheets were engineered as previously described [19, 24]. Briefly, smooth muscle cells were seeded onto laminin coated wavy molds made of Sylgard with longitudinal grooves and allowed to align. Five days following smooth muscle alignment, neural progenitor cells were collected and suspended in a mixture of 10% FBS, 1X DMEM, 1X antibiotic–antimycotic, 10 µg/mL mouse laminin and 0.4 mg/mL type I rat tail collagen. The resuspended neural progenitor cells were laid on top of the aligned smooth muscle. Neural differentiation media was supplemented every other day for 10 days.

Human innervated pyloric smooth muscle sphincters were engineered using our previously described technique [25]. A suspension of 200,000 enteric neural

progenitor cells was suspended in a gel mix similar to the one described above. The mixture was pipetted on a Sylgard-coated plate that had a central cylindrical post and allowed to gel for about 20 minutes at 37°C. Pyloric smooth muscle cells were trypsinized and 500,000 cells were obtained. The cells were resuspended in a similar gel mixture as described earlier. The mixture was then pipetted on top of the first neural layer. Following gelation, differentiation media was supplemented every other day for 10 days.

The formed engineered human innervated smooth muscle sheets were circumferentially wrapped around the tubular scaffolds as described previously to mimic the circular muscle layer [19]. The inner tubing of the mold was left inside the lumen of the tissue to retain its lumen and prevent the opposing walls from collapsing. The ends of the tissues were left open. The gut-sphincter complex was left in culture for 2 days until the time of implantation.

#### *2.4. Implantation of the engineered tubular gut-sphincter complex:*

Athymic rats (n=6) were used as recipients of the tubular human gut-sphincter complexes. Surgical procedures described in this work were performed following the guidelines set forth by IACUC. Rats were anesthetized by continuous isoflurane masking throughout the surgery. The surgical area was shaved and aseptically prepared. A midline skin incision of up to 5 cm was made in the abdominal wall. The engineered tubular gut-sphincter complex was implanted lateral and parallel to the midline followed. The tissue was then stabilized using 5-0 prolene sutures to mark the tissue at the time of harvest. The rats were

allowed to recover in their cages in standard fashion and were given the appropriate analgesics.

### *2.5. In vivo intraluminal pressure measurement:*

Four weeks following implantation, the rats were brought back to the procedure room. The rats were anesthetized by continuous isoflurane masking. The surgical site was re-accessed. The implants were located by the prolene sutures. An air-charged catheter with 4 consecutive circumferential sensors (7 mm spacing between the sensors) was used to measure in vivo the luminal pressure of the tubular implants. The catheter was inserted into the tubular implant entering from the gut part until the first sensor of the catheter reached the sphincteric area. The remaining 3 sensors were measuring pressure at the gut part of the tubular implant. Luminal pressure was recorded using InSIGHT Acquisition (version 5.2.4, Sandhill scientific Inc, Highland Ranch, CO, USA, [www.sandhillsci.com](http://www.sandhillsci.com)). The recorded pressures were analyzed using BioVIEW system (version 5.6.3.0 Sandhill scientific Inc, Highland Ranch, CO, USA, [www.sandhillsci.com](http://www.sandhillsci.com)). Following pressure readings, the rats were euthanized. The implants were dissected from the surrounding tissue. The harvested implants were further evaluated.

## *2.6. Mechanical properties of the implants:*

### **a) Tensile properties:**

Immediately after harvest, the implants were tested for their tensile properties using a uniaxial load test machine (Instron model # 5544, Issaquah, WA, USA). Tubular specimens were obtained and hooked onto the machine equipped with a 2kN load cell. Tensile strength, elongation at break and Young's modulus were obtained. Rat native intestines with intact cell layers served as control.

### **b) Burst pressure strength:**

A pressure transducer catheter with an inflatable balloon was used to measure the burst strength pressure of the implants. The catheter was inserted into the lumen of the tissues and the luminal pressure was increased until failure occurred. The pressure was slowly increased until failure occurred and the pressures were recorded. Rat duodena were used as control.

## *2.7. Histological and immunofluorescence evaluation of the implant:*

Immediately after harvest, sections of the sphincter and the gut tissues were fixed in formaldehyde, processed and paraffin embedded. Sections were deparaffinized and stained with hematoxylin and eosin (H&E) for morphological analysis. Phenotype of smooth muscle and differentiated neurons were analyzed by incubating the sections in primary antibodies directed against smoothelin and  $\beta$ -III tubulin, respectively. Neuronal nitric oxide synthase (nNOS) and choline acetyltransferase (ChAT) antibodies were used to confirm the presence of

inhibitory and excitatory motor neurons, respectively. Vascularization was confirmed by immunostaining of the sections with von Willebrand (vWF) factor. Appropriate fluorophore-conjugated secondary antibodies were used.

### *2.8. Physiological analysis of the implant:*

Circular strips of the harvested sphincters and gut tissues were also immediately obtained after euthanasia of the rats, and evaluated for physiological functionality. A force transducer apparatus (Harvard Apparatus, Holliston, MA) was used to measure real time force generation. The tissues were hooked to a stationary fixed pin from one side and to the measuring arm of the force transducer from the other side. The tissues were kept in a warm tissue bath throughout the experiments. Establishment of basal tone by the sphincters, electromechanical coupling integrity of the smooth muscle of both the sphincters and the gut tissues, and the functionality of the differentiated neurons were evaluated as described before [19, 25].

Electromechanical coupling integrity was evaluated in the presence of 60mM potassium chloride (KCl). Functionality of neurons was evaluated using electrical field stimulation (EFS) in the absence and presence of neurotoxin, tetrodotoxin (TTX) and nitric oxide synthase (nNOS) blocker *N*<sub>ω</sub>-Nitro-L-arginine methyl ester hydrochloride (L-NAME).

### **2.9. Statistical analysis:**

The difference in tensile strength, elongation at break and Young's modulus between the implants and the native rat intestines was evaluated by Student's *t*-test. Analysis of acquired force data was conducted using Powerlab and exported to GraphPad Prism 5.0 for Windows (GraphPad Software, San Diego CA; [www.graphpad.com](http://www.graphpad.com)). Second order Savitzky–Golay smoothing was applied to data. Student paired *t*-test was used to compare the means of forces in the absence and presence of inhibitors. All values were expressed as means  $\pm$  SEM. A *p*-value less than 0.05 was considered significant.

## **3. Results:**

### **3.1. Harvest of the implant:**

Gut-sphincter complex were engineered by combining innervated human smooth muscle sheets and engineered innervated human pyloric sphincters around tubular chitosan scaffolds (**Figure 37**). The engineered innervated human smooth muscle sheets were wrapped circumferentially around the tubular scaffolds to form the circular muscle layer. The sheets constituted the gut part of the gut-sphincter complex. The engineered sphincters of the complex were placed at one end of the scaffolds. The bioengineered human tissues were implanted subcutaneously in the abdomen of athymic rats for 4 weeks. At the end of 4 weeks implantation, the engineered gut became integrated with the engineered sphincter and formed a single continuous functional unit. The implants showed healthy pink color upon harvest. The implants were 3 cm in length and 0.5 cm diameter. The luminal patency of the implants was maintained



for 4 weeks post-implantation. There were no signs of inflammation, infection or tissue necrosis. Neovascularization was visually demonstrated by the presence of blood vessels around the implants. The ends of the tubular tissues were refreshed and the inner tubing was taken out.

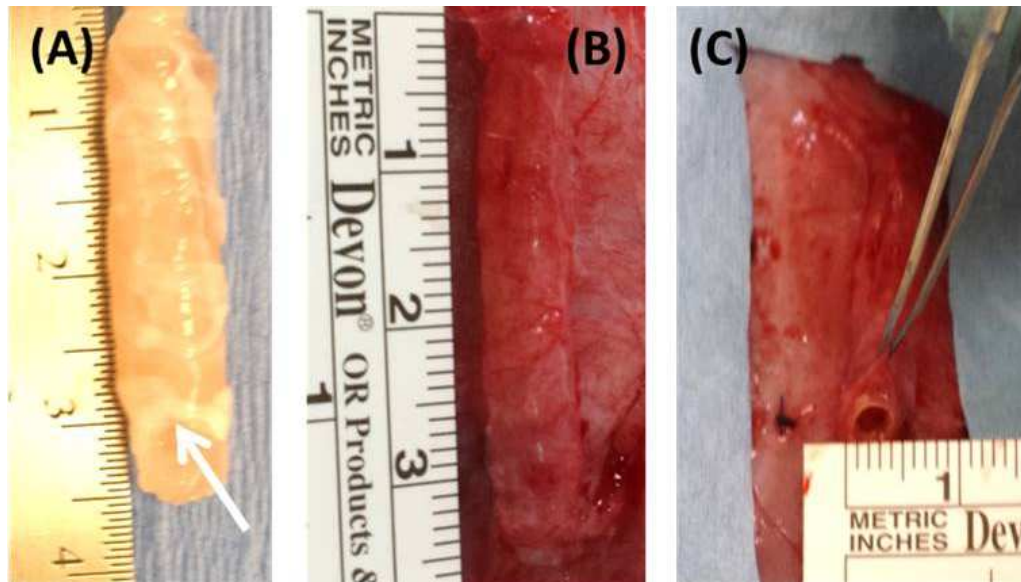


**Figure 37:** Harvest of the gut-sphincter complex after 4 weeks of implantation. (A) The complex pre-implantation, 3 cm in length, shows a gut part and a sphincter part (white arrow). (B) After 4 weeks of subcutaneous implantation in the abdominal wall shows vascularization of the complex. (C) The complex maintained its luminal patency (0.3 cm internal diameter).

### 3.2. *In vivo intraluminal pressure:*

The rats were anesthetized by continuous isoflurane masking. The implants were re-accessed. The catheter with circumferential sensors was calibrated before any measurement. The pressure reading was set to zero prior to insertion of the catheter into the lumen of the implant. The catheter was inserted into the lumen of the implant by increment of 1 sensor at a time until all sensors were inserted

**(Figure 38).** Pressures started increasing as the catheter was inserted into the tissue. Pressure reading from each sensor was reflected on a separate channel. The catheter was inserted from the gut side of the implant (opposite end of the sphincter). Pressure reading of the sphincter is shown on the top graph. The other 3 lower channels were measuring the gut part of the complex. The mean luminal pressure (of all sensors) of the gut zone was  $(21 \pm 2 \text{ mmHg})$ . The mean pressure recorded at the sphincter zone was  $(52 \pm 3 \text{ mmHg})$ . The basal tone of the sphincter increased gradually to reach the highest zone. After that, the pressures were stable over time. The luminal patency was further confirmed by completely inserting the catheter through the length of the implant without obstruction.

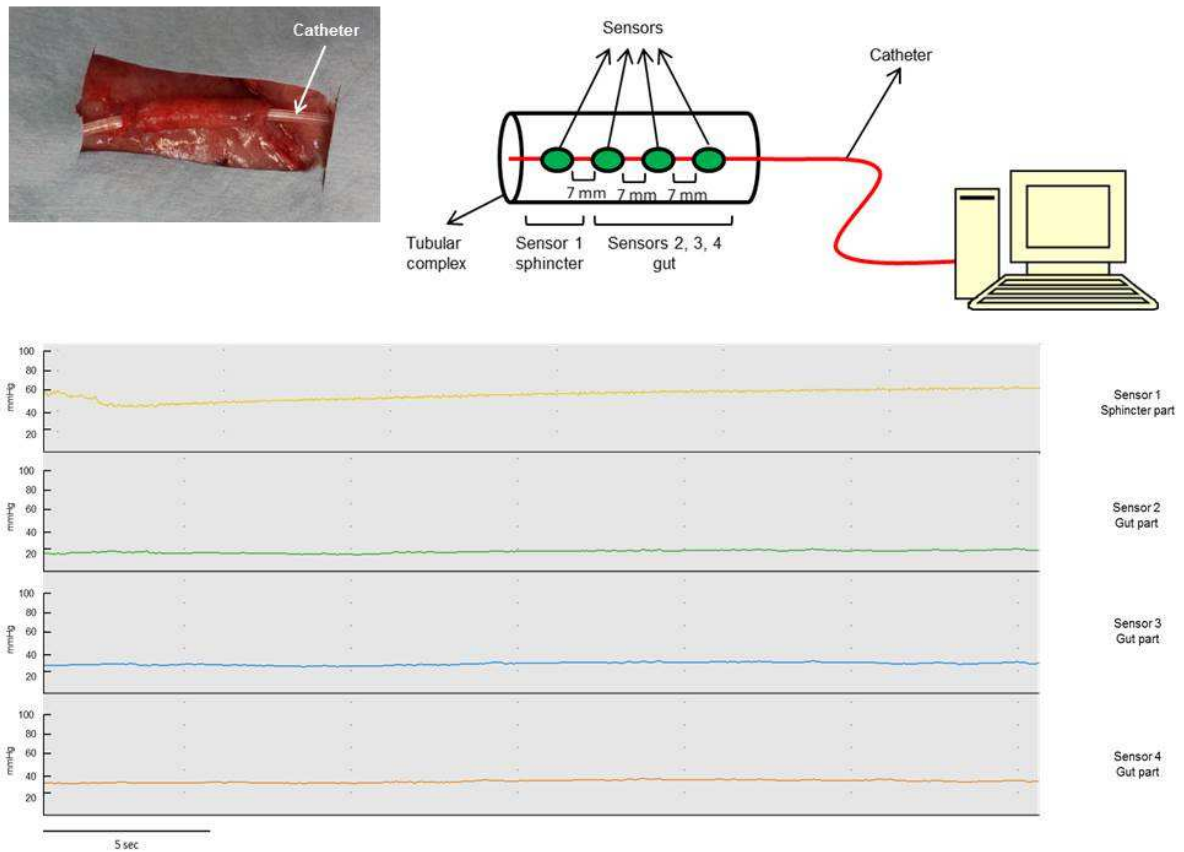


**Figure 38:** In vivo intraluminal pressure measurement. The rats were anesthetized and the complex was accessed. A catheter with 4 circumferential sensors was inserted into the complex to measure luminal pressure. The catheter was connected to Sandhill equipment that records the pressures (as shown in the diagram). Mean gut luminal pressure was  $21 \pm 2$  mmHg while the sphincteric pressure was  $52 \pm 3$  mmHg.

### 3.3. Mechanical properties of the implants

#### a) Tensile properties:

Uniaxial tensile properties of the implants were compared to those of native rat intestine. The tensile strength was significantly different between the implants and the native rat intestine (**Figure 39**). The tensile strength of the native rat

intestine was  $0.054 \pm 0.005$  MPa whereas the average tensile strength of the implants was  $0.043 \pm 0.007$  MPa ( $n = 4$ ,  $p = 0.12$ ). Elongation at break and Young's modulus of the implants were lower than those of the native rat intestine, however, they were not significantly different ( $n = 4$ ,  $p = 0.1$  and  $p = 0.37$  respectively). Elongation at break and Young's modulus were  $230 \pm 13$  % and  $0.12 \pm 0.01$  MPa, respectively for the native rat intestine. The implant's elongation at break and Young's modulus averaged  $171 \pm 30$  % and  $0.1 \pm 0.01$  MPa, respectively.

**b) Burst pressure strength:**

A pressure transducer catheter with an inflatable balloon was inserted inside the lumen of the tubular implants. Pressure was increased gradually until failure of the implant. The pressure at failure was recorded as the burst pressure strength. The mean burst pressure strength of the implants was  $1396 \pm 60$  mmHg compared to  $1655 \pm 56$  mmHg in rat duodena ( $p = 0.06$ ).

**3.4. Histology and immunofluorescence:**

**a) H&E:**

Paraffin cross sections of the harvested engineered sphincters and gut tissues of 6  $\mu$ m thickness were prepared. Representative H&E staining of both the engineered sphincters and gut tissues after implantation is shown in **Figure 40**. The engineered innervated smooth muscle sheets were wrapped circumferentially around the tubular scaffolds to form circular muscle layer. The

smooth muscle of the engineered sphincters was also circumferentially aligned. H&E stains showed maintenance of smooth muscle alignment around the lumen of the tubular tissues for both the gut segment and the sphincter. H&E shows dense aligned smooth muscle.

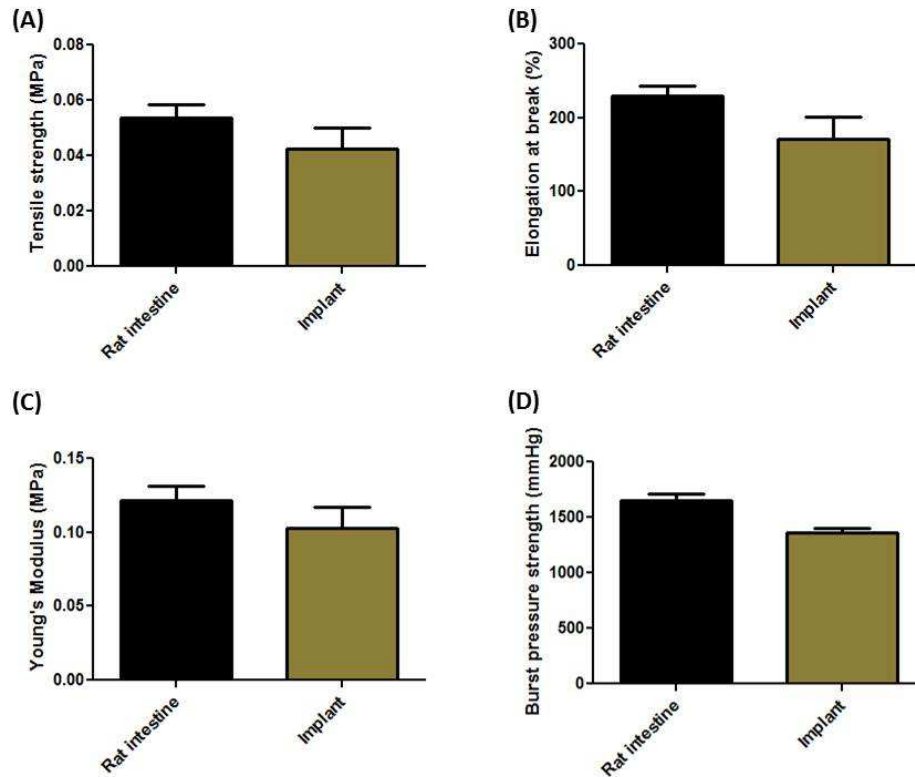


**Figure 39:** Mechanical properties of the implanted complex. The tensile properties of the complex were lower than those of the native rat intestine; however they were not significantly different. (A) The tensile strength of the complex was  $0.043 \pm 0.007$  MPa compared to  $0.054 \pm 0.005$  MPa for the native rat intestine. (B) Elongation at break of the implant was  $171 \pm 30$  % compared to  $230 \pm 13$  % for the native rat intestine. (C) Young's modulus of the implanted complex was  $0.1 \pm 0.01$  MPa compared to  $0.12 \pm 0.01$  MPa for the native rat intestine. (D) Burst pressure strength of the implant was  $1396 \pm 60$  mmHg while that of rat duodena was  $1655 \pm 56$  mmHg ( $p = 0.06$ ).

**b) Immunofluorescence:**

**Figure 41** shows immunofluorescence evaluation of the implants. Sections of both the engineered sphincters and the engineered gut segments stained positive for the smooth muscle specific marker smoothelin. This indicated that smooth muscle contractile phenotype of both the engineered sphincter and the gut segment was maintained over a period of 4 weeks post-implantation. Engineered tissues also stained positive for pan-neuronal marker,  $\beta$ III-tubulin, indicating the presence of differentiated neurons in the engineered complex 4 weeks post-implantation. Additional positive staining for neural nitric oxide synthase (nNOS) and choline acetyltransferase (ChAT) indicate the presence of inhibitory and excitatory motor neurons in the implanted complex. Positive stain for vWF confirmed the vascularization of the implants.

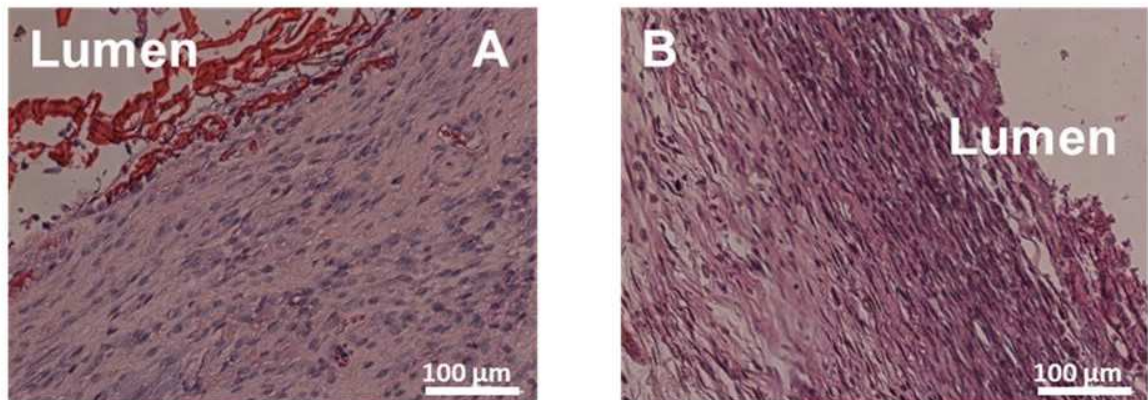


**Figure 40:** Histological evaluation of the implants. Representative images of H&E for the (A) sphincter and (B) gut parts of the complex show maintenance of the circular alignment of the smooth muscle around the lumen of the tubular graft.

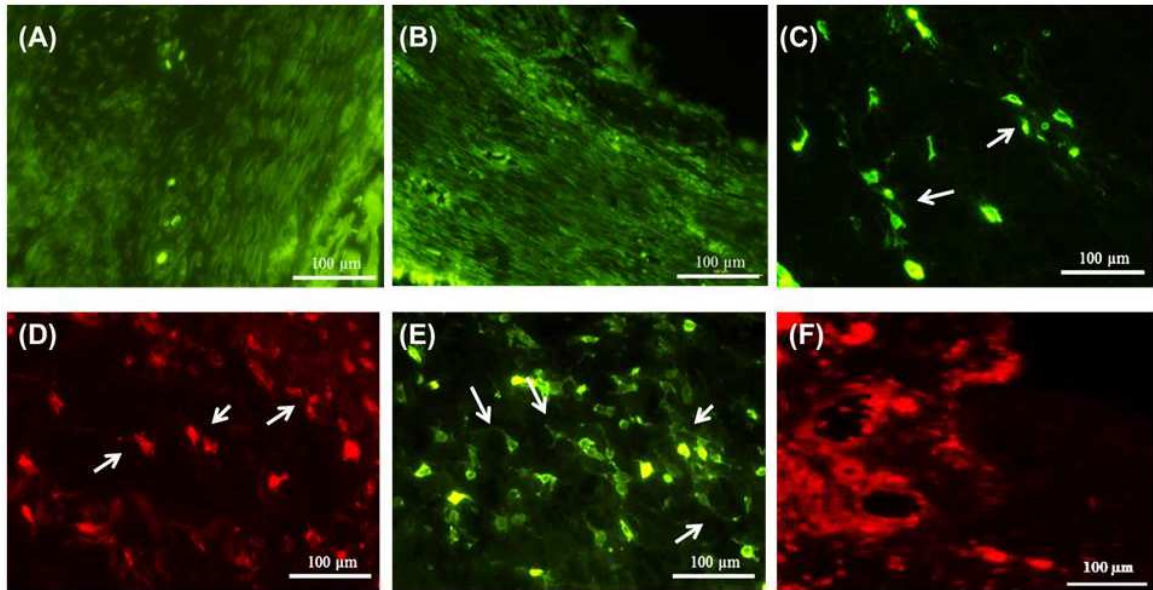


**Figure 41:** Immunofluorescence of the implants. Smooth muscle of (A) the sphincter and (B) the gut parts of the complex maintained their contractile phenotype as shown by positive stain for smoothelin after 4 weeks of implantation. (C) Innervation of the complex was demonstrated by positive stain with  $\beta$ III tubulin, indicating that the neural progenitor cells differentiated into neurons. (D) The presence of excitatory motor neurons was demonstrated by positive stain with ChAT. (E) Inhibitory motor neurons stained positive with nNOS. (F) Vascularization was demonstrated by positive stain with von Willebrand factor.

### 3.5. *Physiological studies:*

Circular strips of implanted engineered sphincter and gut segments were hooked to a force transducer measuring arm and allowed to establish baseline (**Figure 42**). The engineered sphincters exhibited the spontaneous ability to generate basal tone that averaged  $382 \pm 79 \mu\text{N}$ . Electromechanical coupling integrity of both the sphincters and the gut segments was demonstrated by the robust contraction of the tissues after the addition of KCl. Sphincters demonstrated a contraction of  $427 \pm 42 \mu\text{N}$  above the basal tone while the gut tissues exhibited a mean peak contraction of  $434 \pm 17 \mu\text{N}$ .

Functionality of neurons in the segment was evaluated by electrical field stimulation (8 Hz and 0.5 ms). Smooth muscle of both the implanted engineered sphincters and the gut segments relaxed following excitation of the nerves (**Figure 43**). Relaxation of the implanted sphincters averaged  $-294 \pm 26 \mu\text{N}$  below the basal tone and the maximal relaxation averaged  $-355 \pm 8 \mu\text{N}$  in the gut segment. The tissues were then washed with fresh warm buffer and pre-treated with TTX. Upon excitation of the nerves, relaxation was completely abolished in both the sphincters and the gut segments. This indicated that the relaxation of the smooth muscle observed following EFS without TTX was due to excitation of neurons only. This also indicates that the neural progenitor cells within the complexes differentiated into functional neurons. Further characterization of the relaxation response was studied in the presence of nNOS inhibitor LNAME. The tissues were pre-treated with LNAME followed by EFS. Relaxation was significantly reduced to  $-140 \pm 6 \mu\text{N}$  in the sphincters (gold trace) and  $-223 \pm 29$  in the gut segments (gold trace). This inhibition indicates that EFS-induced relaxation of the smooth muscle was partially mediated by functional nitrergic neurons.

#### **4. Discussion:**

Surgical intervention (resection of the diseased segment of the gut followed by anastomosis or creation of a permanent stoma) remains the gold standard treatment for GI disorders at least for the short term. However, long term patient satisfaction needs to be achieved. Depending on the location of the



resection, loss of gut segments can be accompanied with loss of sphincteric integrity and function. In this study, we provide an approach to both lengthen the gut and restore sphincter integrity and function. To our knowledge, this is the first case of engineering a single functional complex composed of a sphincter part and a gut part. The engineered complex became vascularized when implanted subcutaneously in the abdomen of athymic rats for 4 weeks. Physiological functionality of the gut and the sphincter parts were maintained. Future studies will look at motility functions of the complex following its anastomosis to the native intestine.

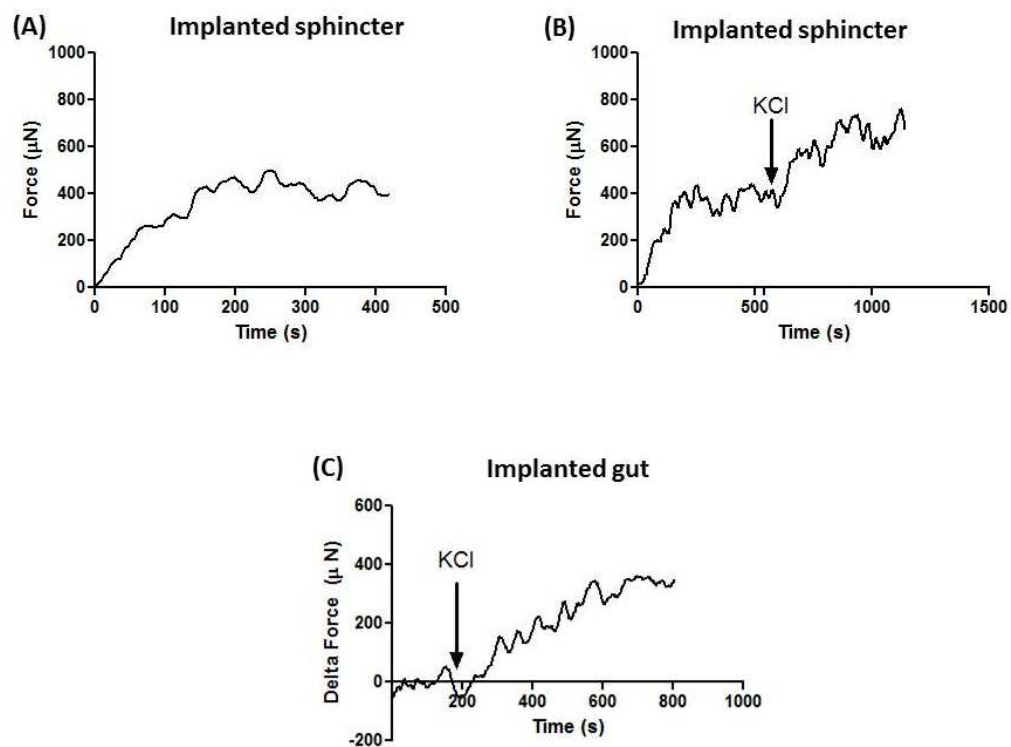


**Figure 42:** In vitro physiological functionality of the implants – myogenic component. (A) The implanted sphincter maintained its capacity to generate a spontaneous basal tone of  $382 \pm 79 \mu\text{N}$ . (B) The addition of potassium chloride (KCl) resulted in a contraction of  $427 \pm 42 \mu\text{N}$  above the basal tone in the sphincter. (C) KCl resulted in a robust and sustained contraction ( $434 \pm 17 \mu\text{N}$ ) in the gut part of the complex.

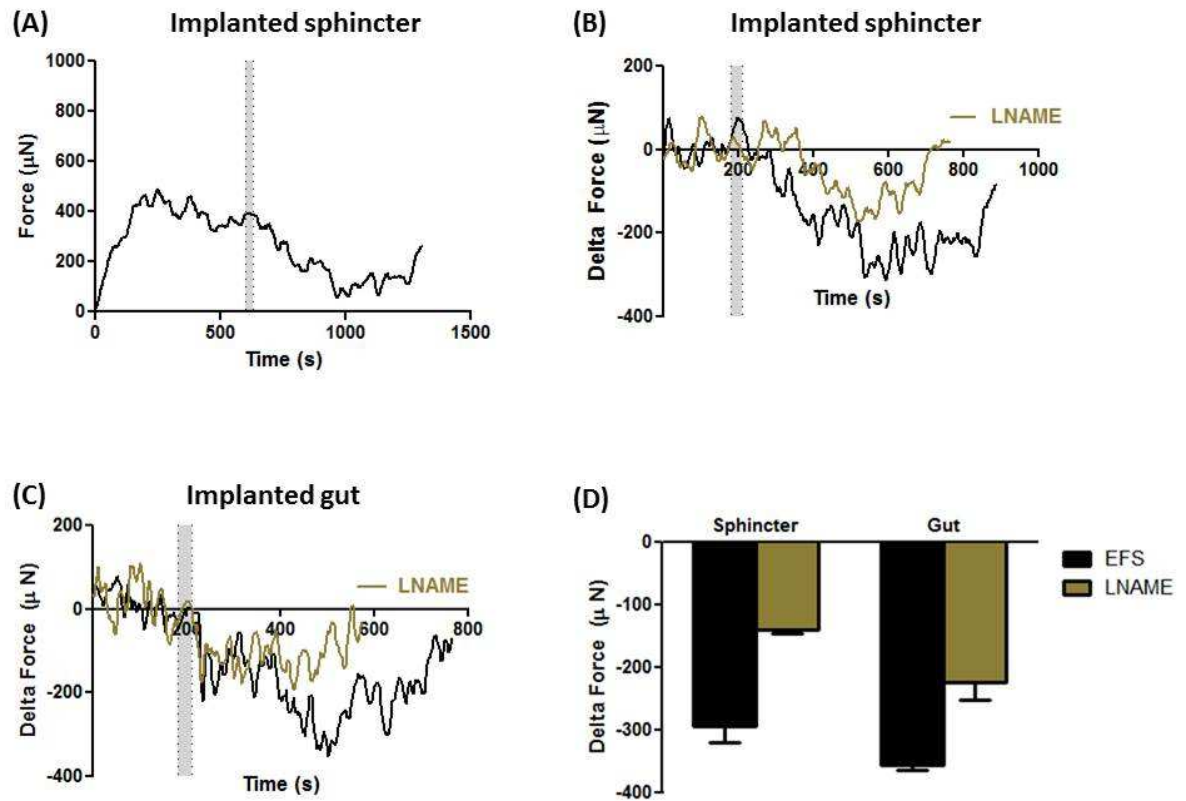


**Figure 43:** In vitro physiological functionality of the implants (neural component). Electrical field stimulation (EFS) of both the (A & B) sphincter and the (C) gut parts of the complex caused relaxation of the smooth muscle (black trace). Pre-incubation of the implants with nNOS inhibitor LNAME significantly reduced the magnitude of relaxation, indicating the presence of functional nitrergic neurons (gold trace).

There are several challenges in the field of GI tissue engineering, in part due to the different types of cells that colonize the gut and due to the different architecture of the cells. The multicellular aspect of the gut sets a challenge for finding an adequate cell source. Organoid units isolated from different parts of the gut (esophagus, stomach, small intestine and colon) have shown

regeneration capacity when seeded onto polymer scaffolds [26-28]. Functional assays have shown the presence of differentiated epithelium [29]. An innervated muscularis layer was demonstrated by immunohistochemistry. Additional functional evaluation of the regenerated muscle will be necessary for motility purposes. The ability to expand organoid units in vitro to generate enough units for seeding might be a limitation.

Intestinal smooth muscle cells are potential candidates for regeneration of the musculature of the gut. In our study, we used 10 cm duodenal tissues to isolate smooth muscle cells and neural progenitor cells. Our previous proliferation assays have demonstrated the potential of isolating these cells from human tissues and growing them to a sufficient number in order to engineer the constructs [30]. Currently, we are using the gut as source of cells. Previous studies investigated the feasibility of isolating enteric neural progenitor cells from Hirschsprung's patients [31, 32]. This is promising when it comes to autologous applications. Our large animal studies have shown that a 1 cm<sup>2</sup> intestinal tissue is enough to generate smooth muscle and neural progenitor cells. A common limitation using primary smooth muscle cells is their ability to maintain their contractile phenotype in a 3D setting. Contractile phenotype reflects normal physiological function of the smooth muscle. Smooth muscle survival following implantation is challenging [33]. Previous studies have looked at different designs of scaffolds in order to maximize survival and function of seeded smooth muscle following implantation [34]. It was found that smooth muscle cells survive better at a higher porosity. In our study, we used smooth muscle cells and enteric

neural progenitor cells isolated from the gut to engineer 3D innervated smooth muscle tissues. The engineered tissues exhibited a contractile phenotype in vitro. After 4 weeks of implantation, those tissues maintained their contractile phenotype as demonstrated by immunohistochemistry and physiological studies. Apart from phenotype, recapitulating the alignment of the smooth muscle is another challenge. It is essential to recapitulate the alignment specific to each muscle layer for proper function. The advantage of our engineering technique lies in the ability to engineer pre-aligned, neo-innervated smooth muscle tissues. The smooth muscle of the tubular gut-sphincter complexes maintained their circular alignment around the lumen of the complexes, mimicking the circular muscle of the gut.

Acellular approaches have been explored in the field of gut bioengineering. Chitosan was recently evaluated in the form of acellular hydrogel for intestinal regeneration [35]. Regeneration of an organized epithelial cell layer was observed in the harvested tissue. A partial regeneration of the smooth muscle layer was observed only after 60 days of implantation of the chitosan hydrogels. In our study, tubular chitosan scaffolds were used as matrices for the engineered gut-sphincter tissues. The engineered complexes exhibited a mature contractile phenotype as early as 2 weeks and then at 4 weeks post implantation. Neuro-muscular activity of the engineered complexes was evaluated by in vivo luminal pressure recordings and in vitro organ bath physiological studies. Even though the forces generated by the engineered complexes were lower than the forces generated by the native intestine, it is important to notice that the force

patterns displayed by the engineered complexes are similar to native tissues [36]. Engineered gut tissues generating lower force than native gut tissues has been a challenge in other studies as well [37]. In future studies involving anastomosis of the engineered complexes to native intestines, it will be interesting to evaluate whether host cells infiltrate the engineered tissues and increase the magnitude of force generated by the engineered tissues.

Current treatments to restore sphincteric function range from diet change, medications, toxin injections or electric stimulation. The efficacy of toxin injection requires further investigations. Electric stimulation has been associated with complications that include infection at the site of implantation of the device. This has led to the removal of the device from patients. Additional studies are needed to confirm the efficacy and effectiveness of those approaches. This has shifted the focus to a regenerative medicine approach to treat neuro-muscular disorders in the gut. In previous studies, skeletal muscle derived cells were injected into the LES and resulted in increased basal LES pressure [38]. Immunofluorescence assays showed that the muscle derived cells differentiated into skeletal muscle rather than smooth muscle. The tonic activity of the sphincter is dominantly due to the smooth muscle component of the sphincter. Restoration of the myogenic tone of the sphincter (smooth muscle component) is therefore critical for reinstating normal sphincter function. In our approach, we provided a bioengineered complex that has both a gut segment and a sphincteric tissue with appropriate neuro-muscular function. The implanted engineered sphincteric tissues maintained their ability to generate spontaneous basal tone when

compared to engineered sphincters pre-implantation [25]. The contractile phenotype of the sphincteric smooth muscle was maintained. Our previous studies have shown that bioengineered IAS tissues became vascularized and maintained viability and functionality when implanted alone as sphincter replacements in rat models [18]. Based on those results, we suggest that the bioengineered complex with a sphincter and a gut part holds a promising option for gut replacement. Our regenerative medicine approach provides a unique continuous complex that contains both a functional sphincteric part and a functional gut part in a single unit. This approach makes it easier for the replacement of any diseased or degenerated sphincter in addition to lengthening the gut.

Long term success of the engineered gut tissues requires additional quality control testing. In previous studies, there has been no emphasis on the mechanical strength of the engineered gut tissues. Some of the main surgical complications that arise following intestinal anastomosis in humans include leakage or stenosis at the anastomosis site. While animal studies involving anastomosis of engineered gut tissues have shown successful outcomes, additional evaluation of the engineered tissues is needed for translational purposes. The engineered complexes exhibited tensile properties similar to native rat intestine following 4 weeks of implantation. This is crucial to avoid any compliance mismatch following anastomosis.

Previous attempts have aimed at regenerating either intestinal replacements or at re-instating sphincteric pressure. In this study, we

demonstrated the successful regeneration of the neuro-muscular components of both sphincters and gut in a single continuous segment. The segment met the basic requirements for motility. However, this study still lacks some additional components to fine tune the muscular component. First, ICCs are believed to be regulators of smooth muscle rhythmic function. Preliminary studies have been initiated in the lab to incorporate ICCs in the engineering process to assess the myogenic activity of the complex. Protocols for isolation of ICCs are established in the literature. Co-culturing smooth muscle cells with ICCs in an engineered construct is currently under consideration [39]. Second, the epithelial component is still missing in our engineered complex. Current studies in our lab are seeking different approaches to regenerate the epithelium as part of the complex. Third, the engineered complex was implanted subcutaneously in the abdominal area. Our future studies plan to anastomose the engineered tissues with the native tissue to evaluate peristalsis and motility.

## **5. Conclusion:**

Neuro-muscular diseases of the GI tract result in motility disorders. Often, these diseases affect a gut segment along with the adjacent sphincter. Different approaches are being developed to restore neuro-muscular functions. In this study, we provide an approach to reconstruct gut sphincter incorporated into a gut segment. We successfully engineered a human-derived tubular neuromuscular tissue. The tissue consisted of an innervated gut smooth muscle and an intrinsically innervated sphincter tissue. The cellular components of the

tissue maintained their alignment, phenotype and physiological functionality following their subcutaneous implantation in rats for 4 weeks. The engineered tubular complex possessed biomechanical properties that make it suitable for gut replacement. Future studies will look at the epithelial regeneration and motility capacity of the engineered tissue.

## **6. Acknowledgment:**

This study was supported by Wake Forest School of Medicine Institutional Funds and NIH/NIDDK 1R42DK105593.

***In this chapter, the engineered human based gut-sphincter complex maintained its survival and function following its subcutaneous implantation for 4 weeks in athymic rats. This work offers a regenerative medicine approach to treat patients who present with diseased gut segments that extended to the adjacent sphincter (i.e. LES achalasia, gastroparesis and fecal incontinence). Having successfully engineered the neuro-musculature of the GI tract, the next step was to regenerate the epithelial component of the gut.***



## 7. References:

- [1] Sanders K. Regulation of smooth muscle excitation and contraction. *Neurogastroenterology & Motility*. 2008;20:39-53.
- [2] Hirano I. Pathophysiology of achalasia and diffuse esophageal spasm. *GI Motility* online. 2006.
- [3] Park W, Vaezi MF. Etiology and pathogenesis of achalasia: the current understanding. *The American journal of gastroenterology*. 2005;100:1404-14.
- [4] Pohl D, Tutuian R. Achalasia: an overview of diagnosis and treatment. *Journal of Gastrointestinal and Liver Diseases*. 2007;16:297.
- [5] Parkman HP, Hasler WL, Fisher RS. American Gastroenterological Association technical review on the diagnosis and treatment of gastroparesis. *Gastroenterology*. 2004;127:1592-622.
- [6] Miller LS, Szych GA, Kantor SB, Bromer MQ, Knight LC, Maurer AH, et al. Treatment of idiopathic gastroparesis with injection of botulinum toxin into the pyloric sphincter muscle. *The American journal of gastroenterology*. 2002;97:1653-60.
- [7] Sprangers M, Taal B, Aaronson N, Te Velde A. Quality of life in colorectal cancer. *Diseases of the colon & rectum*. 1995;38:361-9.
- [8] Engel J, Kerr J, Schlesinger-Raab A, Eckel R, Sauer H, Hölzel D. Quality of life in rectal cancer patients: a four-year prospective study. *Annals of surgery*. 2003;238:203.
- [9] Levitt MA, Peña A. Anorectal malformations. *Orphanet J Rare Dis*. 2007;2:1-13.
- [10] Bai Y, Yuan Z, Wang W, Zhao Y, Wang H, Wang W. Quality of life for children with fecal incontinence after surgically corrected anorectal malformation. *Journal of pediatric surgery*. 2000;35:462-4.

- [11] Patwardhan N, Kiely E, Drake D, Spitz L, Pierro A. Colostomy for anorectal anomalies: high incidence of complications. *Journal of pediatric surgery*. 2001;36:795-8.
- [12] Hamid C, Holland A, Martin H. Long-term outcome of anorectal malformations: the patient perspective. *Pediatric surgery international*. 2007;23:97-102.
- [13] Pena A, Migotto-Krieger M, Levitt MA. Colostomy in anorectal malformations: a procedure with serious but preventable complications. *Journal of pediatric surgery*. 2006;41:748-56.
- [14] Bitar KN, Zakhem E. Is bioengineering a possibility in gastrointestinal disorders? *Expert review of gastroenterology & hepatology*. 2015:1-3.
- [15] Hecker L, Baar K, Dennis RG, Bitar KN. Development of a three-dimensional physiological model of the internal anal sphincter bioengineered in vitro from isolated smooth muscle cells. *American Journal of Physiology-Gastrointestinal and Liver Physiology*. 2005;289:G188-G96.
- [16] Raghavan S, Lam MT, Foster LL, Gilmont RR, Somara S, Takayama S, et al. Bioengineered three-dimensional physiological model of colonic longitudinal smooth muscle in vitro. *Tissue Engineering Part C: Methods*. 2010;16:999-1009.
- [17] Gilmont RR, Raghavan S, Somara S, Bitar KN. Bioengineering of physiologically functional intrinsically innervated human internal anal sphincter constructs. *Tissue Engineering Part A*. 2014;20:1603-11.
- [18] Raghavan S, Miyasaka EA, Gilmont RR, Somara S, Teitelbaum DH, Bitar KN. Perianal implantation of bioengineered human internal anal sphincter constructs intrinsically innervated with human neural progenitor cells. *Surgery*. 2014;155:668-74.

- [19] Zakhem E, Elbahrawy M, Orlando G, Bitar KN. Successful implantation of an engineered tubular neuromuscular tissue composed of human cells and chitosan scaffold. *Surgery*. 2015;158:1598-608.
- [20] Rego SL, Zakhem E, Orlando G, Bitar KN. Bioengineering functional human sphincteric and non-sphincteric gastrointestinal smooth muscle constructs. *Methods*. 2015.
- [21] Zakhem E, Rego SL, Raghavan S, Bitar KN. The Appendix as a Viable Source of Neural Progenitor Cells to Functionally Innervate Bioengineered Gastrointestinal Smooth Muscle Tissues. *Stem cells translational medicine*. 2015:sctm. 2014-0238.
- [22] Zakhem E, Raghavan S, Gilmont RR, Bitar KN. Chitosan-based scaffolds for the support of smooth muscle constructs in intestinal tissue engineering. *Biomaterials*. 2012;33:4810-7.
- [23] Zakhem E, Bitar KN. Development of Chitosan Scaffolds with Enhanced Mechanical Properties for Intestinal Tissue Engineering Applications. *Journal of Functional Biomaterials*. 2015;6:999-1011.
- [24] Raghavan S, Bitar KN. The influence of extracellular matrix composition on the differentiation of neuronal subtypes in tissue engineered innervated intestinal smooth muscle sheets. *Biomaterials*. 2014;35:7429-40.
- [25] Rego SL, Zakhem E, Orlando G, Khalil B. Bioengineered human pyloric sphincters using autologous smooth muscle and neural progenitor cells. *Tissue engineering*. 2015.
- [26] Grikscheit TC, Ochoa ER, Ramsanahie A, Alsberg E, Mooney D, Whang EE, et al. Tissue-engineered large intestine resembles native colon with appropriate in vitro physiology and architecture. *Annals of surgery*. 2003;238:35-41.

- [27] Sala FG, Kunisaki SM, Ochoa ER, Vacanti J, Grikscheit TC. Tissue-engineered small intestine and stomach form from autologous tissue in a preclinical large animal model. *The Journal of surgical research*. 2009;156:205-12.
- [28] Grikscheit TC, Siddique A, Ochoa ER, Srinivasan A, Alsberg E, Hodin RA, et al. Tissue-engineered small intestine improves recovery after massive small bowel resection. *Annals of surgery*. 2004;240:748.
- [29] Grant CN, Mojica SG, Sala FG, Hill JR, Levin DE, Speer AL, et al. Human and mouse tissue-engineered small intestine both demonstrate digestive and absorptive function. *American Journal of Physiology-Gastrointestinal and Liver Physiology*. 2015;308:G664-G77.
- [30] Rego SL, Zakhem E, Orlando G, Bitar KN. Bioengineered human pyloric sphincters using autologous smooth muscle and neural progenitor cells. *Tissue Engineering Part A*. 2015;22:151-60.
- [31] Wilkinson DJ, Bethell GS, Shukla R, Kenny SE, Edgar DH. Isolation of enteric nervous system progenitor cells from the aganglionic gut of patients with Hirschsprung's disease. *PloS one*. 2015;10:e0125724.
- [32] Rollo BN, Zhang D, Stamp LA, Menheniott TR, Stathopoulos L, Denham M, et al. Enteric Neural Cells From Hirschsprung Disease Patients Form Ganglia in Autologous Aneuronal Colon. *CMGH Cellular and Molecular Gastroenterology and Hepatology*. 2016;2:92-109.
- [33] Qin HH, Dunn JC. Small intestinal submucosa seeded with intestinal smooth muscle cells in a rodent jejunal interposition model. *Journal of Surgical Research*. 2011;171:e21-e6.
- [34] Walthers CM, Nazemi AK, Patel SL, Wu BM, Dunn JC. The effect of scaffold macroporosity on angiogenesis and cell survival in tissue-engineered smooth muscle. *Biomaterials*. 2014;35:5129-37.

- [35] Denost Q, Adam J-P, Pontallier A, Montembault A, Bareille R, Siadous R, et al. Colorectal tissue engineering: A comparative study between porcine small intestinal submucosa (SIS) and chitosan hydrogel patches. *Surgery*. 2015.
- [36] Zakhem E, Elbahrawy M, Orlando G, Bitar KN. Successful implantation of an engineered tubular neuromuscular tissue composed of human cells and chitosan scaffold. *Surgery*. 2015.
- [37] Nakao M, Ueno T, Oga A, Kuramitsu Y, Nakatsu H, Oka M. Proposal of intestinal tissue engineering combined with Bianchi's procedure. *Journal of pediatric surgery*. 2014.
- [38] Pasricha PJ, Ahmed I, Jankowski RJ, Micci M-A. Endoscopic injection of skeletal muscle-derived cells augments gut smooth muscle sphincter function: implications for a novel therapeutic approach. *Gastrointestinal endoscopy*. 2009;70:1231-7.
- [39] Rego SL, Shannon B, Zakhem E, Bitar KN. Su1859 Incorporation of Interstitial Cells of Cajal in Bioengineered Intrinsically Innervated Smooth Muscle Constructs. *Gastroenterology*. 2015;148:S-535.

## **CHAPTER X: TRANSLATIONAL APPLICATION OF THE TISSUE-ENGINEERED GUT (TEG)**

### **Short bowel syndrome:**

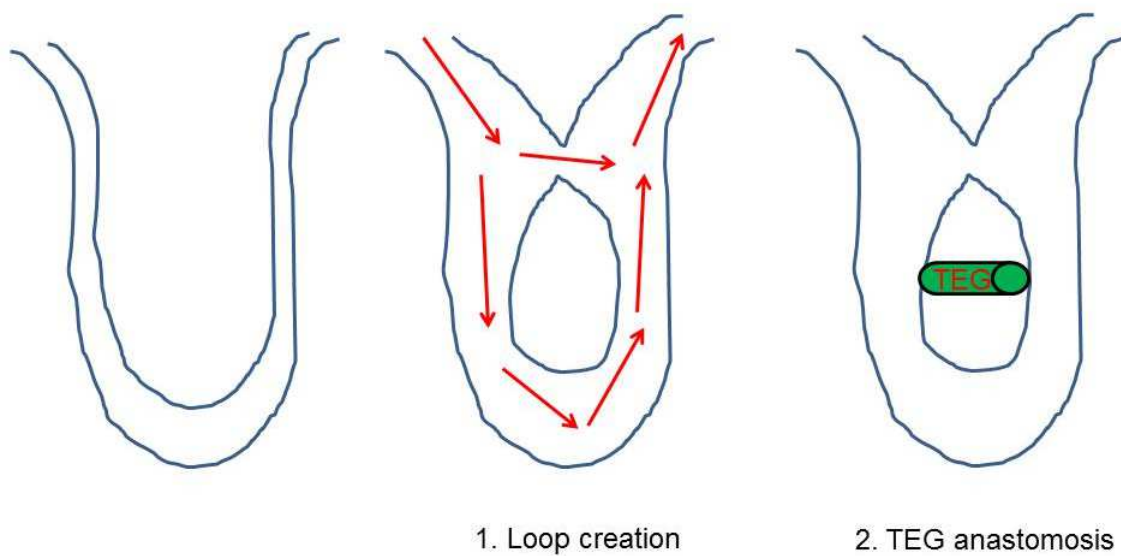
Short bowel syndrome is a condition that results from loss of a large surface area of the small intestine <sup>1</sup>. Patients suffer from inadequate digestion and absorption of nutrients resulting in malnutrition. Management of patients with short bowel syndrome ranges from dietary to surgical <sup>2, 3</sup>. Dietary management, special diets and total parenteral nutrition are different treatment options. There is a high risk of morbidity and mortality in patients undergoing total parenteral nutrition, usually associated with infections and liver disease with low survival rate. Other complications include catheter occlusion. Surgical management of short bowel syndrome includes intestinal transplantation. This approach is limited by the availability of donors, graft rejection, non-functional graft, organ failure and others.

A tissue engineered intestine is needed to lengthen the gut, restore motility and to re-establish the nutritional balance in patients with short bowel syndrome <sup>4</sup>. The complexity of the intestine imposes several requirements on the newly generated intestine. First, the neo-intestine must possess the properties needed for restoring motility and propulsion of luminal content. Second, the restoration of the absorptive characteristic is essential for nutrition. Finally, the intestine's

immune and endocrine functions must be taken into consideration. Several previous approaches have worked on regenerating the different cellular components of the intestine. The use of organoid units seeded onto polymer scaffolds resulted in the formation of a multilayered intestine <sup>5, 6</sup>. Assays have shown the regeneration of a functional epithelium <sup>7</sup>. Motility and physiological properties of the regenerated neuro-musculature is missing. We have previously demonstrated the ability to engineer tubular neuro-muscular tissues that maintained their biomechanical properties following their subcutaneous implantation <sup>8</sup>. The goal of this study was to implant the engineered tubular tissues in the omentum of the rats followed by their anastomosis to the native intestine. The hypothesis of this study was that anastomosis of the engineered tubular neuro-muscular tissue will allow epithelial cell migration into the tissue and formation of the intestinal epithelium. The schematic diagram of the surgical process is illustrated in **Figure 44**. The first surgical step involves implantation of TEG in the peritoneal fold followed by the formation of the intestinal loop. The second surgical step involves the anastomosis of TEG with the native intestine in the loop part. The loop was formed to create 2 ways for luminal flow; one through the loop and the other through the neck in order to avoid any obstruction that may be caused by TEG.

## Engineering TEG:

Aligned innervated smooth muscle sheets were formed as previously described. Briefly, smooth muscle cells were isolated from human small intestine and seeded onto laminin-coated plates that have longitudinal grooves. Following smooth muscle alignment, neural progenitor cells isolated from human small intestine were suspended in collagen gel and laid on top of the aligned smooth muscle. Following formation of the sheets, the neural progenitor cells were allowed to differentiate before wrapping the sheets around the mechanically



reinforced tubular chitosan scaffolds. Chitosan scaffolds had circumferentially aligned chitosan fibers on the outer side of the scaffold.

**Figure 44:** Schematic diagram of the surgical process for TEG anastomosis.

*(The red arrows show the 2 paths for luminal flow).*



## **Implantation of TEG followed by the formation of the intestinal loop:**

Athymic female rats were used for this study. Surgical procedures described in this work were performed following the guidelines set forth by IACUC. Rats were anesthetized by continuous isoflurane masking throughout the surgery. The surgical area was shaved and aseptically prepared. A midline abdominal incision of up to 5 cm was made and the peritoneal fold was explored. TEG was implanted intra-abdominally and wrapped with the peritoneal fold (Figure 45). The tissues were returned back to the abdominal cavity. Up to 10 cm of the native intestine was used to form a loop and the neck of the loop was anastomosed in a side-to-side fashion as shown in Figure 46. The intestine was returned back to the abdominal cavity and the rats were allowed to recover in their cages in standard fashion and were given the appropriate analgesics.



**Figure 45:** Implantation of TEG in the peritoneal fold.

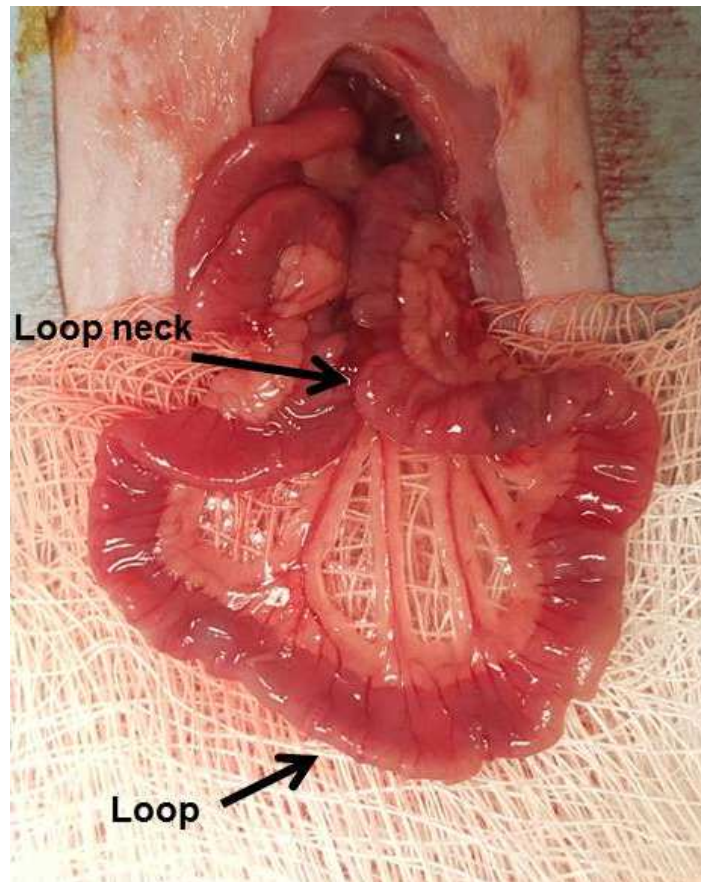


**Figure 46:** Creation of the intestinal loop.

### **Anastomosis of TEG to the native intestine:**

Rats were brought back to the procedure room and prepared for the second surgery of anastomosis. An abdominal midline incision was made and the peritoneal fold was explored. TEG was identified and the intestinal loop was located. The ends of TEG were refreshed and biopsies were obtained for physiological and histological analysis. TEG was then anastomosed with the native intestine in the initially created intestinal loop (**Figure 47**). The intestines

were returned back to the abdominal cavity. The abdominal wall and skin were sutured and the rats were allowed to recover in their cages in standard fashion and were given the appropriate analgesics.

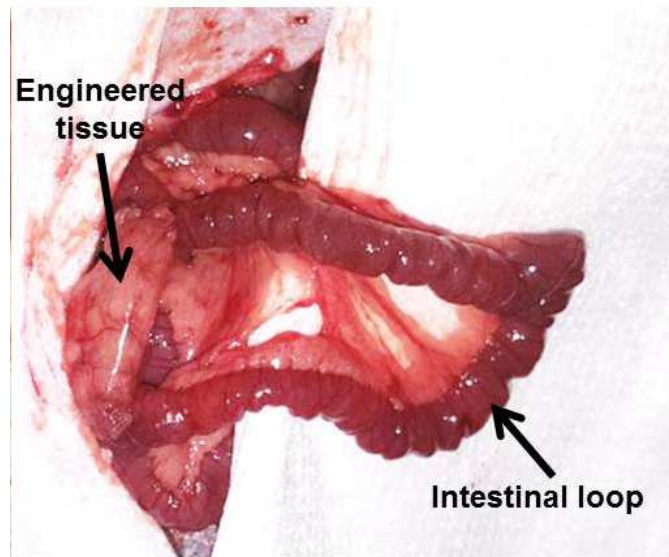


**Figure 47:** Anastomosis of the engineered tissue with the native intestine in the created loop area.

### **Physiological functionality of the implant:**

Four weeks post TEG anastomosis, the rats were euthanized. The anastomosed TEG was harvested. A circular strip of the implant was used for organ bath studies (**Figure 48**). The protocol was previously described. Briefly, the tissues were hooked to a force transducer arm in a warm tissue bath. Smooth muscle electromechanical coupling integrity was tested by administering potassium chloride. Neural functionality was tested using electrical field stimulation. Following equilibration and establishing baseline, potassium chloride was administered to the tissue. A contraction of 466  $\mu$ M was observed. The tissue

was then washed and allowed to establish baseline again. Electrical field stimulation was applied and caused relaxation of the implant to  $-270\ \mu\text{M}$ .

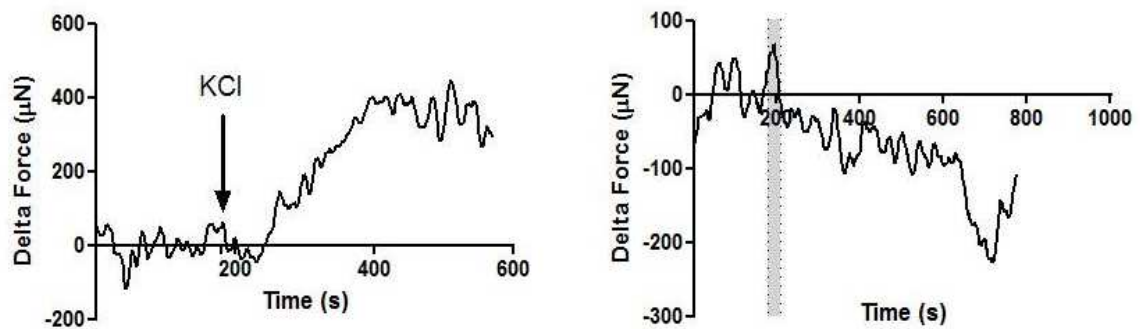


**Figure 48:** Organ bath studies using potassium chloride and electrical field stimulation indicated the preservation of both the smooth muscle and neural components of the implanted tissue.

## Histological evaluation of the implant:

At 4 weeks post-anastomosis of TEG, implants were harvested. Cross sections of the implant were fixed in formaldehyde, processed and embedded. Paraffin sections of  $6\ \mu\text{m}$  thickness were obtained and stained with hematoxylin and eosin (H&E) for morphological analysis. H&E analysis of the implants revealed re-epithelialization of the implants (**Figure 49**). Epithelial cells were seen in the implant even though not fully differentiated.

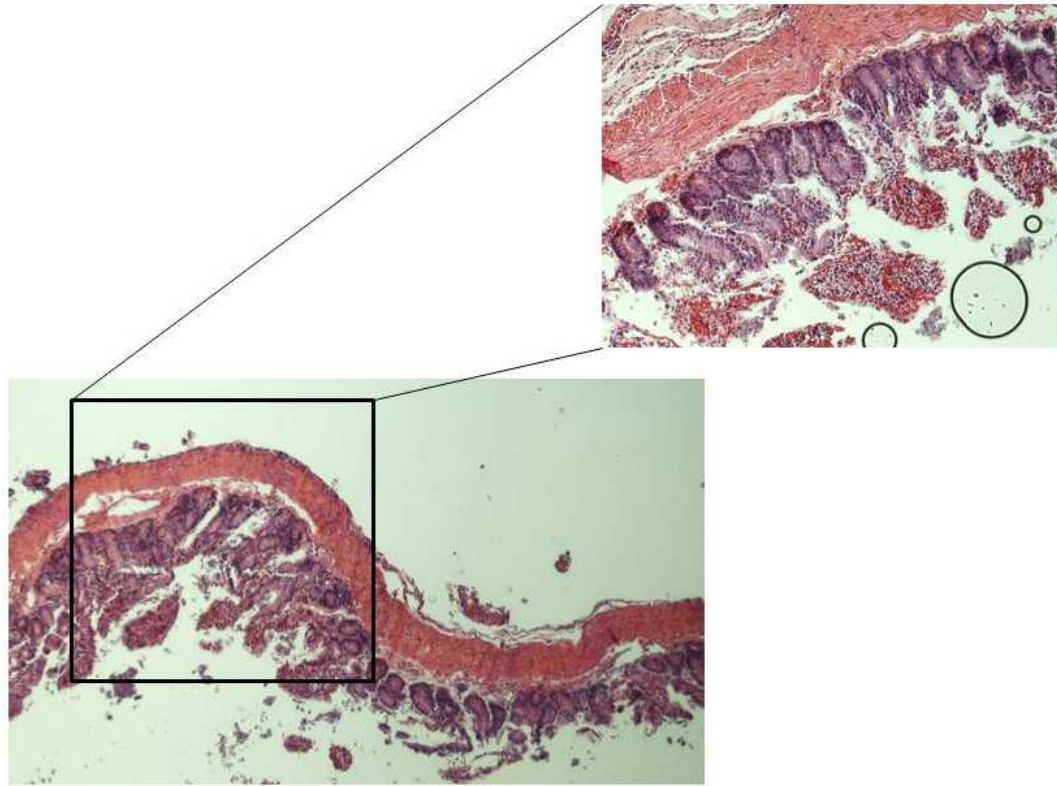


**Figure 49:** H&E analysis of the implant indicated the re-epithelialization of the engineered tissue following anastomosis with the rat native intestine.

## Discussion:

This study demonstrated the feasibility of anastomosing the engineered tubular neuro-muscular tissue with the native intestine of the rat. The anastomosis site was completely healed following surgery without any signs of leakage. The intestinal bypass surgery performed during implantation of the engineered tissue aimed to alleviate any potential obstruction from the implanted engineered tissue. Following 4 weeks of implantation of the engineered tissue, the implant remodeled and became vascularized.

Physiological functionality of the implant showed that the neuromuscular components of the engineered tissue were preserved. Contraction in response to potassium chloride indicated that depolarization of the smooth muscle membrane caused activation of voltage dependent calcium channels and allowed the influx of calcium into smooth muscle resulting in the observed contraction. Additional studies will look at the specific phenotype of each component. Electrical field stimulation induced the release of neurotransmitters from the neural component of the engineered tissue. Neurotransmitters caused relaxation of the smooth muscle.

Previous studies have shown that the epithelial cells increase their proliferation rate following mechanical manipulation of the native intestine <sup>9</sup>. This has led to our hypothesis that anastomosis between the engineered tissue and the native intestine will result in epithelial cell proliferation, migration into the engineered tissue and epithelialization of the tissue. Histological analysis showed evident re-epithelialization of the engineered tissue following anastomosis. The epithelium did not look uniformly differentiated. A longer period than 4 weeks of anastomosis will be needed to determine the maturity of the newly generated epithelium. Additional studies will characterize the different cell type present in the newly generated epithelium and their function.

In conclusion, this study is promising in providing a solution for patients with short bowel syndrome. Our engineering technique provides a tubular tissue with the necessary components for restoring motility. Following anastomosis, the tissue

has the ability to become epithelialized to provide the absorptive component needed for these patients.

## **Future directions**

Our preliminary results in this study have shown the regeneration of an epithelial component in the engineered tubular neuromuscular tissue following its anastomosis to native rat intestine. Further studies will characterize the epithelial differentiation and function. The presence of the 4 differentiated types of epithelial cells is important for a functional epithelium. Stains such as villin for enterocytes, chromogranin-A for enteroendocrine, mucin-2 for goblet cells and lysozyme for Paneth cells will be performed. Once these stains have been conducted, functionality of the regenerated epithelium will be confirmed using functional assays. Enzymatic activity of maltase and sucrase will be measured by checking the hydrolysis of the respective sugars through the amount of glucose released.

The work performed in this thesis was in a small animal model. Future studies will look at scaling up the engineering process to develop scaffolds with larger diameter to match large animals. The scaffolds will be tested for maintenance of mechanical strength. Anastomosis of the scaled up engineered tubular tissue to the native intestine of a large animal model will be performed as a way to lengthen the gut.

## 8. References:

1. Seetharam, P. & Rodrigues, G. Short bowel syndrome: a review of management options. *Saudi Journal of Gastroenterology* **17**, 229 (2011).
2. Buchman, A.L., Scolapio, J. & Fryer, J. AGA technical review on short bowel syndrome and intestinal transplantation. *Gastroenterology* **124**, 1111-1134 (2003).
3. Schalamon, J., Mayr, J. & Höllwarth, M. Mortality and economics in short bowel syndrome. *Best Practice & Research Clinical Gastroenterology* **17**, 931-942 (2003).
4. Ladd, M.R., Niño, D.F., March, J.C., Sodhi, C.P. & Hackam, D.J. Generation of an artificial intestine for the management of short bowel syndrome. *Current opinion in organ transplantation* **21**, 178-185 (2016).
5. Grikscheit, T.C. et al. Tissue-engineered small intestine improves recovery after massive small bowel resection. *Annals of surgery* **240**, 748-754 (2004).
6. Sala, F.G., Kunisaki, S.M., Ochoa, E.R., Vacanti, J. & Grikscheit, T.C. Tissue-engineered small intestine and stomach form from autologous tissue in a preclinical large animal model. *Journal of Surgical Research* **156**, 205-212 (2009).
7. Grant, C.N. et al. Human and mouse tissue-engineered small intestine both demonstrate digestive and absorptive function. *American Journal of Physiology-Gastrointestinal and Liver Physiology* **308**, G664-G677 (2015).



8. Zakhem, E., Elbahrawy, M., Orlando, G. & Bitar, K.N. Successful implantation of an engineered tubular neuromuscular tissue composed of human cells and chitosan scaffold. *Surgery* **158**, 1598-1608 (2015).
9. Koga, H. et al. Distraction-induced intestinal enterogenesis: Preservation of intestinal function and lengthening after re-implantation into normal jejunum. *Annals of surgery* **255**, 302 (2012).

## CHAPTER XI: SUMMARY AND CONCLUSIONS

The hypothesis of this thesis was that tubular chitosan scaffolds will mediate the reconstruction of the neuro-musculature of the GI tract. The studies conducted in this thesis were devised to address this hypothesis. Given that the natural polymer chitosan hasn't been previously tested for its potential use in gut tissue engineering, the first step of this thesis was to evaluate the in vitro biocompatibility of chitosan using smooth muscle cells and neural progenitor cells. Smooth muscle cells maintained their contractile phenotype, alignment and functionality around chitosan scaffolds. The neural progenitor cells differentiated into functional neurons when seeded with smooth muscle cells on chitosan scaffolds. The next step of this thesis was to develop tubular chitosan scaffolds with mechanical properties that match those of a native intestine. Compliance matching between the engineered gut and the native gut is necessary for successful anastomosis. Different tubular scaffolds were engineered and were mechanically reinforced by embedding chitosan fibers circumferentially around the scaffolds in different patterns. Reinforced chitosan scaffolds had increased tensile strength, elongation at break and burst pressure than scaffolds without fibers.

The next step of the work outlined in this dissertation was to evaluate the biocompatibility and remodeling of the engineered tissues in vivo. Aligned human gut smooth muscle sheets were engineered and innervated using gut-derived neural progenitor cells. The sheets were circumferentially wrapped around

mechanically reinforced tubular chitosan scaffolds to form an innervated circular smooth muscle layer around tubular chitosan scaffolds. The tissues were implanted subcutaneously in the back of athymic rats for 2 weeks. The implants became vascularized and maintained their luminal patency. The smooth muscle maintained its circumferential alignment around the lumen of the scaffold, maintained its contractile phenotype and maintained its innervation as demonstrated histologically and functionally.

The application of the engineered tubular neuro-muscular tissues can be extended to replace gut segments along with the adjacent sphincter. The tubular innervated circular smooth muscle tissues were engineered as described above. Human sphincteric tissues were also engineered and placed around the same scaffold on one end to form a gut-sphincter complex. The tissue was implanted subcutaneously in the abdomen of athymic rats for 4 weeks. At the time of harvest, the tissues displayed luminal pressures with the sphincter zone exhibiting a higher pressure than the gut zone, consistent with physiological characteristic of sphincters in the gut. The mechanical properties and burst pressures of the implants matched those of a native rat intestine. Histological studies indicated that the alignment and the phenotype of both the muscular and the neural components were preserved. This was further confirmed by organ bath studies that indicated the preservation of the smooth muscle contractility and the neural functionality.

Lastly, the last aim of this thesis was to regenerate the epithelial component in the newly generate gut tissue. The engineered tissues were

implanted in the omentum of athymic rats followed by the creation of an intestinal loop through side to side anastomosis of the small intestine. Following maturation of the engineered tissue, anastomosis of the engineered tissue and the native small intestine was performed in the loop area. Histological studies showed evident epithelial regeneration in the engineered gut tissue. This indicated the possibility of the epithelial cells to migrate from the native intestine into the engineered tissue. Those results are promising and require further investigation.

In conclusion, we were successful in reconstructing the neuro-musculature of the gut using a tubular chitosan scaffold and an innervated aligned smooth muscle sheet. The reconstructed neuro-muscular tissues maintained viability in vivo, maintained their phenotype and functionality and exhibited mechanical properties that make them suitable for gut repair. Those engineered tissues provide a potential solution to either replace an intestinal segment or to replace a gut segment along with the adjacent sphincter.

# SCHOLASTIC VITA

## Elie Zakhem

2462 Southmont Drive, Apt 208  
Winston-Salem, NC 27103

☎ 248-835-5505

✉ ezakhem@wakehealth.edu

---

### EDUCATION

- **Wake Forest University School of Medicine**  
*PhD in Molecular Medicine and Translational Sciences-* 2012- 2016  
Concentration: Cell and Tissue Engineering
- **Wayne State University, Detroit, MI**  
*Masters in Biomedical Engineering –* 2008-2010  
Concentration: Tissue Engineering
- **University of Balamand, Tripoli , Lebanon**  
*Bachelors in Biology-* 2004-2007

### PEER-REVIEWED PUBLICATIONS

- Bitar, K.N. & **Zakhem, E.** Bioengineering the gut: future prospects of regenerative medicine. *Nature Reviews Gastroenterology and Hepatology* (Accepted July 2016).
- **Zakhem, E.**, Elbahrawy, M., Orlando, G. & Bitar, K.N. Biomechanical Properties of an Implanted Engineered Tubular Gut-Sphincter Complex”. *Journal of Tissue Engineering and Regenerative Medicine* 2016. (Accepted July 2016).
- **Zakhem, E.**, Murphy, S.V., Davis, M.L., Raghavan, S. & Lam, M.T. IMAGE AND VIDEO ACQUISITION AND PROCESSING FOR CLINICAL APPLICATIONS. *Biomedical Engineering and Computational Biology* **7**, 35 (2016).

- Rego, S.L., **Zakhem, E.**, Orlando, G. & Bitar, K.N. Bioengineered human pyloric sphincters using autologous smooth muscle and neural progenitor cells. *Tissue Engineering Part A* **22**, 151-160 (2015).
- Bitar, K.N. & **Zakhem, E.** Is bioengineering a possibility in gastrointestinal disorders? *Expert review of gastroenterology & hepatology* **9**, 1463-1465 (2015).
- **Zakhem, E.** & Bitar, K.N. Development of chitosan scaffolds with enhanced mechanical properties for intestinal tissue engineering applications. *Journal of functional biomaterials* **6**, 999-1011 (2015).
- Rego, S.L., **Zakhem, E.**, Orlando, G. & Bitar, K.N. Bioengineering functional human sphincteric and non-sphincteric gastrointestinal smooth muscle constructs. *Methods* **99**, 128-134 (2016).
- **Zakhem, E.**, Elbahrawy, M., Orlando, G. & Bitar, K.N. Successful implantation of an engineered tubular neuromuscular tissue composed of human cells and chitosan scaffold. *Surgery* **158**, 1598-1608 (2015).
- Rego, S.L., Raghavan, S., **Zakhem, E.** & Bitar, K.N. Enteric neural differentiation in innervated, physiologically functional, smooth muscle constructs is modulated by bone morphogenic protein 2 secreted by sphincteric smooth muscle cells. *Journal of tissue engineering and regenerative medicine* (2015).
- **Zakhem, E.**, Rego, S.L., Raghavan, S. & Bitar, K.N. The appendix as a viable source of neural progenitor cells to functionally innervate bioengineered gastrointestinal smooth muscle tissues. *Stem cells translational medicine* **4**, 548 (2015).
- Bitar, K.N. & **Zakhem, E.** Design strategies of biodegradable scaffolds for tissue regeneration. *Biomedical Engineering and Computational Biology* **6**, 13 (2014).

- Bitar, K.N., Raghavan, S. & **Zakhem, E.** Tissue engineering in the gut: developments in neuromusculature. *Gastroenterology* **146**, 1614-1624 (2014).
- **Zakhem, E.**, Raghavan, S. & Bitar, K.N. Neo-innervation of a bioengineered intestinal smooth muscle construct around chitosan scaffold. *Biomaterials* **35**, 1882-1889 (2014).
- Bitar, K.N. & **Zakhem, E.** Tissue engineering and regenerative medicine as applied to the gastrointestinal tract. *Current opinion in biotechnology* **24**, 909-915 (2013).
- **Zakhem, E.**, Raghavan, S., Gilmont, R.R. & Bitar, K.N. Chitosan-based scaffolds for the support of smooth muscle constructs in intestinal tissue engineering. *Biomaterials* **33**, 4810-4817 (2012).
- **Zakhem, E.** & Bitar, K.N. Tissue Engineering and Regenerative Medicine: Gastrointestinal Application. Translating Regenerative Medicine to the Clinic 2015. Book Chapter
- Bitar, K.N., Raghavan, S., Somara, S., **Zakhem, E.** & Rego, S.L., Advances in neo-innervation of the gut". Translational Regenerative Medicine 2014. Book Chapter

## **RESEARCH AND WORK EXPERIENCE**

### **Graduate Student Research Assistant** (August 2012 – Present)

Wake Forest Institute for Regenerative Medicine, Wake Forest School of Medicine, Winston-Salem, NC.

- Extensive experience in isolating and culturing smooth muscle cells and enteric neural stem cells from human, rabbits and rodents.

- Designed and developed mechanically reinforced tubular scaffolds for gut tissue engineering
- Utilized a perfusion flow bioreactor system to orient smooth muscle cells on tubular scaffolds.
- Bioengineering a continuously innervated functional gut replacement using primary isolated smooth muscle and enteric neural progenitor cells derived from rabbits and humans.
- Evaluation of mechanical properties of tubular scaffolds using tensile testing machine.
- Evaluation of the engineered gut segments in vivo in athymic rats.
- Evaluation of engineered gut segments biochemically and functionally using force transducer set up.
- Provided surgical assistance in large animal survival surgeries involving implantation of engineered anal sphincters.
- Experience in small and large animal care, Occupational Health & Safety, Regulatory and IACUC Compliance.
- Experience in wet bench molecular biology.
- Trained and experienced in conducting GLP studies and standard operating procedure.

**Research Lab Assistant** (June 2011 – July 2012)

Wake Forest Institute for Regenerative Medicine, Wake Forest School of Medicine, Winston-Salem, NC.

- Bioengineered innervated intestinal circular smooth muscle constructs
- Bioengineered intrinsically innervated smooth muscle constructs using smooth muscle and neural stem cells.



- Tested physiological functionality of innervated smooth muscle constructs.
- Studied nerve differentiation and migration along smooth muscle constructs around biodegradable scaffolds.
- Tested the biological and mechanical properties of the scaffolds.

**Research Lab Assistant** (September 2010 – June 2011)

Gastrointestinal motor lab, Biomedical Engineering, University of Michigan, Ann Arbor, MI.

- Developed scaffolds for intestinal replacement using a combination of different biodegradable materials (chitosan, collagen, hydrogels).
- Studied the biocompatibility of different biomaterials and their immobilization with different glycosaminoglycans.

**Directed Study** (January 2010 – May 2010)

Matthew Lab, Biomedical Engineering, Wayne State University, Detroit, MI.

- Studied the behavior of primary isolates of intrahepatic biliary tree cells known as cholangiocytes under different concentrations of vascular endothelial growth factor (VEGF).

**Medical internship** (June 2009 – August 2009)

Rochester Medical Center, Rochester, MI.

- Conducted CT/CTA scans (heart, brain, bone density, abdomen) and analyzed the studies.
- Assisted in nuclear medicine, gained experience in Enhanced External Counter Pulsation (EECP), observed general ultrasound and cardiac ultrasound.

## **PODIUM PRESENTATIONS**

- “Development of a Tubular Gut-Sphincter Complex (TGSC) that Maintains Biomechanical Properties In Vivo”. Digestive Disease Week annual meeting 2016. San Diego, CA
- “Implantation of a Human-Based Engineered Neuro-Muscular Tubular Gut Tissue”. North Carolina Tissue Engineering and Regenerative Medicine Society (NCTERMS) 2015. Winston Salem, NC.
- “Implantation of a Chitosan-Based Bioengineered Tubular Neuromuscular Tissue For Gut Lengthening”. Biomedical Engineering Society (BMES) 2015. Tampa, FL.
- “Chitosan-based neuromuscular tubular tissue with improved biomechanical properties suitable for gut lengthening in a rat model”. Tissue Engineering and Regenerative Medicine International Society (TERMIS) meeting World Congress 2015. Boston, MA.
- “The appendix as a viable source of neural progenitor cells to functionally innervate bioengineered gastrointestinal smooth muscle tissues”. Digestive Disease Week (DDW) 2015. Washington, D.C.
- “Neo-innervation of a bioengineered smooth muscle construct by an intrinsically innervated construct located on the same scaffold”. Digestive Disease Week annual meeting 2012. San Diego, California.
- “A bioengineered segment of colonic smooth muscle tissue demonstrates the capabilities of expansion and decompression similar to native tissue”. Digestive Disease Week annual meeting 2012. San Diego, California.
- “Manufacturing a hollow organ on a novel biodegradable chitosan scaffold in intestinal tissue engineering with physiologically functional circular smooth muscle layer”. Digestive Disease Week annual meeting 2011. Chicago, Illinois.

## **POSTER PRESENTATIONS**

- “Bioengineered sphincters for aging population”. Rejuvenation Biotechnology 2015. *San Francisco, California.*
- “Successful implantation of a Tissue-Engineered Gut (TEG) using human smooth muscle and human enteric neural progenitor cells”. Digestive Disease Week (DDW) 2015. *Washington, D.C.*
- “Surgical Implantation of a Bioengineered Human Smooth Muscle Tubular Hollow Organ”. Tissue Engineering and Regenerative Medicine International Society (TERMIS) 2014. *Washington, D.C.*
- “Tissue Engineered Esophagus Using Primary Isolated Smooth Muscle Cells”. Biomedical Engineering Society (BMES) 2013. *Seattle, WA.*
- “A Tissue Engineered Esophageal Construct Demonstrates Physiological Functionality In Vitro”. Tissue Engineering and Regenerative Medicine International Society (TERMIS) 2013. *Atlanta, Georgia.*
- “Tubular Esophageal Tissue Construct Bioengineered from Isolated Esophageal Circular Smooth Muscle Cells”. Digestive Disease Week annual meeting 2013. *Orlando, Florida.*
- “A bioengineered segment of colonic smooth muscle tissue demonstrates the capabilities of expansion and decompression similar to native tissue”. Digestive Disease Week annual meeting 2012. *San Diego, California.*
- “Manufacturing a hollow organ on a novel biodegradable chitosan scaffold in intestinal tissue engineering with physiologically functional circular smooth muscle layer”. Upper Midwest Biomaterials Day 2011. *Ann Arbor, Michigan.*

## **AWARDS AND ACHIEVEMENTS**

- Certificate of recognition for scientific accomplishment as an early stage investigator, Digestive Disease Week (DDW) meeting, San Diego, CA. 2016.
- Certificate of recognition for scientific accomplishment as an early stage investigator, Digestive Disease Week (DDW) meeting, Washington, D.C. 2015.
- Lead Guest Editor, Special issue on Image and Video Acquisition and Processing for Clinical Applications “Biomedical Engineering and Computational Biology” journal, 2015.
- Rejuvenation Biotechnology Travel Award, San Francisco 2015.
- Poster of Distinction – Digestive Disease Week (DDW) meeting, 2013, 2015 & 2016.
- Student co-chair for “Naturally-derived/Inspired Biomaterials” session at Tissue Engineering and Regenerative Medicine International Society (TERMIS) meeting, Washington, D.C. 2014.
- Travel Awards – School of Biomedical Engineering and Sciences, 2013.
- Travel Awards – Department of Molecular Medicine and Translational Sciences, 2015-2016
- Student Travel Award, Wake Forest Graduate School, 2015
- Poster of Distinction – Digestive Disease Week (DDW) meeting, 2013.
- Graduate Student Fellowship –Wake Forest University School of Medicine, 2012-2016.
- Secretary, Biomedical Engineering Society Student Chapter, Wake Forest University, 2014 – Present.
- Member, Biomedical Engineering Society 2012 – Present.